

NAME



AD A 0 7 8 2 3 3

AD A 0 7 8 2 3 3

TECHNICAL REPORT ARBRL-TR-02199

(Supersedes IMR No. 323)

AMMUNITION FOR LAW ENFORCEMENTS: PART I  
METHODOLOGY FOR EVALUATING RELATIVE  
STOPPING POWER AND RESULTS

William J. Bruchey, Jr.

October 1979



US ARMY ARMAMENT RESEARCH AND DEVELOPMENT COMMAND  
BALLISTIC RESEARCH LABORATORY  
ABERDEEN PROVING GROUND, MARYLAND

Approved for public release; distribution unlimited.

REPRODUCED BY  
NATIONAL TECHNICAL  
INFORMATION SERVICE  
U.S. DEPARTMENT OF COMMERCE  
SPRINGFIELD, VA. 22161

87004

208

Destroy this report when it is no longer needed.  
Do not return it to the originator.

Secondary distribution of this report by originating  
or sponsoring activity is prohibited.

Additional copies of this report may be obtained  
from the National Technical Information Service,  
U.S. Department of Commerce, Springfield, Virginia  
22151.

The findings in this report are not to be construed as  
an official Department of the Army position, unless  
so designated by other authorized documents.

*The use of trade names or manufacturers' names in this report  
does not constitute indorsement of any commercial product.*

NOV 12 1982

UNCLASSIFIED

SECURITY CLASSIFICATION OF THIS PAGE (When Data Entered)

REPORT DOCUMENTATION PAGE		ACQUISITIONS	READ INSTRUCTIONS BEFORE COMPLETING FORM
1. REPORT NUMBER TECHNICAL REPORT ARBRL-TR-02199	2. GOVT ACCESSION NO.	3. RECIPIENT'S CATALOG NUMBER	
4. TITLE (and Subtitle) AMMUNITION FOR LAW ENFORCEMENTS: PART I METHODOLOGY FOR EVALUATING RELATIVE STOPPING POWER AND RESULTS		5. TYPE OF REPORT & PERIOD COVERED Final	
		6. PERFORMING ORG. REPORT NUMBER	
7. AUTHOR(s) William J. Bruchey, Jr.		8. CONTRACT OR GRANT NUMBER(s)	
9. PERFORMING ORGANIZATION NAME AND ADDRESS US Army Ballistic Research Laboratory ATTN: DRDAR-BLT Aberdeen Proving Ground, Maryland 21005		10. PROGRAM ELEMENT, PROJECT, TASK AREA & WORK UNIT NUMBERS	
11. CONTROLLING OFFICE NAME AND ADDRESS US Army Armament Research & Development Command US Army Ballistic Research Laboratory ATTN: DRDAR-BL Aberdeen Proving Ground, Maryland 21005		12. REPORT DATE October 1979	
		13. NUMBER OF PAGES 213	
14. MONITORING AGENCY NAME & ADDRESS (if different from Controlling Office)		15. SECURITY CLASS. (of this report) Unclassified	
		15a. DECLASSIFICATION/DOWNGRADING SCHEDULE	
16. DISTRIBUTION STATEMENT (of this Report) Approved for public release; distribution unlimited.			
17. DISTRIBUTION STATEMENT (of the abstract entered in Block 20, if different from Report)			
18. SUPPLEMENTARY NOTES This report supersedes Interim Memorandum Report No. 323 dated December 1974.			
19. KEY WORDS (Continue on reverse side if necessary and identify by block number) Penetration                      Tissue Simulant Incapacitation                  Cavity Formation Small Arms                        Bullets Ammunition                        Handgun Ammunition			
20. ABSTRACT (Continue on reverse side if necessary and identify by block number) → A comprehensive study was conducted for the Department of Justice to determine what factors influence human incapacitation by handgun bullets. An evaluation of the effectiveness of nearly all commercial handgun bullets was made. The report describes the methodology developed and the application of this methodology to handgun ammunition evaluation. Data on the individual test rounds fired are published in the following companion reports: Ammunition For Law Enforcement: Part II, Data Obtained For Bullets			

UNCLASSIFIED

SECURITY CLASSIFICATION OF THIS PAGE(When Data Entered)

Penetrating Tissue Simulant, BRL Report No. 1940, "Ammunition For Law Enforcement: Part III: Photographs of Bullets Recovered After Impacting Tissue Simulant," BRL Memorandum Report No. 2673.

UNCLASSIFIED

SECURITY CLASSIFICATION OF THIS PAGE(When Data Entered)

TABLE OF CONTENTS

	Page
LIST OF ILLUSTRATIONS . . . . .	5
LIST OF TABLES . . . . .	13
I. INTRODUCTION . . . . .	19
II. TERMINOLOGY . . . . .	20
III. METHODOLOGY . . . . .	22
A. Relative Stopping Power (RSP) . . . . .	23
B. Ricochet and Penetration Performance . . . . .	29
IV. EXPERIMENTAL TECHNIQUES . . . . .	29
A. Data Storage and Retrieval . . . . .	32
B. Calculation of the Relative Incapacitation Index . . . . .	33
V. THEORETICAL CAVITY MODEL . . . . .	34
VI. RESULTS . . . . .	38
A. Effect of Aiming Error on the Hit Distribution . . . . .	38
B. Effect of Aiming Error on the RII for Handguns . . . . .	41
C. Determination of the RII for Commercially Available Handgun Bullets . . . . .	43
D. Determination of the RII for Commercially Available Cartridges . . . . .	47
E. Predictions Based on the Analytical Cavity Model . . . . .	50
F. Effect of Accuracy and Aim Point on Stopping Power . . . . .	52
G. Comparison with other Techniques of Calculating RSP . . . . .	52
H. Penetration/Ricochet Characteristics . . . . .	53
VII. CONCLUSIONS . . . . .	58
A. Bullet Velocity . . . . .	58
B. Caliber . . . . .	58
C. Bullet Mass . . . . .	59
D. Bullet Shape . . . . .	59
E. Deformation and Bullet Construction . . . . .	59
F. Shooter Accuracy . . . . .	60

TABLE OF CONTENTS (continued)

	Page
G. Point of Aim . . . . .	60
H. Hazard to Bystanders . . . . .	60
VIII. RECOMMENDATIONS . . . . .	60
DISTRIBUTION LIST . . . . .	<b>207</b>

## LIST OF FIGURES

Figure	Page
1. Flow Chart Used to Develop Relative Stopping Power For Handgun Ammunition. . . . .	62
2. Sketch of the Computer Man . . . . .	63
3. Top View of Typical Cross Section of the Computer Man (Shoulder Region) . . . . .	64
4. Sketch of Tissue Response to Bullet Penetration . . . . .	65
5. Comparison of Measured Maximum Temporary Cavity (MTC) Formed in Animal Tissue and a Momentum Transfer Model Prediction. . . . .	65
6. Comparison of the Maximum Temporary Cavity For A Steel Sphere Penetrating Animal Tissue and Tissue Simulant . . . . .	66
7. Sketch of Calculational Procedure For Obtaining RII . . . . .	67
8. Theoretical Cavity Model. . . . .	67
9. Aiming Error as a Function of Engagement Range. . . . .	68
10. Group A Hit Distribution Superimposed on a Computer Man Silhouette at 3.0 Meter Range . . . . .	69
11. Group A Hit Distribution Superimposed on a Computer Man Silhouette at 6.0 Meter Range . . . . .	70
12. Group A Hit Distribution Superimposed on a Computer Man Silhouette at 12.1 Meter Range. . . . .	71
13. Group B Hit Distribution Superimposed on a Computer Man Silhouette at 3.0 Meter Range . . . . .	72
14. Group B Hit Distribution Superimposed on a Computer Man Silhouette at 6.0 Meter Range . . . . .	73
15. Group B Hit Distribution Superimposed on a Computer Man Silhouette at 12.1 Meter Range. . . . .	74
16. Vulnerability Index for Handguns at a Range of 3 Meters for the Group A Hit Distribution. . . . .	75

LIST OF FIGURES (continued)

Figure	Page
17. Vulnerability Index for Handguns at a Range of 6 Meters for the Group A Hit Distribution . . . . .	75
18. Vulnerability Index for Handguns at a Range of 12 Meters for the Group A Hit Distribution . . . . .	76
19. Vulnerability Index for Handguns at a Range of 6 Meters for the Group B Hit Distribution . . . . .	76
20. High Aim Point Hit Distribution Superimposed on a Computer Man Silhouette for Group A Shooters at a 6.0 Meter Range. . . . .	77
21. High Aim Point Hit Distribution Superimposed on a Computer Man Silhouette for Group B Shooters at a 6.0 Meter Range . . . . .	78
22. Vulnerability Index For Handguns at a Range of 6 Meters for the Group A Hit Distribution Using a High Aim Point . . . . .	79
23. Vulnerability Index for Handguns at a Range of 6 Meters for the Group B Hit Distribution Using a High Aim Point . . . . .	79
24. Relative Incapacitation Index for 90 Grain, Caliber .353, JSP, JFP Bullets. . . . .	80
25. Relative Incapacitation Index for 100 Grain, Caliber .353, FJ Bullets. . . . .	80
26. Relative Incapacitation Index for 100 Grain, Caliber .353, PP Bullets. . . . .	81
27. Relative Incapacitation Index for 100 Grain, Caliber .353, JSP, JFP Bullets. . . . .	81
28. Relative Incapacitation Index for 100 Grain, Caliber .353, JHP, JHC Bullets. . . . .	82
29. Relative Incapacitation Index for 115 Grain, Caliber .353, FJ Bullets. . . . .	82
30. Relative Incapacitation Index for 115 Grain, Caliber .353, PP Bullets. . . . .	83

LIST OF FIGURES (continued)

Figure	Page
31. Relative Incapacitation Index for 115 Grain, Caliber .353, JHP, JHC Bullets. . . . .	83
32. Relative Incapacitation Index for 124 Grain, Caliber .353, FJ Bullets. . . . .	84
33. Relative Incapacitation Index for 125 Grain, Caliber .353, RN Bullets. . . . .	84
34. Relative Incapacitation Index for 125 Grain, Caliber .353, JSP Bullets . . . . .	85
35. Relative Incapacitation Index for 90 Grain, Caliber .357, JSP, JFP Bullets. . . . .	85
36. Relative Incapacitation Index for 90 Grain, Caliber .357, HEM1JSP Bullets . . . . .	86
37. Relative Incapacitation Index for 90 Grain, Caliber .357, MP Bullets. . . . .	86
38. Relative Incapacitation Index for 95 Grain, Caliber .357, JHP Bullets . . . . .	87
39. Relative Incapacitation Index for 100 Grain, Caliber .357, JHP, JHC Bullets. . . . .	87
40. Relative Incapacitation Index for 110 Grain, Caliber .357, JSP Bullets . . . . .	88
41. Relative Incapacitation Index for 110 Grain, Caliber .357, JHP, JHC Bullets. . . . .	88
42. Relative Incapacitation Index for 125 Grain, Caliber .357, JSP, JFP Bullets. . . . .	89
43. Relative Incapacitation Index for 125 Grain, Caliber .357, JHP, JHC Bullets. . . . .	89
44. Relative Incapacitation Index for 140 Grain, Caliber .357, JHP Bullets . . . . .	90
45. Relative Incapacitation Index for 146 Grain, Caliber .357, JHP Bullets . . . . .	90

LIST OF FIGURES (continued)

Figure	Page
46. Relative Incapacitation Index for 148 Grain, Caliber .357, WC Bullets. . . . .	91
47. Relative Incapacitation Index for 150 Grain, Caliber .357, L, LRN, RN Bullets. . . . .	91
48. Relative Incapacitation Index for 150 Grain, Caliber .357, JSP, JFP Bullets. . . . .	92
49. Relative Incapacitation Index for 150 Grain, Caliber .357, JHP, JHC Bullets. . . . .	92
50. Relative Incapacitation Index for 158 Grain, Caliber .357, L, LRN, RN Bullets. . . . .	93
51. Relative Incapacitation Index for 158 Grain, Caliber .357, SWC Bullets . . . . .	93
52. Relative Incapacitation Index for 158 Grain, Caliber .357, LHP Bullets . . . . .	94
53. Relative Incapacitation Index for 158 Grain, Caliber .357, JSP, JFP Bullets. . . . .	94
54. Relative Incapacitation Index for 158 Grain, Caliber .357, JHP, JHC Bullets. . . . .	95
55. Relative Incapacitation Index for 158 Grain, Caliber .357, MP Bullets. . . . .	95
56. Relative Incapacitation Index for 185 Grain, Caliber .357, JHP Bullets . . . . .	96
57. Relative Incapacitation Index for 200 Grain, Caliber .357, L Bullets . . . . .	96
58. Relative Incapacitation Index for ALL Grain, Caliber .357, SS Bullets. . . . .	97
59. Relative Incapacitation Index for ALL Grain, Caliber .357, SSG Bullets . . . . .	97
60. Relative Incapacitation Index for 170 Grain, Caliber .410, JHP, JHC Bullets. . . . .	98

LIST OF FIGURES (continued)

Figure	Page
61. Relative Incapacitation Index for 200 Grain, Caliber .410, JHP Bullets. . . . .	98
62. Relative Incapacitation Index for 210 Grain, Caliber .410, L Bullets . . . . .	99
63. Relative Incapacitation Index for 210 Grain, Caliber .410, JSP Bullets. . . . .	99
64. Relative Incapacitation Index for 210 Grain, Caliber .410, JHP, JHC Bullets . . . . .	100
65. Relative Incapacitation Index for 220 Grain, Caliber .410, JSP Bullets... . . . .	100
66. Relative Incapacitation Index for 180 Grain, Caliber .429, JSP Bullets. . . . .	101
67. Relative Incapacitation Index for 180 Grain, Caliber .429, JHP Bullets. . . . .	101
68. Relative Incapacitation Index for 200 Grain, Caliber .429, JHP Bullets. . . . .	102
69. Relative Incapacitation Index for 225 Grain, Caliber .429, JHP Bullets. . . . .	102
70. Relative Incapacitation Index for 240 Grain, Caliber .429, SWC Bullets. . . . .	103
71. Relative Incapacitation Index for 240 Grain, Caliber .429, JSP Bullets. . . . .	103
72. Relative Incapacitation Index for 240 Grain, Caliber .429, JHP Bullets. . . . .	104
73. Relative Incapacitation Index for 170 Grain, Caliber .450, HEM1JHP Bullets. . . . .	104
74. Relative Incapacitation Index for 185 Grain, Caliber .45 , JHP Bullets. . . . .	105
75. Relative Incapacitation Index for 185 Grain, Caliber .450, WC Bullets . . . . .	106
76. Relative Incapacitation Index for 200 Grain, Caliber .450, SWC Bullets. . . . .	106

LIST OF FIGURES (continued)

Figure	Page
77. Relative Incapacitation Index for 200 Grain, Caliber .450, JHP Bullets. . . . .	107
78. Relative Incapacitation Index for 225 Grain, Caliber .450, JHP Bullets. . . . .	107
79. Relative Incapacitation Index for 230 Grain, Caliber .450, FJ, FMJ Bullets. . . . .	108
80. Relative Incapacitation Index for 230 Grain, Caliber .450, MC Bullets . . . . .	108
81. Relative Incapacitation Index for 250 Grain, Caliber .450, SWC Bullets. . . . .	109
82. Relative Incapacitation Index for 255 Grain, Caliber .450, L, LRN, RN Bullets . . . . .	109
83. Relative Incapacitation Index Computer Prediction for Lead Spheres . . . . .	110
84. Relative Incapacitation Index Computer Predictions of a .357 Caliber Bullet with $C_D = .30$ and Mass = 110 grains (Data points are 9mm, 115 and 100 grain FJ bullets). . . . .	110
85. Relative Incapacitation Index Computer Predictions for .357 Caliber Bullets with $C_D = .30$ . . . . .	111
86. Relative Incapacitation Index Computer Predictions for .357 Caliber Bullets with $C_D = .30$ and Mass = 110 grains (Data are .357, 90 grain Hemi-JSP). . . . .	111
87. Relative Incapacitation Index Computer Predictions for a .357 Caliber Bullets with $C_D = .37$ and Mass = .125 grains. . . . .	112
88. Relative Incapacitation Index Computer Predictions for a .357 Caliber Bullets with $C_D = .37$ and Mass = 158 grains (Data are .357, 158 Grain LRN Bullets). . . . .	112
89. Relative Incapacitation Index Computer Predictions for a .357 Caliber Bullets with $C_D = .45$ and Mass = 110 grains. . . . .	113

LIST OF FIGURES (continued)

Figure	Page
90. Relative Incapacitation Index Computer Predictions for a .357 Caliber Bullets with $C_D = .45$ and Mass = 125 Grains (Data are .357, 125 Grain JSP Bullets). . . . .	113
91. Relative Incapacitation Index Computer Predictions for a .357 Caliber Bullets with $C_D = .45$ and Mass = 158 Grains (Data are .357, 158 Grain JSP Bullets). . . . .	114
92. Relative Incapacitation Index Computer Predictions for a .357 Caliber Bullets with $C_D = 1.20$ . . . . .	114
93. Relative Incapacitation Index Computer Predictions for a .357 Caliber Bullets with $C_D = .45$ and Mass = 158 Grains (Data are .357, 148 Grain WC Bullets) . . . . .	115
94. Relative Incapacitation Index Computer Predictions for a .45 Caliber Bullets with $C_D = .30$ . . . . .	115
95. Relative Incapacitation Index Computer Predictions for a .45 Caliber Bullet with $C_D = .45$ and Mass = 230 Grains (Data are .45, 230 Grain Bullets) . . . . .	116
96. Relative Incapacitation Index Computer Predictions for a .45 Caliber Bullet with $C_D = .37$ . . . . .	116
97. Relative Incapacitation Index Computer Predictions for a .45 Caliber Bullet with $C_D = .37$ and Mass = 230 Grains (Data are .45, 255 Grain LRN Bullets) . . . . .	117
98. Relative Incapacitation Index Computer Predictions for a .45 Caliber Bullet with $C_D = .45$ . . . . .	117
99. Relative Incapacitation Index Computer Predictions for a .45 Caliber Bullet with $C_D = 1.20$ . . . . .	118
100. Comparison of a Measured Cavity Contour for a .357, 158 Grain JSP Bullet at 372 m/s Velocity and Model Generated Cavity Contour for a Similar Non-Deforming Bullet. . . . .	118
101. Effect of Engagement Range of the Relative Incapacitation Index. . . . .	119

LIST OF FIGURES (continued)

Figure	Page
102. Effect of Shooter Accuracy on Relative Incapacitation Index. (Good = Group B Shooters; Average = Group A Shooters). . . . .	119
103. Effect of Aim Point on Relative Incapacitation Index (Group A Shooters) . . . . .	120
104. Effect of Aim Point on Relative Incapacitation Index (Group B Shooters) . . . . .	121
105. Relationship Between Probability of Instant Incapacitation and Relative Incapacitation Index . . . . .	122
106. Relationship Between Energy Deposit and Relative Incapacitation Index . . . . .	122
107. Relationship Between Hatcher's Formula and Relative Incapacitation Index . . . . .	123
108. Instogram of Bullet Fragmentation on Ricochet. . . . .	123
109. Effect of Impact Angle and Velocity on Bullet Breakup. . . . .	124
110. Safety Range for Lead Fragments. . . . .	124
111. Safety Range for Bullet Jacket Fragments . . . . .	125
112. Impact of a .357 Magnum, 125 grain, JHP Bullet Against 1/8 inch Plate Glass. Velocity - 284 mps (933 fps). . . . .	126
113. Impact of a .357 Magnum, 125 grain, JHP Bullet Against 1/8 inch Plate Glass. Velocity - 194 mps (637 fps). . . . .	127
114. Impact of a .357 Magnum, 125 grain, JHP Bullet Against 1/8 inch Plate Glass. Velocity - 270 mps (887 fps). . . . .	128
115. Impact of a .357 Magnum KTW Metal Piercing Bullet Against 1/4 inch Laminated Glass. Velocity - 644 mps (2114 fps) . . . . .	129
116. Impact of a .357 Magnum, 125 grain, JHP Bullet Against 1/4 inch Laminated Glass. Velocity - 205 mps (674 fps). . . . .	130
117. Impact of a .357 Magnum Safety Slug Against 1/4 inch Laminated Glass. Velocity - 601 mps (1972 fps). . . . .	131
118. Impact of a .41 Magnum, 170 grain, JHP Bullet Against 1/4 inch Laminated Glass. Velocity - 350 mps (1151 fps). . . . .	132

## LIST OF TABLES

Table	Page
I. Sedov's Ricochet Parameters. . . . .	133
II. Sample Scan Output. . . . .	134
III. Vulnerability Index Parameters . . . . .	135
IV. RII Data for JSP, JFP, 90 Grains, .353 to .355 Caliber Bullets. . . . .	136
V. RII Data for FJ, 100 Grains, .353 to .355 Caliber Bullets. . . . .	137
VI. RII Data for PP, 100 Grains, .353 to .355 Caliber Bullets. . . . .	138
VII. RII Data for JSP, JFP, 100 Grains, .353 to .355 Caliber Bullets. . . . .	139
VIII. RII Data for JHP, JHC, 100 Grains, .353 to .355 Caliber Bullets. . . . .	140
IX. RII Data for FJ, 115 Grains, .353 Caliber Bullets. . . . .	141
X. RII Data for PP, 115 Grains, .353 to .355 Caliber Bullets. . . . .	142
XI. RII Data for JHP, JHC, 115 Grains, .353 to .355 Caliber Bullets. . . . .	143
XII. RII Data for FJ, 124 Grains, .353 to .355 Caliber Bullets. . . . .	144
XIII. RII Data for RN, 125 Grains, .353 to .355 Caliber Bullets. . . . .	145
XIV. RII Data for JSP, 125 Grains, .353 to .355 Caliber Bullets. . . . .	146
XV. RII Data for JSP, JFP, 90 Grains, .357 Caliber Bullets. . . . .	147
XVI. RII Data for HEMIJSP, 90 Grains, .357 Caliber Bullets. . . . .	148

LIST OF TABLES (continued)

Table	Page
XVII. RII Data for MP, 90 Grains, .357 Caliber Bullets. . . . .	149
XVIII. RII Data for JHP, 95 Grains, .357 Caliber Bullets. . . . .	150
XIX. RII Data for JHP, JHC, 100 Grains, .357 Caliber Bullets. . . . .	151
XX. RII Data for JSP, 110 Grains, .357 Caliber Bullets. . . . .	152
XXI. RII Data for JHP, JHC, 110 Grains, .357 Caliber Bullets. . . . .	153
XXII. RII Data for JSP, JFP, 125 Grains, .357 Caliber Bullets. . . . .	156
XXIII. RII Data for JHP, JHC, 125 Grains, .357 Caliber Bullets. . . . .	157
XXIV. RII Data for JHP, 140 Grains, .357 Caliber Bullets. . . . .	159
XXV. RII Data for JHP, 146 Grains, .357 Caliber Bullets. . . . .	160
XXVI. RII Data for WC, 148 Grains, .357 Caliber Bullets. . . . .	161
XXVII. RII Data for L, LRN, RN, 150 Grains, .357 Caliber Bullets. . . . .	162
XXVIII. RII Data for JSP, JFP, 150 Grains, .357 Caliber Bullets. . . . .	163
XXIX. RII Data for JHP, JHC, 150 Grains, .357 Caliber Bullets. . . . .	164
XXX. RII Data for L, LRN, RN, 158 Grains, .357 Caliber Bullets. . . . .	165
XXXI. RII Data for SWC, 158 Grains, .357 Caliber Bullets. . . . .	166

LIST OF TABLES (continued)

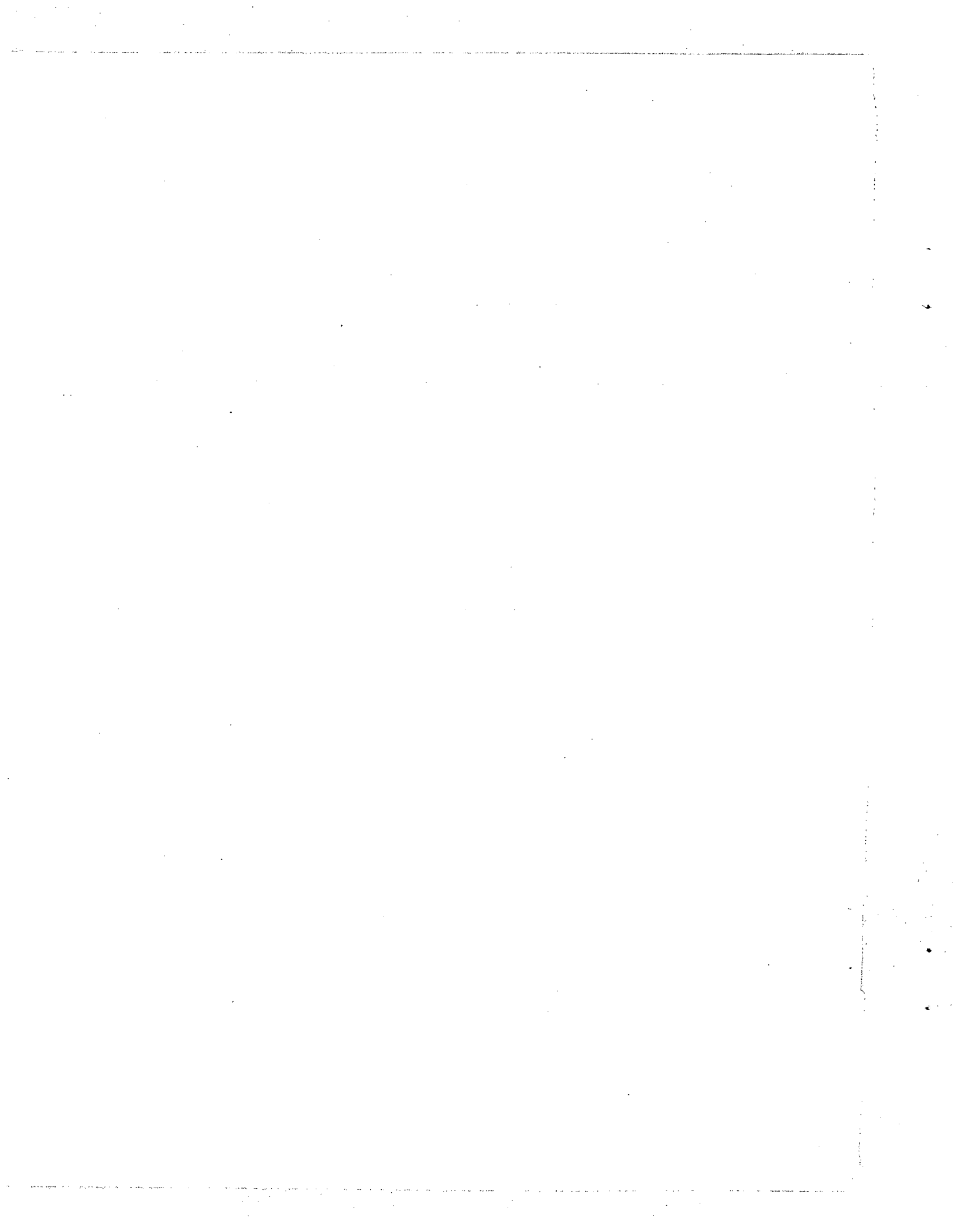
Table	Page
XXXII. RII Data for LHP, 158 Grains, .357 Caliber Bullets. . . . .	167
XXXIII. RII Data for JSP, JFP, 158 Grains, .357 Caliber Bullets. . . . .	168
XXXIV. RII Data for JHP, JHC, 158 Grains, .357 Caliber Bullets. . . . .	170
XXXV. RII Data for MP, 158 Grains, .357 Caliber Bullets . . . . .	172
XXXVI. RII Data for JHP, 185 Grains, .357 Caliber Bullets . . . . .	173
XXXVII. RII Data for L, 200 Grains, .357 Caliber Bullets. . . . .	174
XXXVIII. RII Data for SS, All Grains, .357 Caliber Bullets. . . . .	175
XXXIX. RII Data for SSG, All Grains, .357 Caliber Bullets. . . . .	176
XL. RII Data for JHP, JHC, 170 Grains, .41 Caliber Bullets. . . . .	177
XLI. RII Data for JHP, 200 Grains, .41 Caliber Bullets. . . . .	178
XLII. RII Data for L, 210 Grains, .411 Caliber Bullets. . . . .	179
XLIII. RII Data for JSP, 210 Grains, .41 Caliber Bullets. . . . .	180
XLIV. RII Data for JHP, JHC, 210 Grains, .41 Caliber Bullets. . . . .	181
XLV. RII Data for JSP, 220 Grains, .41 Caliber Bullets. . . . .	182
XLVI. RII Data for JSP, 180 Grains, .427 to .429 Caliber Bullets. . . . .	183

LIST OF TABLES (continued)

Table	Page
XLVII. RII Data for JHP, 180 Grains, .429 Caliber Bullets. . . . .	184
XLVIII. RII Data for JHP, 200 Grains, .429 Caliber Bullets. . . . .	185
XLIX. RII Data for JHP, 225 Grains, .427 to .429 Caliber Bullets. . . . .	186
L. RII Data for SWC, 240 Grains, .427 to .429 Caliber Bullets. . . . .	187
LI. RII Data for JSP, 240 Grains, .427 to .429 Caliber Bullets. . . . .	188
LII. RII Data for JHP, 240 Grain, .429 Caliber Bullets. . . . .	189
LIII. RII Data for HEMIJHP, 170 Grains, .45 Caliber Bullets. . . . .	190
LIV. RII Data for JHP, 185 Grain, .45 Caliber Bullets. . . . .	191
LV. RII Data for WC, 185 Grains, .45 to .454 Caliber Bullets. . . . .	192
LVI. RII Data for SWC, 200 Grains, .45 to .454 Caliber Bullets. . . . .	193
LVII. RII Data for JHP, 200 Grains, .45 to .454 Caliber Bullets. . . . .	194
LVIII. RII Data for JHP, 225 Grains, .45 to .454 Caliber Bullets. . . . .	195
LIX. RII Data for FJ, FMJ, 230 Grains, .45 to .454 Caliber Bullets. . . . .	196
LX. RII Data for MC, 230 Grains, .45 to .454 Caliber Bullets. . . . .	197
LXI. RII Data for SWC, 250 Grains, .45 to .454 Caliber Bullets. . . . .	198

LIST OF TABLES (continued)

Table	Page
LXII. RII Data for L, LRN, RN, 225 Grains, .45 to .454 Caliber Bullets. . . . .	199
LXIII. Effective Coefficients for Typical Bullet Shapes Assuming No Perforation. . . . .	200
LXIV. Matrix of Nondeforming Projectiles Examined with the Cavity Model. . . . .	205



## I. INTRODUCTION

Pistols and revolvers are used primarily as personal defense weapons. Every law enforcement officer may at some time in his life depend on these type weapons for his safety. As the number of encounters between the law enforcement officer and felon has increased in recent years police officers are becoming increasingly concerned with the effectiveness or stopping power of their side arms. They are concerned primarily with the ability of this weapon to immediately render an assailant incapable of further aggressive acts. Clinical lethality, i.e., death, is not of interest per se. Any handgun is capable of inflicting a fatal wound; but many handguns do not possess sufficient stopping power, that is, the ability to put the assailant out of the fight instantly. A typical example of this is the "lowly" .22 caliber rimfire cartridge. It is perhaps one of the most "deadly" cartridges in history. More people, by number, have been killed by this bullet than any other in the civilian community, however, its ability to instantly incapacitate is relatively small.

If all bullets are highly lethal, why is the law enforcement community so concerned with stopping power? The officer is working under a very stringent limitation on the use of his weapon which arises from two basic constraints: (1) he can use his weapon only in a "last ditch" situation, that is, his life is in immediate jeopardy and all other alternatives have been exhausted, and (2) experience has shown that the average engagement range is approximately six meters (21 feet). When his weapon is used in this situation, he cannot wait hours or even minutes for death or complete incapacitation to eventually occur. At such short distances, this is far too long because of the immediate threat to his life. Incapacitation must be near instantaneous with a well placed shot.

A number of theories on the subject have been proposed over the years. Perhaps the most well known is the Hatcher theory.<sup>1</sup> General Hatcher, in 1935, proposed that stopping power was proportional to the bullet's impact momentum times its cross-sectional area. In 1960, and later in 1969, the U.S. Army advanced the theory that incapacitation was a function of the kinetic energy deposited in 15 centimeters of gel tissue simulant.<sup>2</sup> More recently, De Maio has applied this kinetic

---

<sup>1</sup>Hatcher, J.S., *Textbook of Firearms Investigation, Identification and Evidence*, Small Arms Technical Publishing Company, 1935.

<sup>2</sup>Sturdivan, L., Bruckey, W., Wyman, D., "Terminal Behavior of the 5.56mm Ball Bullet in Soft Targets", *Ballistic Research Laboratory Report 1447*, August 1969.

theory to handgun effectiveness by utilizing a ballistic pendulum.<sup>3</sup>

Each of these theories on stopping power have certain shortcomings. Hatcher's theory is based only on the striking conditions of the bullet, i.e., its mass, velocity, and caliber. It considers that a bullet striking anywhere on the body with a fixed set of parameters will produce the same stopping power. The kinetic energy deposit theory is an advancement over the Hatcher theory. It considers that only the portion of the bullet's energy left in the assailant is capable of effecting stopping power. Its primary drawback is that energy deposited anywhere in the body is equally important, and like the Hatcher theory, it considers any hit on the body to be equally important. Where then can the law enforcement community obtain more complete and objective information necessary to make the correct choice of handgun ammunition? What are the factors effecting stopping power? To what extent does increasing stopping power also increase hazards to innocent bystanders relative to over-penetration and ricochet?

In December 1972, the National Institute of Law Enforcement and Criminal Justice of the Law Enforcement Assistance Administration approved and funded a project, submitted by the Law Enforcement Standards Laboratory (LESL) of the National Bureau of Standards, to conduct a study of the terminal effects of police handgun ammunition. LESL late in 1973 contracted with the U.S. Army Ballistic Research Laboratory (BRL) to conduct the study and prepare a report of its findings. The purpose of the study was to provide federal, state, and local law enforcement agencies with a criteria for use in selection of handgun ammunition. The criteria would consider not only the offensive capabilities of the ammunition, but also the safety factors concerning innocent bystanders. The purpose was not to refute or invalidate studies by previous investigators were wrong but to bring the salient features of these previous studies together with a more detailed and updated description of the entire scenario in order to produce a unified approach to the problem which would allow an objective evaluation of handgun effectiveness.

## II. TERMINOLOGY

Relative Stopping Power, RSP - A descriptive term used in contemporary literature to indicate the relative ability of a shot to render an adversary instantly incapable of further aggression. For the purpose of this report, the terms Relative Stopping Power and Instant Incapacitation will be used interchangeably.

---

<sup>3</sup>De Maio, V.J.M., et al, "Comparison of Wounding Effects of Commercially Available Ammunition Suitable for Police Use", FBI Law Enforcement Bulletin Volume 43, No. 12, 1974.

Instant Incapacitation - Immediately after penetration by a kinetic energy projectile, an adversary must be incapable of posing a threat to the safety of a law enforcement officer by means of a hand-held weapon. Instant Incapacitation may mean clinical death, unconsciousness, biomechanical dysfunction, etc. Pain is not considered a deterrent to continued aggression.

Velocity - The speed of the bullet. Unless specified otherwise, velocity refers to the bullet velocity just prior to impact.

Mass - The quantity of matter in a body. The mass of a bullet is determined by dividing its weight by the acceleration of gravity.

Kinetic Energy - The energy which the bullet possesses as a consequence of its motion. It is equal to one-half the product of its mass and the square of its velocity.

Kinetic Energy Deposit - That portion of a bullet's energy which is lost as a result of penetration of a material. Total Kinetic Energy Deposit is not necessarily equal to the Kinetic Energy before penetration.

Momentum - That property of a moving bullet equal to the product of mass and velocity.

Bullet - The projectile shot from a rifle or handgun.

Calibre - The diameter of a bullet or other projectile in decimals of an inch or in millimeters.

Cartridge - A complete unit of ammunition.

Point of Aim - That point with which a firearm's sights are aligned.

Point of Impact - That point which a bullet strikes.

Pressure - Force per unit area.

Vulnerability Index,  $V_I$  - A measure of the relative importance of body tissue to stopping power along the path the bullet travels through the body.

Relative Incapacitation Index, RII - The measure of relative stopping power. It takes into account the size and shape of the maximum temporary wound cavity and the likelihood this wound tract will encounter vital organs.

Maximum Temporary Cavity (MTC) - The size and shape of the near instantaneous distention of the tissue simulant caused by bullet penetration. The MTC is often many times the size and shape of the permanent hole left in the simulant.

Ricochet - The skipping or rebounding of a bullet after striking a surface at some angle.

Ricochet Angle - The angle of incidence of a bullet which ricochets from a surface as measured from a perpendicular to the surface.

### III. METHODOLOGY

Any selection of police handgun ammunition for duty use must be made with due regard to the effectiveness against the criminal as defined by maximum stopping power and maximum safety to citizens. This choice may be a seemingly simple one for the patrolman, that is, continual escalation to more powerful weapons, but it is actually a very complex problem which also must be dealt with by the particular law enforcement and local government agency involved. These agencies must consider every effect which a change of duty ammunition may have on the community at large. Among the many factors which have entered into this decision in the past have been personnel preference, tradition, department or local government policy, advertised ammunition performance and public pressure. Influencing many of these factors have been the numerous published articles which have evaluated particular handgun cartridges in terms of muzzle velocity, muzzle energy, muzzle drop, momentum, range, sectional density, ballistic co-efficient, bullet expansion, relative stopping power according to one or another formula or test method, penetration, ricochet, and other fragments. In the past, the solution to the problem has not always been based on an objective technical approach.

To place the question of handgun effectiveness on the level of an objective approach, that is, as an input into the general problem of weapon/ammunition selection, three primary terminal characteristics of handgun ammunition had to be addressed in this study.

1. Relative incapacitation of human targets, (i.e., relative stopping power).
2. Ricochet hazards.
3. Material penetration characteristics.

The focus of this study was on commercially available handgun ammunition in the caliber range from .355 (9mm) through .45. For the purpose of analysis and discussion, the program was broken into two parts; relative stopping power and hard target performance, each of which is described separately in the following sections.

#### A. Relative Stopping Power (RSP)

Perhaps the primary drawback in past studies relating to RSP has been a lack of detailed consideration of all the factors which could effect the RSP. Hatcher, for example, considered RSP to be a function of only four variables: mass, impact velocity, presented area and shape factor. The U.S. Army, and later De Maio, "black boxed" RSP by lumping all the parameters into one, the deposited energy. The present study expands on both of these through investigation of the effects of the following:

1. Shape
2. Velocity
3. Mass
4. Caliber
5. Construction
6. Aim Point
7. Aiming Error

The methodology employed integrates these parameters into a single measure of effectiveness which incorporates a system analysis approach to relative stopping power. Figure 1 shows a flow chart of the methodology used to accomplish this task.

The core of this effort is the BRL Computer Man,<sup>4</sup> i.e., the target. The Computer Man is an elaborate three-dimensional computer code of the human anatomy. It consists of volume elements of the body of a man in the form of rectangular parallepipeds approximately 5mm x 5mm x 25mm in size. A frontal view of the Computer Man, depicting the horizontal sectioning of the body, as he would "appear" in the computer, is shown in Figure 2. Within each of these volume elements, the predominant tissue type was identified and coded. For the purpose of this study, each of these volume elements was assessed by a team of medical doctors from the University of Maryland Shock Trauma Unit<sup>5</sup> as to its relative importance to stopping power and as such were called injury criteria component vulnerability numbers.

The assessment by the medical doctors was based on a probable situation in which an officer would employ his weapon. That is, the officer is at a decided disadvantage. He cannot indiscriminately employ his weapon against a felon. He must be certain that one of two situations exist: (1) his life is in immediate jeopardy, or

<sup>4</sup>Stanley, C.H., Brown, M., "A Computer Man Model", *Ballistic Research Laboratory Report ARBRL-TR-02060*, May 1978.

<sup>5</sup>U.S. Army Contract DAAD05-75-6-0730.

(2) the lives of others are in immediate jeopardy by the felon. In either case, the officer must wait until the last possible moment to use his weapon to ensure his own safety and that of others. Additionally, the engagement ranges at which many encounters occur is very short, often on the order of a few meters. In this situation, the officer cannot wait hours, minutes, or even 30 seconds for incapacitation to occur. What is desired is a weapon which, with a well placed shot, will render the felon immediately noncombatant, i.e., instantly incapacitated.

Within this framework, the doctors were presented with the following scenario:

An armed felon has been placed in a situation where he feels that only an act of aggression on his part will prevent the loss of his life or that his freedom can be gained only through a violent action directed at the law enforcement officer. The felon is armed with some type of hand-held lethal weapon (pistol, knife, club, brick, etc.) and is being approached by the officer. In this situation the officer must administer an instantaneous incapacitating injury to the felon.

Each doctor was then asked to rank each volume element of the Computer Man as to its overall importance with regards to instant incapacitation. A top view of a typical horizontal cross-section showing the numerically ranked volume elements through a shoulder section of the Computer Man is depicted in Figure 3. The numerical scores range from 0 to 10; that is, they range from no importance to one of extreme importance relative to instant incapacitation. The complete set of these numbers, called component vulnerability numbers, results in a three-dimensional mapping of the human body in terms of its importance to stopping power. However, what is really required of a bullet which produces a known distribution of damage along a wound tract is the average relative importance of the tissue affected because, for any given weapon, shooter, or ammunition combination, the different areas of the body do not have equal likelihood of being hit. For example, when a police officer aims at the center of mass of the felon, he is not likely to shoot him in the left foot. To account for this effect, a hit distribution characterizing the ability of a shooter/weapon/ammunition combination to place a well aimed shot is combined with the Computer Man.

This spatial distribution of possible trajectories for the bullets is obtained once the engagement range and standard deviation of shots about the aim point have been determined. Using this standard deviation or aiming error and the assumption that shots are normally distributed about the aim point, Monte Carlo sampling techniques

are used to determine the directions and impact points for a set of "shots fired" at the Computer Man. That is, the computer simulates the trajectories fired by the shooter and traces them through the body.

As these trajectories are being traced, the computer keeps track of the relative importance of the body at each increment of penetration. A resultant average component vulnerability for any typical hit distribution, called the Vulnerability Index ( $V_T$ ), which the bullet "sees" as it traverses the body, is then generated. It should be noted at this point that the model is attempting to simulate what the bullet sees "on the average" as it penetrates the body because a police officer under stress may miss his intended target or not score a hit at the optimal location on the body. The model takes this into account because whenever a "shot" misses the Computer Man, zeros are used for the component vulnerability numbers along the whole trajectory. The result is that the final determination of stopping power is dependent on the ability of the office to place a well aimed shot.

It is important to note that at this point no mention has been made of the bullet (i.e., its mass, velocity, shape, construction, or caliber). Only the trajectories along which the bullets move have been mentioned. This is intentional and, as will be apparent later, allows for inclusion of the shooter/weapon effects independent of bullet design. Thus, trade-off studies in both areas can be conducted independently to provide an optimal stopping power solution for a given situation.

Returning to the Flow Chart in Figure 1, one can observe that the effects of bullet design are also considered in the methodology. The Vulnerability Index tells us the importance of tissue along the average wound trajectory. What is needed now in the model is a method for quantifying the mechanical damage produced by the bullet as it penetrates the body. However, before outlining the method for describing the mechanical damage as a function of depth of penetration into the body by a given bullet, a simulant material must first be chosen for comparing one bullet to another. That the human body is a highly complex structure goes almost without saying. It is a composite of many tissue types and shapes all separated by various configurations of interface surfaces. Additionally, the "toughness" of tissue varies from animal to animal and tissue type to tissue type. To describe in detail the exact equations of motion for the bullet passing through these structures and the response of each tissue type and interface would be a near insurmountable task. Recall that what we are trying to do is to generate a measure of expected damage and here the emphasis is on measure. We are not trying to predict physiological response of the individual but of the average. For the purpose of this methodology then it was assumed that the body material is homogeneous and can be approximated by 20 percent gelatin (20 percent gelatin, 80 percent water by weight).

The choice of 20 percent gelatin as the target material rather than another simulant is based on many previous experiments from which the following was established:

1. The similarity between bullet retardation in gelatin and animal tissue.
2. The similarity between the size and shape of the temporary cavity in gelatin and tissue.
3. The similarity between the permanent cavity remaining in tissue and gelatin after the passage of a bullet.
4. The homogeneity/reproducibility of the gelatin response to bullet penetration.

Comprehensive wound ballistics experiments in the 1940's and 1950's established that trauma such as bone fracture, hemorrhage and nerve damage could occur beyond the permanent wound tract of complete tissue maceration. By 1962, when the U.S. Office of the Surgeon General published a treatise on wound ballistics,<sup>6</sup> the mechanism of kinetic energy wounding was generally accepted to be cavitation. The basic idea, as illustrated in Figure 4, is that as the bullet penetrates soft tissue it cuts and tears tissue directly in its path. In addition, the bullet transfers some of its momentum to the neighboring tissue setting it in motion radially outward. This outward motion can be thought of as rings of tissue expanding about the projectile path. Often this expansion severely stretches or tears the tissue and trauma results. Experimental evidence has shown that the rate at which bullets transfer momentum to the surrounding tissue as a function of penetration distance is very similar to that observed in gelatin. This can be seen in Figure 5 which compares the maximum temporary cavity, MTC, formed in animal tissue and a momentum transfer model which was used to predict the MTC. The law of penetration for soft tissue has been shown to be the same as the law for gelatin, based on the observation that projectile penetration into both materials exhibit comparable retardation. This is due primarily to the fact that both 20 percent gelatin and animal tissue are of about the same density (both gelatin and animal tissue are approximately 80 percent water by weight).

It has been shown for the wounding mechanism of cavitation that the strains are monotonic functions of tissue displacement. Consequently, the extent of tissue failure is a monotonic function of maximum tissue displacement. This maximum displacement corresponds to the envelope of the maximum temporary cavity. Hence, the maximum

---

<sup>6</sup>"Wound Ballistics", Office of the Surgeon General, 1962.

temporary cavity envelope can be interpreted as a relative measure of a bullet's capacity to do damage as a function of penetration. This temporary cavity explains the so-called explosive effects often noted with high velocity and deforming bullets. It is in this explosive effect which differentiates high velocity or deforming bullets from low velocity, non-deforming bullets. One of the earliest and still more popular theories was that this effect was connected with a shock wave generated on bullet impact. However, this wave moves through the tissue at a rate of approximately 1250 m/sec (4100 ft/sec) with very small associated particle displacements and is well beyond the wound region before the temporary cavity expansion occurs. The same type response is observed in gelatin.

The crucial missing link which allows the use of gelatin as a tissue simulant is the quantitative correspondence between the easily observed temporary cavities formed in gelatin and the temporary cavities formed in tissue. During the conduct of this study, experimental data were obtained to show the correspondence between the cavities in the two materials. Figure 6 shows the contour of the maximum temporary cavity (MTC) formed in gelatin and animal tissue for a 6.35mm (.25 inch) diameter sphere. The data points correspond to measurements of maximum radius of expansion as measured using a multi-flash x-ray system. As seen in this figure, the gelatin data closely follows that for tissue. The differences are due to the fact that tissue samples were not as thick as the gelatin samples.

The above reasons for the use of gelatin are not meant to imply that it is the only material which could be used to simulate tissue. There well may be other viscoelastic materials which simulate the response of tissue as well. Materials such as clay, sand, soap, and telephone books do not fall into this category and while they may simulate one aspect of the penetration/response phenomena, they are not viscoelastic in nature and do not simulate the overall characteristics of penetration as well as gelatin. Additionally, even though there may be other materials which may do as well as gelatin, another reason for perpetuating its use is the massive data bank compiled for different projectiles over the years. By using the same material, a direct comparison between any projectiles previously evaluated and any new projectiles is possible.

Once the target material has been chosen, it must be determined how the projectile characteristics affect formation of the MTC. The purpose here was to investigate the effects of projectile geometry or shape, caliber, orientation on impact and during penetration, construction, and how it effects break-up and deformation and lastly, the effect of changing striking velocity. In the general problem where all of these effects may be present they will not be independent of one another.

Because of the complexity of the general problem an experimental approach was used. The experimental information on the penetration behavior of the bullets was organized to allow assessments based on manufacturer, type construction, mass, caliber, and velocity of the bullet or any desired combination of these factors.

This was accomplished by observing the bullet behavior, i.e., deformation rate of slow down, tumbling, etc. during penetration of the gelatin by means of high-speed photography and flash x-rays. The details of these experiments will be described later. Also to be described later is an analytical model which permits the computation of the MTC and Relative Incapacitation Index for rigid non-tumbling bullets. Many observers consider this class of bullet as an attractive alternative to deforming bullets. This model permits one to parametrically study the effects of shape, caliber, mass, velocity, and density of the bullet. This includes all full-jacket and metal piercing bullets and all lead bullets at velocities less than 240m/s.

With the two inputs, MTC and the Vulnerability Index, we now have the pieces necessary to provide a figure of merit for a shooter/weapon/ammunition combination: average vulnerability of the body versus depth of penetration and damage versus depth of penetration. The convolution of these two functions yields a single number for the measure of effectiveness defined as the Relative Incapacitation Index, RII. That is, the vulnerability function is used as a weighting function in the calculation of wound volume to indicate the relative importance of causing damage at a given depth of penetration. Computationally, this is accomplished by taking each small increment of cavity volume and multiplying it by the Vulnerability Index at the corresponding depth of penetration. The sum of all these weighted volume increments is the RII. The actual formula for calculating the RII is:

$$RII = \int_{x=0}^{x = \text{max penetration depth}} \pi \cdot R^2(x) \cdot V_I(x) dx,$$

where,  $R(x)$  is the cavity envelope radius and  $V_I(x)$  is the Vulnerability Index at a penetration depth of  $x$  as shown in Figure 7. It is this weighted volume of damage or RII which is used as the figure of merit for a hit distribution/projectile combination. The RII then is the measure of relative stopping power.

## B. Ricochet and Penetration Performance

The penetration/ricochet interface for handgun bullets occurs in the case of relatively thin targets. Typical targets which fall into this class are passenger cars and other similar vehicles, interior building structures, wood or plastic walls, glass windows, signs and other non-load bearing structures to be found in both rural and urban environments. The primary interest in this study was to investigate the penetration/ricochet hazard in terms of the potential risk to bystanders caused by unspent bullets shot during a fire-fight.

For the type projectiles and targets involved, projectile penetration is controlled by local impact effects without involvement of bending or gross structural failure. Roughly speaking, this occurs when the time required for the projectile to penetrate the target is small compared with the time for a bending wave to reach the nearest support member. At normal ordnance velocities for handgun bullets, the force resisting penetration is proportional to the density of the target material, its shear resistance and the density of the projectile itself. The mass and velocity of the major projectile fragments after penetration controls the hazard to bystanders caused by penetration. The resultant equation for residual velocity after penetration is a function of impact velocity, impact angle, mass, construction and caliber for each material as well as the other parameters mentioned above.

One of the earlier and most complete analytical treatments of ricochet is provided by Sedov in the study of water impact by seaplanes. Sedov found that the significant parameters in non-dimensional form governing ricochet to be eleven in number, as shown in Table I. Clearly, the current handgun ricochet problem excludes some of these parameters and adds others. The last three parameters are most important to water ricochet and are not important at all in ricochet from solid targets. In order to obtain a scientifically based characterization of handgun ammunition at the level of sophistication shown in Sedov's work one would have to carefully measure at least the necessary variables to evaluate the first eight parameters in Table I. The criteria chosen as the measure of the hazard to bystanders was the minimum velocity for penetration of the skin. The rationale being that any bullet or fragment having sufficient mass and velocity to penetrate the skin had the potential to produce a serious wound.

## IV. EXPERIMENTAL TECHNIQUES

Laboratory investigation of significantly different handgun bullets in the caliber range 9mm to .45, which were currently available to law enforcement agencies in the United States, was conducted. These experiments included the following:

a. A determination of each bullet's behavior on striking and penetrating ordnance gelatin, as a function of its impact velocity.

b. Measurement of the formation and subsequent development of the temporary cavity produced in the gelatin by each projectile, using high-speed motion pictures.

c. Measurement of the dynamic behavior of each bullet as it penetrated the gelatin, i.e., its stability and deformation, using flash x-ray photography.

d. Measurement of the impact velocity of factory-loaded ammunition corresponding to each bullet under study, when fired from various handguns currently used by law enforcement agencies.

e. Measurements designed to determine the ricochet and penetration potentials of each bullet, as a function of angle of incidence and velocity, when striking various common materials.

Details of the experimental techniques, tissue simulant preparation and data reduction technique can be found, along with the data gathered for each test round, in the following documents:

a. "Ammunition For Law Enforcement: Part II, Data Obtained for Bullets Penetrating Tissue Simulant", W. Bruchey, et. al., Ballistic Research Laboratory Report No. 1940, 1976.

b. "Ammunition For Law Enforcement: Part III, Photographs of Bullets Recovered After Impacting Tissue Simulant", W. Bruchey, et. al., Ballistic Research Laboratory Memorandum Report No. 2673, 1976.

The ammunition used in this study consisted primarily of hand loaded cartridges in calibers .9mm through .45. Bullet velocities were adjusted such that striking velocities varied nominally between 120 m/sec (400 ft/sec) and 700 m/sec (2300 ft/sec). The bullets were obtained from commercial manufacturers within the United States. All weights and type bullets either available from or supplied by these manufacturers were evaluated. The manufacturers were chosen such that the vast majority of bullets used in commercial handgun cartridges could be evaluated. The actual bullet manufacturers considered were:

1. Winchester-Western
2. Remington-Peter
3. Super Vel
4. Smith & Wesson
5. High Precision
6. Zero
7. Hornady
8. Sierra

9. Speer
10. Glaser
11. MB Associates
12. KTW

Obviously, the above list does not include all manufacturers of ammunition for two reasons. First, many manufacturers use the above bullets in their loaded cartridges and differences in stopping power would only depend on velocity, and second, this list comprises over 90 percent of the bullets available on the market. Concurrence in using the above list was given by the LESL project officer.

For the actual gelatin firings, typical police handguns were not used. Since one of the more important parameters under investigation was the effect of bullet velocity on stopping power, it was necessary to examine velocity levels below and well above those experienced from standard cartridges from standard weapons. In the case of high velocity testing, chamber pressures exceeded those permissible in standard handguns. For safety, then, Mann test barrels were used. At this point it should be noted that even though stopping power results will be presented up to velocities approaching 700 m/sec, the powder charges necessary to attain these velocities from standard handguns may be well above acceptable safety limits and should be approached with caution.

The justification for testing at non-standard velocities was manyfold. As is well documented in previous studies by many investigators, different type bullets deform differently as a function of velocity. It was the purpose of this study to develop a general criteria which requires that stopping power be known as a continuous function of velocity. To this end it was important to know the degree of degradation experienced in stopping power if lower than standard velocities are used, i.e., velocities below which deformation of the bullet occurs. Also it was important to determine if the effects of possible excess deformation or fragmentation of the bullet at higher than standard velocities enhances or degrades stopping power. Additionally, if only commercial loadings were used and stopping power was reported for these particular cartridges, future changes in loading specifications by a manufacturer to alter velocity would make the stopping power estimates of limited usefulness.

For both the determination of the ricochet/penetration characteristics and the velocity/accuracy measurements actual commercially available cartridges and handguns were used. These included the following cartridge manufacturers:

Winchester-Western  
Remington-Peters  
Super Vel  
Smith & Wesson  
3-D  
Speer  
Browning  
Federal  
Deadeye Associates  
MB Associates

A. Data Storage and Retrieval

The data gathered in this study and tabulated in the above references is stored on a Wang 2200 Computer DISK. The storage program contains extensive information on each projectile. For example, the bullets are described by manufacturer, caliber, mass and construction type such as jacketed soft point, lead round nose, etc. The experimental data stored in the computer consists of striking velocity, flash x-ray penetration versus time data, and x-ray bullet expansion measurements in gelatin. Lastly, the symmetrized cavity envelope contour as measured from high-speed movies is stored for each round. The cavity measurements were taken at approximately 5mm (6.2 inch) increments of penetration. By using the phrase "symmetrized cavity envelope" we mean the array of depths of penetration and maximum cavity radii for each depth measured. The radii are taken to be one-half of the cavity dimension which is perpendicular to the projectile path. This symmetrization procedure is justified on the basis of numerous observations. For example, in 1957, M. Kraus published x-ray pictures of temporary cavities in animal tissue showing nearly circular transverse cross-sections. This is not to imply that the permanent cavity is circular in cross-sections; in fact it is not. The reason temporary cavities are nearly circular in cross-section is based on the principle of minimization of energy for any physical system, vis. the cavity boundary seeks a configuration of minimum surface area. Furthermore, although neither the longitudinal nor transverse cross-sections for any particular cavity are exactly symmetric, the variations from symmetry occur in the nature of statistical fluctuations, and no significant trend was observed. In addition to the information stored in the computer, the BRL maintains all of the original x-ray sequences and high-speed movies on file.

A software retrieval code for the data stored on the Wang 2200 DISK was developed to aid in the analysis of the data. The retrieval program allows the user to scan all the rounds for any combination of the following:

1. Manufacturer
2. Bullet types
3. Calibers
4. Bullet masses
5. Striking velocities

Table II is an example of scan output. The rounds which satisfy a scan are saved on the DISK. The program has the capability for modifying and updating scans.

In addition to listing the scans, for a selected aim error/aim point, the RII can be calculated for each round in a scan. For this purpose each set of  $V_I$  data generated is also stored on the DISK. Another output option is plotting graphs of RII versus striking velocity with a unique plotting symbol for each manufacturer. Curve fitting and curve plotting options are also available for these graphs. Lastly, the symmetrized cavity envelope contours can be plotted for any round.

#### B. Calculation of the Relative Incapacitation Index

As described in the program methodology, the measure chosen for relative stopping power is the RII. To calculate RII each small increment of cavity volume is multiplied by the vulnerability index,  $V_I$ , at the corresponding depth of penetration. The sum of these weighted volume increments is the RII and is given by the following formula:

$$RII = \int_{x=0}^{x = \text{max penetration}} \pi \cdot R^2(x) \cdot V_I(x) dx \quad (2)$$

The data recorded for each round consists of the maximum radius of expansion of the cavity at approximately 0.5cm increments of penetration. The  $V_I$  curves were tabulated at 1cm increments of penetration. The actual calculations were performed using this digitized information and the following formula:

$$RII = \pi \cdot \sum_{x=0}^{x_{\text{max}}} R^2(x) \cdot V_I(x) \quad (3)$$

where

$x$  = depth of penetration in 1.0cm increments

$x_{\max}$  = max depth of penetration or 30cm whichever is larger

$R(x)$  = cavity radius, cm, at depth of penetration,  $x$

$V_I(x)$  = vulnerability index at a depth of penetration,  $x$

When the measured radius was not recorded at a given depth of penetration, the preceding and succeeding data points were used in interpolate for the radius at a depth,  $x$ ; i.e.,  $R(x)$ .

#### V. THEORETICAL CAVITY MODEL

When one considers the time and expense involved in procurement, testing and data reduction, it is highly desirable to have a mathematical model for relating the bullet parameters to the corresponding temporary cavity envelopes formed in gelatin. At this time a provisional model describing the cavity formation has been completed and made operational.<sup>7</sup> The basic idea of the model is illustrated in figure 8. Here the projectile is moving through the target medium along the X-axis with instantaneous velocity,  $V(Z)$ . The dynamic pressure,  $P(Z)$ , at the surface of the projectile can be represented by:

$$P(Z) = \frac{1}{2} \rho_0 C_D V^2(Z) + \sigma_0 \quad (4)$$

where  $\rho_0$  is the density of the target medium,  $C_D$  is the drag coefficient and  $\sigma_0$  is the flow stress of the target medium. The choice of the above equation is not unique but has been found to represent the "slow-down" of the bullet in the target with acceptable accuracy.

For the instant shown in Figure 8, the dynamic pressure is interpreted to be the source for a stress wave propagating spherically outward from the point  $Z$ , the instantaneous position of the bullet.

---

<sup>7</sup>Dubin, H.C., "A Cavitation Model For Kinetic Energy Projectiles Penetrating Gelatin", Ballistic Research Laboratory Memorandum Report No. 2423, December 1974.

Consider an arbitrary observation point, Q. The local stress at Q,  $P_Q$ , due to the spherical wave originating at Z can be represented by:

$$P_Q = P(Z) e^{-R/\lambda} (1/R) \quad (5)$$

The factor  $(1/R)$  is the geometric attenuation for the amplitude of a spherical wave, where R is defined in Figure 8. The exponential factor is an empirical device to account for losses to the target medium.  $\lambda$  is an effective screening length and was determined for the gelatin material through data analysis. This screening length is characteristic of the distance the stress waves could propagate before being opposed by the medium.

The heuristic motivation for the model is based on the following:

$$\begin{aligned} \text{pressure} &= \text{impulse flux} \\ \text{force/area} &= (\text{force} \cdot \text{time}) (1/(\text{time} \cdot \text{area})) \end{aligned} \quad (6)$$

From this relation we see that integrating an impulse flux over time is the same as integrating a pressure overtime. Furthermore, if all of the impulse is delivered in a short time, one can approximate the total impulse per unit area by summing all of the pressure contributions which are present. In this way one can approximate what will be called the total "push" felt at Q with the following integral:

$$["\text{push}" \text{ at } Q] = \left[ \frac{\text{impulse}}{\text{area}} \text{ at } Q \right] \approx \int_0^{Z_Q} P(Z) \frac{e^{-R/2}}{R} dz \equiv D(Z_Q, r_Q) \quad (7)$$

In terms of the model geometry one sums all the contributions to the pressure at Q due to the dynamic pressure at the bullet from the time it enters the target until it passes by the observation point  $Z_Q$ .

This quantity is designated as  $D(Z_Q, r_Q)$ . Experimental evidence shows that very little displacement of the medium occurs until after the bullet passes by, thus, supporting the assumption of a sudden impulse.

An important restriction on the applicability of the model is that the bullet must be moving slowly enough that the outgoing stress waves do not interfere with each other. This occurs when the bullet velocities are less than Mach 0.8 in the target medium. For gelatin, the speed of sound, Mach 1.0, is comparable to that in water; about 1450 meters per second. Similarly, the speed of sound for fat tissue

has been measured to be 1440 meters per second and for muscle to be 1570 meters per second. Consequently, the model should only be applied to projectile velocities less than 1000 meters per second.

The final step in the model is to postulate the existence of a critical value of  $D(Z_Q, r_Q)$ . The value, called  $D_c$ , is the impulse of a unit area which delineates the temporary cavity envelope. This results in the following criteria for calculating the contour of the temporary cavity formed by bullet penetration:

1. If  $D(Z_Q, r_Q) > D_c$ , the point, Q, lies within the cavity envelope.
2. If  $D(Z_Q, r_Q) < D_c$ , the cavity will never advance as far as Q.
3. If  $D(Z_Q, r_Q) = D_c$ , then the point, Q, lies on the cavity boundary.

The cavity model is then of the form:

$$D_c = \int_0^{Z_Q} [P(Z) \cdot e^{-R/\lambda} / R] dZ \quad (8)$$

such that the maximum temporary cavity envelope is found by finding the locus of pairs of coordinates  $(Z_Q, r_Q)$  at which the above equation is satisfied.

To implement the cavity calculation, an expression is required for the dynamic pressure,  $P(Z)$ , as a function of penetration distance,  $Z$ . This accomplished by using equation (4):

$$P(Z) = \frac{1}{2} \rho_o C_o V^2(Z) + \sigma_o$$

which can also be written, by definition, as

$$F/A = \text{Force/Area} = P(Z)$$

$$F = P(Z) \cdot A$$

$$m \frac{d^2 Z}{dt^2} = P(Z) \cdot A$$

$$mV \frac{dV}{dZ} = P(Z) \cdot A$$

$$V dV = \frac{A}{m} P(Z) dZ$$

Integrating from the striking velocity,  $V_0$ , at penetration distance,  $Z = 0$ , to the velocity,  $V$ , at penetration distance,  $Z$ , and using equation (4) for  $P(Z)$ ,

$$\int_{V_0}^V V dV = \frac{A}{m} \int_0^Z \left[ \frac{1}{2} \rho_0 C_D V^2 + \sigma_0 \right] dZ$$

$$V^2(Z) = V_0^2 e^{-\rho_0 C_D \frac{A}{m} Z} + \frac{2\sigma_0}{\rho_0 C_D} (e^{-\rho_0 C_D \frac{A}{m} Z} - 1)$$

Substituting this expression into equation (4) results in the required expression for  $P(Z)$  as a function of  $Z$ . The cavity model then becomes:

$$D_c = \int_0^{Z_0} \left[ \frac{1}{2} \rho_0 C_D \left( V_0^2 e^{-\rho_0 C_D \frac{A}{m} Z} + \frac{2\sigma_0}{\rho_0 C_D} (e^{-\rho_0 C_D \frac{A}{m} Z} - 1) \right) + \sigma_0 \right] e^{-\frac{R}{\lambda}} \frac{dZ}{R} \quad (9)$$

where  $A$  is the presented area of the bullet and  $m$  is its mass. Values of  $C_D$  were empirically determined for bullets of different shapes and  $\sigma_0$  are listed in the results section. The numerical values of the remaining parameters are:

$$\rho_0 = 1.07 \text{ g/cc}$$

$$\tau_0 = 2470 \text{ dynes/cm}^2$$

$$D_c = 1.4 \times 10^8 \text{ dynes/cm}^2$$

$$\lambda = 3.945 \sqrt{A} \text{ cm}$$

## VI. RESULTS

### A. Effect of Aiming Error on the Hit Distribution

As stated earlier, the desired characteristic of a hit distribution model is the ability to represent the spatial distribution of possible trajectories for bullets fired from a given weapon. For small arms fire this characterization is obtained once the range is known and the standard deviation of shots about the aim point has been determined. Using these standard deviations, the assumption was made that shots are normally distributed about the aim point and horizontal and vertical miss distances are independent. Monte Carlo sampling techniques were used to determine the directions and impact points for a set of "shots fired" at the Computer Man.

The aiming error, as determined from actual impact points on a silhouette target, consists of two components; one due to the shooter and the other due to the ammunition/weapon. No attempt was made to generate experimental data on aiming errors. However, two sets of data were available from other sources. The first set of data was made available by the Human Engineering Laboratories (HEL) at APG. It consists of the aiming error as a function of range for soldiers firing the M1911A1 pistol under "stress" conditions. By "stress" conditions is meant that the soldiers, Group A, were instructed that their prime purpose was to hit a pop-up silhouette target as quickly as possible after exposure. These targets appeared in random sequences out to a range of 30 meters.

The second set of data were taken from a report prepared by the H.P. White Laboratories for the U.S. Army Land Warfare Laboratory (LWL) at APG. These tests consisted of timed fire by highly trained police officers, Group B, using .38 Special revolvers. B-21 silhouette targets were used.

The composite curves of aiming error versus range for both sets of data are shown in Figure 9. As can be seen, the Group A curve lies considerably higher than the Group B curves and the aiming error in both cases decreases with increasing range. The difference in level between the two curves is due primarily to the

test conditions since both groups were familiar with their weapons. Timed fire at an exposed silhouette target is less difficult than firing at randomly exposed targets. It is felt that the conditions experienced by Group A more closely approximate those encountered in law enforcement situations; consequently, Group A data were used as the basic hit distribution for calculations of stopping power in this study. Group B data were used to demonstrate the effects of increased shooter accuracy on stopping power.

The second factor to be observed from these two curves is that aiming error decreases as range increases. This observation is consistent with independent tests conducted in other small arms studies. Conjecture is that this phenomenon is due to the shooter taking more deliberate aim and making better use of the gun sights, especially at longer ranges; thus, as the range increases, the "point and fire" tendency of the shooter is replaced by "aim and fire."

Figures 10 through 12 show the Group A hit distribution on a silhouette of the Computer Man for random sample of 4 shots. A similar set of plots are shown based on the Group B curves in Figures 13 through 15.

In both sets of figures, the ranges correspond to the average engagement range, six meters (approximately 21 feet), and one-half and double this value. The circles and ellipses show separate regions of constant standard deviation about the aim point, denoted by the "X" in the figure. The zones correspond to:

Zone 1 - shots impacting within innermost circle or ellipse, corresponding to one standard deviation radius or less.

Zone 2 - shots impacting outside Zone 1 and less than the outermost circle or ellipse, correspond to a standard deviation of one or two.

Zone 3 - shots impacting outside Zones 1 and 2, corresponding to a standard deviation greater than two.

The purpose of presenting these figures is illustrative only. They are to give the reader a better appreciation for the locations of impact points on the Computer Man and a visual picture of the magnitude of aiming error expressed in mils. For the actual computations in the Computer Man program, the trajectories are traced through a three-dimensional target. Additionally, 10,000 "shots" were used in the actual program rather than the 4 used in the illustrations.

As stated previously, the aiming error, as depicted in Figure 9 contains contributions due to the shooter and the ammunition/weapon used. Data gathered in previous studies show that shooter error and ammunition error can be treated as statistically independent; that is, the square of the aiming error,  $\tau_t$ , is the sum of the squares of the shooter error,  $\tau_s$ , and ammunition error,  $\tau_a$ , i.e.,

$$\tau_t^2 = \tau_s^2 + \tau_a^2 \quad (10)$$

The Group A and Group B data do not indicate what part of  $\tau_t$  is due to the shooter and what part is due to ammunition. To determine the importance of  $\tau_a$  as it affects stopping power and how it varies with weapon, choice of ammunition, bullet velocity, etc., a series of tests were carried out to measure  $\tau_a$  for three variations.

The ammunition used consisted of more than 100 different types (i.e., bullet construction, manufacturer, and mass). The weapons were fired from a machine rest at paper targets (28cm x 36cm) fifteen meters away. The vertical and horizontal impact points on the target were measured from an arbitrary reference point. The standard deviation, S.D., of the shots about the center of the shot pattern was then computed. The ammunition error,  $\tau_a$ , is the standard deviation converted to mil units, i.e.,

$$\tau_a = \frac{\text{S.D. (cm)}}{\text{Range (cm)}} \times 1000 \quad (11)$$

For the over 100 different tests run, with one exception, the average ammunition error was 0.98 mils with a standard deviation of 0.8 mils. The total aiming error,  $\tau_t$ , for ranges from three meters to twelve meters, varies from 35 mils to 30 mils for Group A and 23 mils to 16 mils for the Group B data. Using the average  $\tau_a$  value, the percent of the total aiming error,  $\tau_t$ , attributable to the ammunition was less than 1%.

The conclusion based on these data is that the inherent accuracy of ammunition from manufacturer to manufacturer, bullet type to bullet type, weapon to weapon, and bullet velocity level were not significant when compared to the shooter error and was not effected by weapon type. In other words, ammunition accuracy

far exceeds shooter accuracy. This conclusion should not be interpreted as saying that total aiming error,  $\tau_t$ , is independent of recoil level associated with a given weapon/ammunition combination. In fact, there should be a strong correlation. For example, with respect to the average police officer, it would be expected that shooter errors are greater when firing the .44 Magnum pistol as compared to the .38 Special pistol even though the inherent accuracy of the ammunition was approximately the same in both cases. Recoil effects on shooter accuracy were not addressed but its effect on stopping could be investigated in a subsequent effort.

The one exception to the above discussion concerning the importance of ammunition error were the tests conducted using the MB Associates' Short Stop Cartridge. Only a limited number of cartridges were available at the time of testing. When fired from a machine rested revolver at a distance of fifteen meters at a target 28cm x 36cm, insufficient hits on the target were obtained to permit computations of ammunition errors. Consequently, as opposed to conventional ammunition, the accuracy of these rounds could adversely affect the stopping power of the weapon/shooter combination being considered. At this time, it is not known if this inaccuracy is inherent in this cartridge or if there is a quality control problem with the particular ammunition tested being of low quality.

#### B. Effect of Aiming Error on the RII for Handguns

The vulnerability index,  $V_I$ , as a function of the depth of penetration into the body is an indicator of the ability of the weapon/shooter system to place a shot in the path of a vulnerable organ and the level of importance of these organs in contributing to stopping power. Here vulnerable organ is defined as an organ, tissue type or computer cell which has a non-zero value of importance to stopping power. Using the hit distribution model, as previously discussed, a random sample of trajectories was fired at the Computer Man and the average vulnerability index as a function of penetration depth was determined. Six different  $V_I(x)$  curves were computed as listed in Table III.

The corresponding  $V_I$  curves for the standard aim point are shown in Figures 16 through 19. Each of these curves is a composite based on the firing of 10,000 trajectories at the Computer Man. The sample size of 10,000 was chosen to ensure numerical stability of the  $V_I$  curves. Since the  $V_I$  is a function of shooter accuracy, or the ability to hit a target, the  $V_I$  curves change as a function of range.

Figures 16 through 18, depicting the Group A data, also show a change in structure as a function of range to the target. This is due to the injury criteria and the spreading out of the shot pattern as the range increases. The injury criteria is a very stringent one, immediate incapacitation, and results in only a limited number of the organs of the body being vulnerable. One of the most vulnerable areas is the cervical spine. This area is highly localized along a narrow strip at a relatively deep depth of penetration. This is why Figure 16 shows a second peak. As the range increases, however, the probability of a shot actually hitting the spine becomes quite small. Thus the peak becomes less apparent as the range increases until at 12 meters it has disappeared. Comparing Figure 17 and Figure 19, it can be seen that for a given range, the tighter hit distribution of the Group B data produces a higher vulnerability index level.

Since the  $V_I$  curves will be used as weighting functions to assess the importance of producing tissue damage at a given depth of penetration, it should be apparent that the resultant stopping power for a given cartridge will change dependent on the range and hit distribution. For a given range, it is possible that increased shooter accuracy can offset the effect of using a potentially less "effective" cartridge. This point will be discussed further when the actual stopping power of cartridge types is presented.

One last factor to be addressed as to its effects on the  $V_I$  curve and subsequent stopping power computations is the location of the shooter aim point. The point chosen for Figures 16 through 19 was the center of mass of the target, i.e., mid-thorax, and corresponds to the aim point on the standard silhouette target. However, the medical assessment showed that the vulnerable organs lie in primarily the upper half of the body. For the Group A hit distribution, many of the hits are on the lower half of the body which does not contain vulnerable organs. The Group B distribution, on the other hand, is tight enough that many of the vulnerable organs above the aim point are not hit. This implies that there may be an optimum aim point which lies higher than the generally accepted aim point.

To determine if in fact a more optimum aim point exists, a second series of vulnerability indices were determined with the aim point shifted to approximately arm pit level. The resultant hit distribution super-imposed on the Computer Man silhouette with this aim point is shown in Figure 20 for the Group A data and Figure 21 for the Group B data. The resultant vulnerability index curves are shown in Figures 22 and 23. Notice that when these two curves are compared with the lower aim point curves, there is a significantly greater area under the curves indicating a higher probability of encountering a vulnerable tissue on any given shot. Additionally, it is evident that the character or shape of the curves has changed.

This is because the higher aim point is now concentrating the shots in an area where the vulnerable tissues lie closer to the front of the man. For this aim point, it is expected that some of the rounds which do not penetrate as deeply as others and do not cause as much damage at greater depths of penetration for the low aim point would be more effective in terms of stopping power if the higher aim point were employed. This point will be addressed later as to its net effect on stopping power.

C. Determination of the RII for Commercially Available Handgun Bullets

The effect of striking velocity on the calculated measure of relative stopping power (RII) for each bullet evaluated in the study is listed in Tables IV through LXI. The data in each table is grouped according to mass, construction type, and caliber for all manufacturers. The tables make use of the following abbreviations:

Caliber: 9mm is listed as a caliber range from .353 to .355  
.357 includes both .38 Special and .357 Magnum bullets  
.41 is listed as .41  
.44 is listed as .429 or .427 to .429  
.45 is listed as .45 to .454

Shape/Construction (for each caliber):

LSP\* - Lead Soft Point  
L, RN, LRN - Lead Round Nose  
WC - Wadcutter  
SWC - Semi-Wadcutter  
LHP - Lead Hollow Point  
JFP, JSP - Jacketed Flat Point, Jacketed Soft Point  
(flat nose)  
JHC, JHP - Jacketed Hollow Point (flat nose)  
FMJ, FJ - Full Jacket  
HEMIJSP - Jacketed Soft Point (round nose)  
HEMIJHP - Jacketed Hollow Point (round nose)  
PP - Power Point, same as FJ but with exposed lead  
MP - Metal Piercing  
SSG - Safety Slug  
SS - Short Stop

<u>Manufacturer:</u>	Hi-Precision	- HI
	Zero	- ZE
	Winchester-Western	- W-W, W-
	Sierra	- SI
	Smith & Wesson	- S+W, S+
	Remington	- RE
	Hornady	- HO
	KTW	- KT
	MB Associates	- MBA, MB
	Deadeye Associates	- Glaser, GL
	Super Vel	- SU
	Speer	- SP

Using computer predictions and actual bullet data, a curve of the form:

$$R_{II} = e^{(A + BV + \frac{C}{V})} \quad (12)$$

where RII = relative incapacitation index

v = striking velocity, fps\*

A, B, C = are curve fitting parameters

or

$$R_{II} = e^{(A + \frac{BV}{D} + \frac{C \cdot D}{V})} \quad (13)$$

where v = striking velocity, mps

D = .3048

was fitted to the RII values for each bullet type using least squares techniques. The numerical values of A, B, and C are printed below each table. This equation provides a means of estimating the average RII for a given bullet construction, mass, and caliber. It can then be used to rank bullets of different manufacture. Two ranking techniques were examined. The first was the average deviation of a given manufacturer's bullet about the fitted curve. That is, each bullet of specified manufacture was compared with the average curve for all bullets of that type and the number of units it was, on the average, above or below the curve was computed. The greater the average deviation, the higher or lower the ranking. In the attached tables,

manufacturers are listed from lowest to highest average deviation. The second method of ranking examined was the percent of a given manufacturer's data which fell above or below the average. The actual values of average deviation can be effected by a "flier" in the sense that, on the average, a manufacturer may rank very high but because of one or two very low data points its position in the ranking is adversely affected. The percent above the average would not be effected as much by these averages. Both the average deviation and percent data points above the average for each manufacturer are given in the tables. By considering both factors together, one can rank bullets by manufacturers.

In addition to the data tables for each bullet type, the curves of average RII versus velocity (calculated with Equation 12) are given for each bullet in Figures 24 through 82. Tables IV through LXI include a notation as to which figure the table applies for ease of cross reference.

Examining these tables, there is no clear cut choice of best manufacturer. However, the data indicates in general that Speer, Winchester-Western, and Remington generally have the highest rankings. Additionally, when bullets from these three manufacturers are compared the order is the same: (1) Speer, (2) Winchester-Western, (3) Remington with few exceptions.

Comparison of the average curves in Figures 24 through 82 is more difficult and subject to interpretation. Intimately built into these curves is manufacturer's construction type. It can be seen in the tables that certain manufacturer's bullets always tend to give low RII's compared to others. Consequently, when one desires to look at average response to rank bullets by type, caliber, and weight, if all the data in one instance came from a low ranking manufacturer, the absolute ranking of a type bullet may be adversely affected.

One of the most frequently asked questions concerning stopping power is: "In the caliber range from 9mm to .45, what is the optimal caliber and weight bullet?" Answering this question was one of the goals of this program even though objective analysis was difficult because of the many factors which enter into the choice of optimal caliber and weight bullet. As evidenced from the test data, the most important factors which hinder an objective choice are:

Construction

Shape/Geometry

Construction is largely related to manufacturer. Not all manufacturers offer bullets of each construction type through the whole caliber range. Consequently, the data base would not be consistent between calibers. For instance, one of the better bullet designs was found to be the LHP. In the caliber range of primary interest, this bullet type is available only in .357 caliber. None are available in 9mm or .45 caliber. When one examines the shape of bullets available in the different caliber, the same is true. A given shape/geometry bullet may not be available in all calibers. This is particularly true when one compares the 9mm and .45 caliber bullets as a group to the remaining calibers as a group. Both the 9mm and .45 caliber bullets are used primarily in semi-automatic handguns. Because these weapons are magazine fed, the bullets are "streamlined" in shape to insure proper feeding into the chamber. However, this "streamlining" is detrimental to stopping power. Consequently, while the 9mm and .45 caliber bullets may rank low in RII, this may not be a true indicator of the potential of these calibers.

To answer the question, one must subjectively re-adjust the bullet type curves to eliminate the construction and geometry bias to arrive at the following results.

Within the caliber range tested, the stopping power increases with caliber, that is the .45 caliber ranks highest. However, the optimal bullet weight is not the heavy standard bullet but one weighing about 170 grains. This can be born out by examining the data. For the .357 data, RII increases with weight up to 158 grains. For the larger caliber data, RII increases with decreasing weight down to 170 grains. This implies that the optimal weight lies somewhere in the range from 158-170 grains.

When one considers why deforming bullets are used it is not surprising that the .45 caliber should rank highest. Deforming bullets cause a sudden increase in presented area on impact. This increases drag in tissue, increases the rate at which energy is deposited by the bullet, and enhances tissue damage. The .357 caliber hollow point bullets expand on impact for this purpose but the .45 caliber bullet is already the size of a deformed .357 even before impact and can only get better once its deformation begins. The .45 caliber bullets as tested suffer primarily from their streamlined shape which inhibits deformation.

The data also indicate that a near optimum velocity is 335m/s (1100 ft/sec). It is at approximately this velocity that the RII's rise very rapidly or have reached a plateau.

Coupled closely with caliber, mass, and velocity is shape. The data indicate that the most effective design is the lead hollow-point (LHP). Hollow-points generally deformed to a greater extent than other types, provided the velocity is high enough. Without the presence of the jacket, a hollow point design deforms to an even greater extent.

D. Determination of the RII for Commercially Available Cartridges

A sample of nearly 100 different commercially available cartridges was test fired from typical police handguns to determine muzzle velocities. Equation 12 or 13 was then used to calculate the relative incapacitation index, RII, for each of these cartridges. The results are given in Table LXII. It should be noted that this table is not all inclusive, but is a sampling of ammunition available at the time of the tests. Manufacturers may change their powder loadings from time to time for one reason or another producing different velocities than those reported. Additionally, different type handguns may give different muzzle velocities than those in the table. Consequently, this table is meant to provide a guide to ammunition selection. In practice, when a law enforcement agency desires to use a cartridge found in Table LXIII or some cartridge using a particular bullet found in Tables IV through LXII, the ammunition should be test fired to determine muzzle velocity. The RII can then be calculated using the following procedure:

1. Determine muzzle velocity (fps)
2. Specify the bullet (not cartridge) type by:
  - a. Manufacturer (this may not be identical to the cartridge manufacturer.
  - b. Construction, i.e., LRN, JHP, SWC, etc.
  - c. Mass in grains
  - d. Caliber
3. Locate the appropriate bullet RII table (between Table IV and LX)
4. Use the values of A, B, and C found in the table in the following equation:

$$RII = e^{(A+Bv+c/v)}$$

5. At the bottom of the table is listed the average deviation of each manufacturer from the above equation. The specific RII for the chosen bullet is given by

$$RII = RII + AVG DEV$$

If the manufacturer is not given in the appropriate table then set AVG DEV equal to zero. To illustrate this procedure, the calculation of the RII for the 125 gr., .357 Magnum, JHP, Remington cartridge follows:

1. Muzzle Velocity: 1366 fps
2. a. Remington  
b. JHP  
c. 125 gr.  
d. .357
3. Reference Table XXIII
4. A = 4.268997<sup>+</sup>  
B = 8.61675<sup>+</sup> E-04 (.000861675<sup>+</sup>)  
C = -2512.29936

$$\begin{aligned} R_{III} &= e^{(A + 1366 \cdot B + C/1366)} \\ &= 36.85 \end{aligned}$$

5. AVG DEV = 3.96  
RII = 40.8

As stated above, Table LXIII is not all inclusive and it should be noted that the RII tables, Tables IV through LXII, contain more manufacturers and bullet types than listed in Table LXIII. Many manufacturers offer many bullets in the form of handloading components and do not make them available in loaded cartridge form. As many of these handloading type bullets as possible were tested and included in the tables. The procedure given above would also be used to calculate RII for these bullets when used in loaded cartridges.

Manufacturers of ammunition, both commercial and wildcat, are continually making changes in bullet design to improve their products. Many of these designs may not be found in Tables IV through LXII. In this event, the determination of RII would have to be made experimentally by firing the bullets into tissue simulant as was done in this study. If this is necessary, the following procedure must be followed:

1. Measure the maximum temporary cavity formed in a gelatin target by following the procedures given in BRL Report 1940, "Ammunition For Law Enforcement: Part II, Data Obtained For Bullets Penetrating Tissue Simulant". This results in a table of cavity radius vs. penetration distance, i.e.,  $R(x)$  vs.  $x$ . As an example, consider the Speer .45 caliber, JHP bullet fired at a velocity of 374 m/s (1227 f/s), Round No. 519, Table LVI. The cavity data taken from the above report is:

x (mm)	R (mm)
0	39
6	43
11	48
17	51
23	55
29	58
35	60
41	62
47	63
53	63
59	64
65	62
71	62
77	61
83	59
89	56
95	54
101	52
107	50
113	47
119	44
125	40
131	37
137	31
143	25
148	24
155	23
161	23
166	22
172	21
178	18
184	15
190	13
196	11
202	9
208	8
214	8
220	6

2. Figure 17 shows the  $V_I(x)$  curve used in the calculation of RII as follows: interpolate the  $R(x)$  vs.  $x$  data to get  $R(x)$  at 1cm increments, calculate  $R^2(x) \cdot V_I(x)$  at each point, sum the results and multiply by  $\pi$ , i.e.,

x(cm)	R(cm)	$V_I$	$R^2 V_I$
0	3.9	0.0	0
1	4.8	.0061	.140
2	5.4	.0169	.493
3	5.8	.0477	1.604
4	6.2	.0608	2.336
5	6.3	.0588	2.333
6	6.4	.0564	2.309
7	6.2	.0458	1.819
8	6.0	.0388	1.396
9	5.6	.0401	1.257
10	5.2	.0405	1.095
11	5.0	.0248	.621
12	4.4	.0238	.460
13	3.7	.0292	.400
14	2.8	.0231	.181
15	2.4	.0227	.131
16	2.3	.0273	.144
17	2.1	.0230	.101
18	1.6	.0247	.063
19	1.3	.0196	.035
20	.9	.0074	.006
21	.8	.0014	.001
22	.6	.0003	.000+

$$\text{Total} = \sum_{x=0}^{x_{\max}} R^2 \cdot V_I = 16.92$$

$$\text{RII} = \pi \cdot \text{Total} = 53.1$$

#### E. Predictions Based on the Analytical Cavity Model

By using the cavity model to generate cavity envelopes, the corresponding RII's can be calculated just as they are for the cavities obtained experimentally. There are two basic applications for these theoretical calculations. The first is to supplement sparse data for velocities in the nondeforming regime. This application is practical only in cases where the drag coefficient  $C_D$  in equation (4) can be closely estimated. Since variations in design for the same bullet type could result in significantly

different drag coefficients, it is difficult to use this technique to replace data. On the other hand, the model calculations can be used to estimate bullet performance and indicate trends. From information already on file at the BRL, penetration versus time data, striking velocity versus residual velocity data for projectiles which excited the gelatin blocks, and striking velocity versus maximum penetration in gelatin, data have been used to estimate "effective" drag coefficients based on equation (4) for various bullet types. Table LXIII lists the drag coefficients evaluated and the general bullet types for which they apply.

The cavity model was then used to generate RII versus striking velocity for the cases listed in Table LXIV.

Figures 83 through 99 display the RII versus velocity curves for the model along with data that are available for bullets having similar caliber, mass, and drag coefficient. The data plotted on these figures with the symbol "X" are not distinguished according to manufacture. Consequently, a broad spectrum of bullet performance with respect to yawing and deformation can occur on some of these graphs.

In general, the model curves represent a lower limit to the data. The higher data points are primarily the result of the projectiles presenting a larger area either initially because of striking yaw or because of deformation occurring during the penetration process. In some cases, the projectiles actually tumbled in the gelatin. Early tumbling usually resulted in exceptionally large RII's, but for the most part the ball rounds tumbled beyond the depth at which the vulnerability index becomes zero. The cases where the actual rounds may fall closer to or below the nontumbling, nondeforming model curves fall into two categories. The first is the high velocity case which results in bullet break-up. The second is exemplified in Figure 100. This figure compares a .357, 158 grain, 372 m/s JSP round with the non-deforming, nontumbling cavity contour generated by equation (8) for the same mass, caliber and striking velocity. The figure shows that in this case the bullet cavity is larger than the model cavity over about the first 7.5cm of penetration due to early bullet expansion. For the remainder of the penetration the bullet cavity was lower than the cavity computed for the nontumbling, nondeforming projectile. This reversal in cavity radius is due to the fact that the actual bullet was slowed down to a greater extent in the expansion state and that after deformation the flat nose has become somewhat rounded making the  $C_D$  lower. Depending on where these phenomena occur with respect to peaks in the vulnerability index curve, various changes in the RII's would be obtained.

On examining the equations of the cavity model it can be seen that the RII trends exhibited in Figures 83-99 follow common sense. The cavity model tells us that, at a given depth of penetration, the cavity envelope radius is a monotonic increasing function of projectile velocity, presented area, and drag coefficient. It is noted that the only influence of projectile mass in the nondeforming case is on how rapidly velocity is lost. This also supports the experimental result that the .45 caliber bullet should be optimal.

#### F. Effect of Accuracy and Aim Point on Stopping Power

The stopping power criteria as developed in this report is dependent not only on the type bullet and velocity used but also on the accuracy of the shooter and the point on the body at which he is aiming. Figures 101 through 104 show the effect of varying these parameters. Figure 101 shows what is intuitively obvious as the engagement range increases stopping power decreases. Figure 102 shows the effect of changing the shooter accuracy. At a range of 6 meters, the Group B "shooter" is nearly twice as accurate as the Group A "shooter". This results in an increase in stopping power of about 18% for a 100% increase in accuracy. The effects of varying the aim point from the standard silhouette target location are shown in Figures 84 and 85. The aim point designated by "High" is that shown in Figures 20 and 21; the "Low" point is the aim point shown in Figures 11 and 14. These figures clearly show that improvements in stopping power can be achieved by raising the aim point to the high location. Comparison of the two figures also shows that the higher aim point used in conjunction with the Group A "shooter" can more than offset the increase in stopping power due to using the more accurate Group B "shooter" with the lower aim point.

#### G. Comparison with other Techniques of Calculating RSP

When one views the methodology presented, the skeptic very logically might observe all that has been presented is a numbers game and bears no resemblance to reality because nowhere during the whole study has a medical doctor been called upon to assess the effects of a wound. The only advice sought from the medical community was a relative ranking of individual computer tissue cells, not classical wound assessment per se. The wounds and a measure of their effects were created in the computer. This was intentional because it was desired to formulate a criteria unbiased by a doctor's preconceived notion of a typical wound or by wounds created by typical projectiles. The final unanswered question concerning the overall methodology is "just how does the RII or stopping power correlate with the probability that an assailant would be rendered non-combatant?" To answer this question, a panel of three medical assessors, not associated with the University of Maryland Hospital, in conjunction

with the University of Colorado, were asked to estimate the probability of instant incapacitation for a series of 100 bullets evaluated in this study.<sup>8</sup> These assessors were:

- (1) The Chief of the Biophysics Laboratory at Edgewood Arsenal.
- (2) The Assistant Medical Examiner for the County of Santa Clara, California.
- (3) The Chief Medical Examiner for King County, Washington, formerly Chief of the Wound Ballistics Section of the Armed Forces Institute of Pathology.

The mean response of these individuals is compared with the computer generated RII in Figure 105 and it can be seen that the RII does in fact correlate properly with the probability of instant incapacitation.

A comparison was also made between RII and two other stopping power theories: Energy deposit and Hatcher's formula. Figure 106 shows how RII compares to energy deposit. It shows that a given level of RII or stopping power can be produced by different values of kinetic energy deposit. That is, stopping power depends not only on whether energy is deposited in the body or not but also on its spatial distribution within the body, i.e., energy must be deposited where the vital organs are most likely to be found.

Figure 107 compares prediction based on Hatcher's formula to RII or stopping power. As with energy deposit, Hatcher's formula could only be judged a general indicator of probability of incapacitation if the data for each of the bullet types all fell on one continuous curve. Of the three criteria the RII is most consistent with medical judgement.

#### H. Penetration/Ricochet Characteristics

The degree and cause of bullet breakup on ricochet emerged as the most significant information obtained from the ricochet tests. Data from the ricochet experiments were sorted on the basis of all recorded categories of information. Only the pairing of impact velocity and degree of break-up produced significant information. The measured residual velocity is always that of the fastest fragment leaving the impact point and passing through the velocity screens. Forty-seven percent of the ricochet cases tested (on non-penetrable targets) failed to satisfactorily function the velocity screens on the ricochet

<sup>8</sup> Hammond, K.R., et.al., "Report to the Denver City Council and Mayor Regarding the Choice of Handgun Ammunition for the Police Department" Institute of Behavioral Science, University of Colorado, March 1975.

side of impact. Most velocity screens on the ricochet side of impact indicated perforation by hundreds of minute particles (less than 0.5mm in hole width). Figure 107 shows the results of sorting cases according to those with one to five or more than five fragments. Cases with seriously doubtful fragment counts were rejected. The mean striking speed and its coefficient of variation were determined for both groups. Approximately 25 percent of the total cases had from one to five fragments. Almost 10 percent of the cases had from six to thirty fragments. The remaining 65 percent of the cases were questionable data for one or more reasons. When the accepted cases were analyzed, the mean velocity and the coefficient of variation were obtained for both break-up categories shown in Figure 108.

The conclusion which has been drawn from this result is that a velocity exists above which one may expect bullets from handguns to break into many fragments. The evidence obtained in these experiments is supportive of that expectation for impacts into concrete, macadam, building block, brick, or heavy steel. The mean velocity at which massive break-up occurred was 335 m/sec (1103 ft/sec) but, break-up of large (massive) projectiles may still leave significant fragments.

In order to check this possibility, the ricochet data was searched for fragments as large as or larger than the .22 Caliber HP (39 grains). The results are shown in Figure 109. The samples for impact angles of 30°, 45°, and 60° are divided into those with speeds greater or less than 335 m/sec. From the figure it is clear that striking velocities less than 335 m/sec hold the dominant number of cases that produced massive fragments. This is significant because more massive fragments have higher ballistic efficiency and retain lethal characteristics to greater ranges.

It is possible to characterize the range at which a given projectile loses its capability to cause a serious wound. The hazard criteria chosen for consideration of safety to bystanders was the minimum velocity necessary to penetrate the skin. It was felt that any fragment with sufficient mass and velocity to penetrate the skin could also cause a serious wound. Using this criteria, the following equation for use as a safety criteria was developed to calculate the maximum tolerable velocity which a given mass fragment could have after ricochet or penetration:

$$v = [(KxM)+B]e^{-C \cdot M \cdot R}$$

$$v = \frac{K \cdot M + B}{\text{Exp}(-C \cdot M \cdot R)}$$

v = velocity (mps) at point of ricochet such that fragments become non-hazardous at a distance R

where  $M = D \cdot \left(\frac{\pi}{m}\right)^{1/3} \left(\frac{3}{4\rho}\right)^{2/3}$

m = fragment mass, grains

R = distance from point of ricochet or penetration to a bystander, cm

$\rho$  = density of fragment, gm/cc. (for lead core  $\rho = 11$ , for copper jacket  $\rho = 8$ )

K = 125

B = 22

C =  $5.75 \times 10^{-4}$

D = 2.49

This equation is plotted in Figures 110 and 111 for four ranges; 3, 6, 12, and 50m. Except for the extremely small fragment masses (less than a few grains), fragments moving at a velocity greater than approximately 50 m/sec (164 ft/sec) pose a threat to safety even out to ranges as far as 50m.

In the figures masses up to 150 grains are considered, but in real events larger masses may be produced in ricochet. The calculations were produced without trajectory considerations and are based on the hydrodynamic drag law. Notice that at the close range, acceptable ricochet speeds are too low to be achieved in practical handgun rounds. On the other hand, the ricochet speeds for fifty meter cleared areas are within the achievable regime, particularly if bullets break into fragments of less than five grains each.

Specially designed ammunition tested in ricochet showed that it is possible to design bullets with substantially reduced risk in ricochet events (e.g., the Safety Slug). On the other hand, certain rounds are particularly hazardous due to ricochet (e.g., KTW bullet and other metal piercing bullets).

One characteristic noted in the ricochet tests should be used in guiding future anti-ricochet designs. Bullets of jacketed design almost always separate the jacket from the lead core in ricochet off any hard materials. Here, hard material means almost any material not penetrated. Data shows, for instance, that if the lead core is replaced by swagged chilled shot (say number nine as with the Safety Slug) that a fairly good hardball round with less severe ricochet characteristics is obtained. Beyond 12 meters, these fragments become "safe".

Several flash x-ray films recorded during ricochet/penetration tests are shown in Figures 112-118. The reader should observe that even so insignificant resistance as 1/8 inch glass is sufficient to cause jacket separation from the core of the bullets shown. From three to five exposures are made on each film. The exposures are for short duration and in rapid sequence showing the progress of the projectile at several times. The lateral displacement of the bullets is due to the x-ray tubes being placed side-by-side thus generating parallax.

One x-ray is the Deadeye Associates Safety Slug penetrating 1/4 inch laminated glass at 600 m/sec. From this test sequence it is clear that even in penetration, this projectile will break-up dramatically.

The issue of unintended wounding does not stop with ricochet. Powerful handguns are quite capable of penetrating urban housing structures, interior walls of office buildings, glass windows, roofs, floors, automobiles, and just about anything else with densities of less than  $15 \text{ kg/m}^2$  ( $10 \text{ lbs/ft}^2$ ). It is true of course, that certain combinations of materials will stop a bullet with much less than  $15 \text{ kg/m}^2$ . But, consider the penetration capability of the .41 Magnum. A 220 grain bullet fired at about the speed of sound from a four-inch barrel .41 Magnum will penetrate about 800 millimeters (30 inches) of tissue simulant. That is equivalent to five people! Even so, the same bullet will not penetrate even 6.35mm (0.25 inch) of rolled homogeneous armor.

All handguns tested in calibers .38 and up will penetrate at least some part of an auto body. No standard automobile doors would stop any of the magnum handgun projectiles at short range. On the other hand, modern lightweight armors are available that could be used covertly to make the occupants of a car safe from handgun attack.

Despite the mythology to the contrary, magnum handguns will not penetrate an entire V-8 motor block. In fact, instantaneous motor stoppage due to attack by handgun is a very low probability event. Radiators, carburetors, and control linkages are all very vulnerable, but all take a finite time to cause engine failure.

One must conclude then that the specifics of penetration of handgun ammunition has enough variation that no rule-of-thumb should be trusted when human life is at stake but the above table, Table LXV, may be used as a guide to expectations.

Comparison of handgun ammunition performance with the effects of military ordnance against unarmored vehicles indicates that the only significant chance of instantaneous stoppage of an automobile is by hitting the driver. Hits on fuel tank, radiator, or tires will provide stops after a certain period of time (ranging from 30 seconds to 30 minutes). Fuel tank fires are not easy to ignite with pistol bullets.

Most rounds fired in a suburban or an urban environment will ricochet if they do not hit their intended target. Building material generally will not be penetrated, especially in the rounds which strike paving, sidewalk, concrete block or major structures. Wall-board and sidings in residential areas will generally be penetrated. Glass used in most shop and housing applications will be penetrated. As a consequence, there is considerable merit to using ammunition which results in bullet break-up prior to ricochet. When a bullet breaks up on impact prior to ricochet there are three advantages: (1) energy is dissipated in the break-up process; (2) the reduced mass of each fragment lowers its lethal potential; (3) the drag to mass ratio of each fragment is greater than that of an intact bullet, reducing the range required to slow down the fragment to non-lethal levels.

Obviously the reduction of the fragment mass to the lowest possible size on impact depends on the break-up process. In the tests conducted for the ricochet study the pure lead, large caliber, heavy bullet at low velocities was the most lethal on ricochet. The 246-grain, .44 Special at 640 feet per second consistently delivered a ricochet of about 237-grains at 400 to 500 feet per second on ricochet. This is to be compared with bullets which consistently break into smaller fragments moving at lower speeds.

However, the likelihood that all officers will be equipped with .357 Magnums with ammunition and barrel lengths that can achieve 335 m/sec with a 158-grain bullet must be compared with the mass of officers who carry .38 Specials in four inch or shorter barrels. It seems clear that a design for ammunition to control ricochet in four inch barreled .38 Specials is desired. Characteristics required are: (1) stopping power at combat ranges; (2) accuracy at combat ranges; (3) tissue penetration up to 15cm; (4) immediate break-up on ricochet; (5) fragment break-up to less than one grain each; (6) retardation in air for fragments such that they become non-lethal within a few feet; and (7) an aggregate wounding capability that is near zero within a few feet after ricochet.

## VII. CONCLUSIONS

### A. Bullet Velocity

In the range of calibers studied, the most important property of a moving handgun bullet affecting its performance in the target medium is its velocity. There are several reasons for this conclusion.

1. The size of the Maximum Temporary Cavity (MTC) depends partly on the striking kinetic energy,  $1/2 mv_0^2$ , i.e., the volume of the MTC depends on the total energy available.

2. There is a threshold velocity, below which a bullet will not deform; deformation of the bullet greatly affects the size and shape of the MTC.

It should be stressed, however, that one cannot use the striking kinetic energy as the sole criterion for ranking handgun bullets. It is the size and shape of the resulting MTC and how it overlaps vital organs that ultimately gives one bullet a higher relative incapacitation index (RII) than another. Some lighter bullets yield a higher RII than heavier ones having the same striking kinetic energy, shape, construction and caliber. From both ricochet considerations and stopping power considerations, a velocity of approximately 335 m/sec (1100 ft/sec) is most effective. At this velocity, the bullets expand sufficiently in soft tissue to provide sufficient stopping power. Additionally, at this and higher velocities, the bullets tend to break-up into smaller fragments on ricochet, thus reducing the hazard to innocent bystanders.

### B. Caliber

The caliber of a bullet, together with its shape, establish the initial value of its area function,  $A(0)$ . It is this area of the interface between the bullet and the target medium that enters the formula for the envelope of the MTC; the sectional area of the bullet (proportional to the caliber squared) cannot be used once the bullet begins to deform. Thus, a larger caliber bullet will yield a higher RII at non-deforming velocities; once deformation is possible, smaller caliber bullets may out-perform larger calibers. The .45 caliber bullet offers the greatest growth potential of the calibers tested. This is not surprising since the initial area function of the .45 caliber bullet is as large as some of the deformed small caliber bullets final area function. Re-design of the .45 caliber bullet similar to the smaller revolver bullets to enhance deformation will result in these bullets out-performing the smaller calibers.

### C. Bullet Mass

The mass of the bullet affects the size and shape of the MTC. A lighter bullet will slow down more rapidly in the target medium and a heavier bullet will penetrate further; this affects the location of the maximum radius of the MTC. Again, it is the location of the temporary cavity with respect to that of vital organs that produces varying degrees of incapacitation. The data show that optimal bullet mass is in the range of 158-170 grains. Combined with conclusion A and B, this mass range bullet in .45 caliber would produce an optimal bullet.

### D. Bullet Shape

The effect of bullet shape (bluntness of the nose) is important only in that it establishes the initial value of the hydrodynamic drag coefficient,  $C_p(0)$ . This coefficient enters the formula for the envelope of the MTC and it is also a part of the formula for the threshold deformation velocity. At velocities too low for deformation to occur,  $C_D$  is a constant and the effect is that blunter bullets (larger  $C_D$ ) yield higher values of RII. The wadcutter (WC) has the largest value of  $C_D$ .

At velocities sufficient to cause deformation of the bullet,  $C_D$  changes as the bullet deforms. Bullets with smaller initial values of  $C_D$  can deform in such a way as to out-perform those with a higher initial  $C_D$ .

### E. Deformation and Bullet Construction

Deformation of a handgun bullet depends strongly on both velocity and construction. Construction involves principally whether the bullet is jacketed or not, the length, thickness and hardness of the jacket material, the presence of hollow noses, cavities or hollow bases and the hardness of the lead. Construction also directly affects fragmentation of the bullet in both hard and soft targets. The ranking of bullet type in order of decreasing RII, is:

- a. Lead hollow point (LHP)
- b. Jacketed hollow point (JHP)
- c. Semi-wadcutter (SWC)
- d. Wadcutter (WC)
- e. Jacketed soft point (JSP)

- f. Lead round nose (LRN)
- g. Full metal jacketed (FMJ)

The low velocity performance of the wadcutter has been discussed under bullet shape. With the exception of the full-metal-jacketed bullet, the onset of deformation occurs at a given velocity for each bullet construction type (a through f); i.e., a hollow-point bullet will begin deforming at a velocity above 215 meters (705 feet) per second and a lead round nose at a velocity above 340 meters (1115 feet) per second. Unless the bullet's muzzle velocity exceeds this threshold value, bullet deformation is highly unlikely. Note that these threshold velocities were obtained by fast x-ray photography; they cannot be obtained by an inspection of the RII vs. velocity figures, although they are consistent with the curves shown there.

#### F. Shooter Accuracy

The relative incapacitation index increases as shooter accuracy increases and accuracy increases as the engagement range decreases. However, the effect of handgun type/cartridge combinations on shooter accuracy has not been systematically addressed in this study; it is the subject of possible future work.

#### G. Point of Aim

The relative incapacitation index is dependent on the aim point chosen by the officer. Assuming a given degree of shooter accuracy, the data indicate that an aim point slightly higher (armpit level) than that used on standard silhouette targets increases stopping power.

#### H. Hazard to Bystanders

A hazard to innocent bystanders can occur if the officer misses his target or if the bullet overpenetrates the target and exists with sufficient velocity to inflict a wound. With regard to the latter, overpenetration can occur if the bullet velocity is too low (absence of deformation) or if it is too high. Overpenetration can be avoided by specifying an acceptable range for bullet muzzle velocity.

### VIII. RECOMMENDATIONS

The current study on handgun effectiveness has shown the advantage of a systems approach to the stopping power question integrating such factors as aim point, shooter error, bullet mass, velocity, construction, shape and caliber into the final assessment. Yet does this study answer all of the questions? For example, it was shown that the ability to place a well aimed shot can increase the stopping power of any bullet, yet there was no effort allotted in this study to investigate

the range of typical aiming errors found throughout the law enforcement community. With the availability of this information, community leaders would be more able to make a trade-off decision between the expense of added training and the use of more powerful ammunition.

Another factor not addressed was the effect of recoil. As the power, recoil energy, muzzle flash and noise increase, accuracy of the shooter from shot to shot decreases. At this time, insufficient data exists to address this question. It was necessary for this phase of the study to assume that the effects of these factors were constant for all handguns. However, it may well be that, independent of training, these factors would make the more powerful handguns less effective than their less powerful counterparts. Again, the inclusion of this information would allow for additional trade-off studies.

It has been shown that for a given velocity, the larger caliber bullets have greater stopping power than their small caliber counterparts. It was also shown that the large caliber bullets, such as the .45 caliber bullet, need not be as massive and yet still retain its stopping power. Masses on the order of 158-170 grains are sufficient. This would indicate that a relatively short large caliber round could be manufactured not weighing much more than a 158-grain .357 magnum cartridge. Additionally, if this cartridge were manufactured, it would be possible to produce a .45 caliber revolver design specifically for this cartridge and not just a modification of an existing "heavy" revolver. The resulting compactness of this new weapon in a large caliber would have the following desirable characteristics:

1. Increased stopping power with a large caliber lightweight cartridge.
2. Relative compactness of the weapon due to short cartridge length;
3. Because muzzle velocities and recoil energies would not be as great as many other weapons, there would be a resultant increase in accuracy and controlability from shot to shot.
4. A new weapon cartridge system could be restricted to only law enforcement agencies.

The feasibility of producing a cartridge/weapon of this type to take advantage of these desirable characteristics should be investigated.

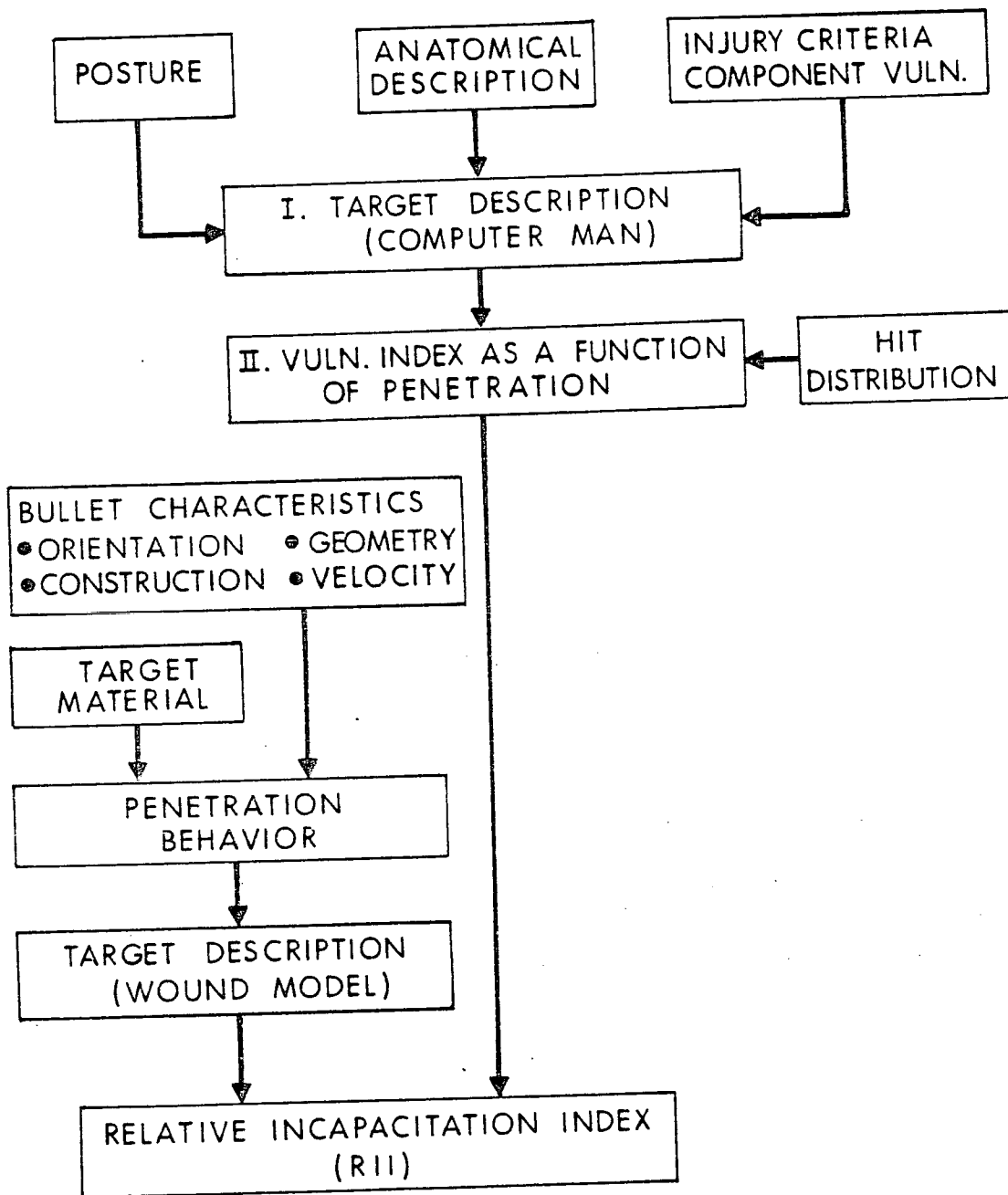


Figure 1. Flow Chart Used to Develop Relative Stopping Power For Handgun Ammunition.

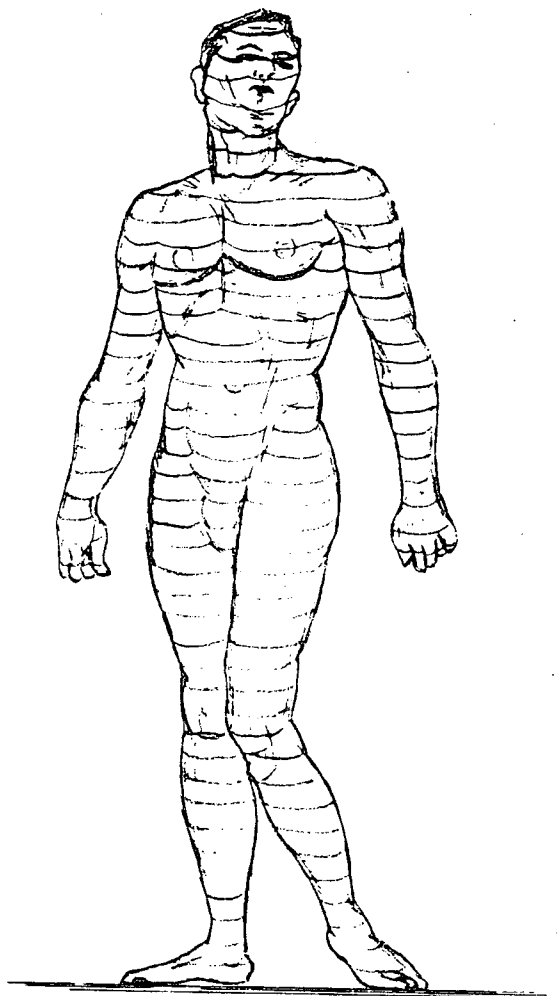


Figure 2. Sketch of the Computer Man

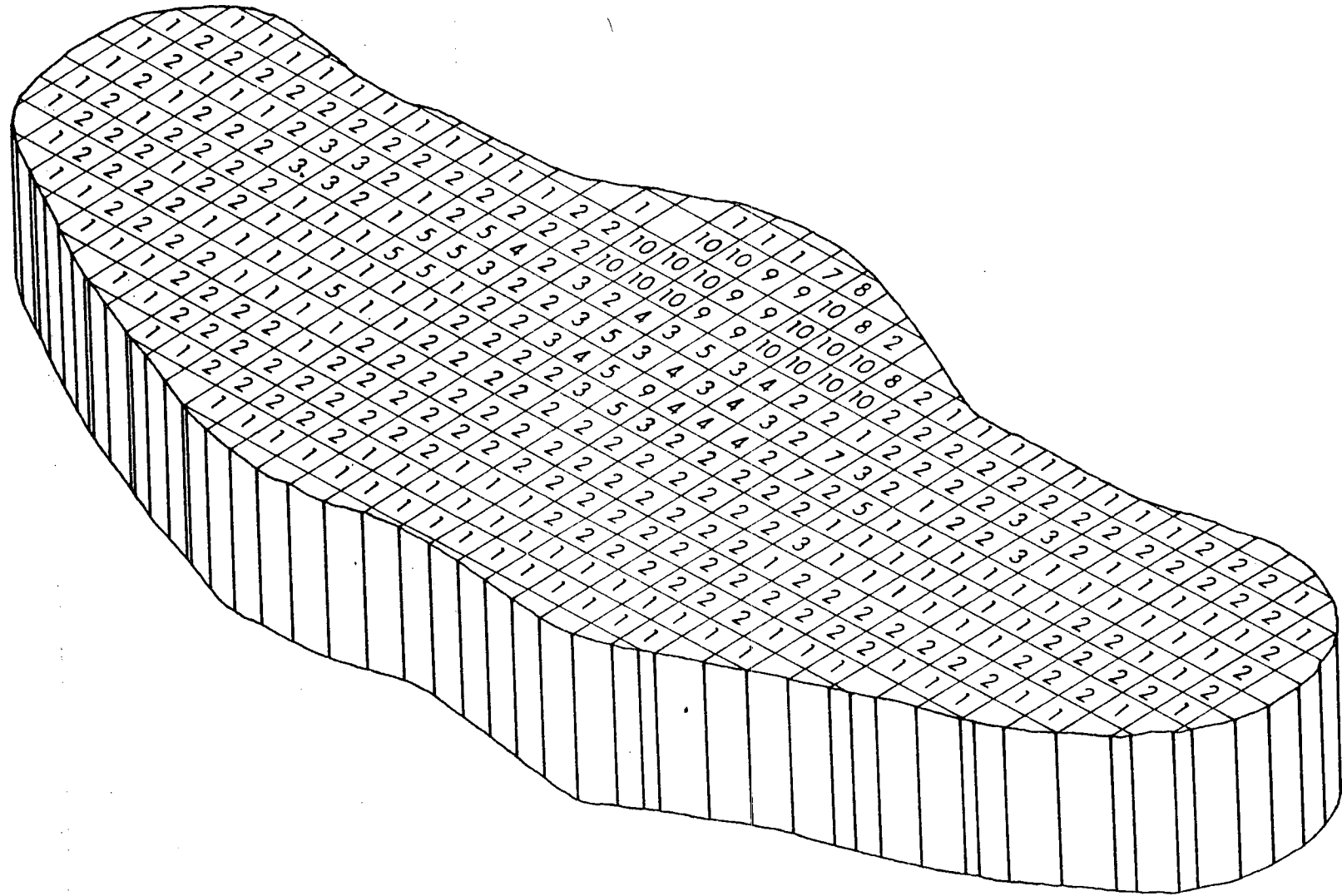


Figure 3. Top View of Typical Cross Section of the Computer Man (Shoulder Region).

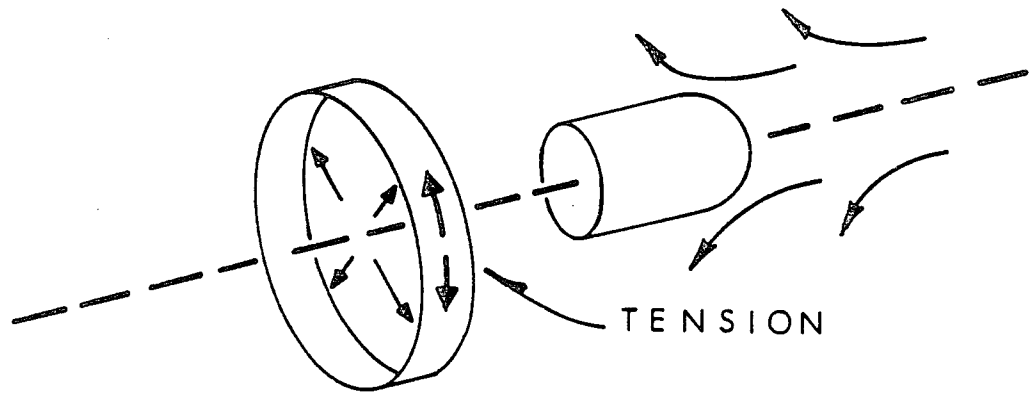


Figure 4. Sketch of Tissue Response to Bullet Penetration.

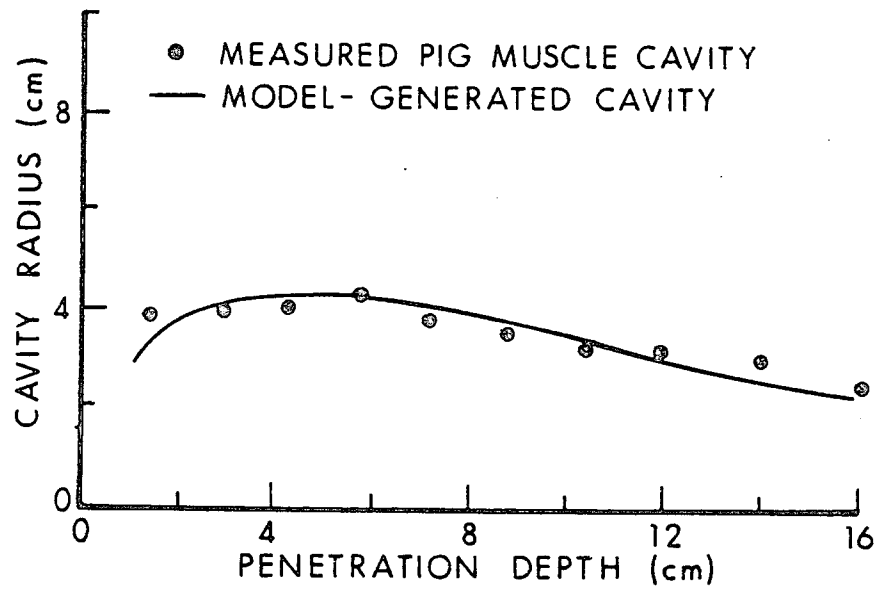


Figure 5. Comparison of Measured Maximum Temporary Cavity (MTC) Formed in Animal Tissue and a Momentum Transfer Model Prediction.

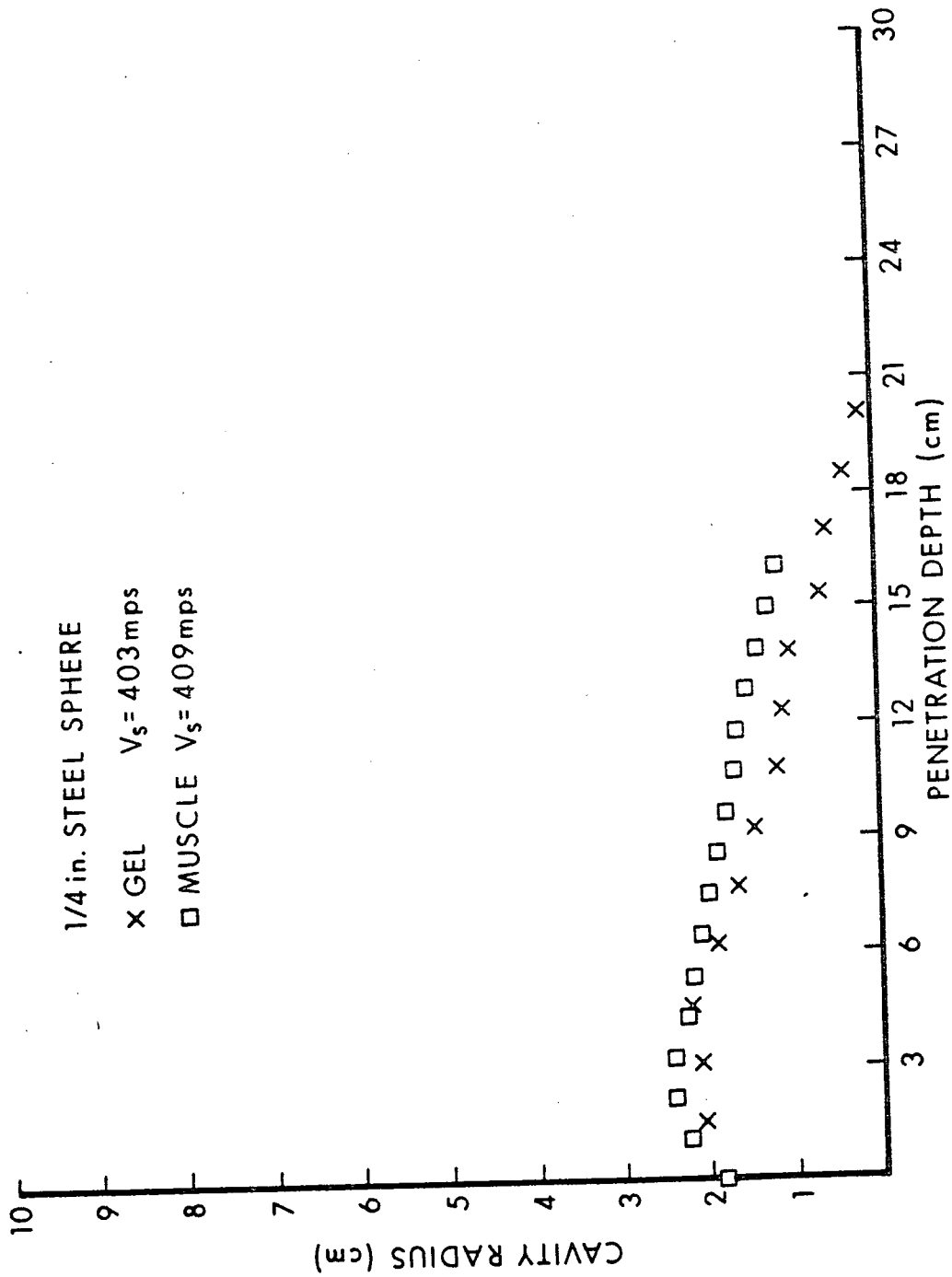


Figure 6. Comparison of The Maximum Temporary Cavity For a Steel Sphere Penetrating Animal Tissue and Tissue Simulant.

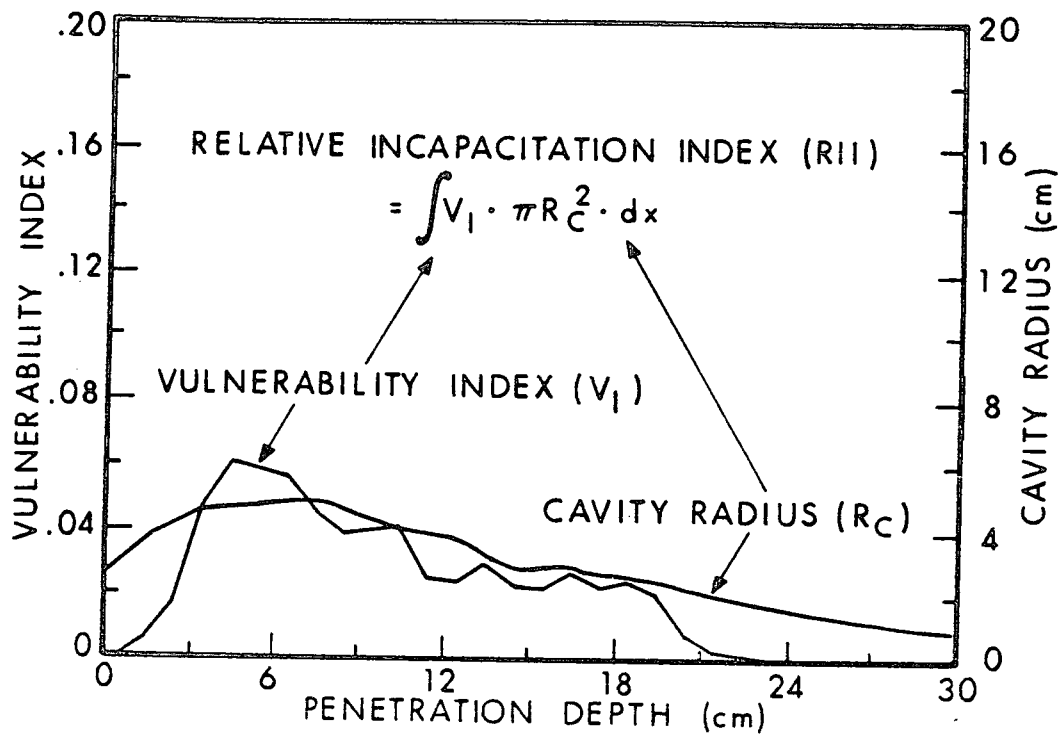


Figure 7. Sketch of Calculational Procedure For Obtaining RII.

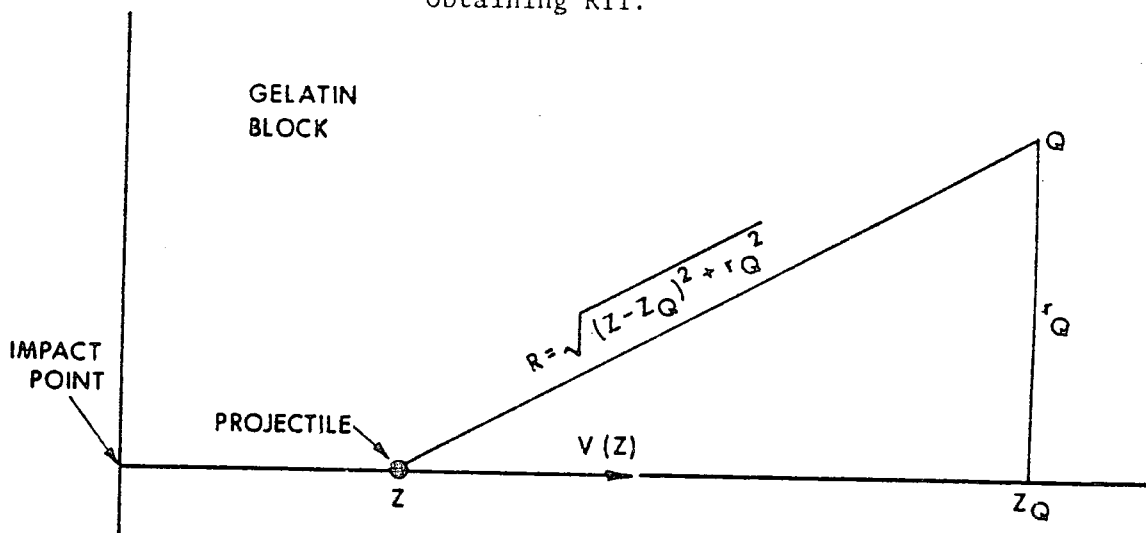


Figure 8. Theoretical Cavity Model

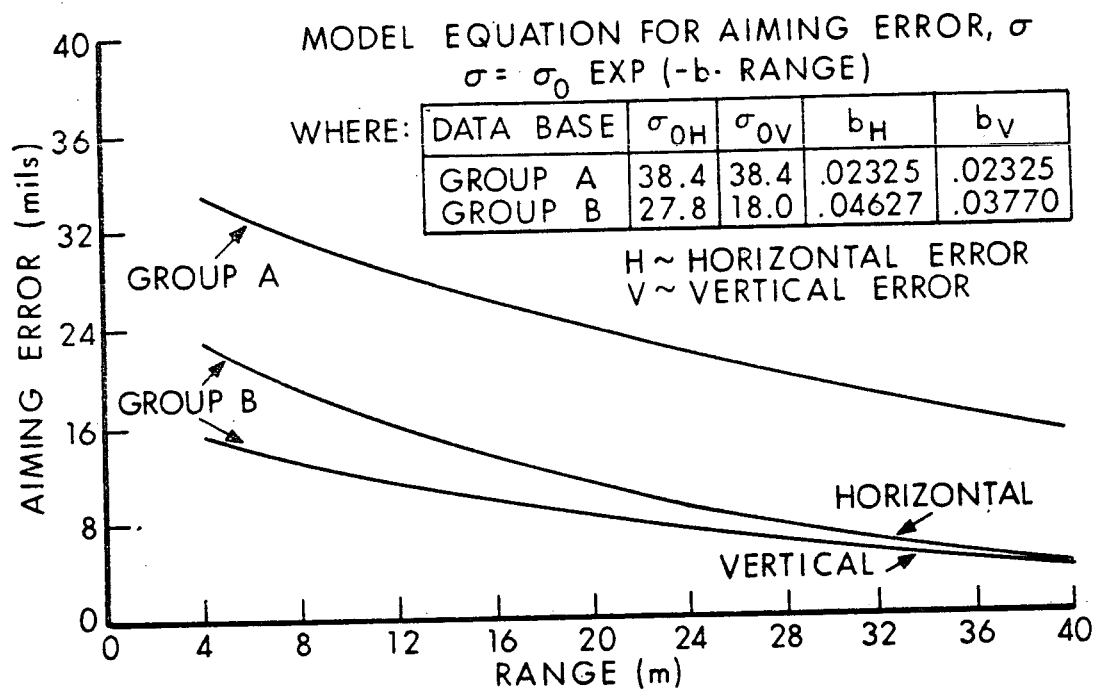


Figure 9. Aiming Error as a Function of Engagement Range.

240 TOTAL SHOTS  
0 SHOTS MISSED  
PLOTING SURFACE

99 SHOTS IN ZONE 1  
109 SHOTS IN ZONE 2  
32 SHOTS IN ZONE 3

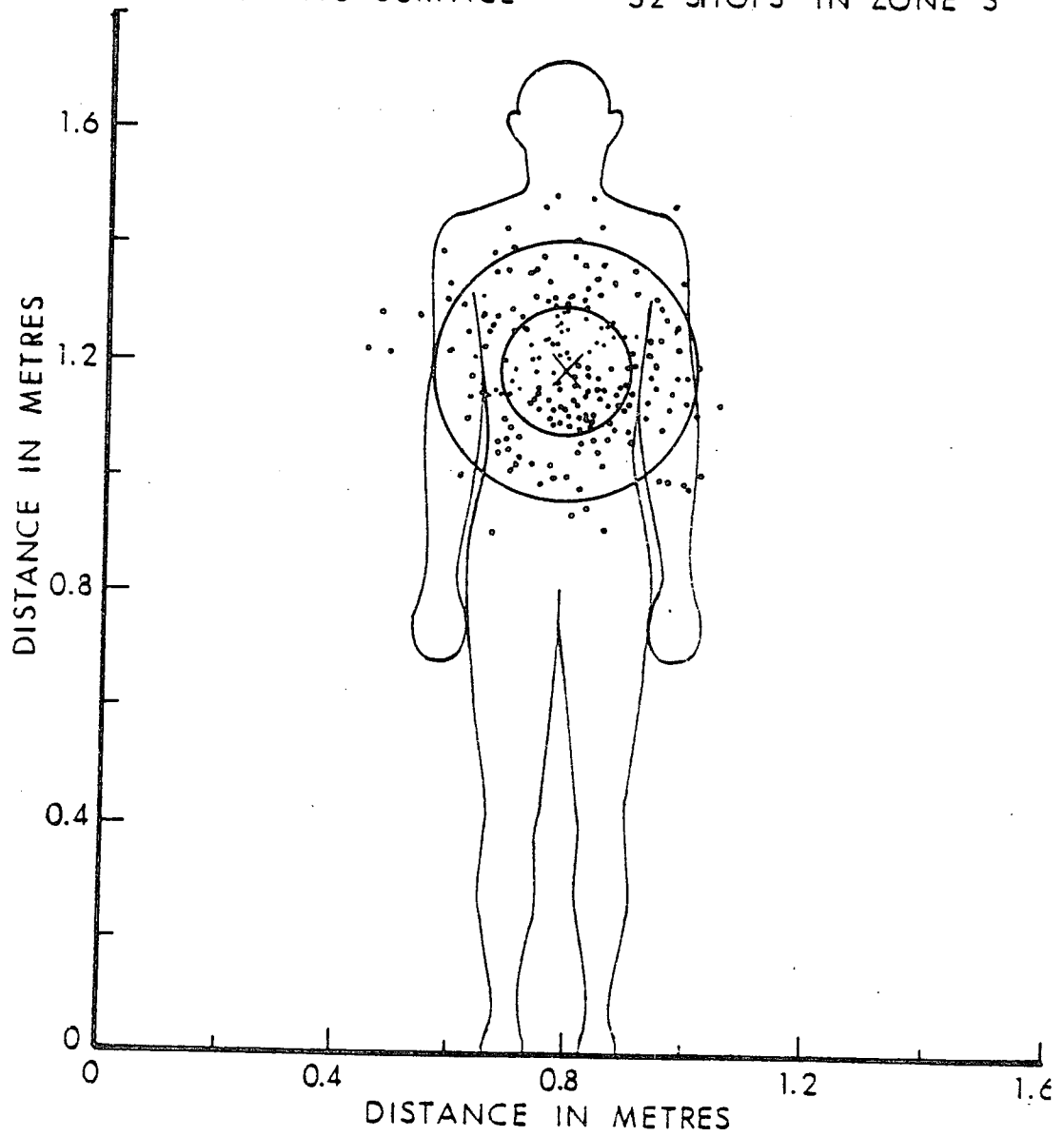


Figure 10. Group A Hit Distribution Superimposed on a Computer Man Silhouette at 3.0 Meter Range.

240 TOTAL SHOTS  
0 SHOTS MISSED  
PLOTING SURFACE

101 SHOTS IN ZONE 1  
105 SHOTS IN ZONE 2  
34 SHOTS IN ZONE 3

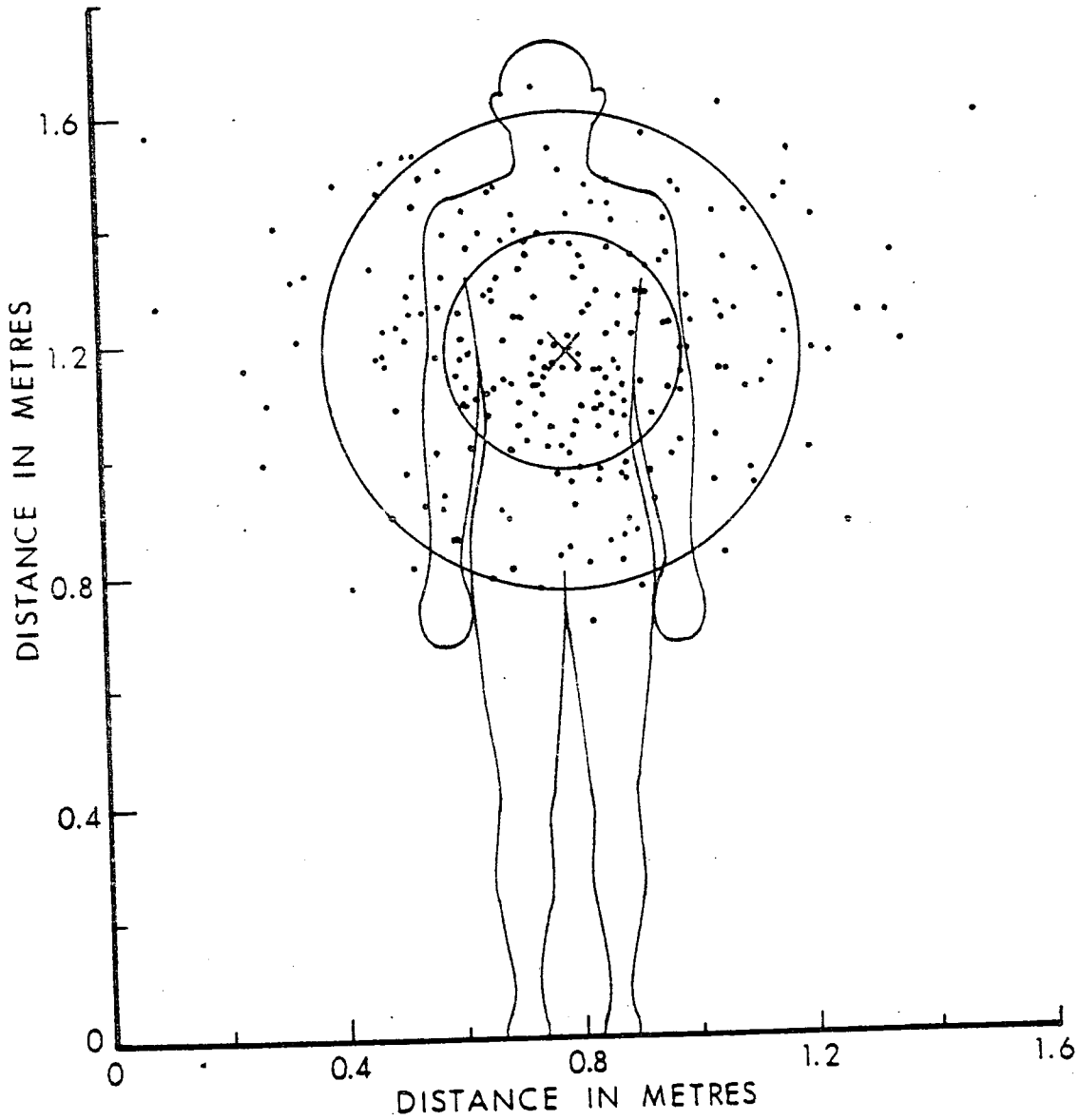


Figure 11. Group A Hit Distribution Superimposed on a Computer Man Silhouette at 6.0 Meter Range.

240 TOTAL SHOTS  
13 SHOTS MISSED  
PLOTING SURFACE

96 SHOTS IN ZONE 1  
122 SHOTS IN ZONE 2  
22 SHOTS IN ZONE 3

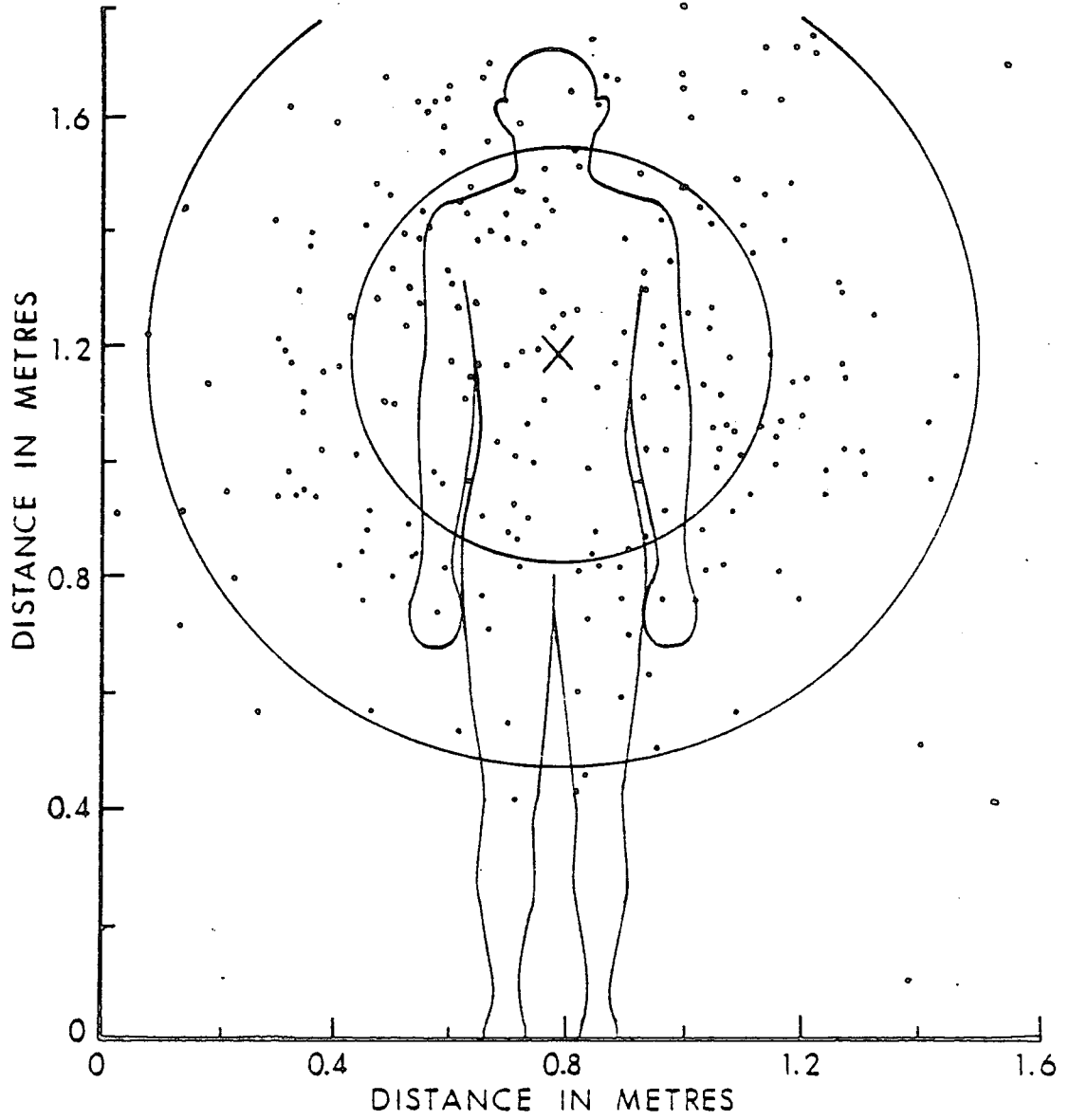


Figure 12. Group A Hit Distribution Superimposed on a Computer Man Silhouette at 12.1 Meter Range.

240 TOTAL SHOTS  
0 SHOTS MISSED  
PLOTTING SURFACE

103 SHOTS IN ZONE 1  
105 SHOTS IN ZONE 2  
32 SHOTS IN ZONE 3

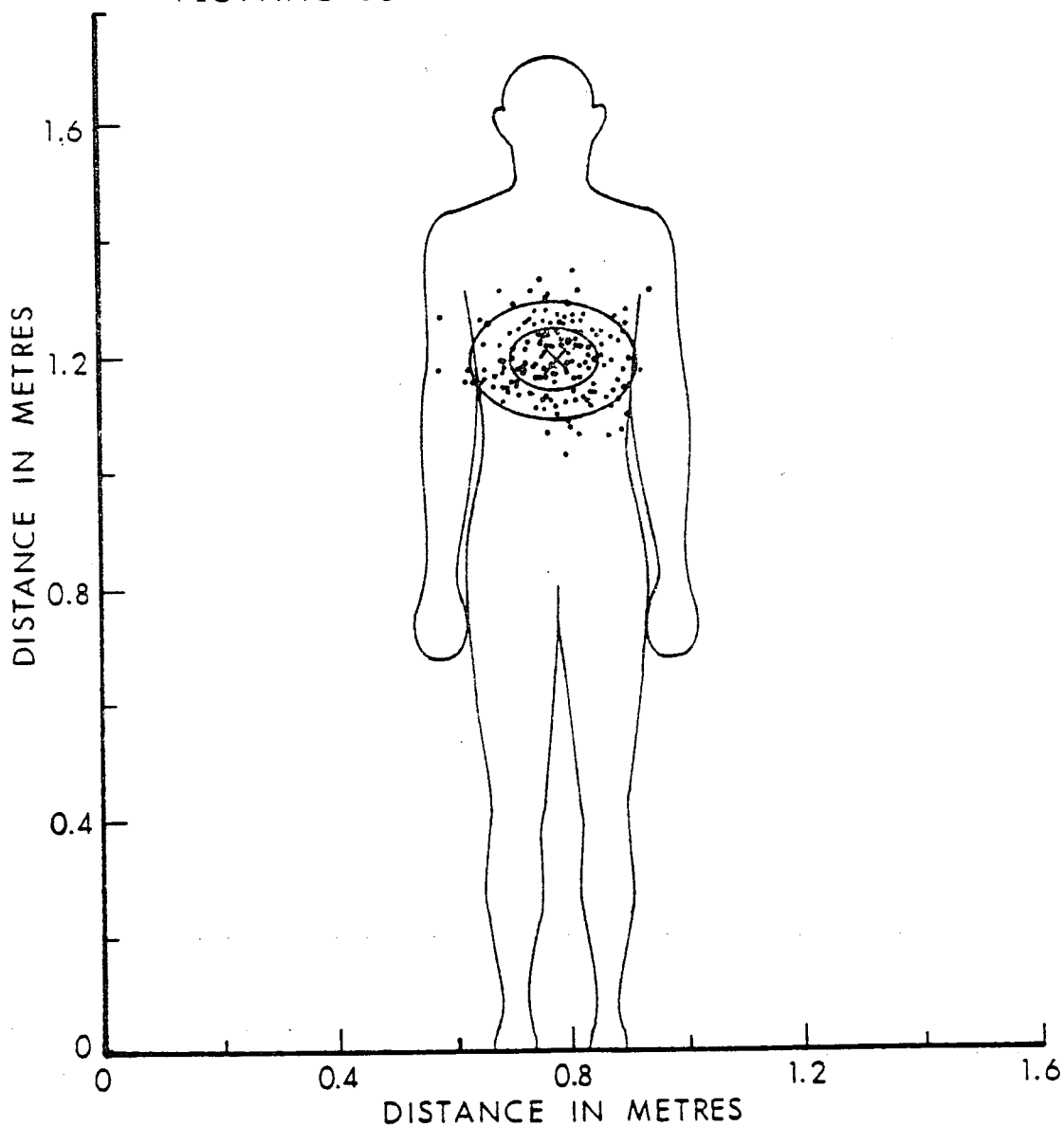


Figure 13. Group B Hit Distribution Superimposed on a Computer Man Silhouette at 3.0 Meter Range.

240 TOTAL SHOTS  
0 SHOTS MISSED  
PLOTTING SURFACE

96 SHOTS IN ZONE 1  
111 SHOTS IN ZONE 2  
33 SHOTS IN ZONE 3

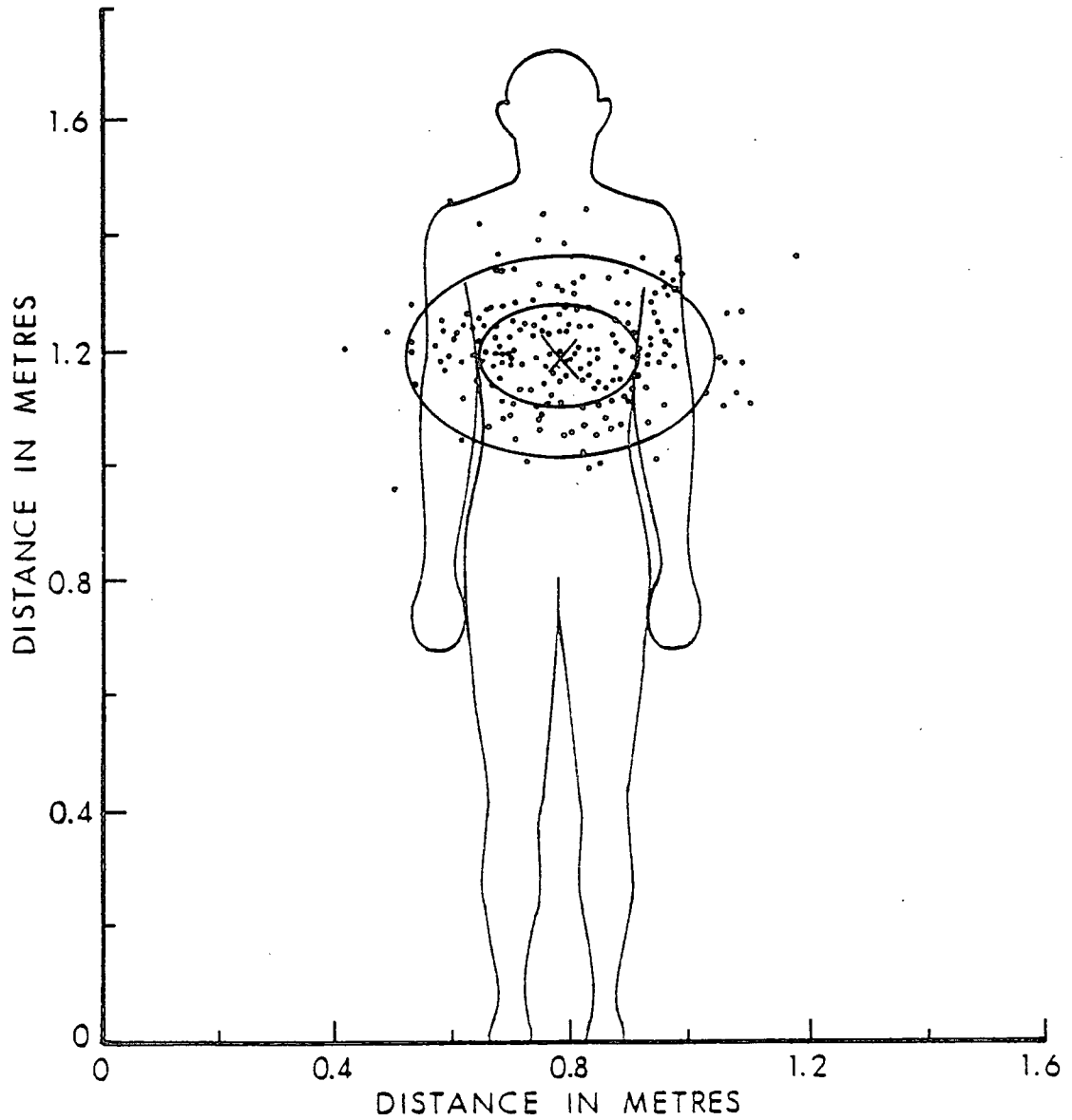


Figure 14. Group B Hit Distribution Superimposed on a Computer Man Silhouette at 6.0 Meter Range.

240 TOTAL SHOTS	105 SHOTS IN ZONE 1
0 SHOTS MISSED	112 SHOTS IN ZONE 2
PLOTTING SURFACE	23 SHOTS IN ZONE 3

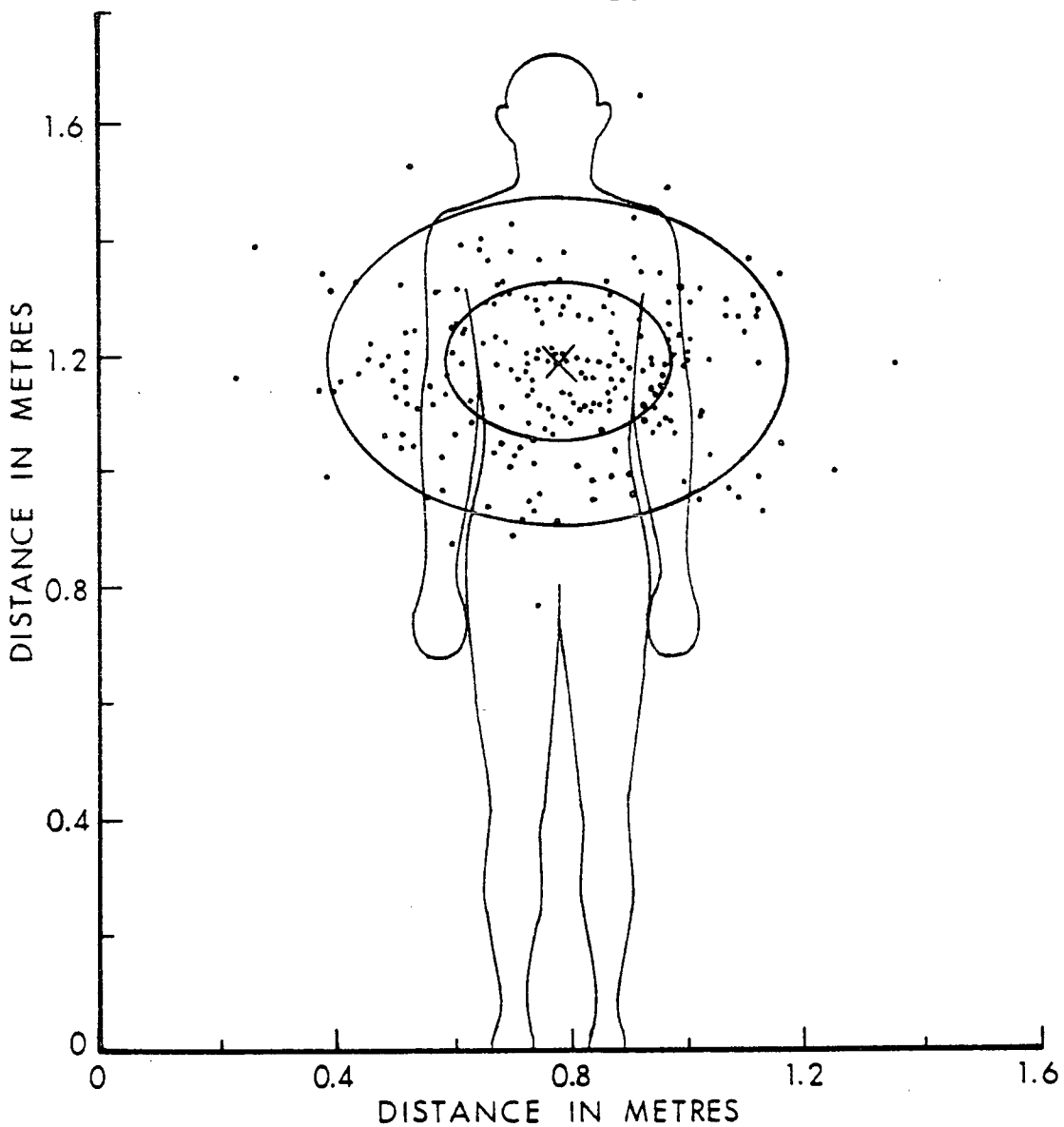


Figure 15. Group B Hit Distribution Superimposed on a Computer Man Silhouette at 12.1 Meter Range.

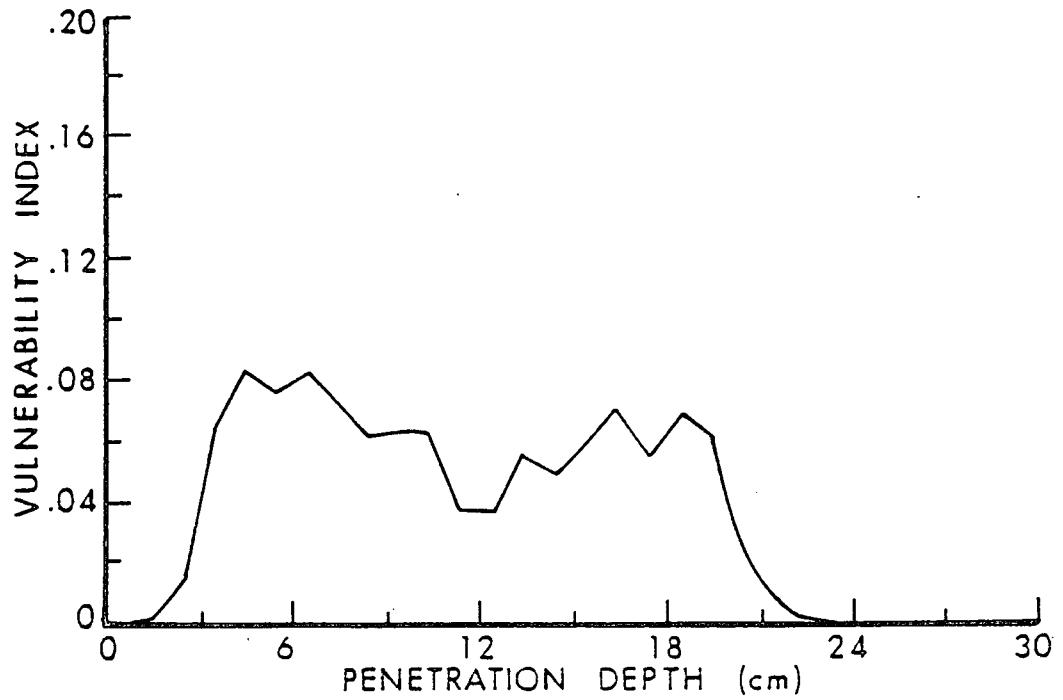


Figure 16. Vulnerability Index for Handguns at a Range of 3 Meters For The Group A Hit Distribution.

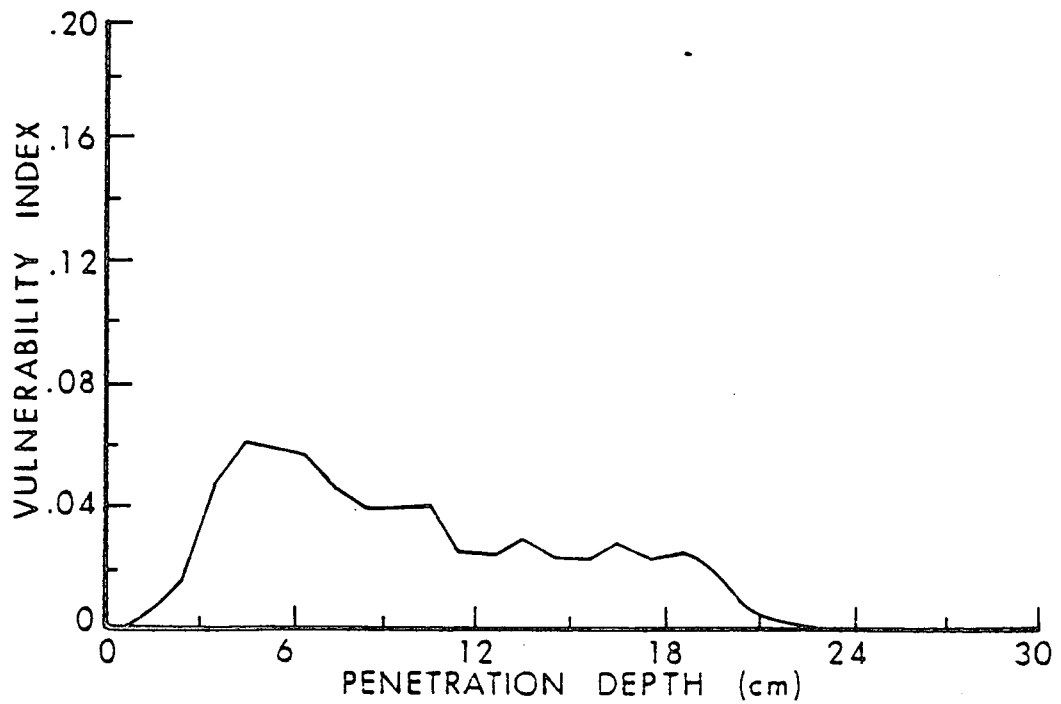


Figure 17. Vulnerability Index For Handguns at a Range of 6 Meters For The Group A Hit Distribution.

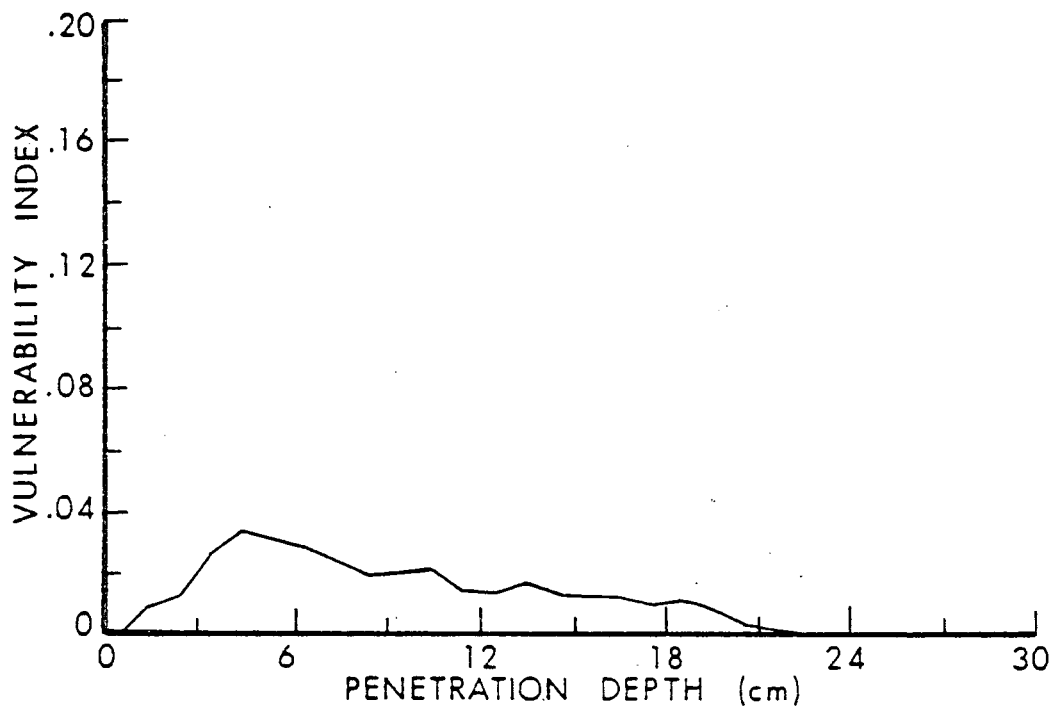


Figure 18. Vulnerability Index For Handguns at a Range of 12 Meters For The Group A Hit Distribution.

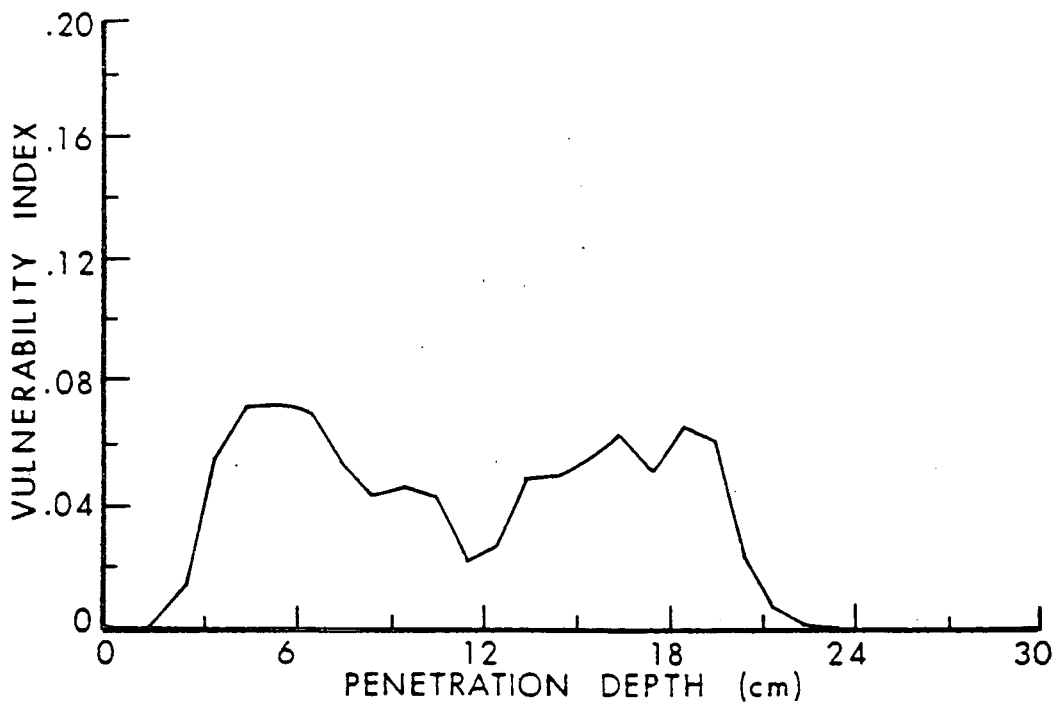


Figure 19. Vulnerability Index For Handguns at a Range of 6 Meters For The Group B Hit Distribution.

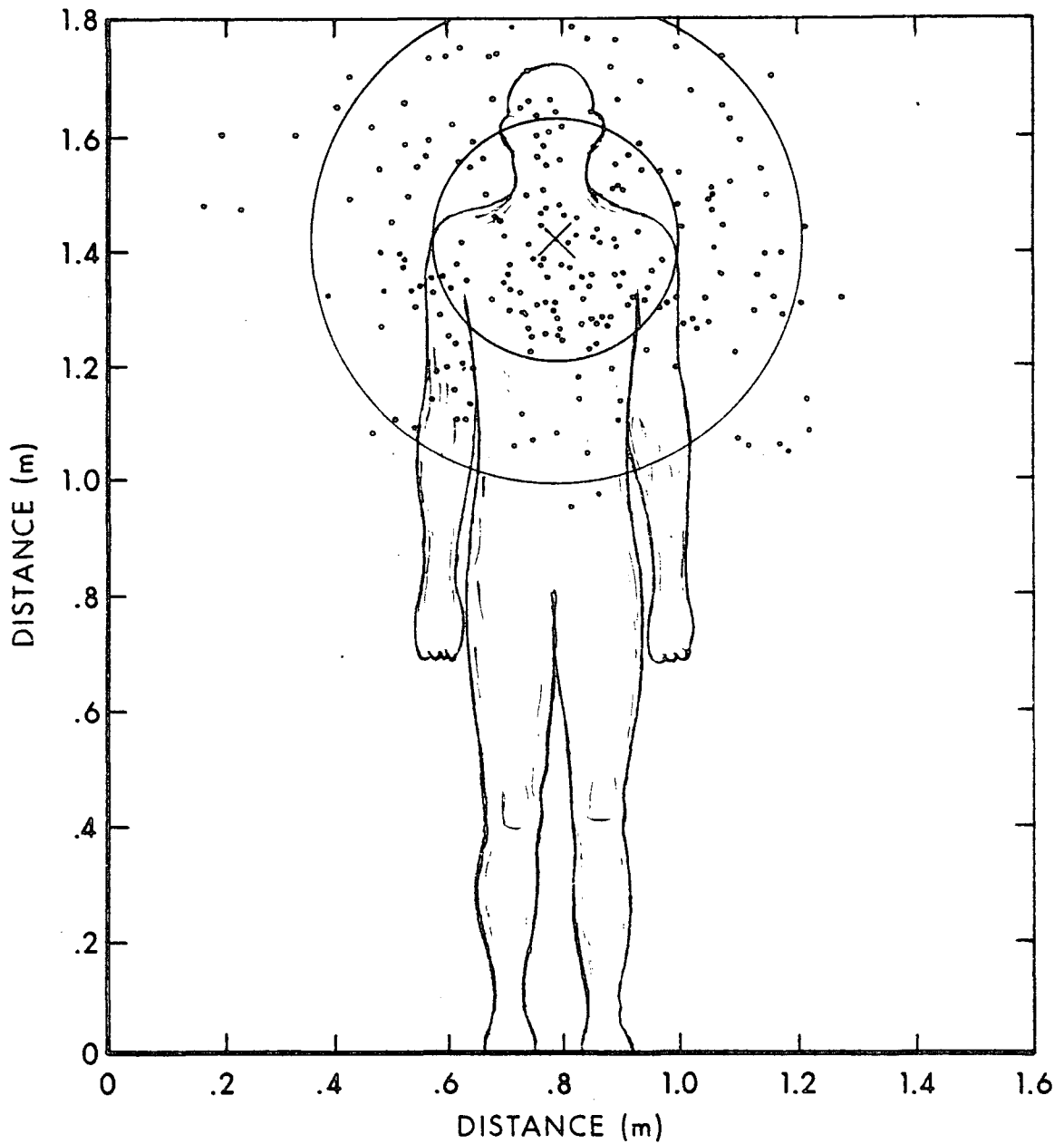


Figure 20. High Aim Point Hit Distribution Superimposed on a Computer Man Silhouette For Group A Shooters at a 6.0 Meter Range.

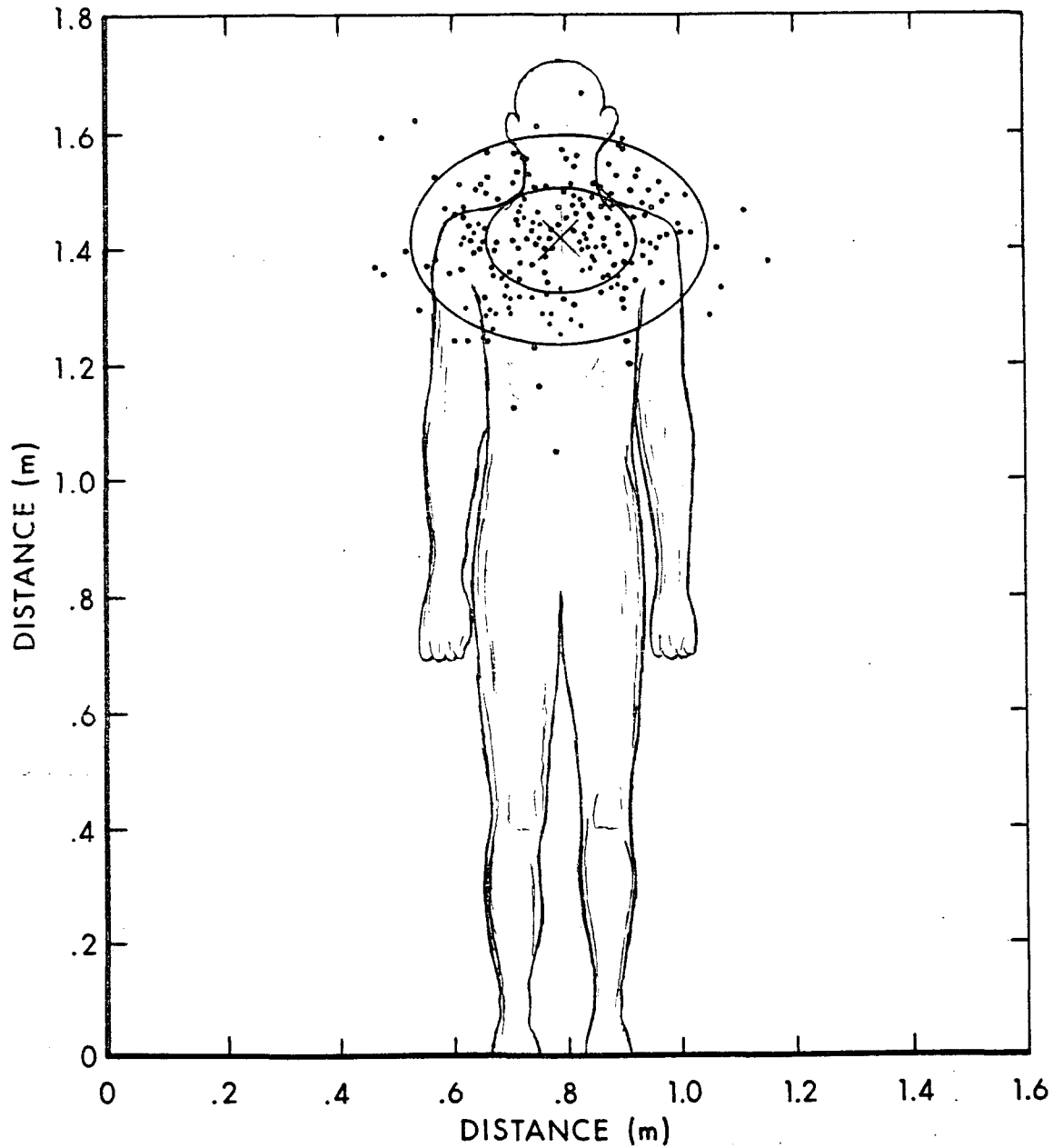


Figure 21. High Aim Point Hit Distribution Superimposed on a Computer Man Silhouette For Group B Shooters at a 6.0 Meter Range.

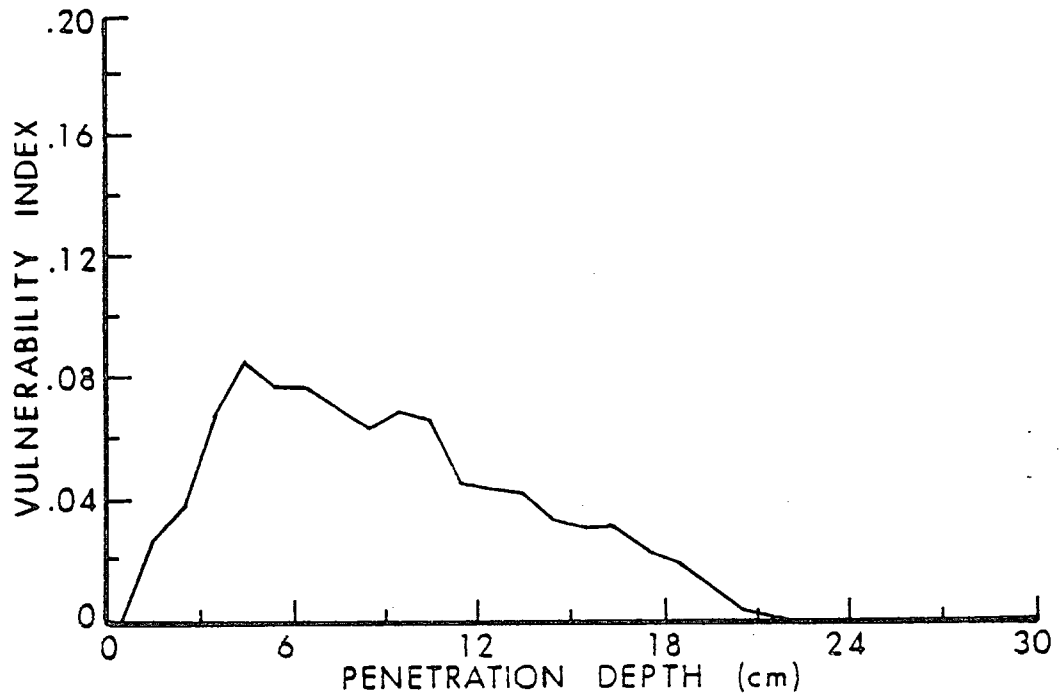


Figure 22. Vulnerability Index For Handguns at a Range of 6 Meters For the Group A Hit Distribution Using a High Aim Point.

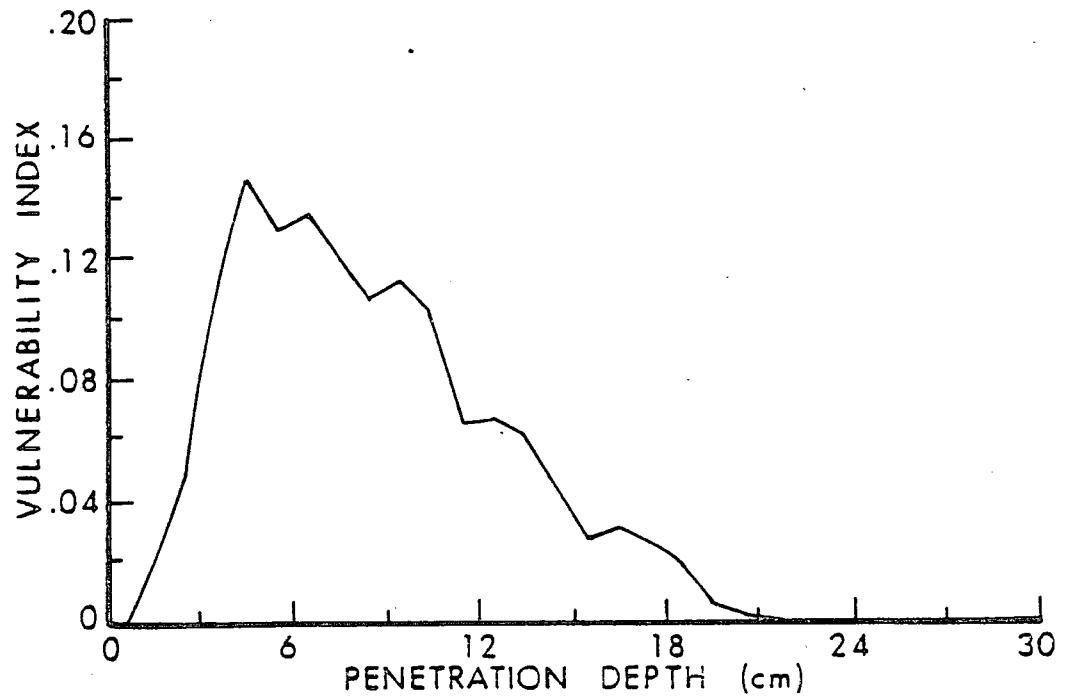


Figure 23. Vulnerability Index For Handguns at a Range of 6 Meters For the Group B Hit Distribution Using a High Aim Point.

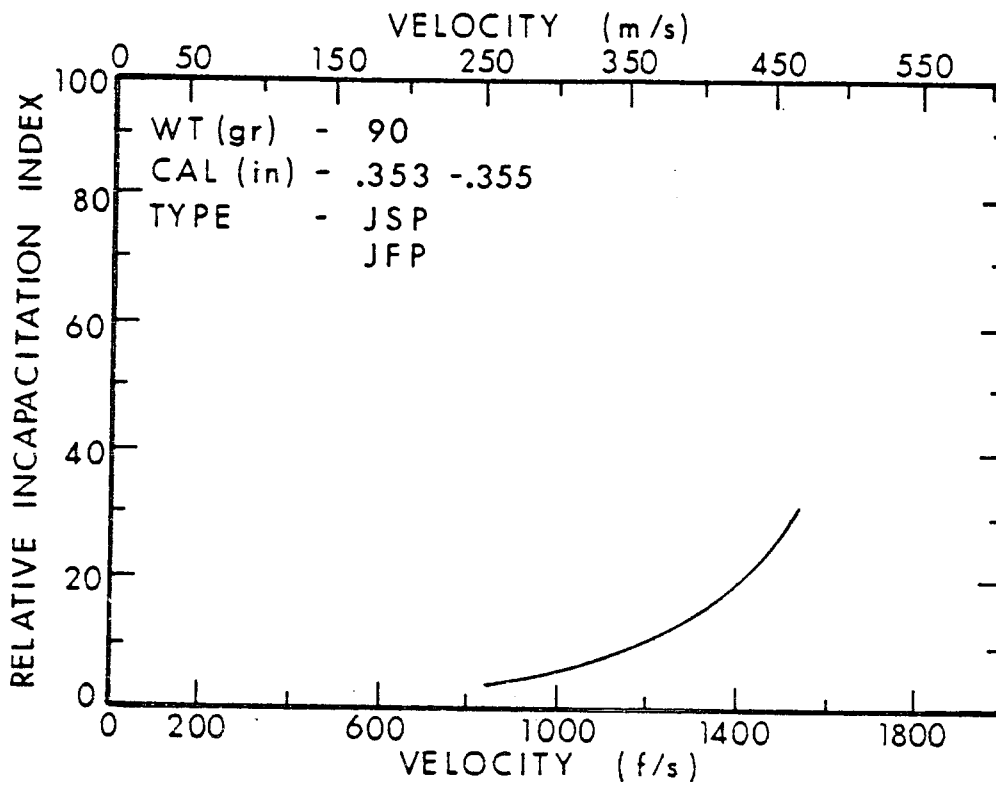


Figure 24. Relative Incapacitation Index For 90 Grain, Caliber .353, JSP, JFP Bullets.

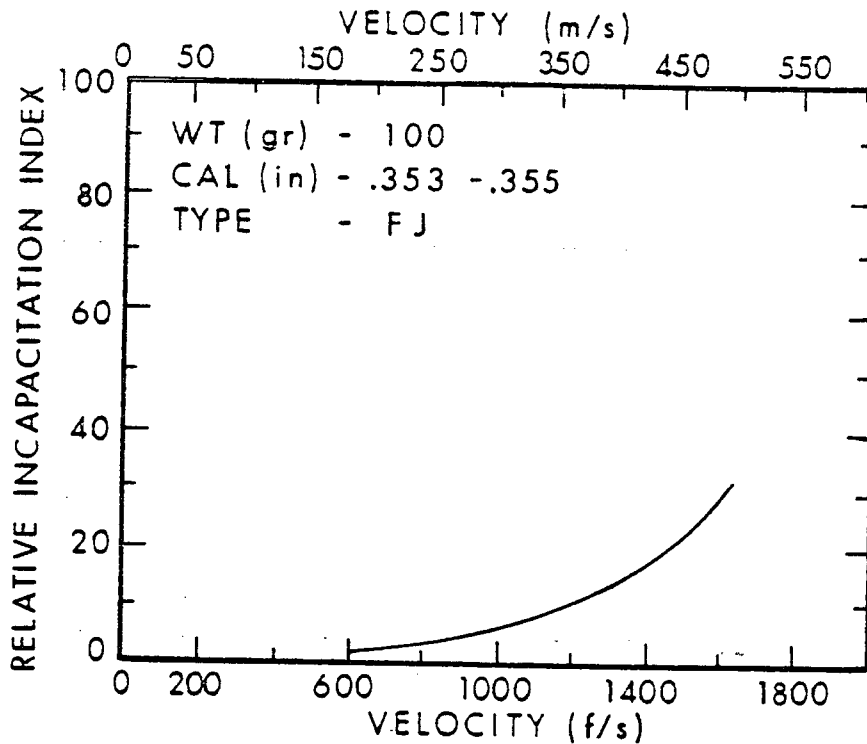


Figure 25. Relative Incapacitation Index For 100 Grain, Caliber .353, FJ Bullets.

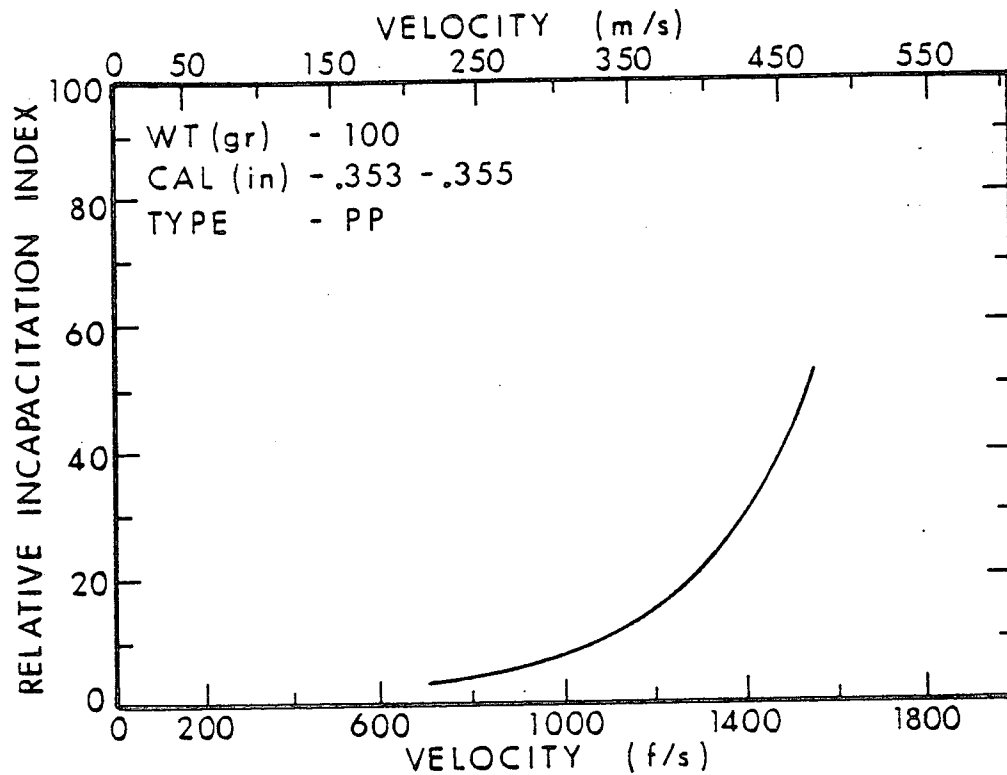


Figure 26. Relative Incapacitation Index For 100 Grain, Caliber .353, PP Bullets.

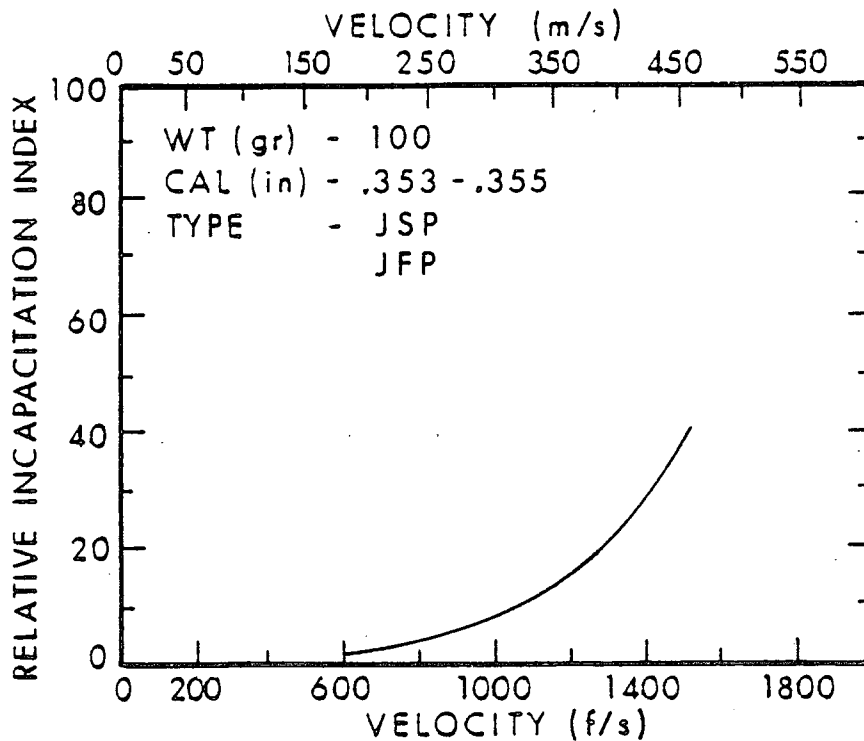


Figure 27. Relative Incapacitation Index For 100 Grain, Caliber .353, JSP, JFP Bullets.

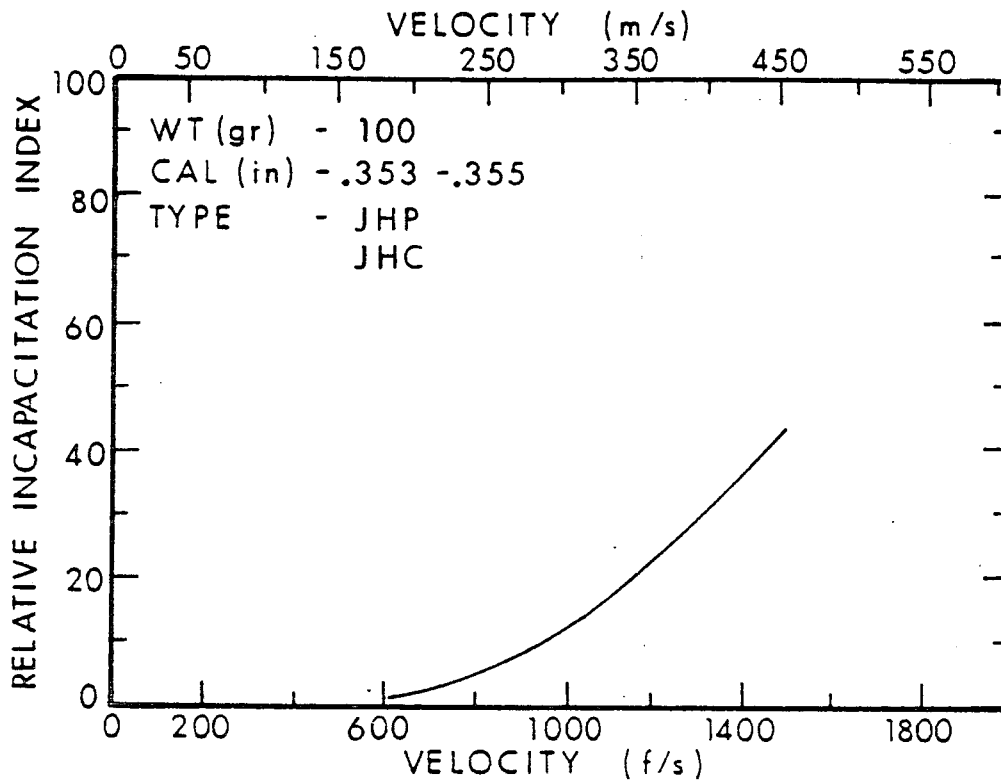


Figure 28. Relative Incapacitation Index For 100 Grain, Caliber .353, JHP, JHC Bullets.

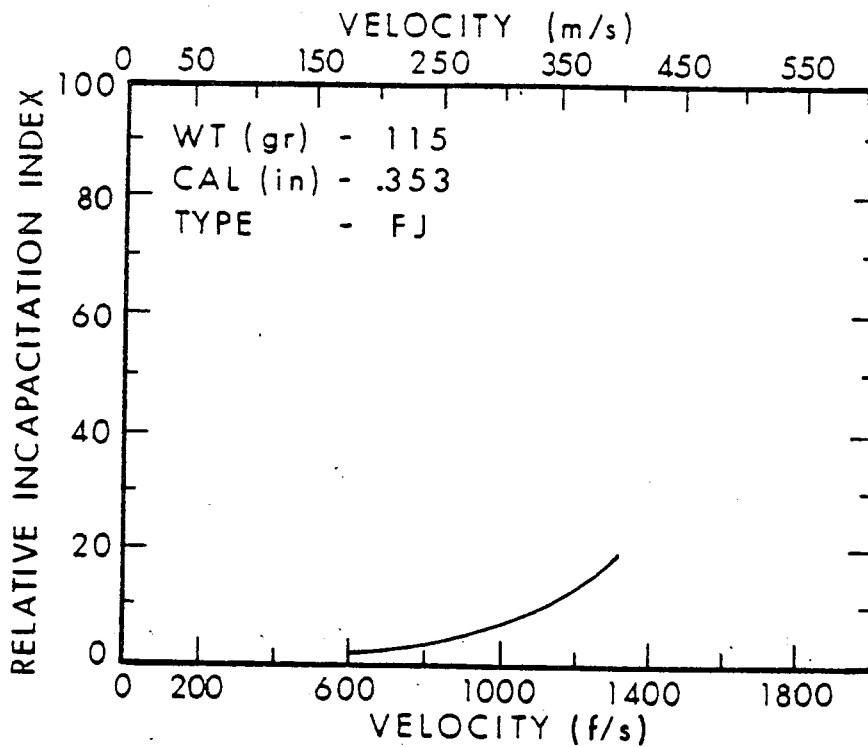


Figure 29. Relative Incapacitation Index For 115 Grain, Caliber .353, FJ Bullets.

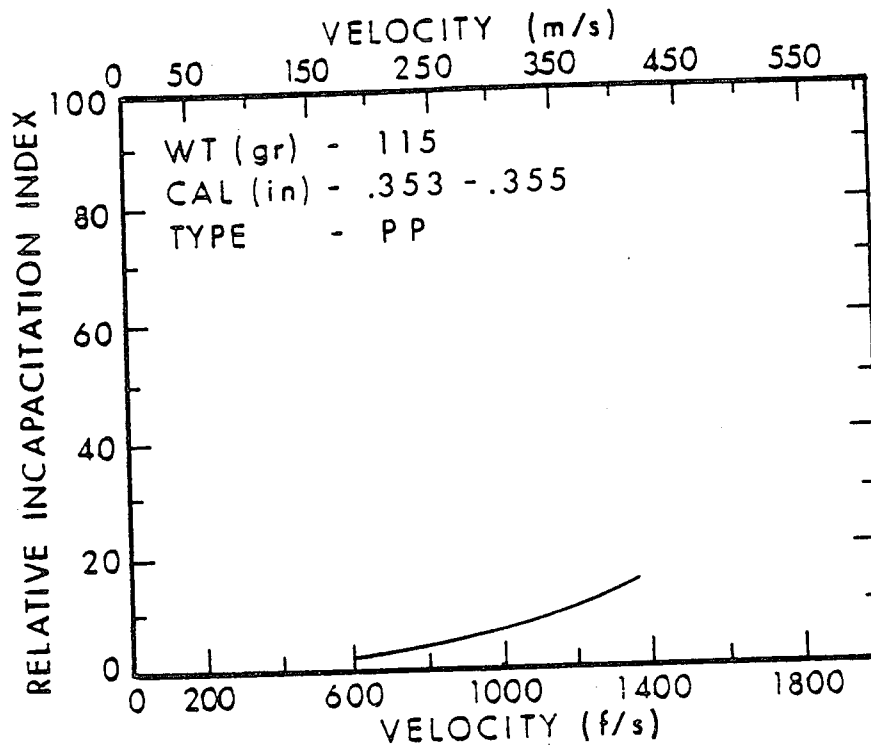


Figure 30. Relative Incapacitation Index For 115 Grain, Caliber .353, PP Bullets.

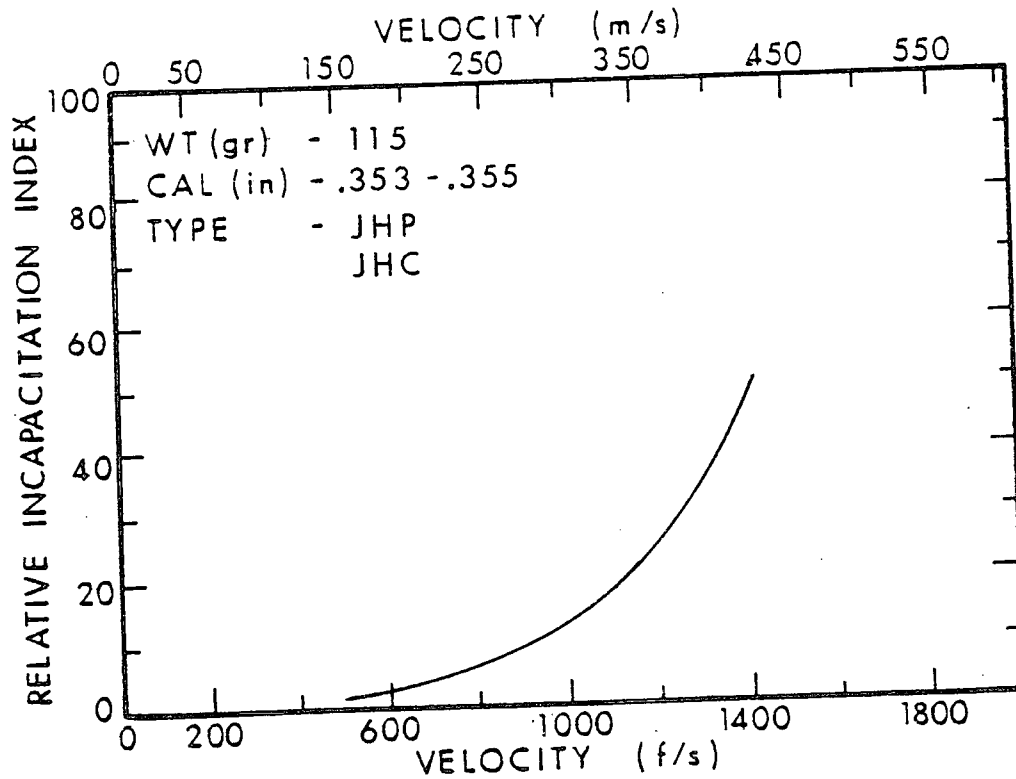


Figure 31. Relative Incapacitation Index For 115 Grain, Caliber .353, JHP, JHC Bullets.

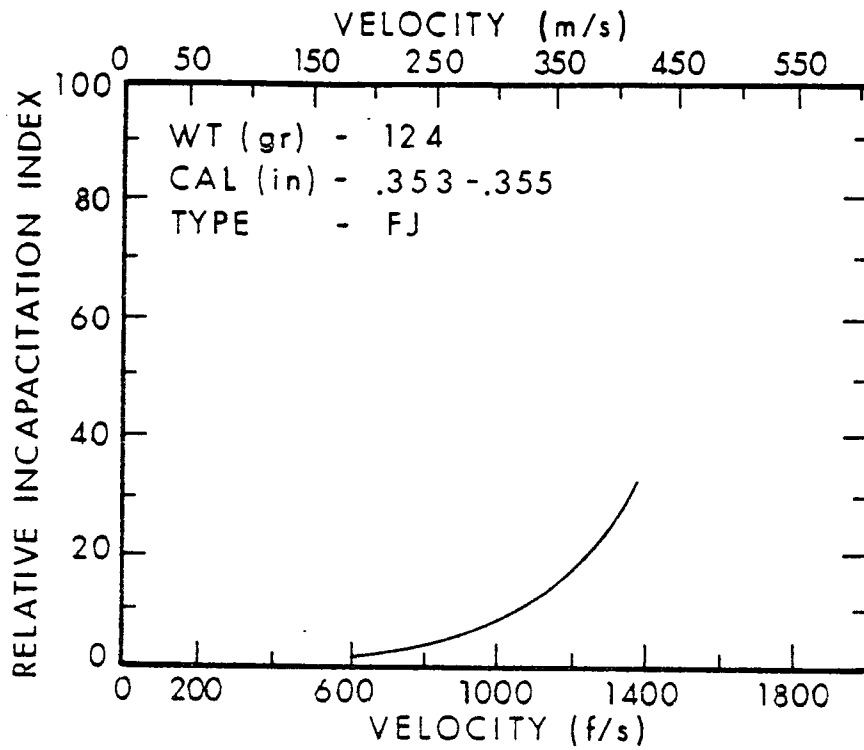


Figure 32. Relative Incapacitation Index For 124 Grain, Caliber .353, FJ Bullets.

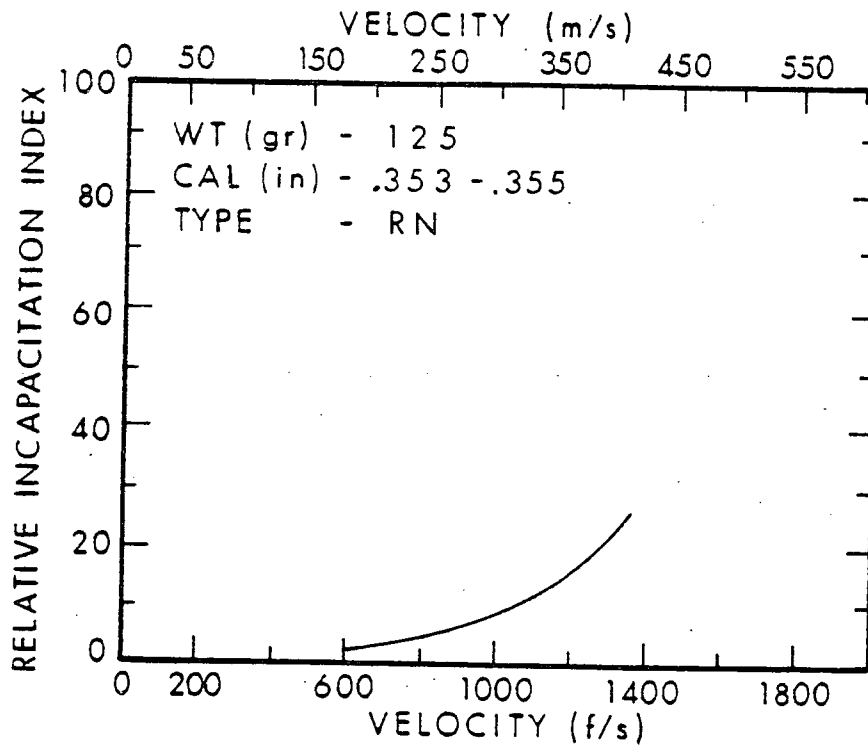


Figure 33. Relative Incapacitation Index For 125 Grain, Caliber .353, RN Bullets.

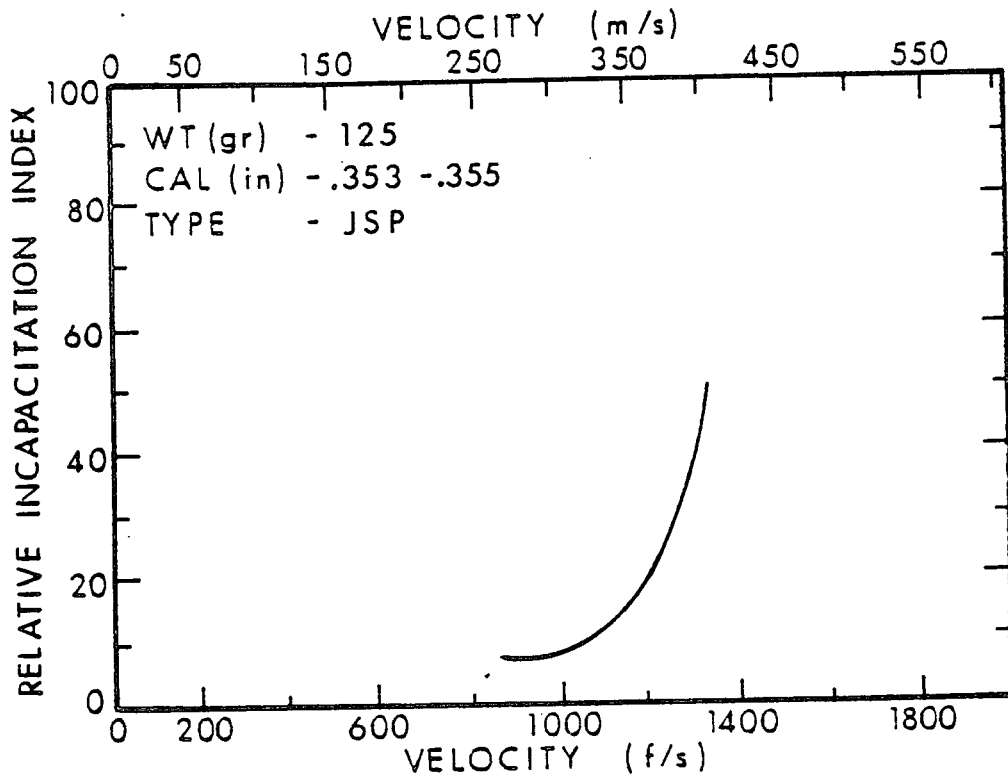


Figure 34. Relative Incapacitation Index For 125 Grain, Caliber .353, JSP Bullets.

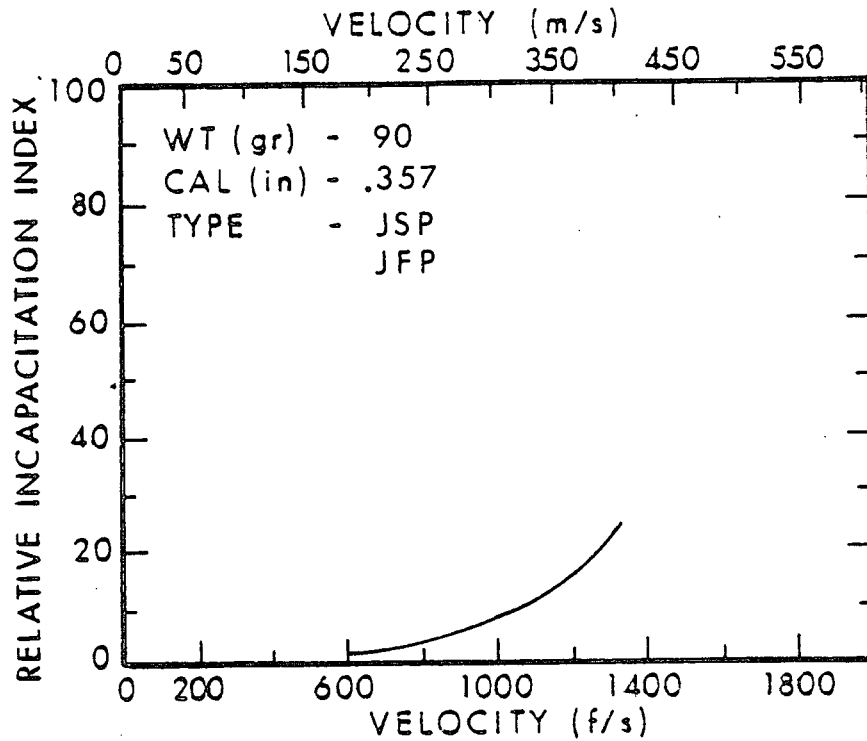


Figure 35. Relative Incapacitation Index For 90 Grain, Caliber .357, JSP, JFP Bullets.

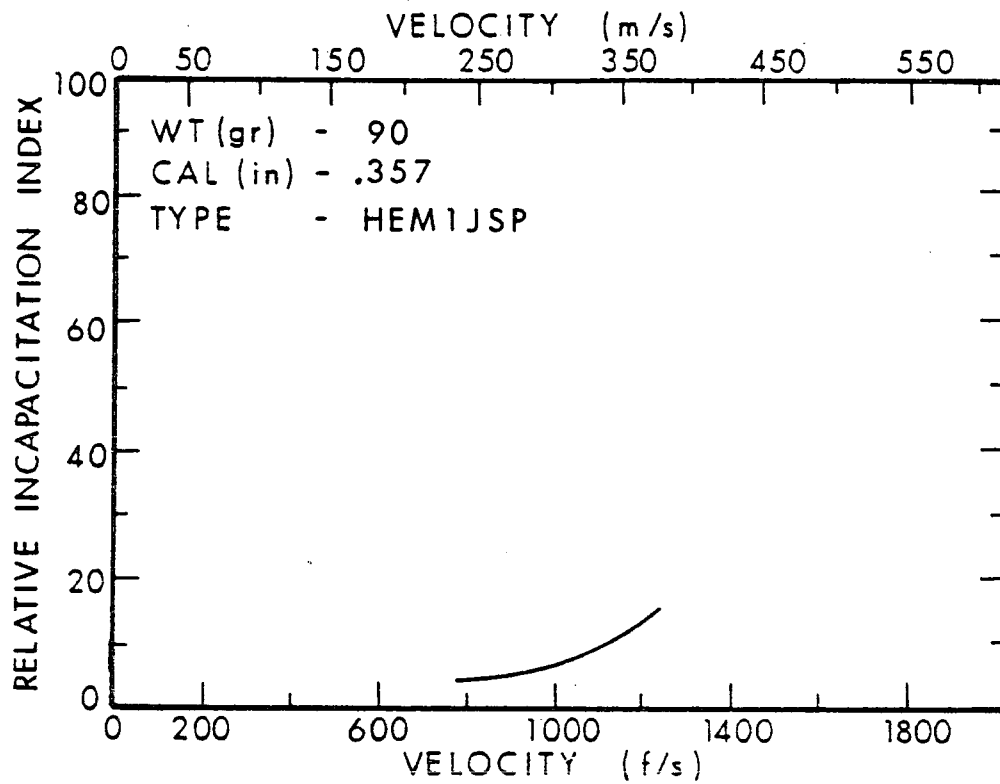


Figure 36. Relative Incapacitation Index For 90 Grain, Caliber .357, HEM1JSP Bullets.

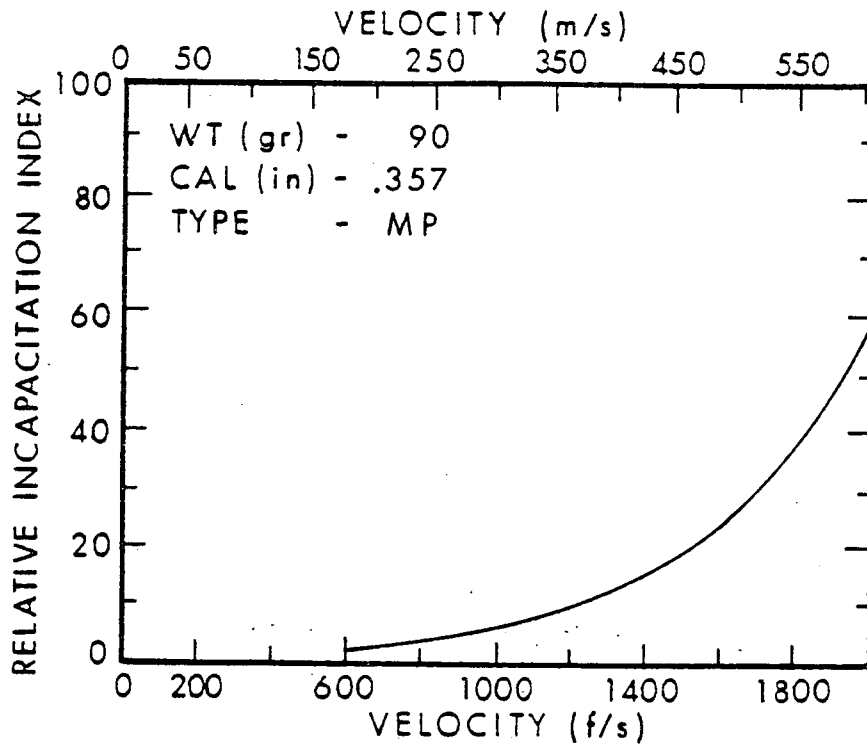


Figure 37. Relative Incapacitation Index For 90 Grain, Caliber .357, MP Bullets.

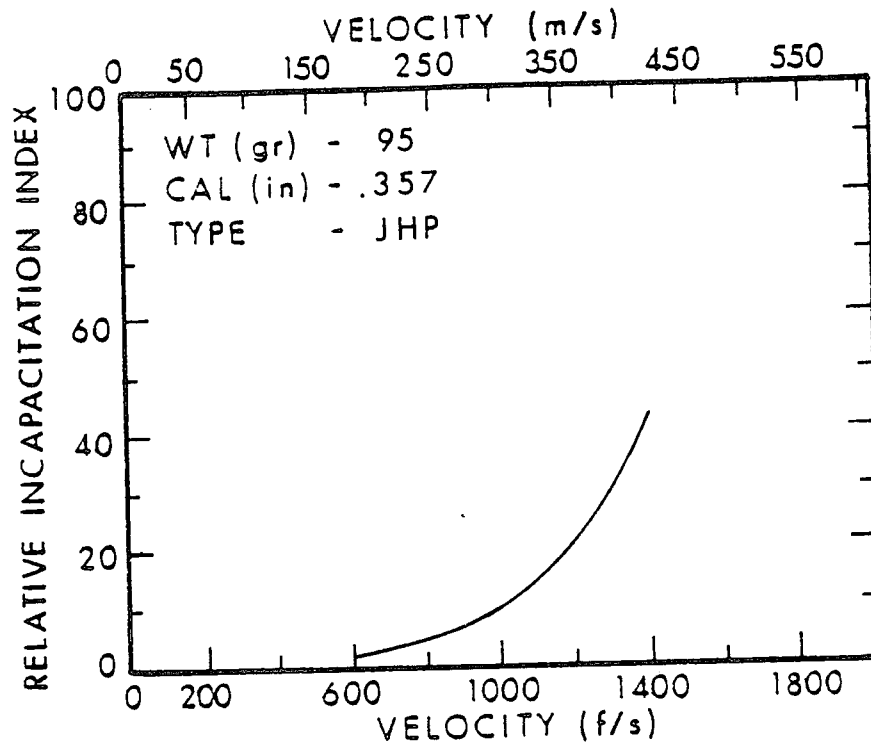


Figure 38. Relative Incapacitation Index For 95 Grain, Caliber .357, JHP Bullets.

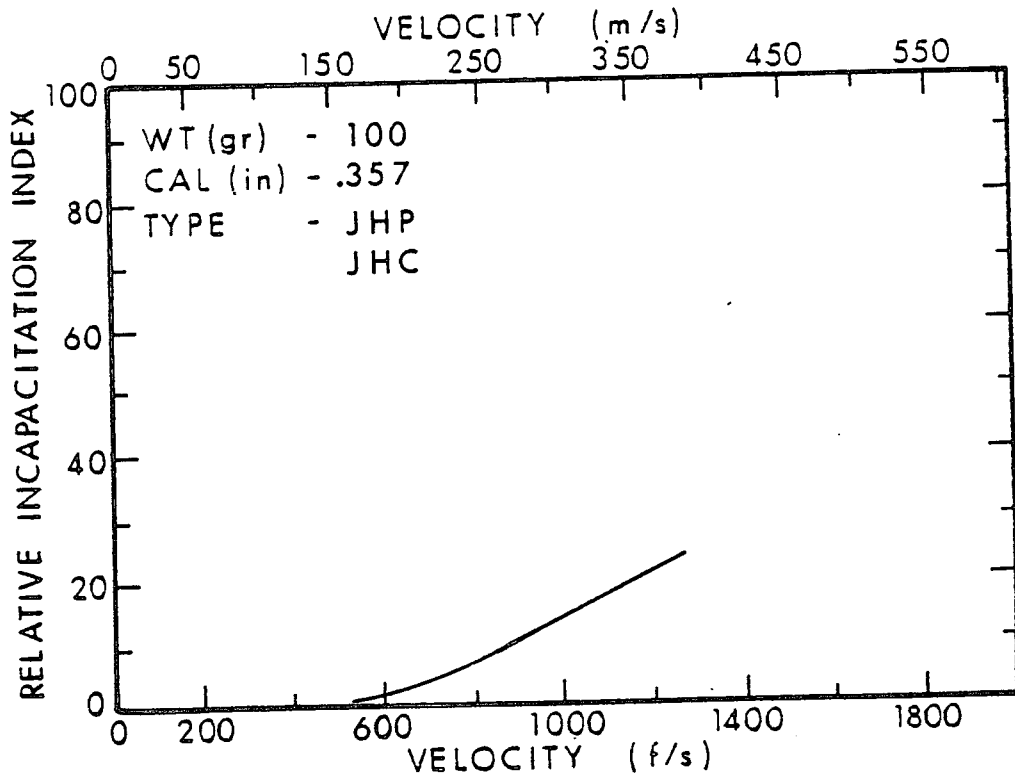


Figure 39. Relative Incapacitation Index For 100 Grain, Caliber .357, JHP, JHC Bullets.

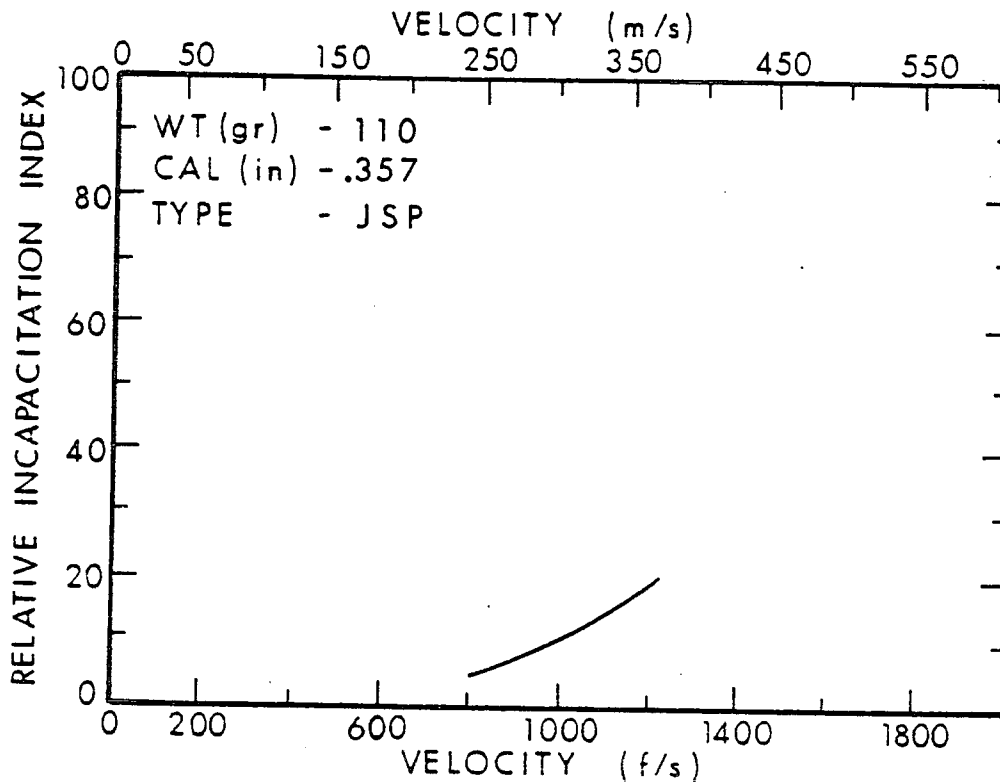


Figure 40. Relative Incapacitation Index For 110 Grain, Caliber .357, JSP Bullets.

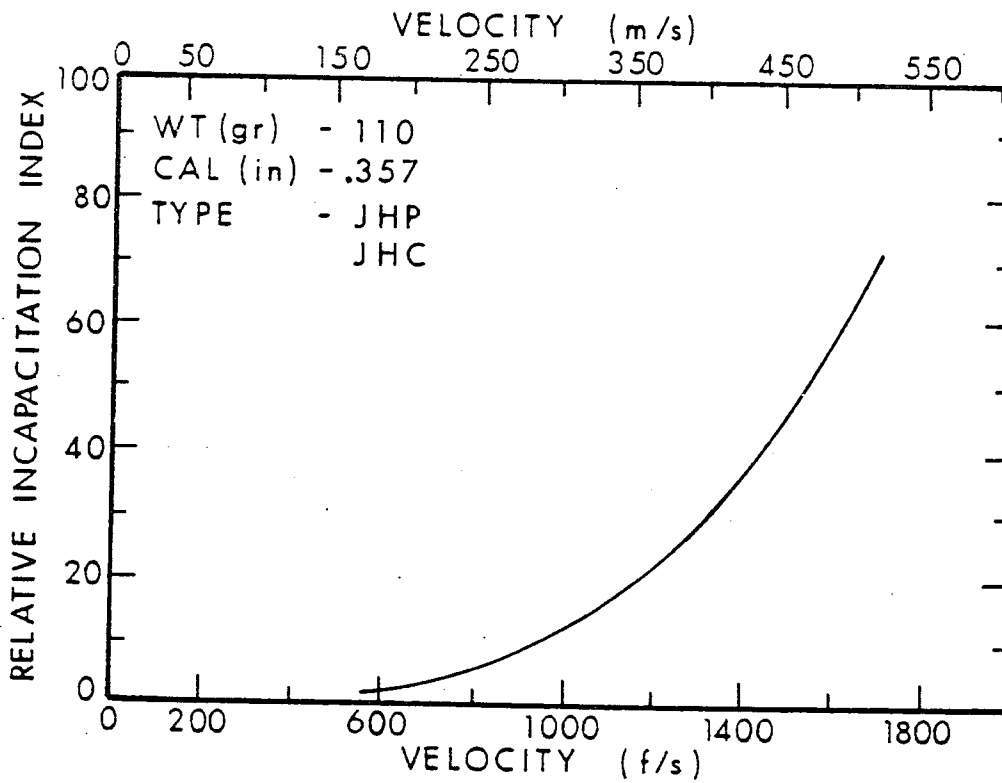


Figure 41. Relative Incapacitation Index For 110 Grain, Caliber .357, JHP, JHC Bullets.

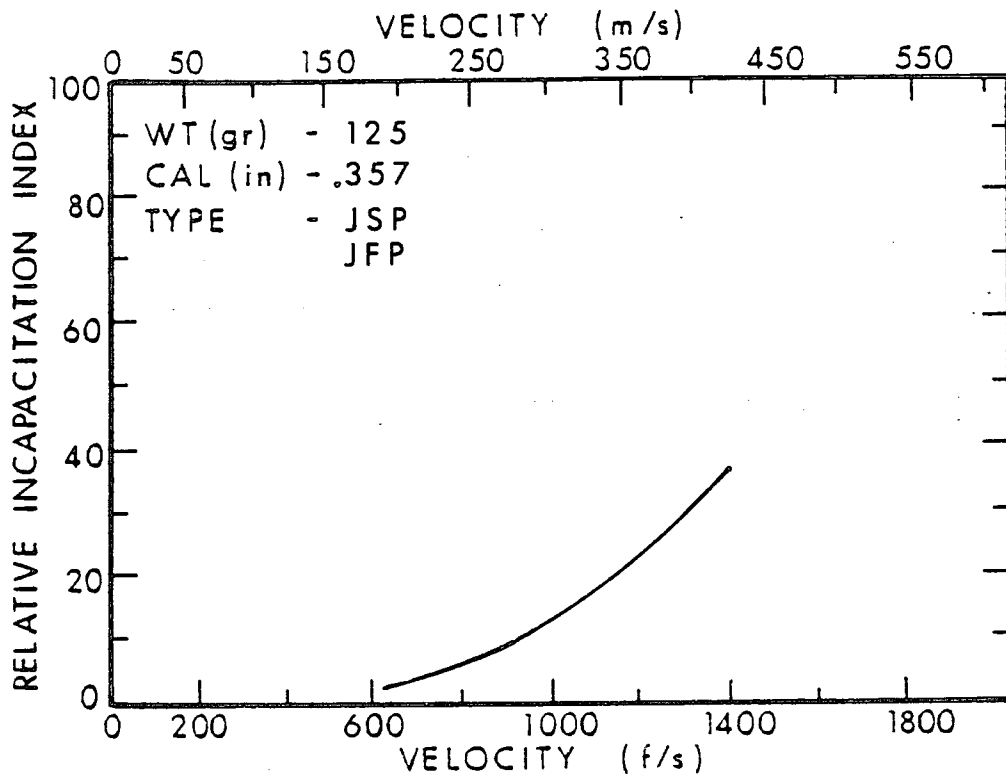


Figure 42. Relative Incapacitation Index For 125 Grain, Caliber .357, JSP, JFP Bullets.

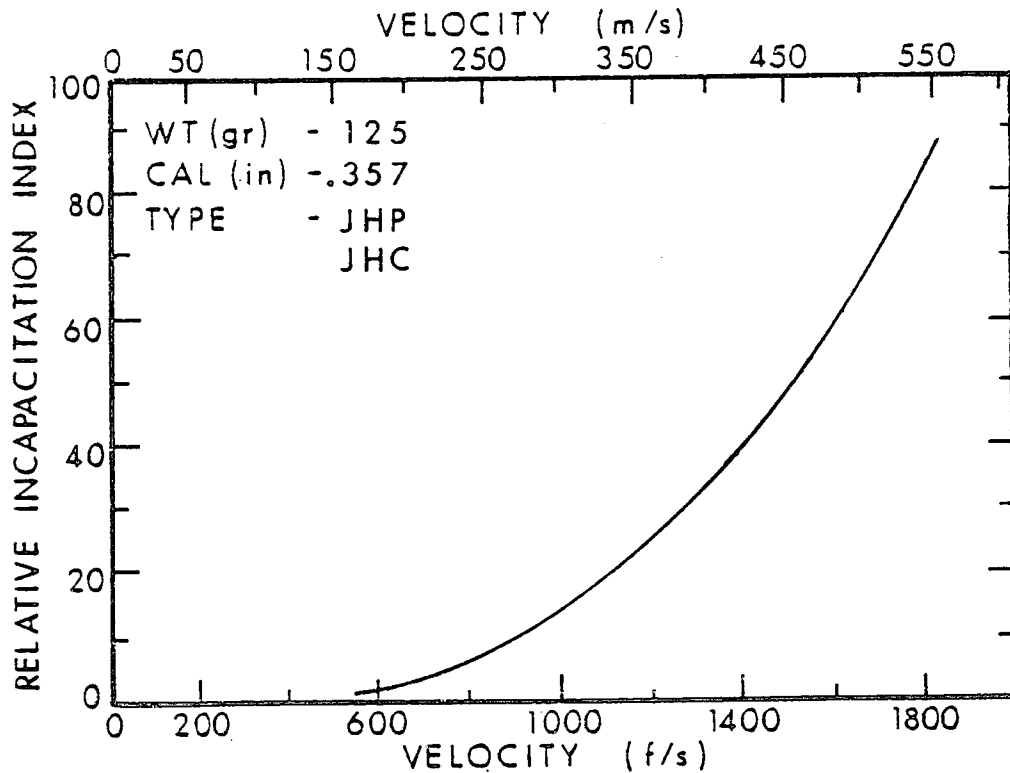


Figure 43. Relative Incapacitation Index For 125 Grain, Caliber .357, JHP, JHC Bullets.

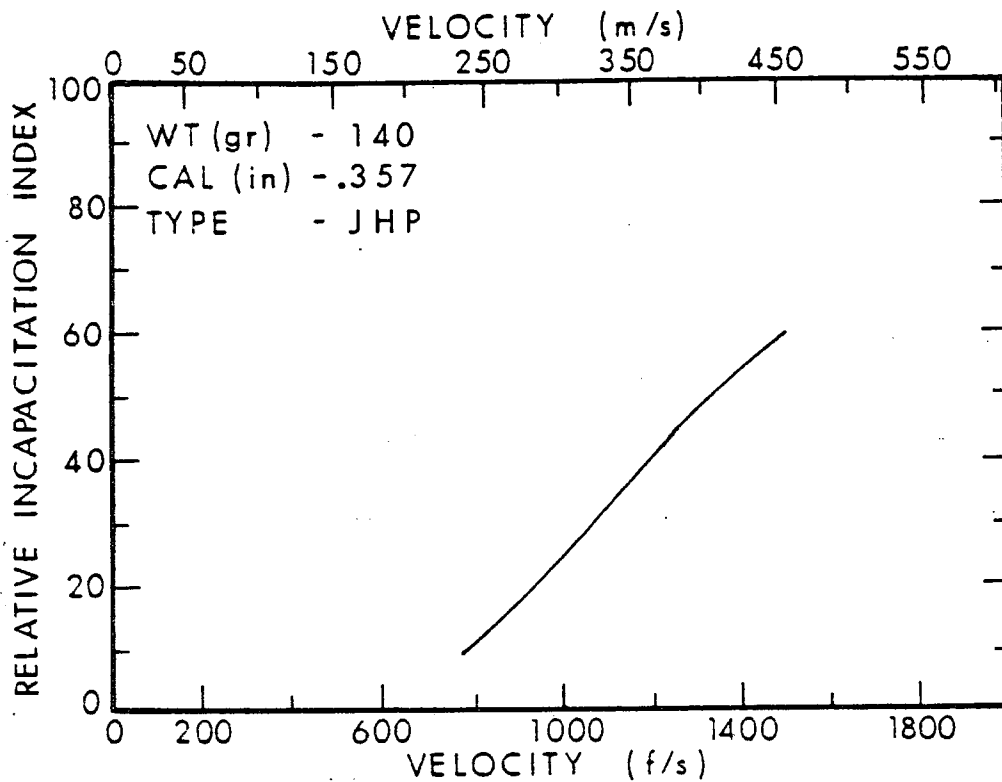


Figure 44. Relative Incapacitation Index For 140 Grain, Caliber .357, JHP Bullets.

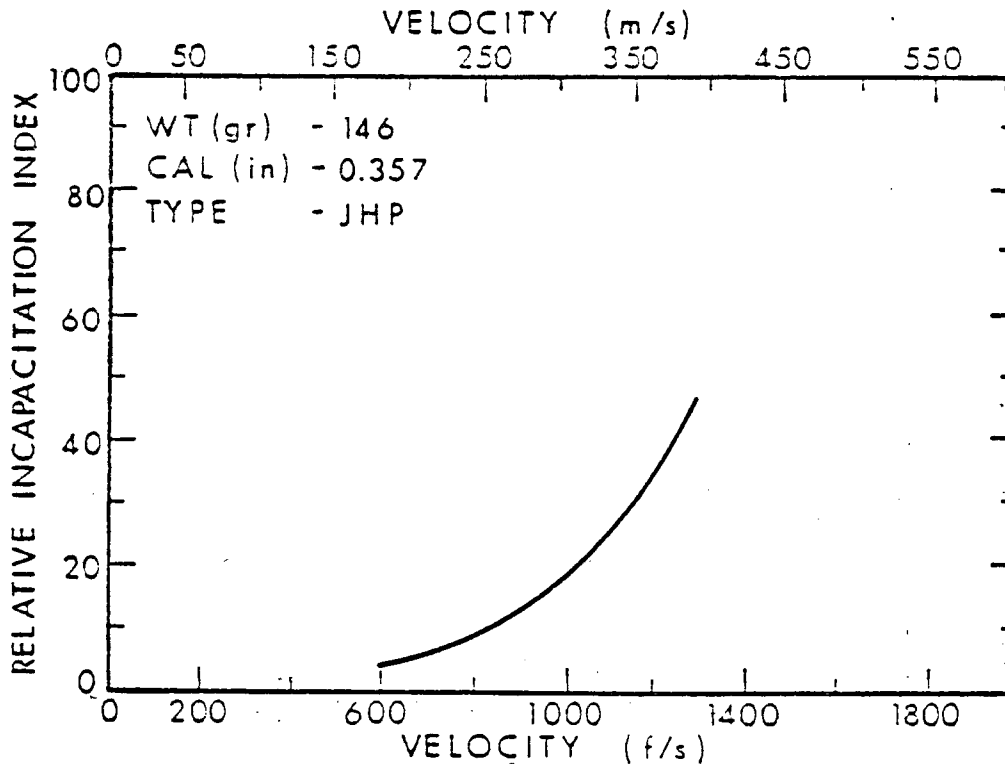


Figure 45. Relative Incapacitation Index For 146 Grain, Caliber .357, JHP Bullets.

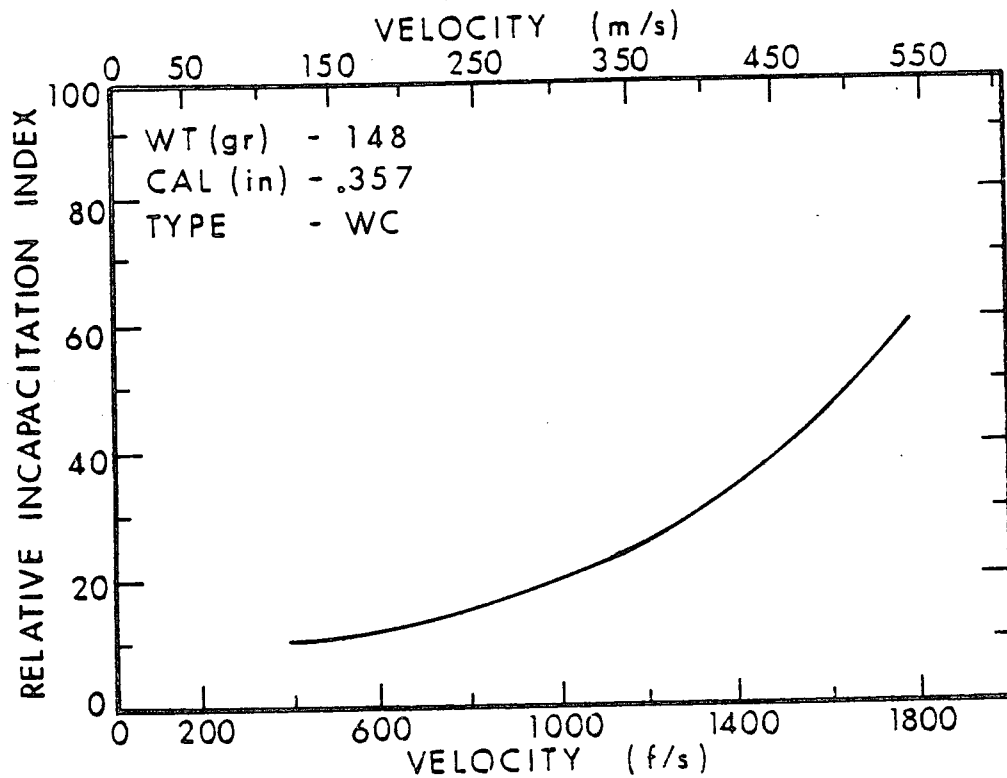


Figure 46. Relative Incapacitation Index For 148 Grain, Caliber .357, WC Bullets.

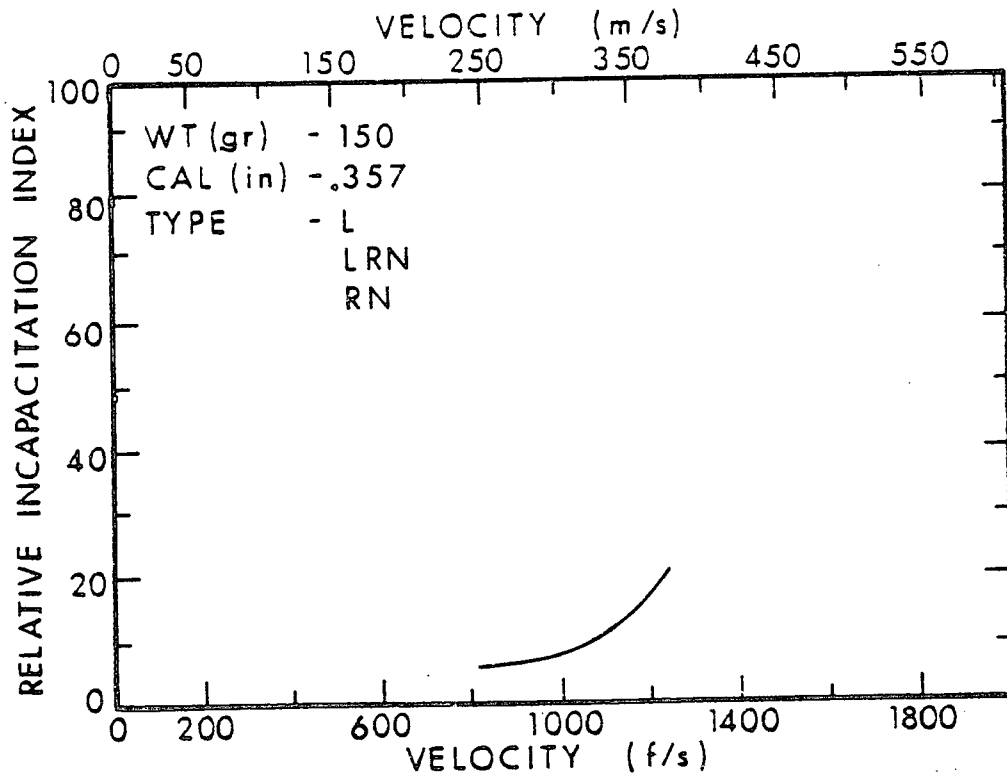


Figure 47. Relative Incapacitation Index For 150 Grain, Caliber .357, L, LRN, RN Bullets.

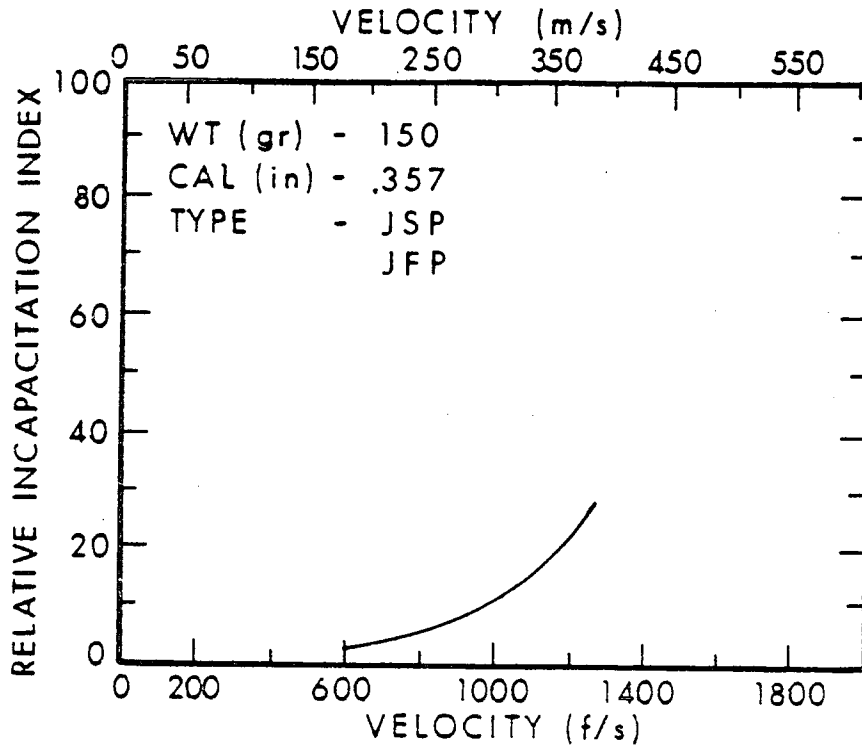


Figure 48. Relative Incapacitation Index For 150 Grain, Caliber .357, JSP, JFP Bullets.

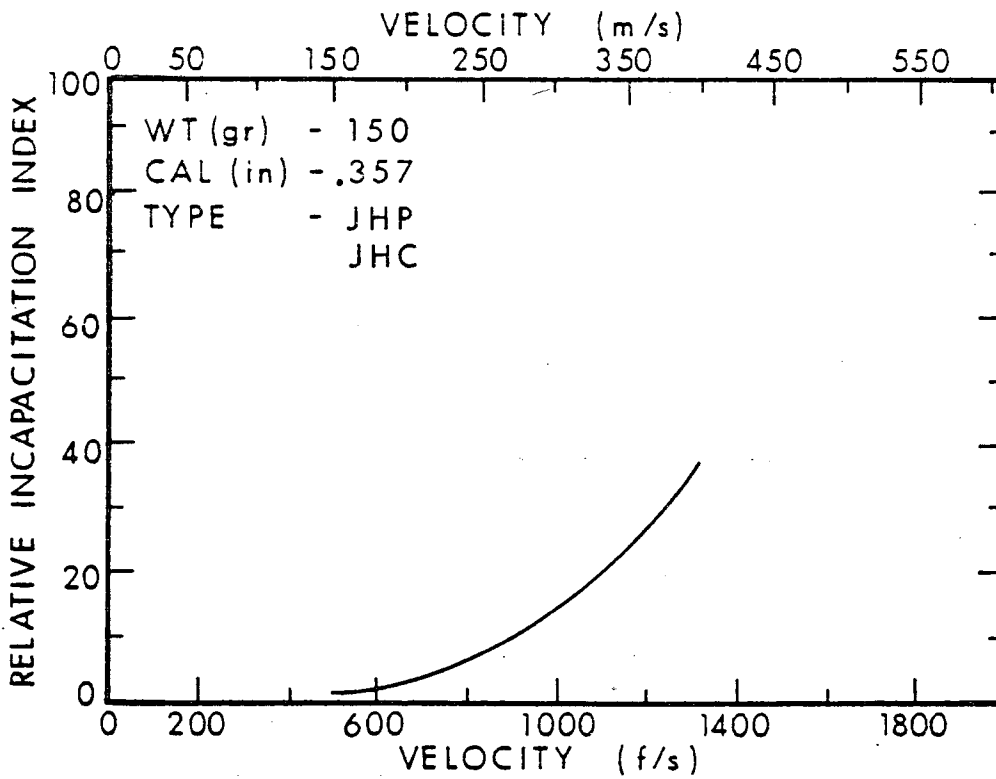


Figure 49. Relative Incapacitation Index For 150 Grain, Caliber .357, JHP, JHC Bullets.

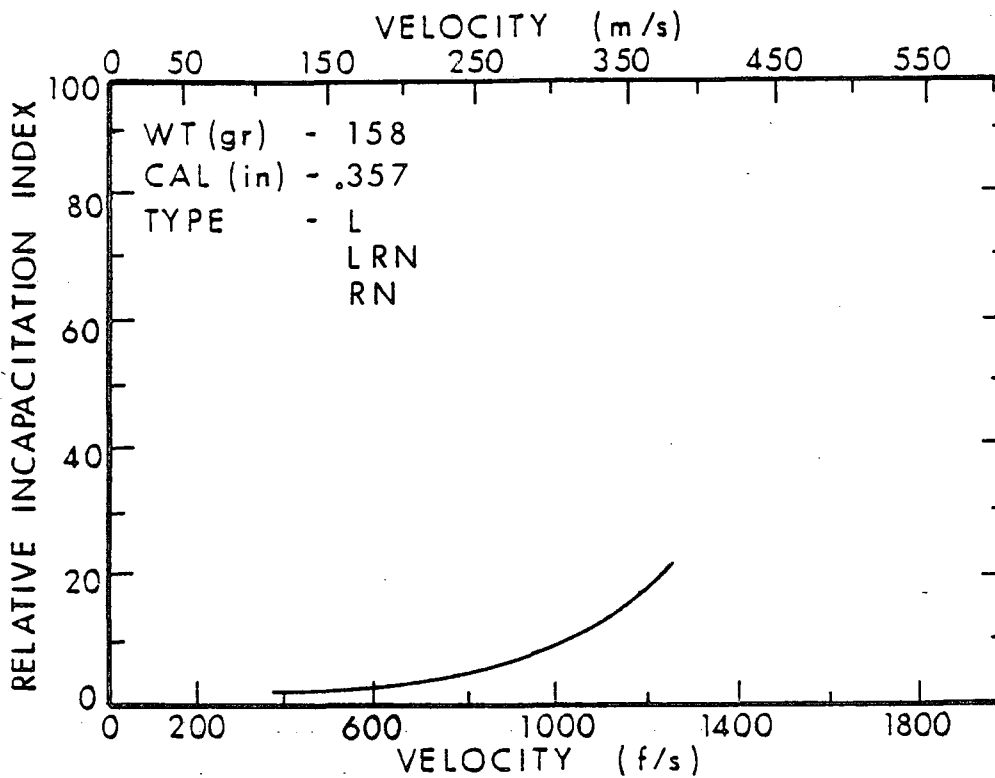


Figure 50. Relative Incapacitation Index For 158 Grain, Caliber .357, L, LRN, RN Bullets.

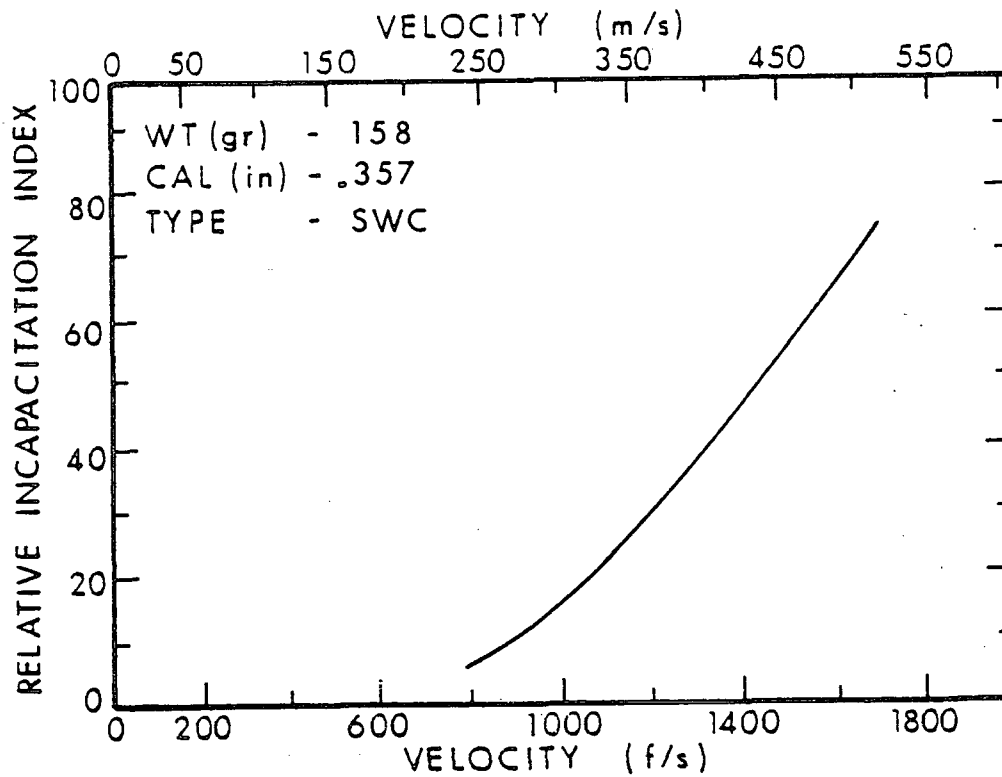


Figure 51. Relative Incapacitation Index For 158 Grain, Caliber .357, SWC Bullets.

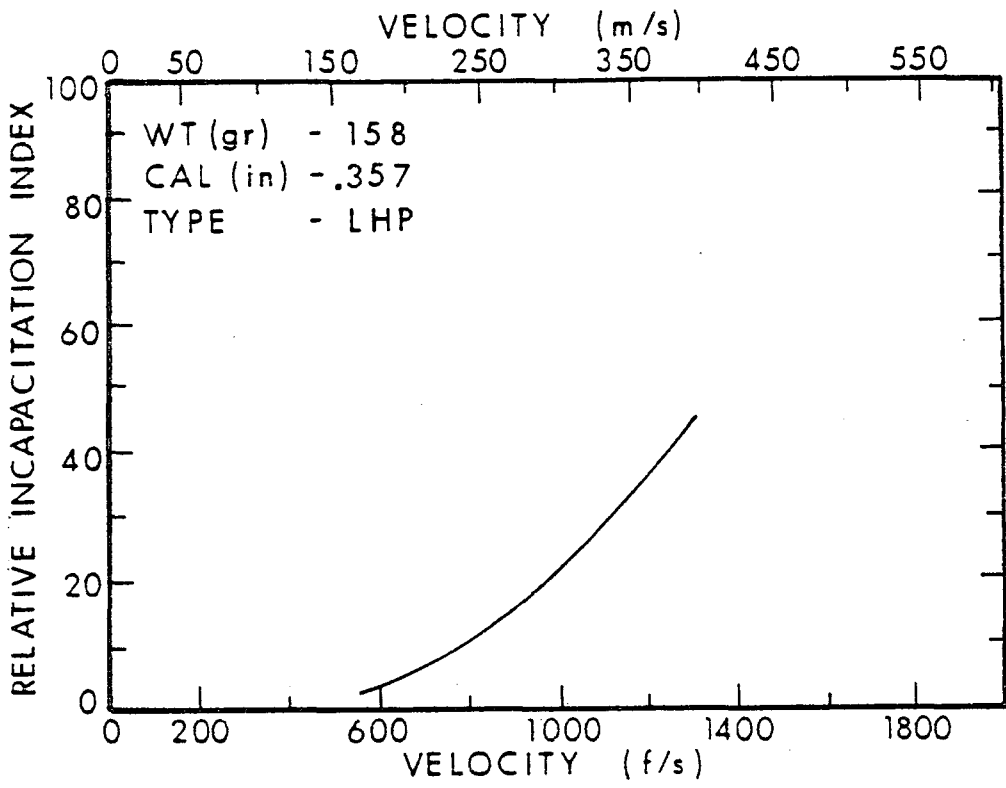


Figure 52. Relative Incapacitation Index For 158 Grain, Caliber .357, LHP Bullets.

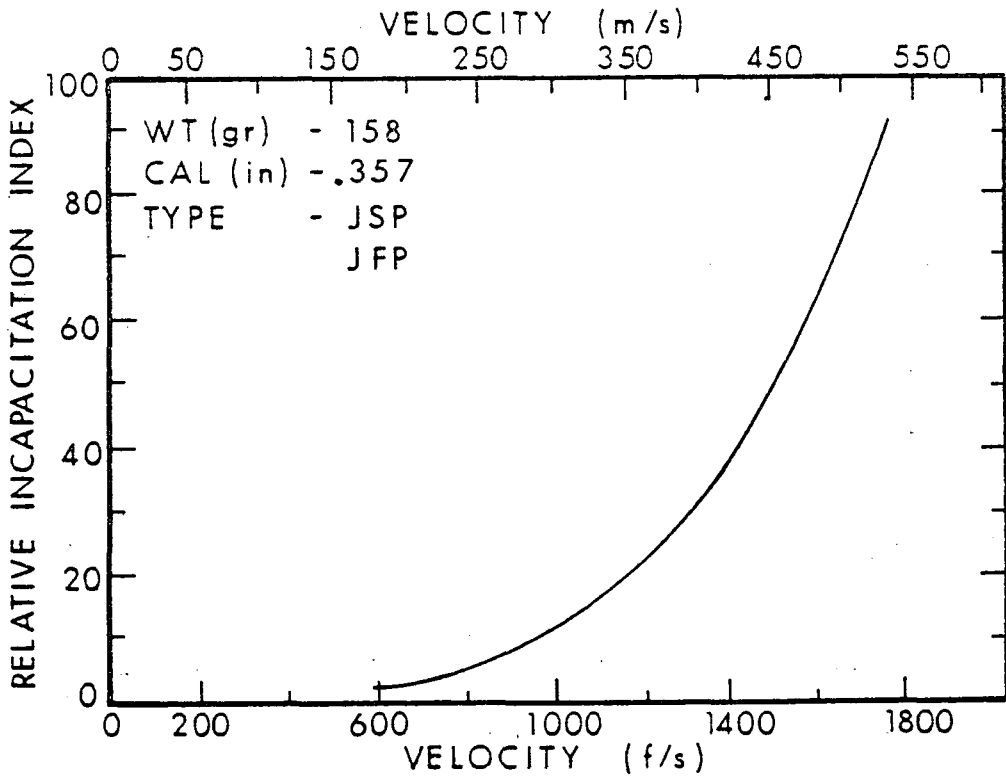


Figure 53. Relative Incapacitation Index For 158 Grain, Caliber .357, JSP, JFP Bullets.

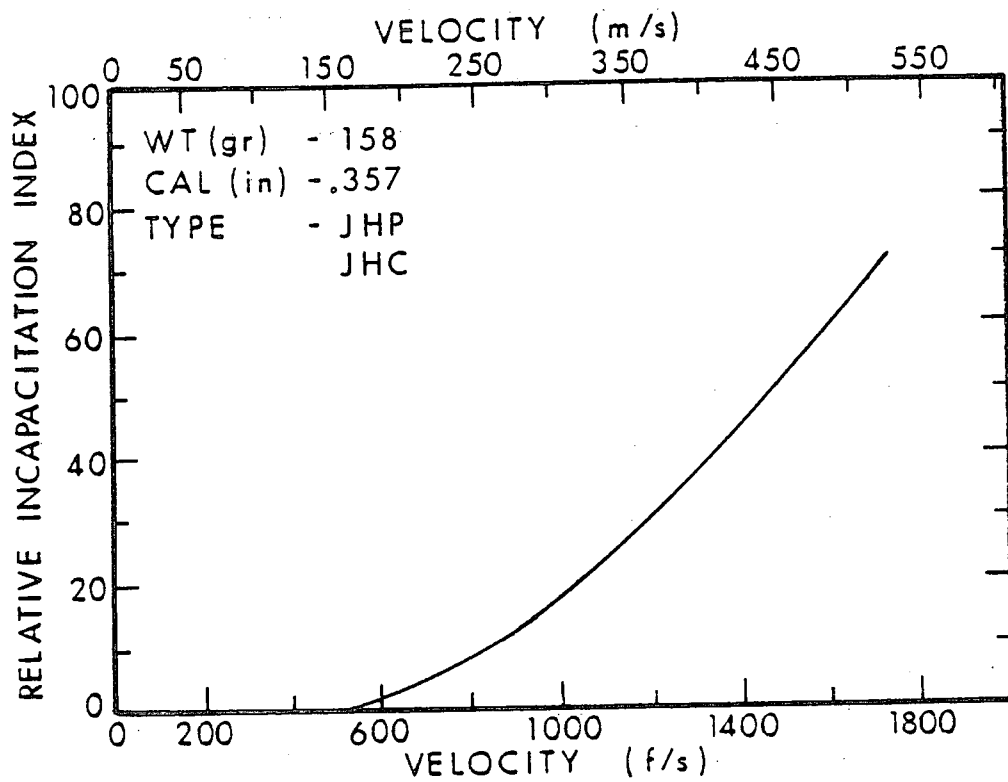


Figure 54. Relative Incapacitation Index For 158 Grain, Caliber .357, JHP, JHC Bullets.

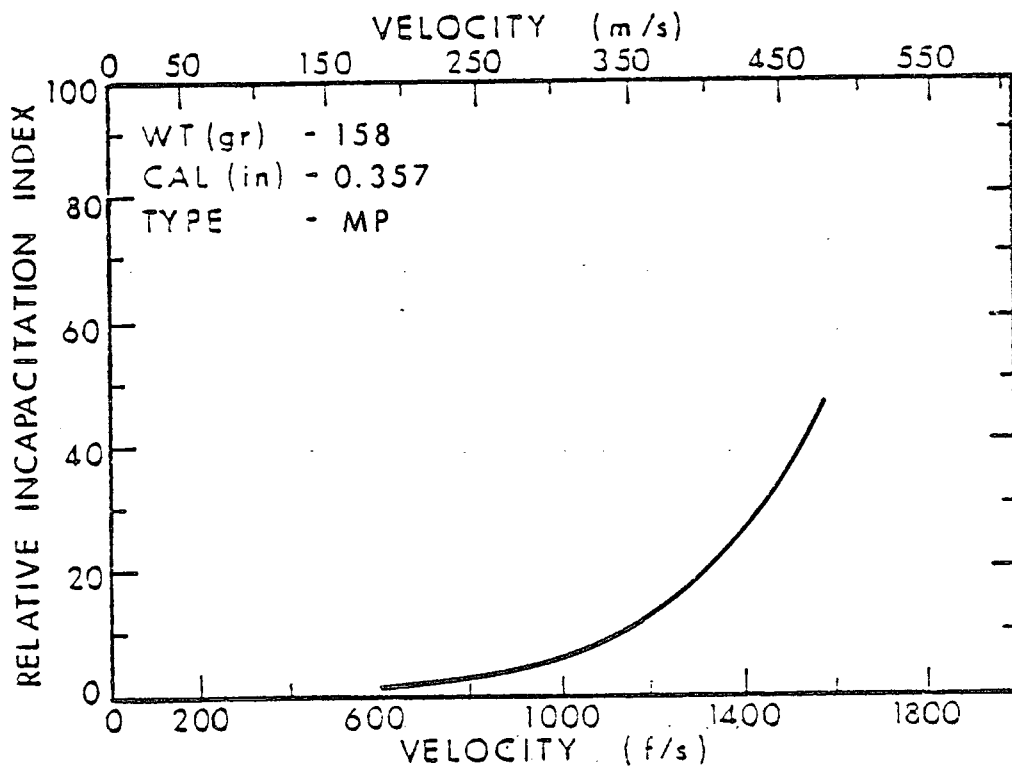


Figure 55. Relative Incapacitation Index For 158 Grain, Caliber .357, MP Bullets.

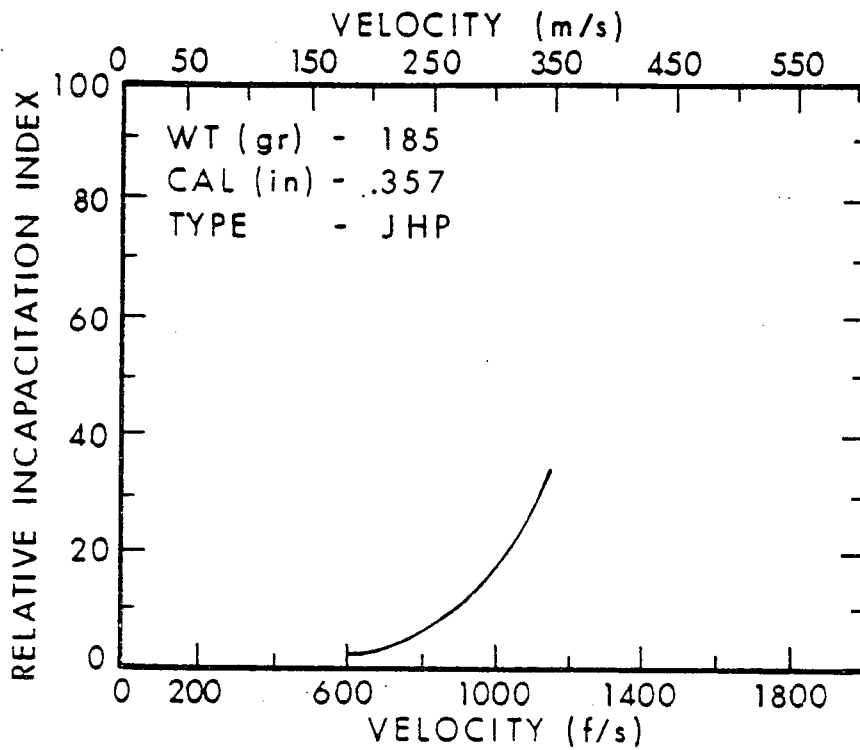


Figure 56. Relative Incapacitation Index For 185 Grain, Caliber .357, JHP Bullets.

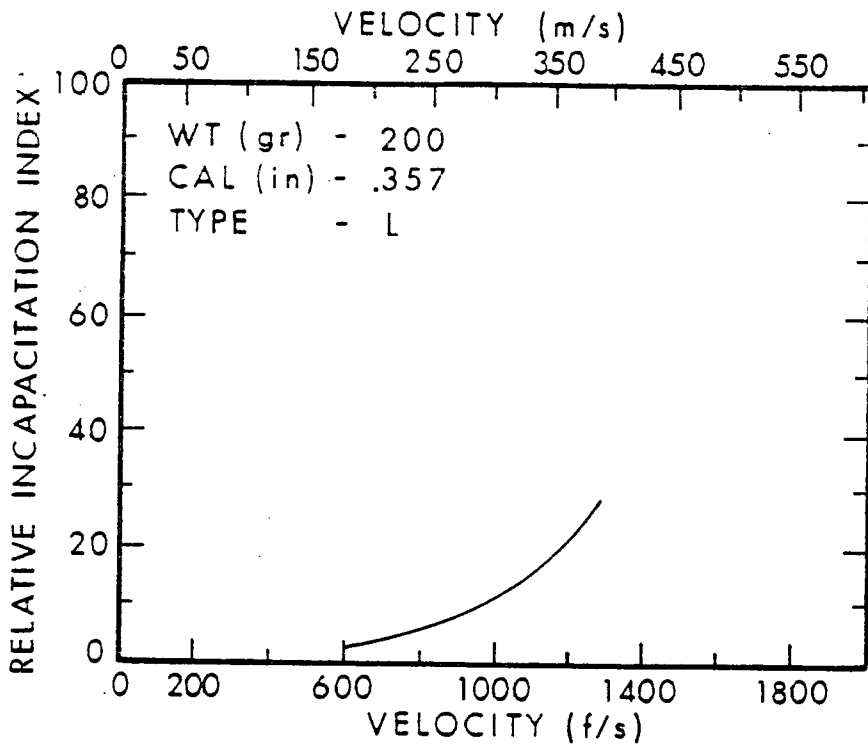


Figure 57. Relative Incapacitation Index For 200 Grain, Caliber .357, L Bullets.

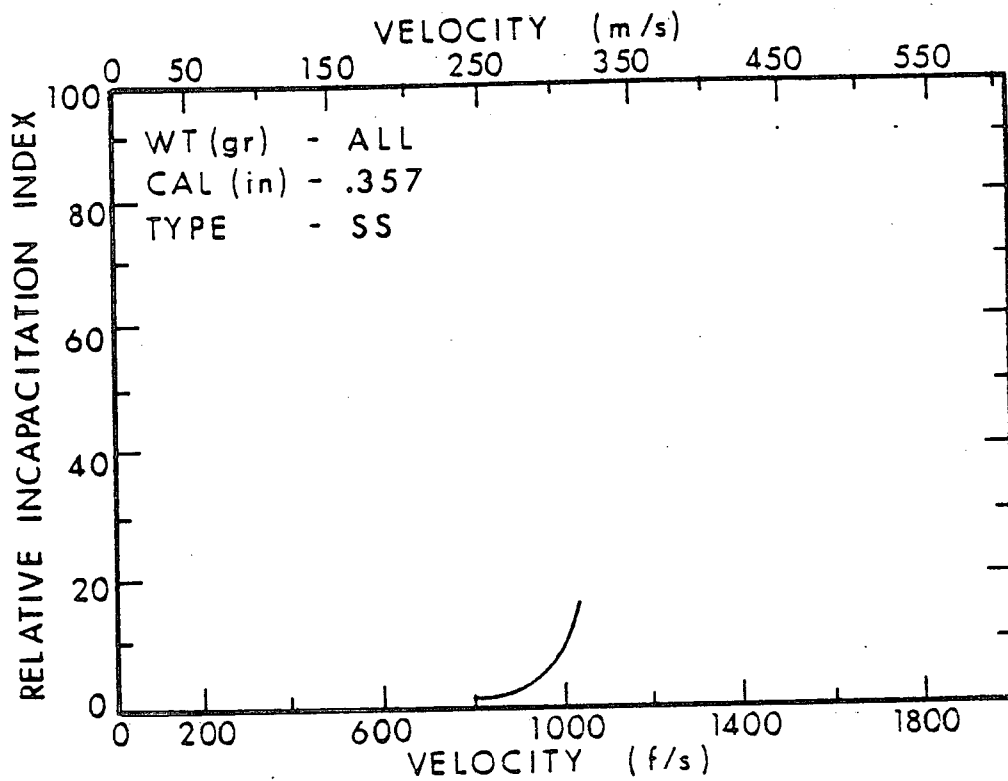


Figure 58. Relative Incapacitation Index For ALL Grain, Caliber .357, SS Bullets.

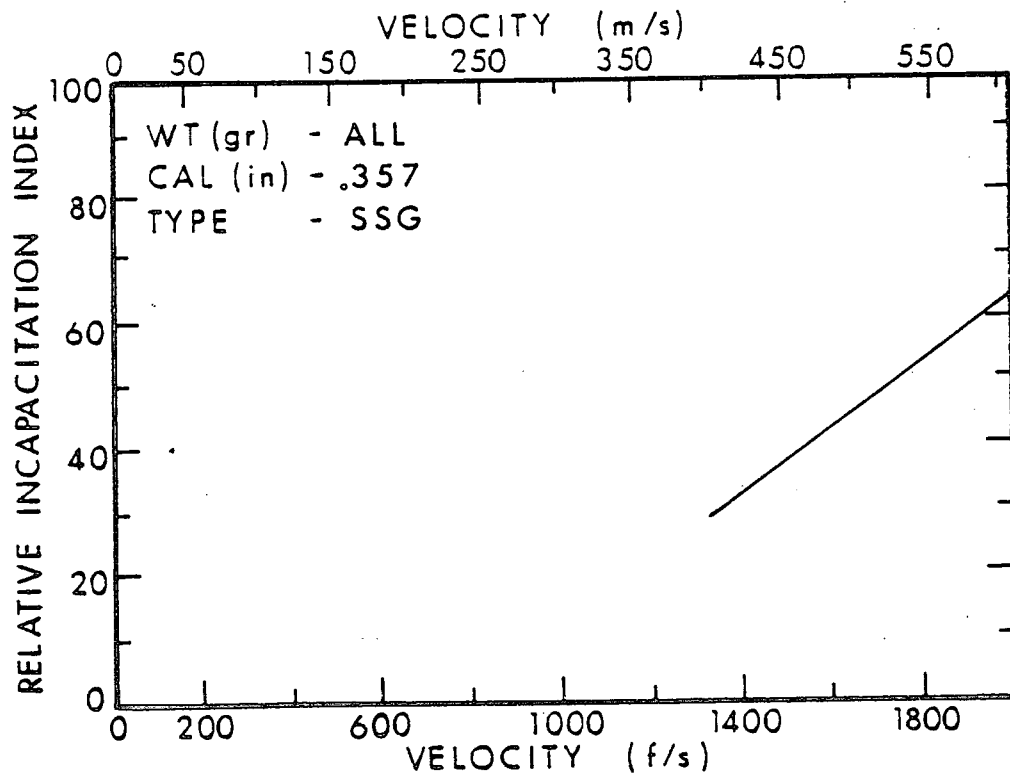


Figure 59. Relative Incapacitation Index For ALL Grain, Caliber .357, SSG Bullets.

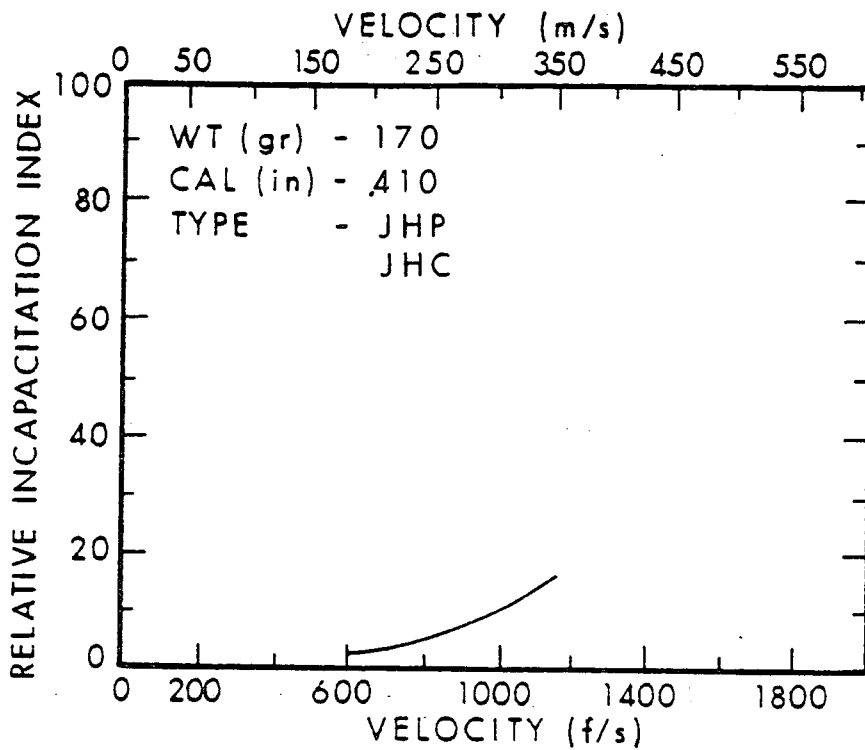


Figure 60. Relative Incapacitation Index For 170 Grain, Caliber .410, JHP, JHC Bullets.

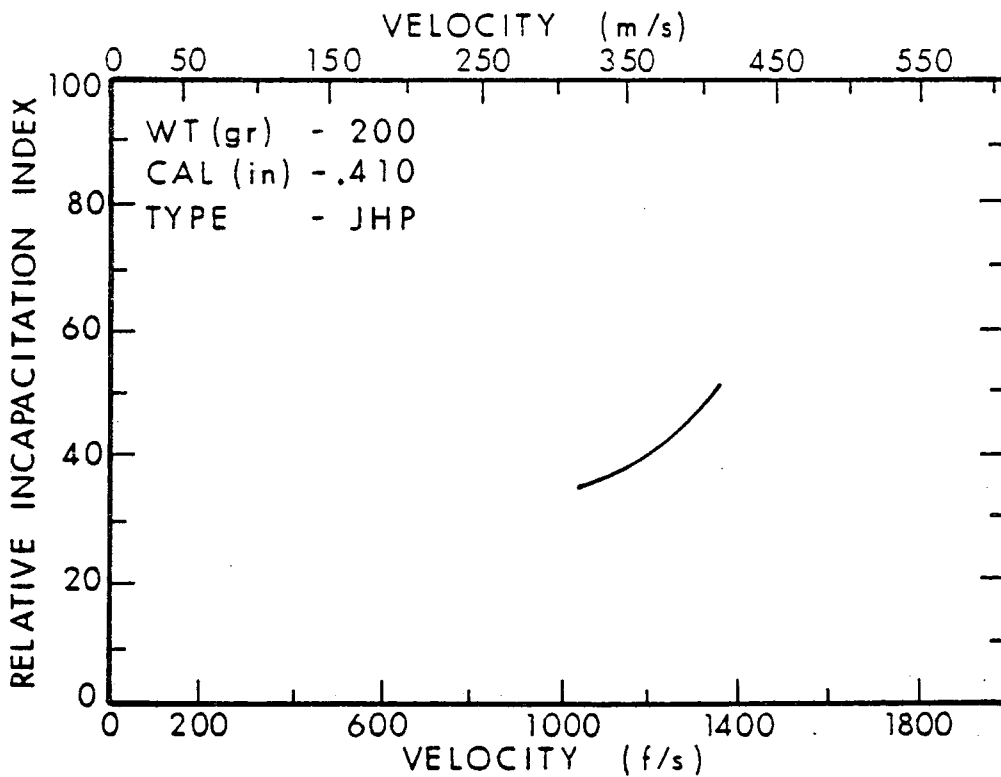


Figure 61. Relative Incapacitation Index For 200 Grain, Caliber .410, JHP Bullets.

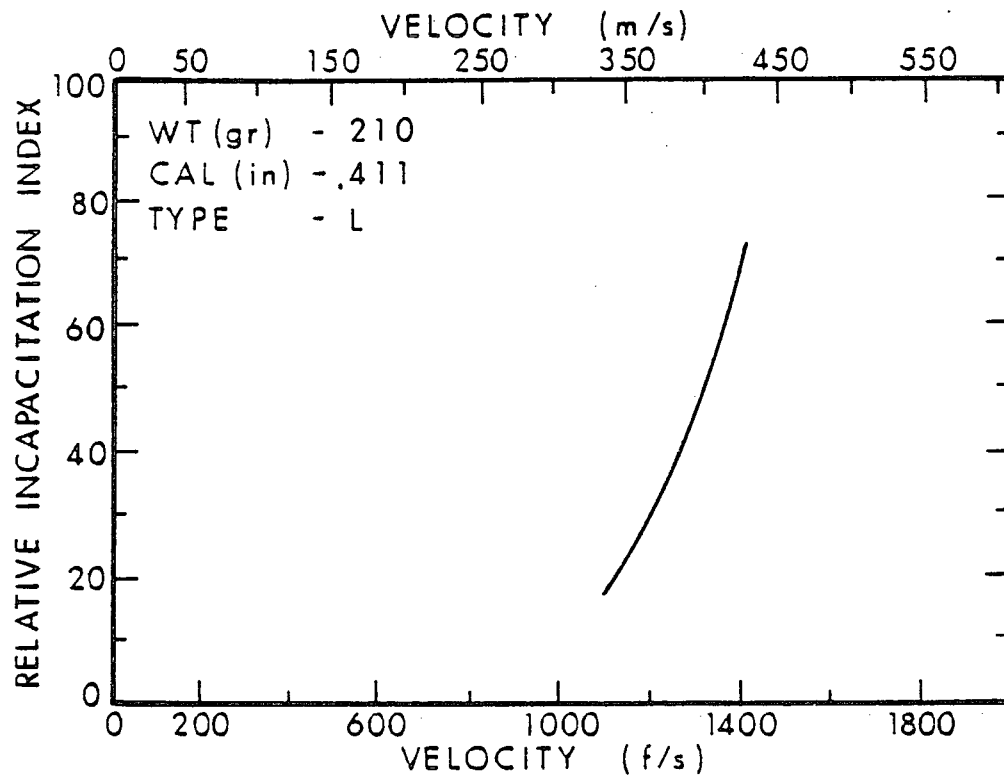


Figure 62. Relative Incapacitation Index For 210 Grain, Caliber .410, L Bullets.

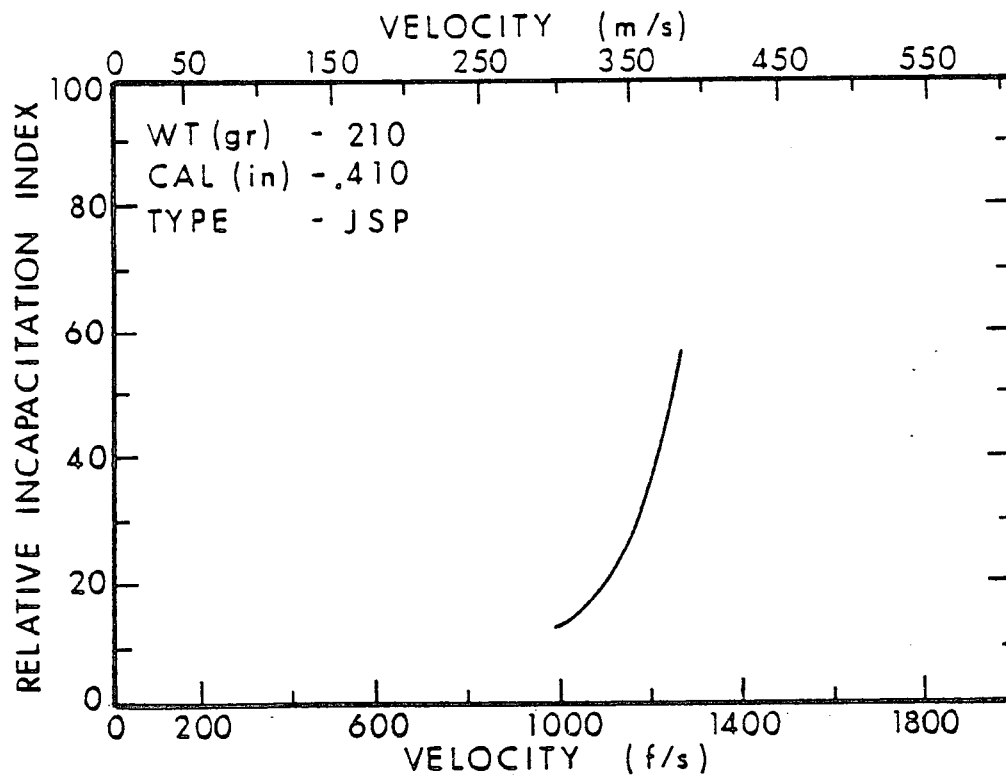


Figure 63. Relative Incapacitation Index For 210 Grain, Caliber .410, JSP Bullets.

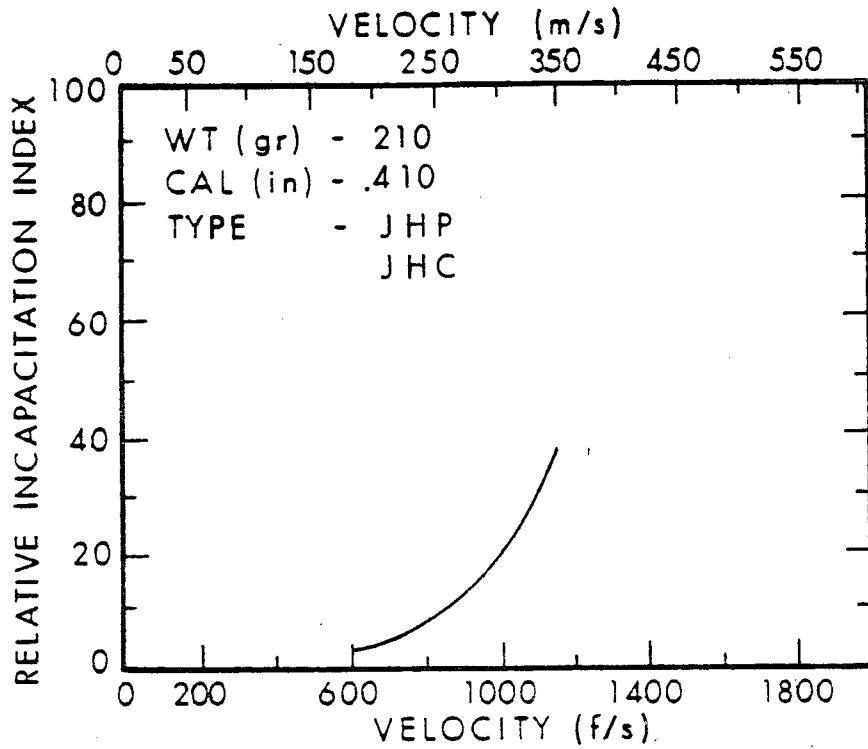


Figure 64. Relative Incapacitation Index For 210 Grain, Caliber .410, JHP, JHC Bullets.

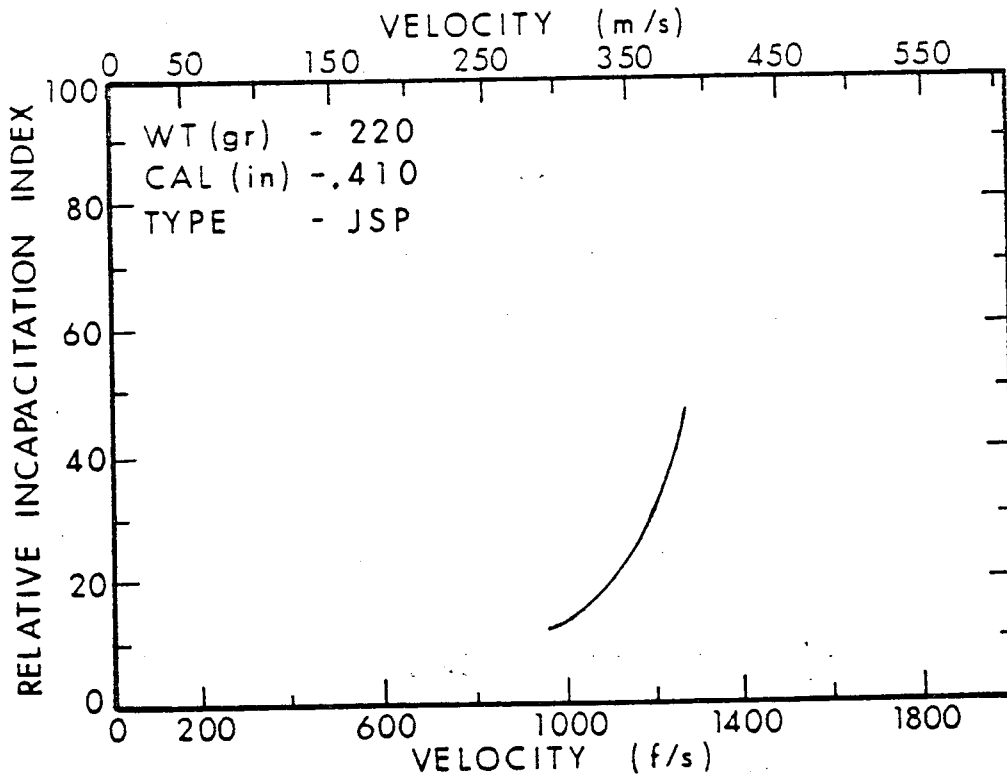


Figure 65. Relative Incapacitation Index For 220 Grain, Caliber .410, JSP Bullets.

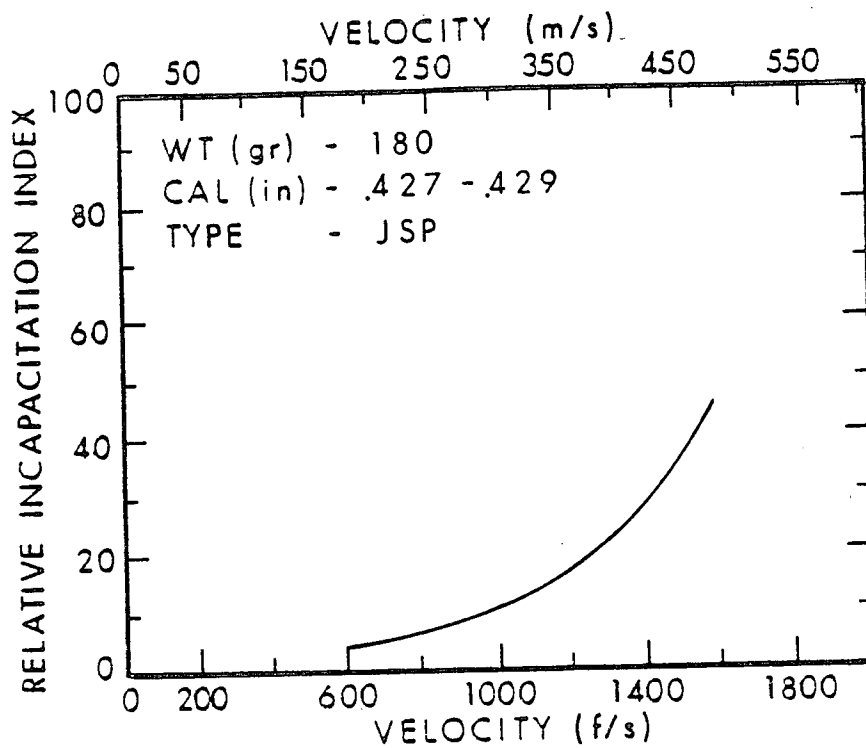


Figure 66. Relative Incapacitation Index For 180 Grain, Caliber .429, JSP Bullets.

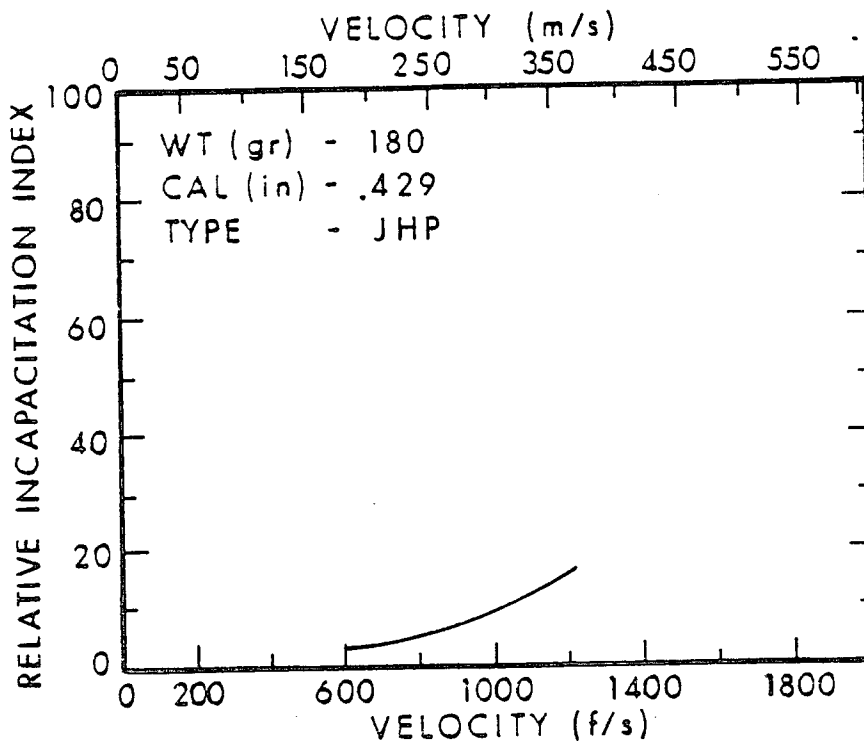


Figure 67. Relative Incapacitation Index For 180 Grain, Caliber .429, JHP Bullets.

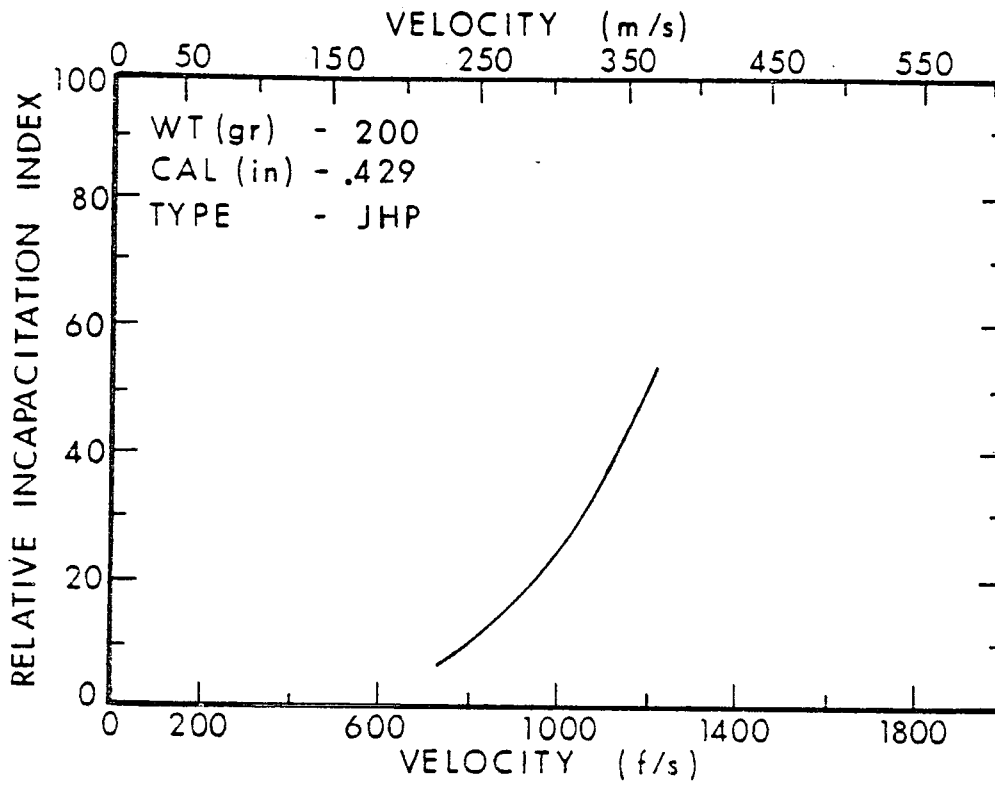


Figure 68. Relative Incapacitation Index For 200 Grain, Caliber .429, JHP Bullets.

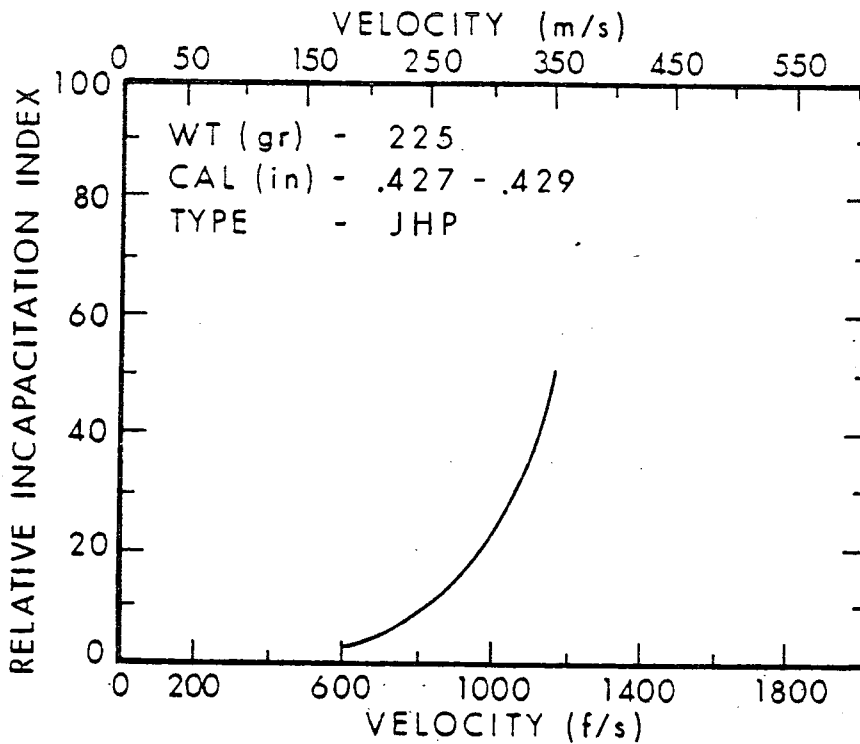


Figure 69. Relative Incapacitation Index For 225 Grain, Caliber .429, JHP Bullets.

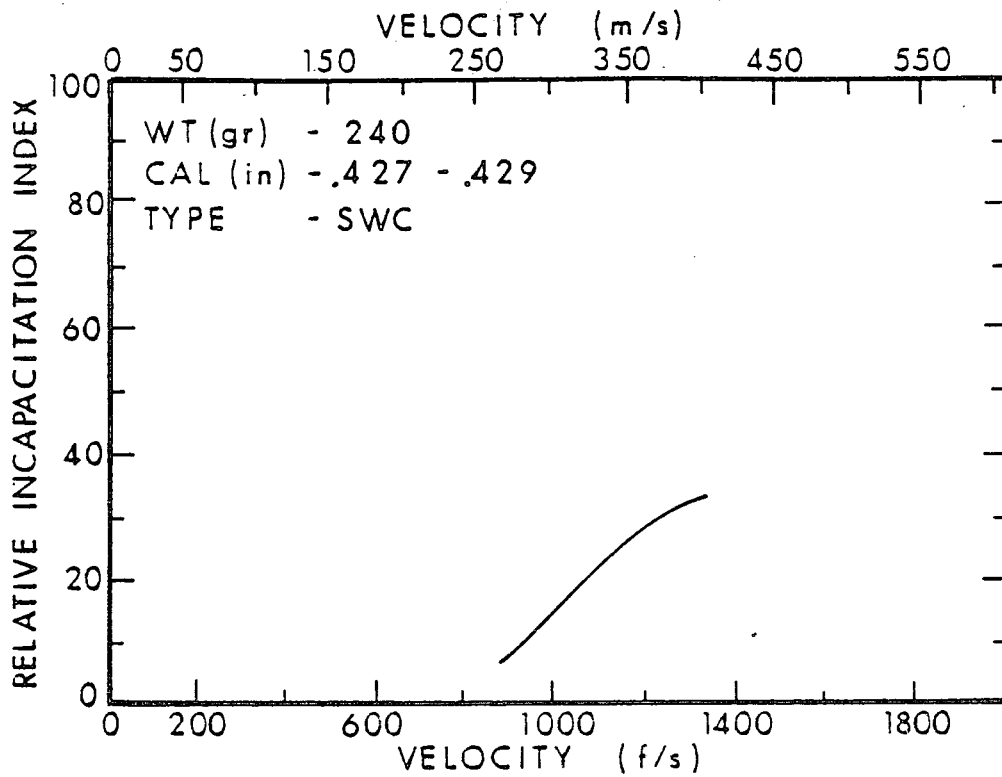


Figure 70. Relative Incapacitation Index For 240 Grain, Caliber .429, SWC Bullets.

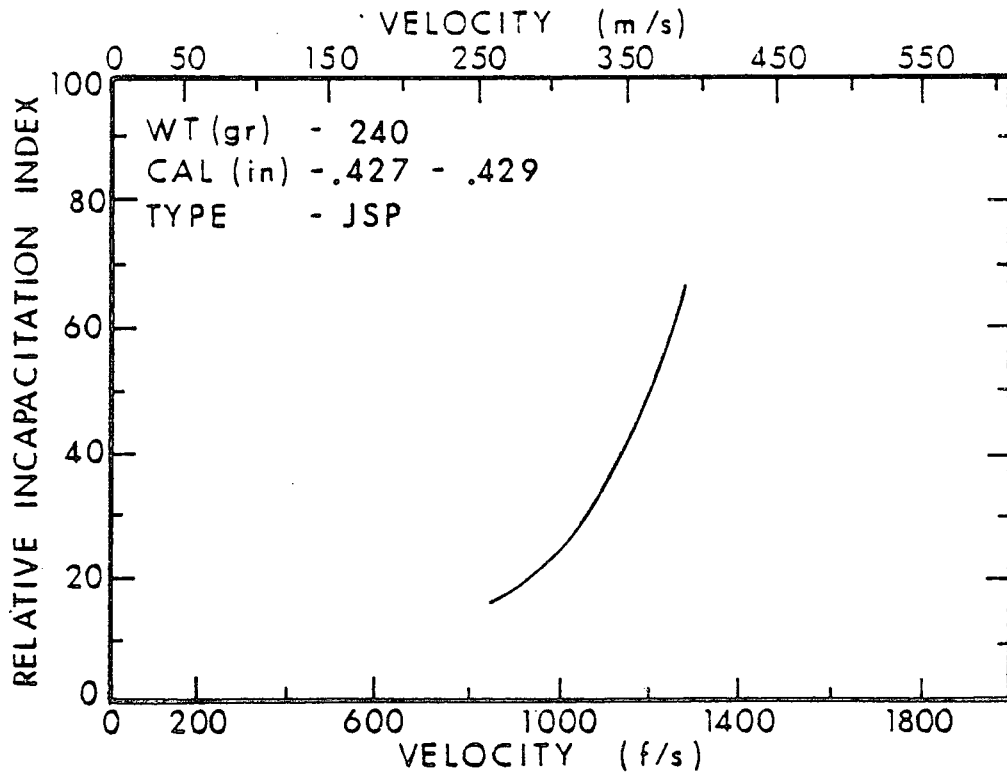


Figure 71. Relative Incapacitation Index For 240 Grain, Caliber .429, JSP Bullets.

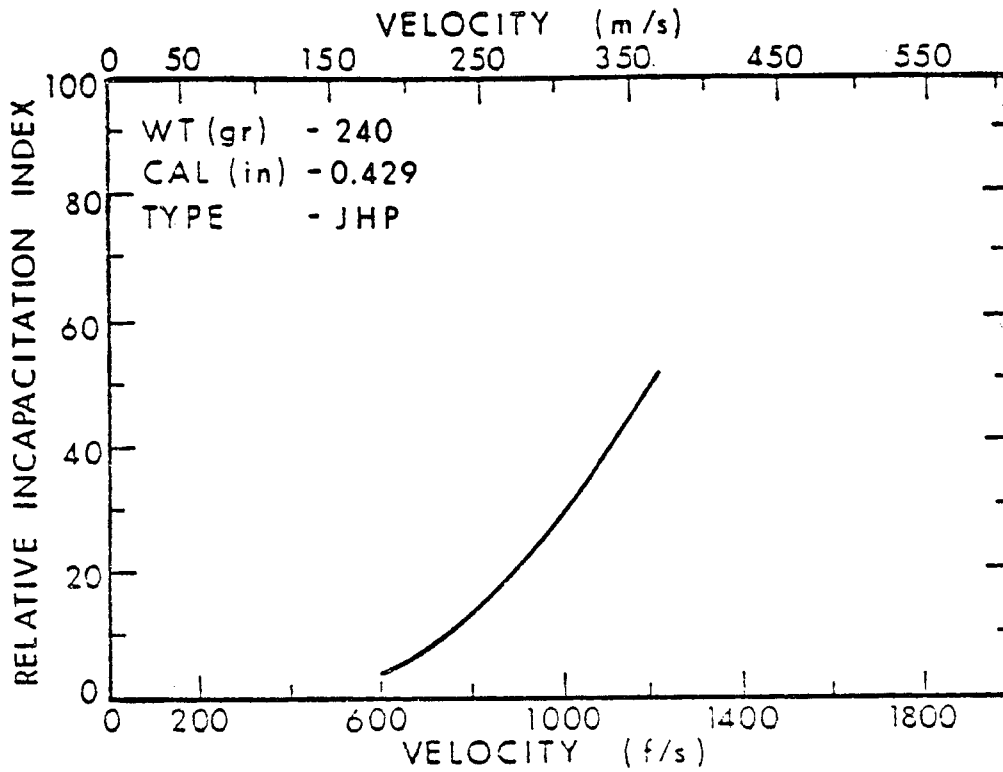


Figure 72. Relative Incapacitation Index For 240 Grain, Caliber .429, JHP Bullets.

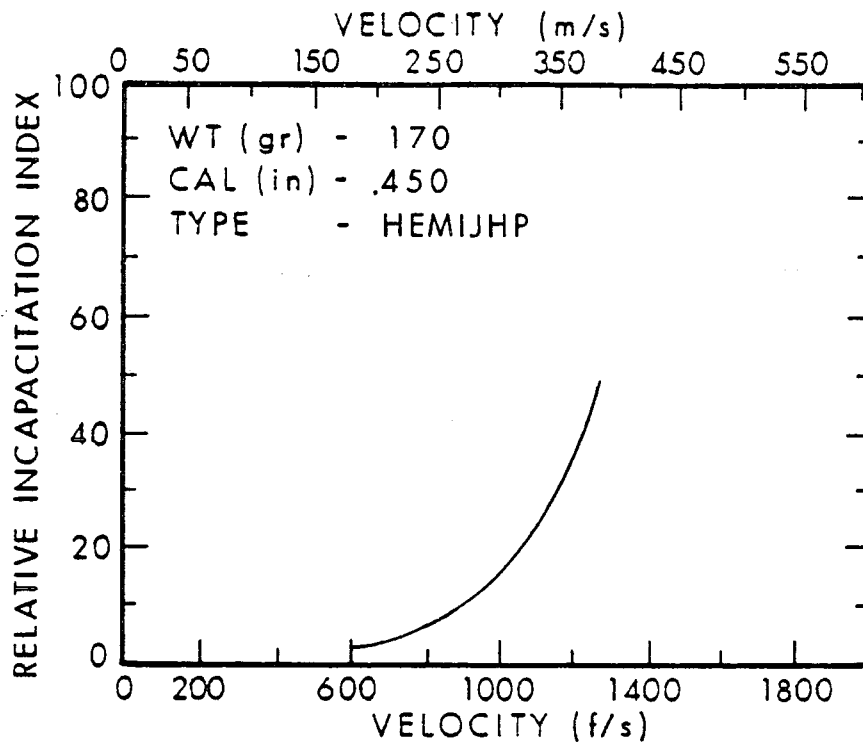


Figure 73. Relative Incapacitation Index For 170 Grain, Caliber .450, HEMIJHP Bullets.

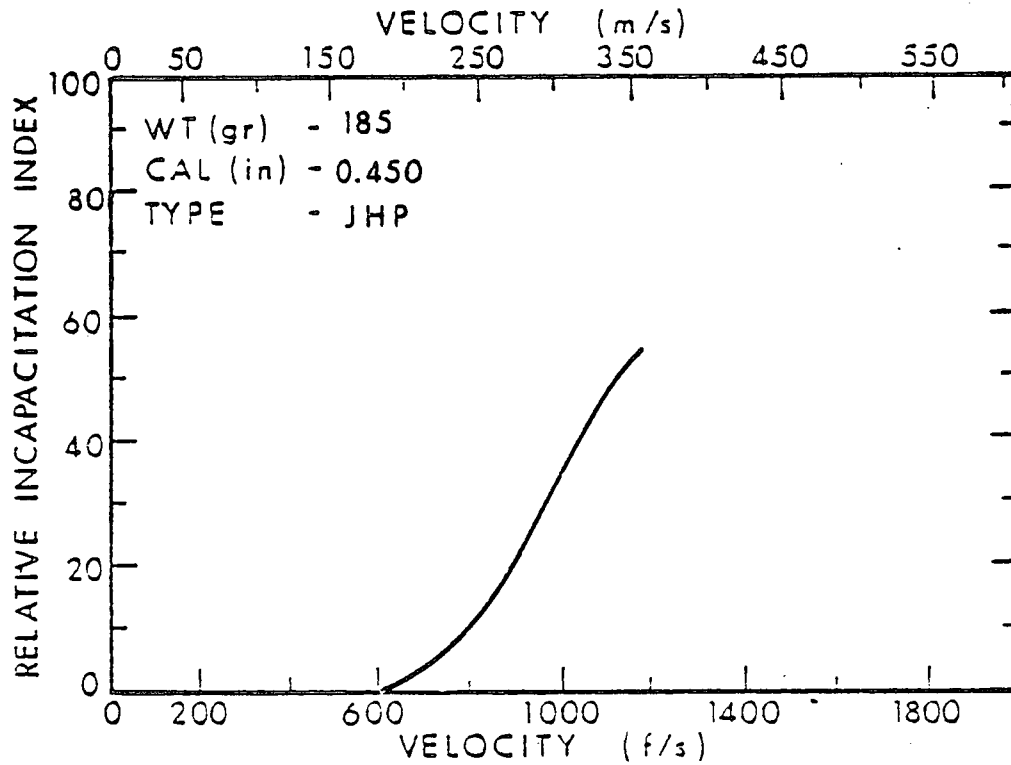


Figure 74. Relative Incapacitation Index For 185 Grain, Caliber .45, JHP Bullets.

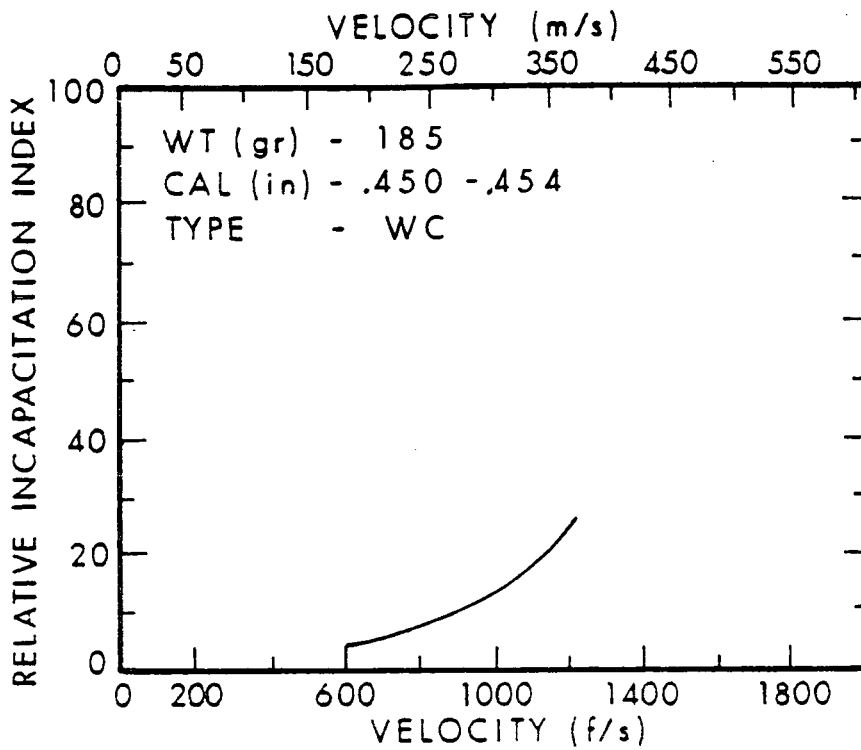


Figure 75. Relative Incapacitation Index For 185 Grain, Caliber .450, WC Bullets.

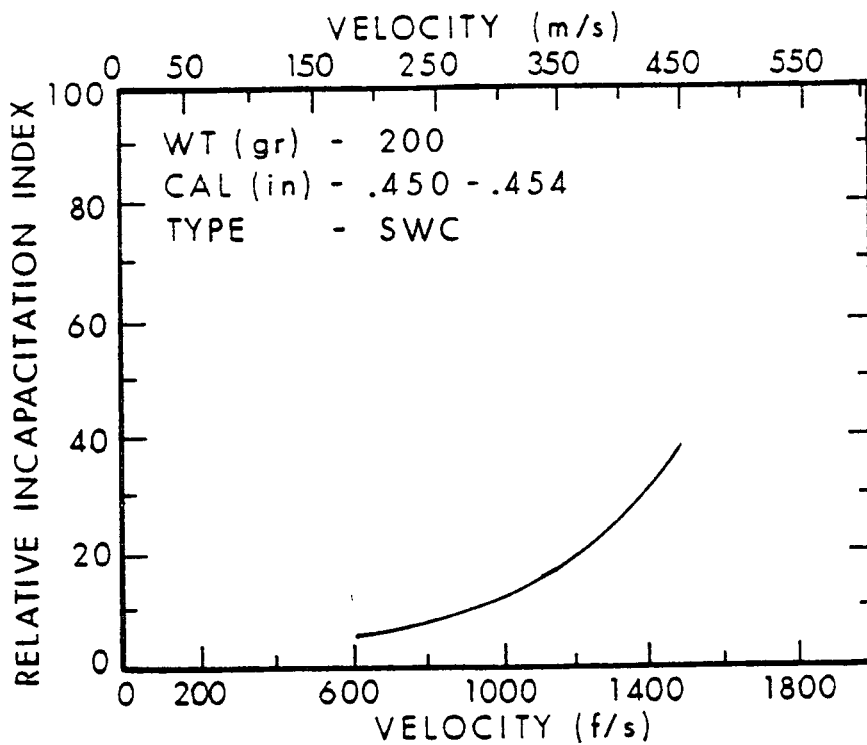


Figure 76. Relative Incapacitation Index For 200 Grain, Caliber .450, SWC Bullets.

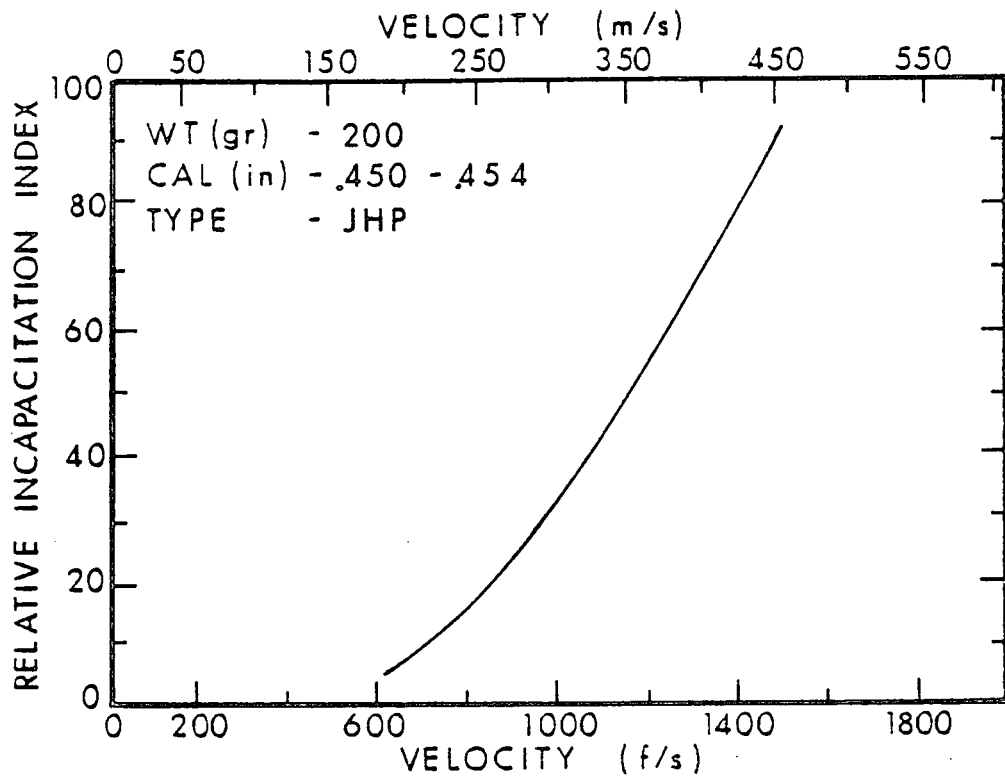


Figure 77. Relative Incapacitation Index For 200 Grain, Caliber .450, JHP Bullets.

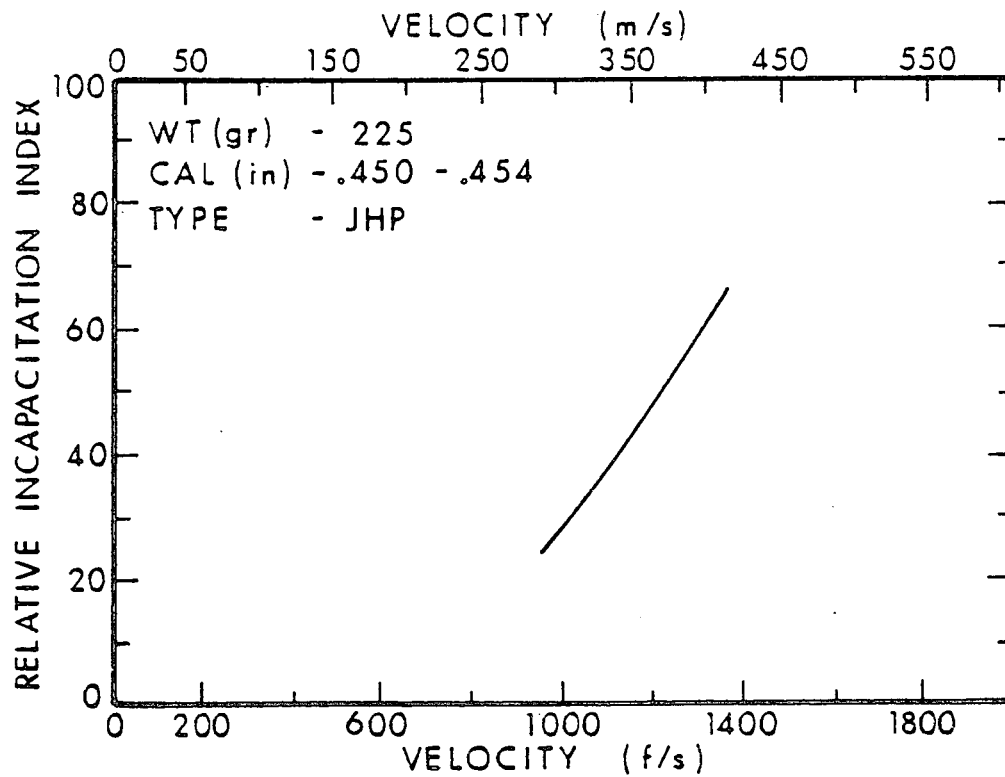


Figure 78. Relative Incapacitation Index For 225 Grain, Caliber .450, JHP Bullets.

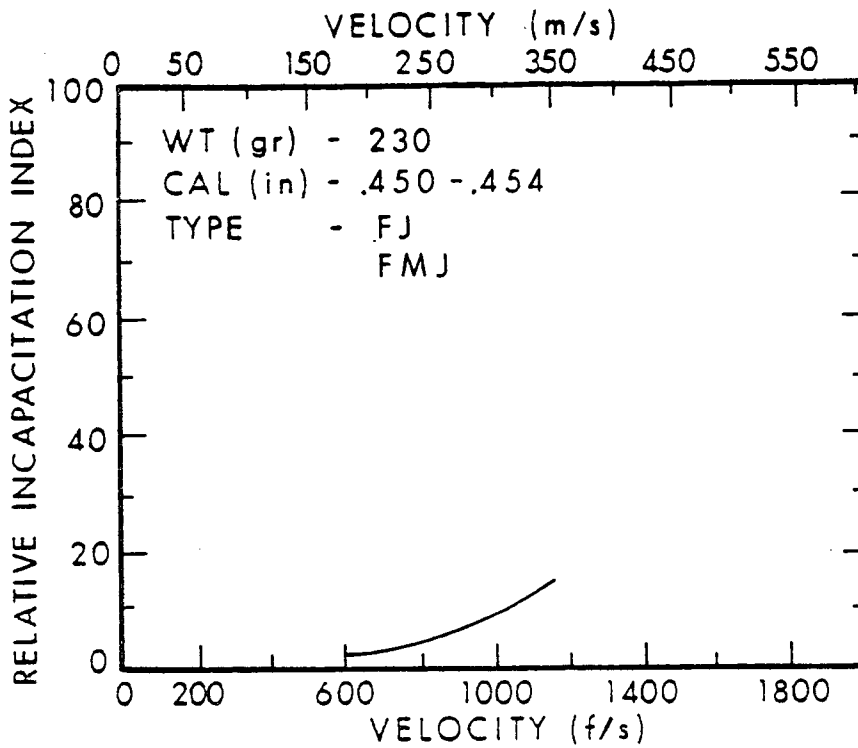


Figure 79. Relative Incapacitation Index For 230 Grain, Caliber .450, FJ, FMJ Bullets.

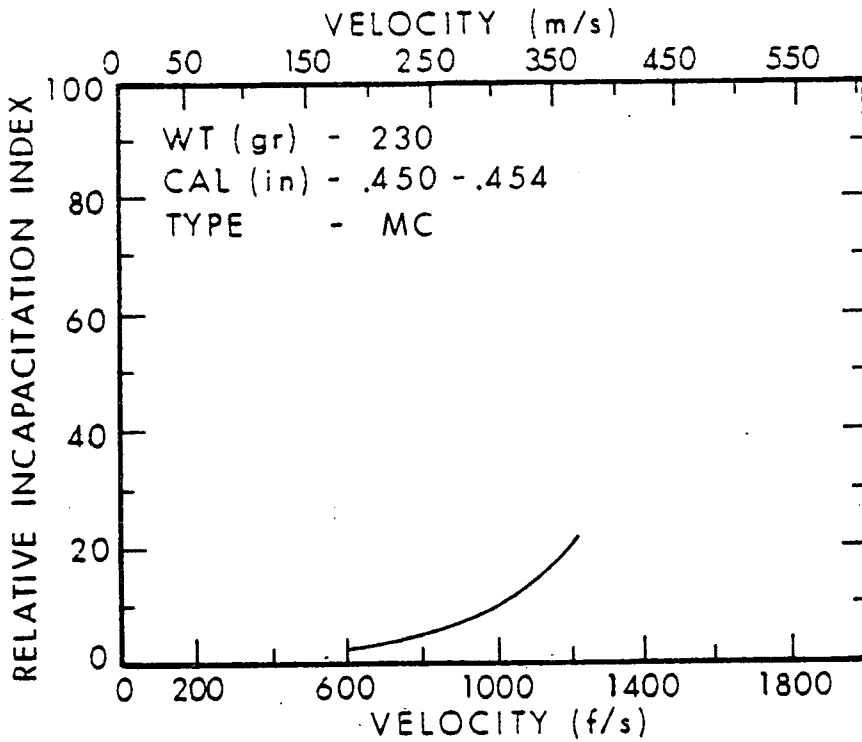


Figure 80. Relative Incapacitation Index For 230 Grain, Caliber .450, MC Bullets.

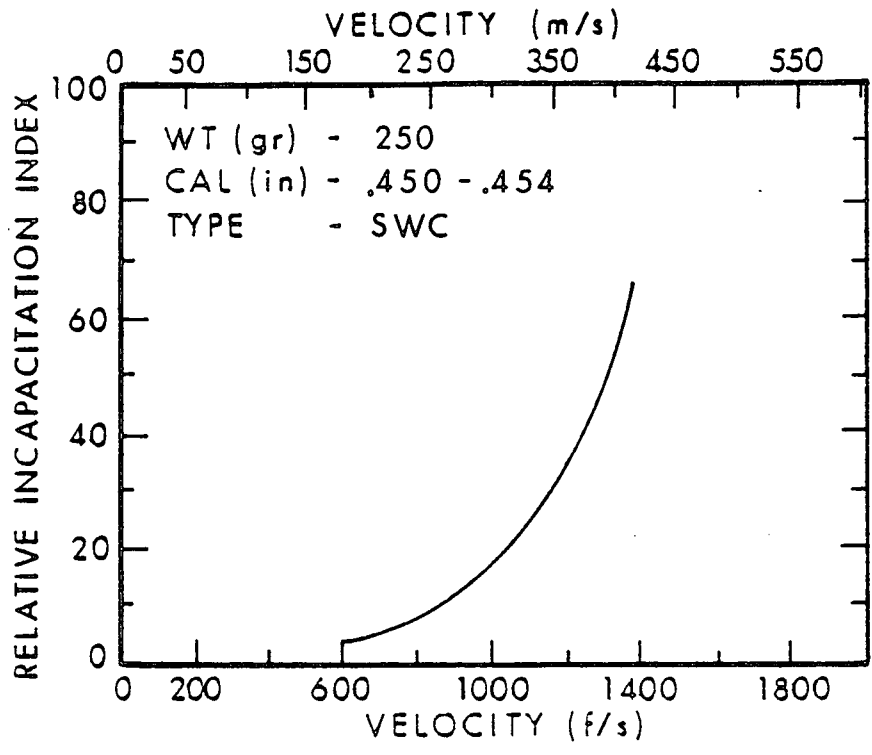


Figure 81. Relative Incapacitation Index For 250 Grain, Caliber .450, SWC Bullets.

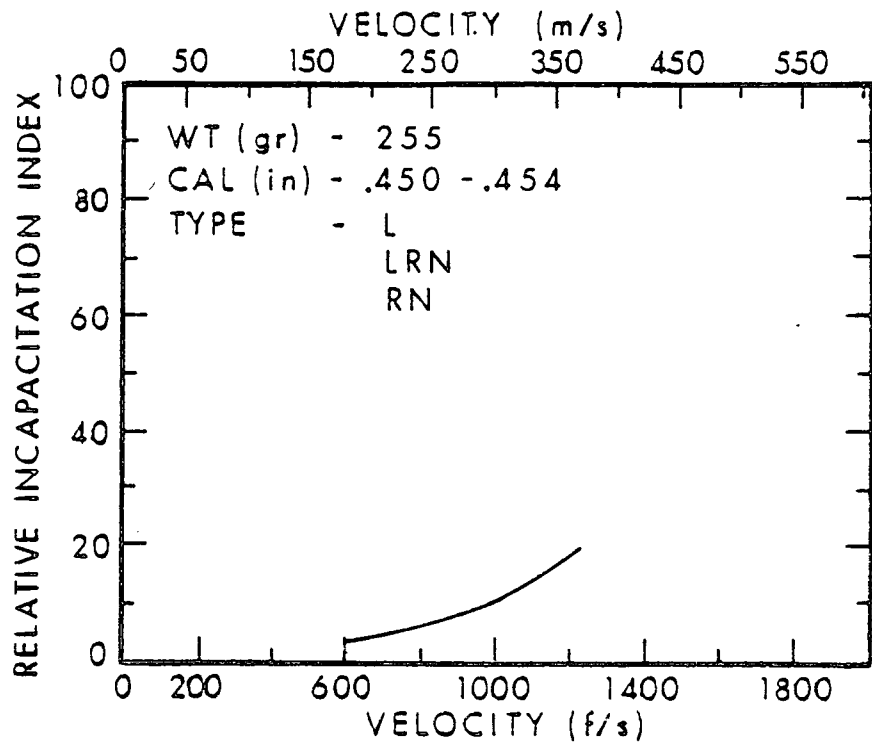


Figure 82. Relative Incapacitation Index For 255 Grain, Caliber .450, L, LRN, RN Bullets.

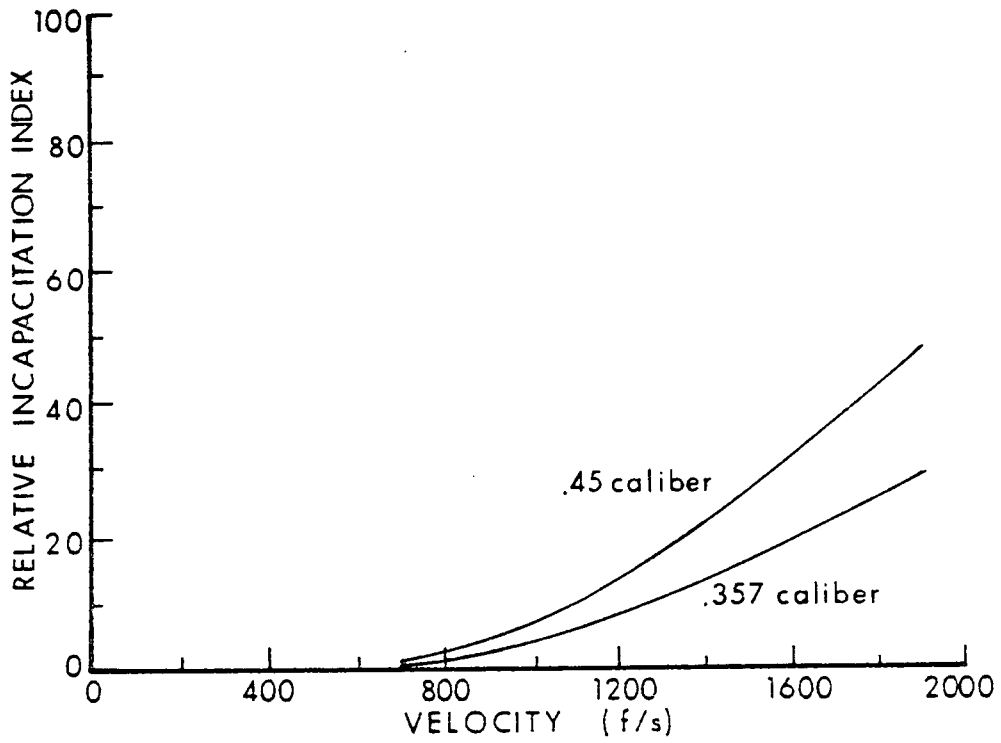


Figure 83. Relative Incapacitation Index Computer Prediction For Lead Spheres.

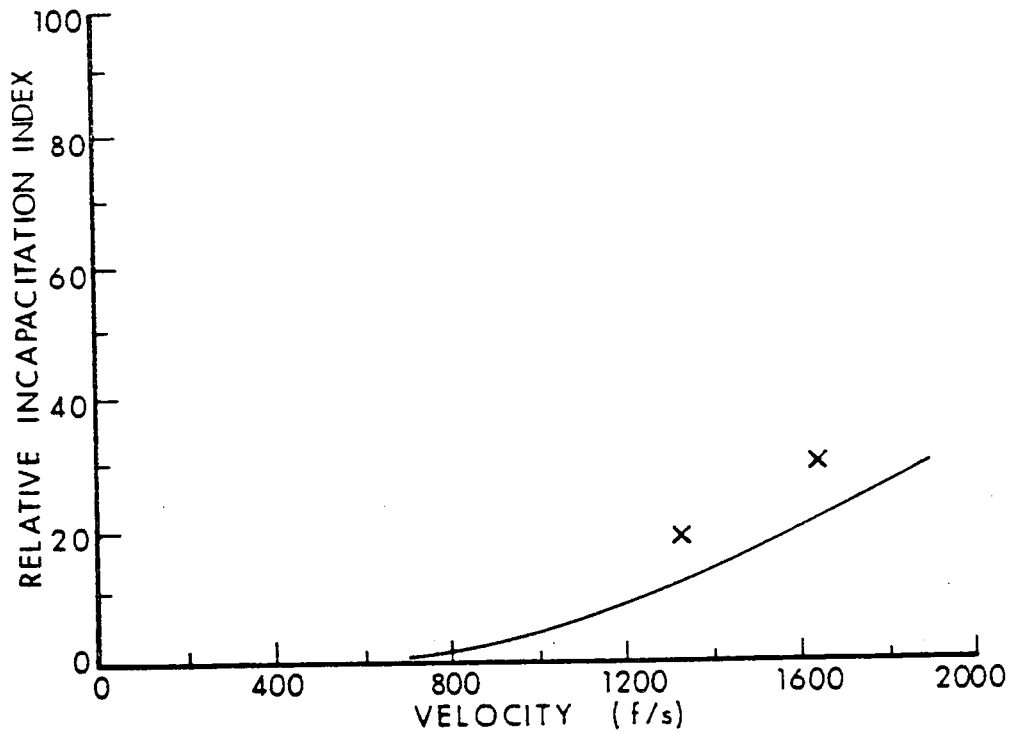


Figure 84. Relative Incapacitation Index Computer Predictions of a .357 Caliber Bullet With  $C_D = .30$  and Mass = 110 grains. (Data points are 9mm, 115 and 100 grain FJ bullets.)

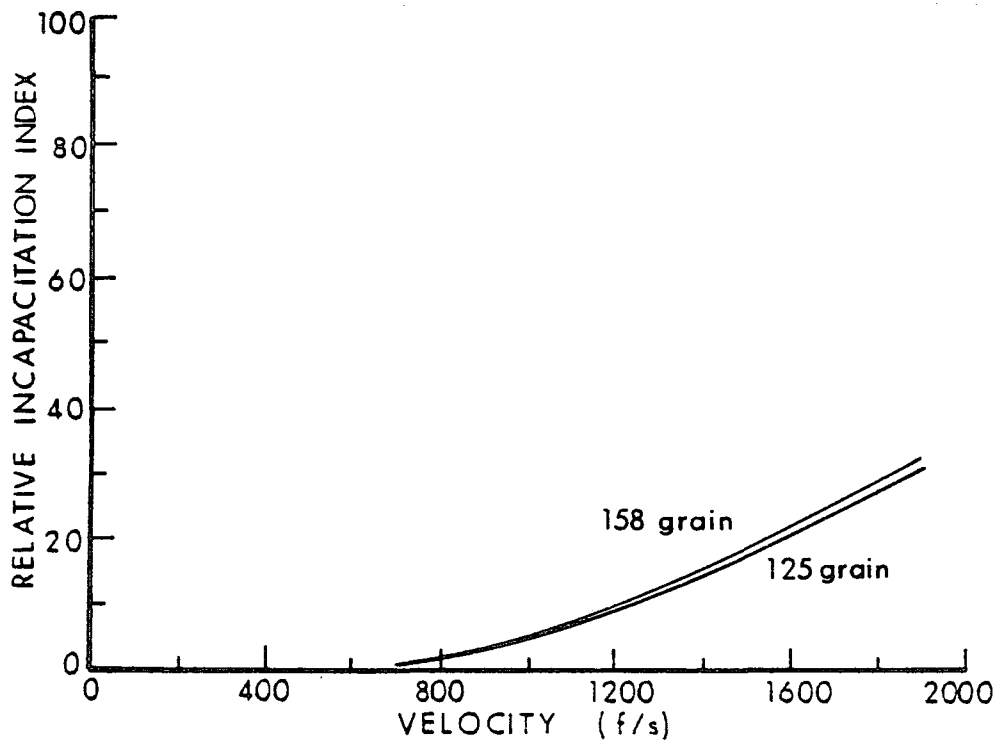


Figure 85. Relative Incapacitation Index Computer Predictions For .357 Caliber Bullets With  $C_D = .50$ .

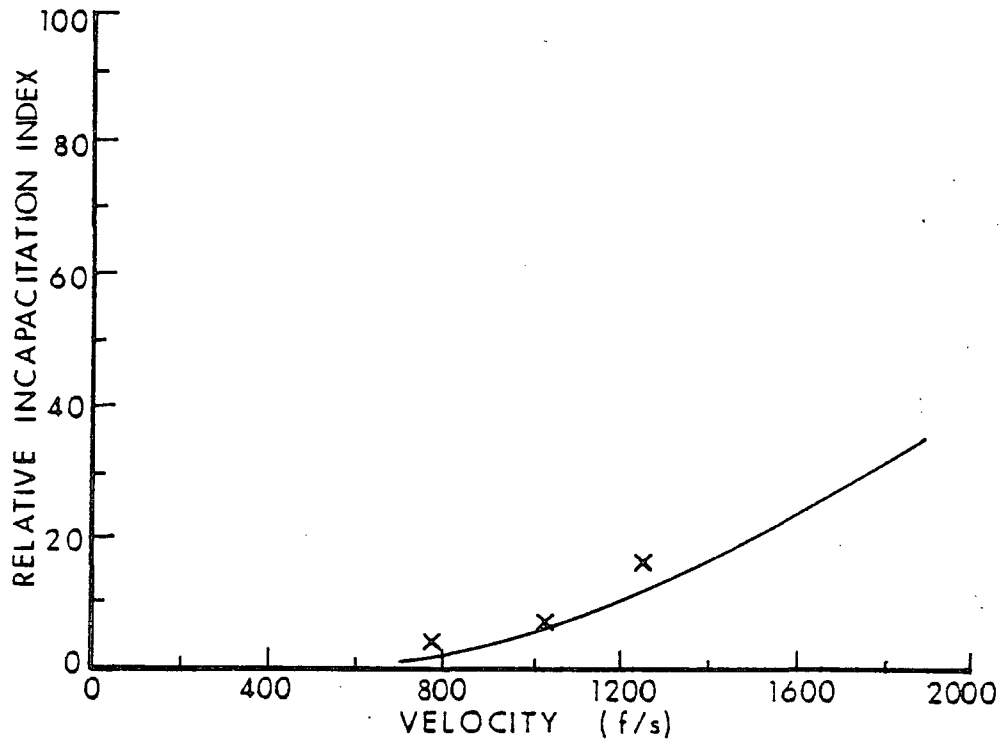


Figure 86. Relative Incapacitation Index Computer Predictions For .357 Caliber Bullets With  $C_D = .30$  and Mass = 110 Grains. (Data are .357, 90 grain Hemi-JSP bullets.)

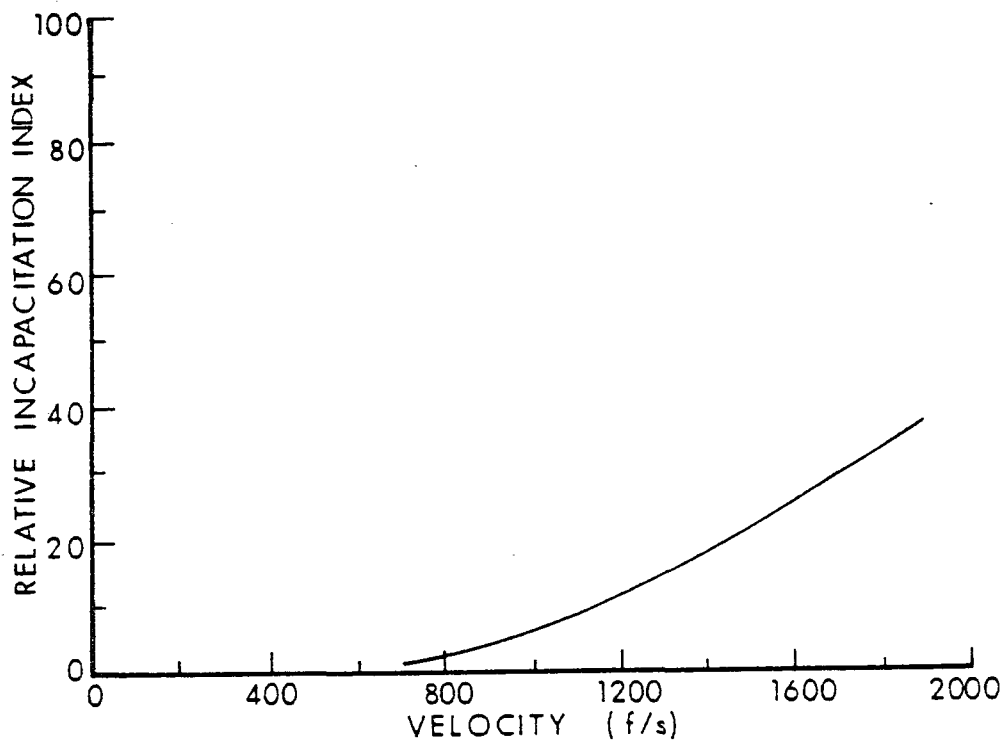


Figure 87. Relative Incapacitation Index Computer Predictions For a .357 Caliber Bullets With  $C_D = .37$  and Mass = 125 Grains.

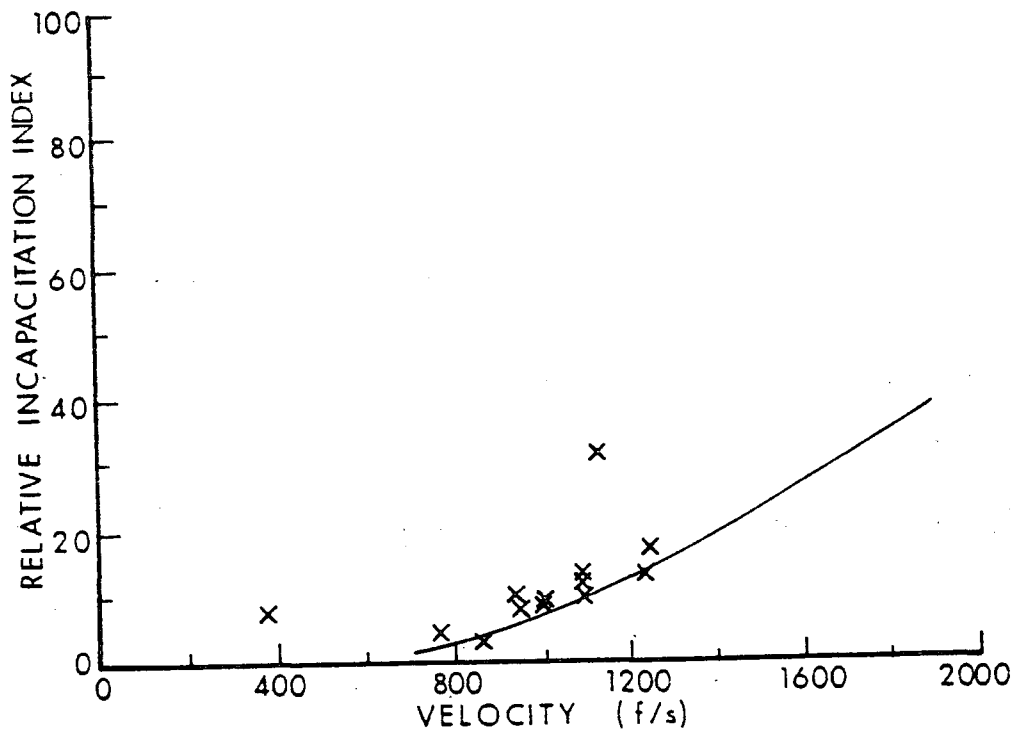


Figure 88. Relative Incapacitation Index Computer Predictions For a .357 Caliber Bullets With  $C_D = .37$  and Mass = 158 Grains. (Data are .357, 158 grain LRN bullets.)

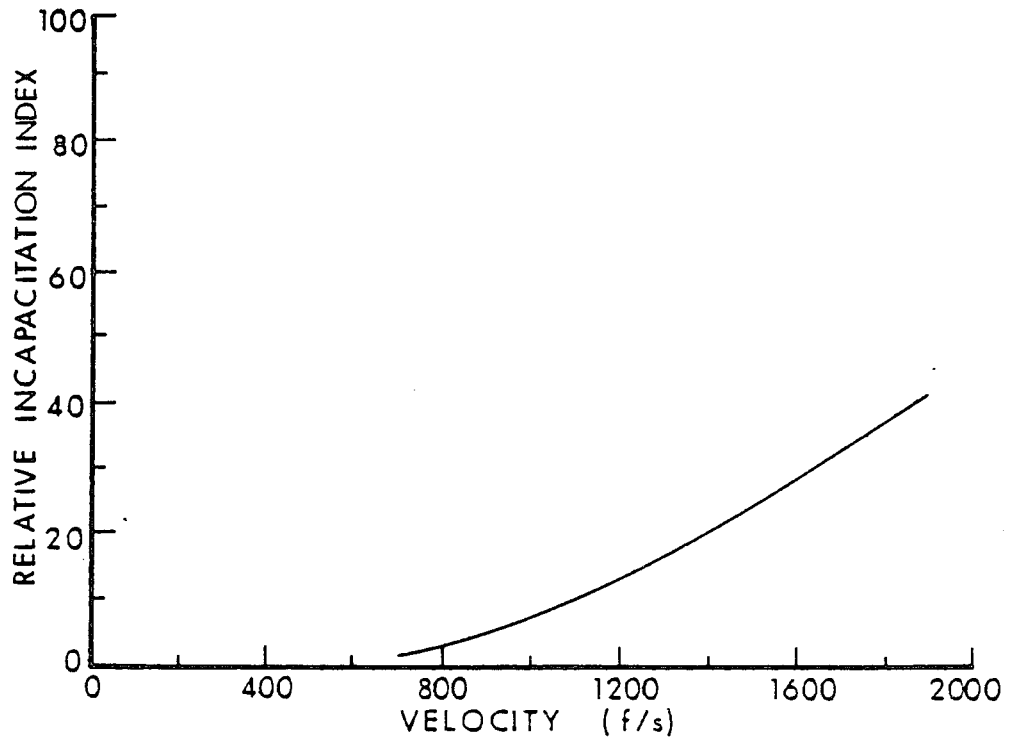


Figure 89. Relative Incapacitation Index Computer Predictions For a .357 Caliber Bullets With  $C_D = .45$  and Mass = 110 Grains.

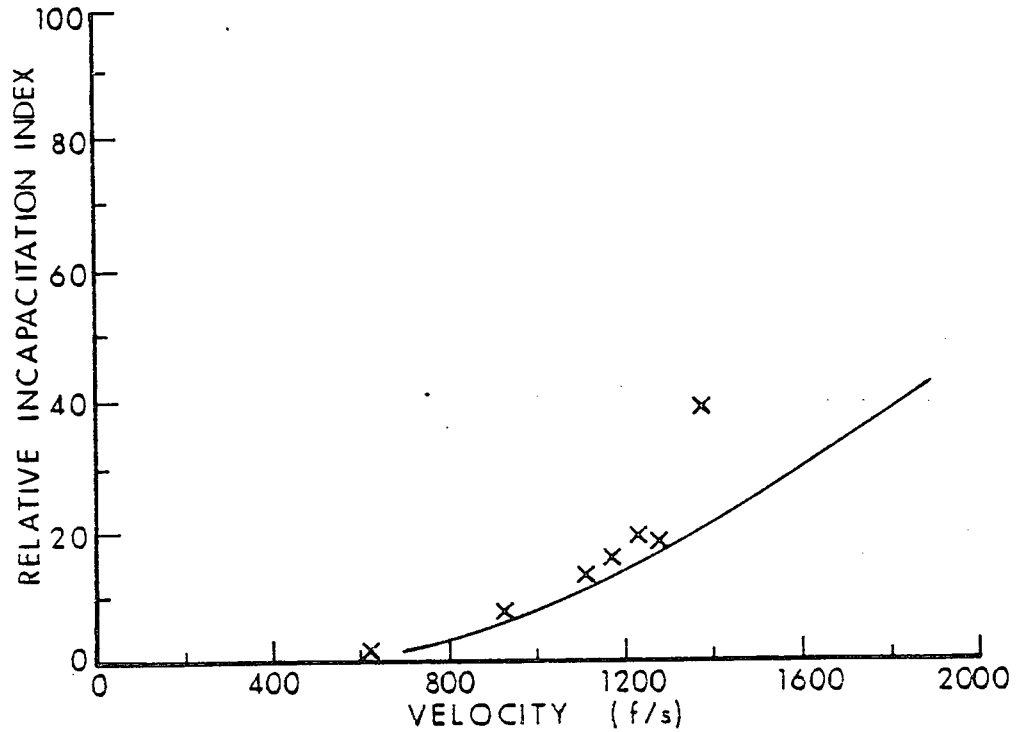


Figure 90. Relative Incapacitation Index Computer Predictions For a .357 Caliber Bullets With  $C_D = .45$  and Mass = 125 Grains. (Data are .357, 125 grain JSP bullets.)

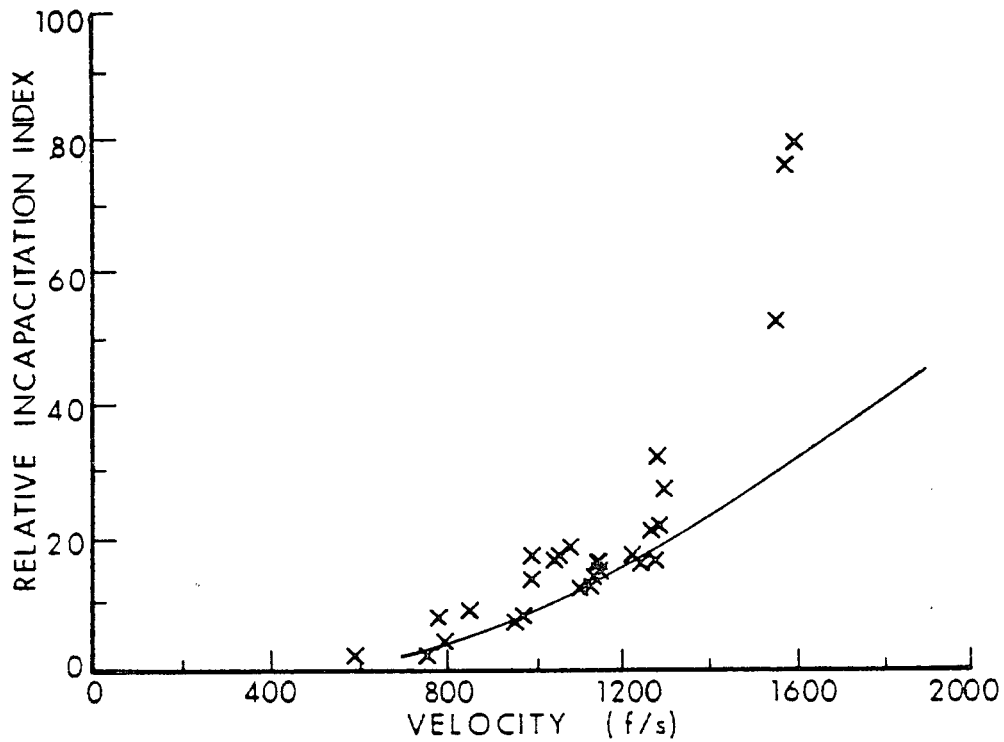


Figure 91. Relative Incapacitation Index Computer Predictions For a .357 Caliber Bullets With  $C_D = .45$  and Mass = 158 grains. (Data are .357, 158 grain JSP bullets.)

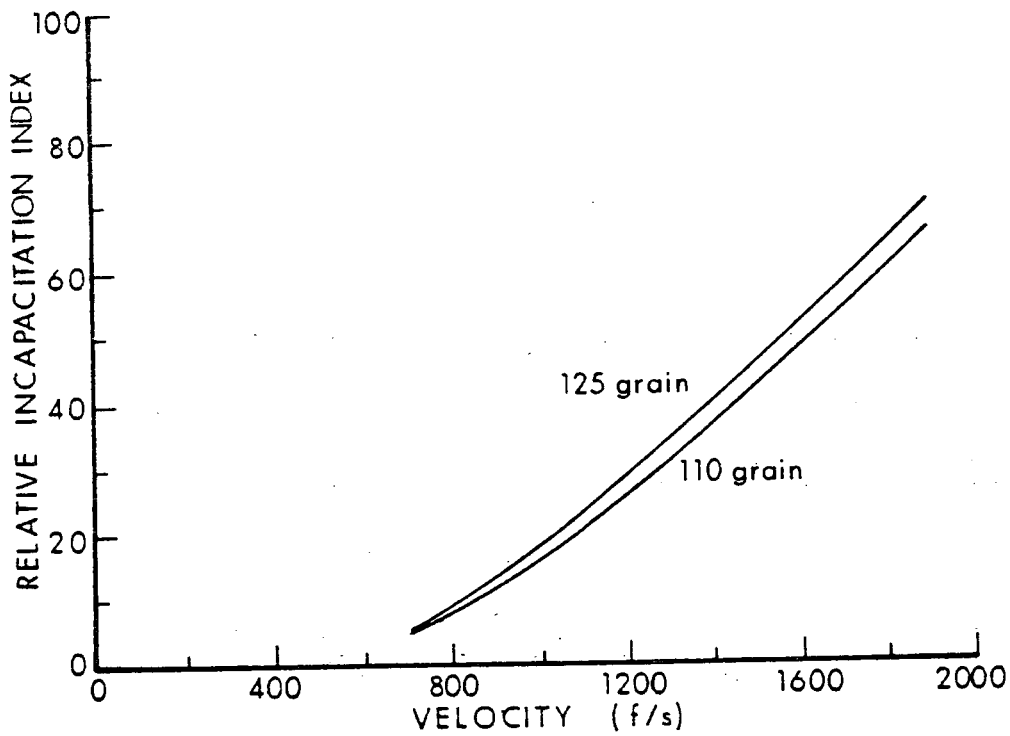


Figure 92. Relative Incapacitation Index Computer Predictions For a .357 Caliber Bullets With  $C_D = 1.20$ .

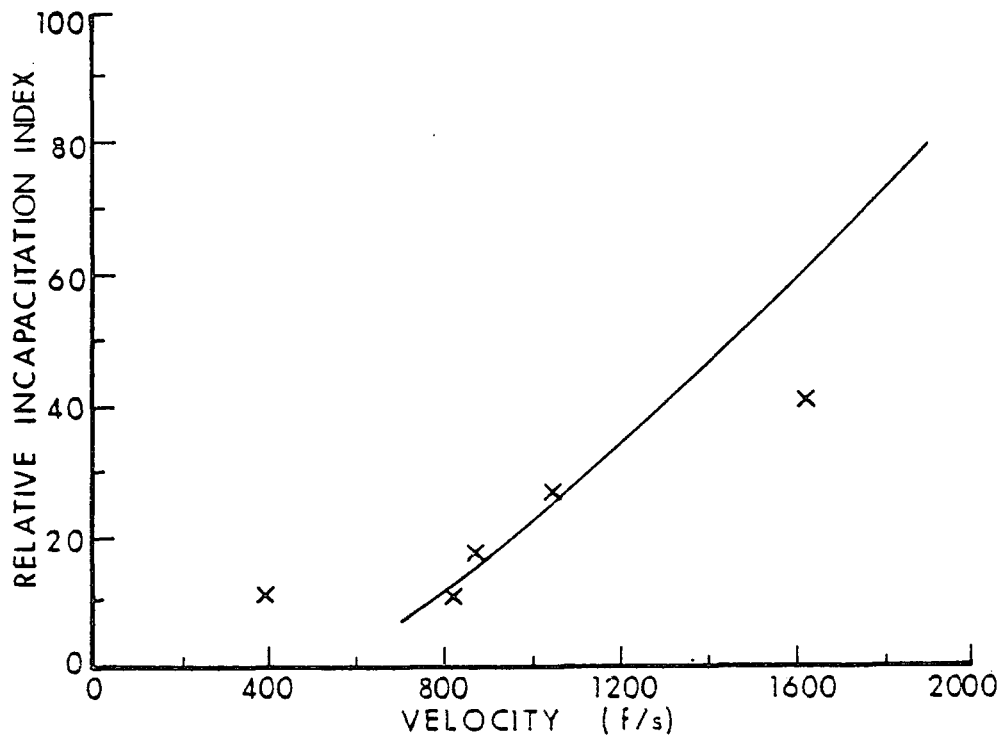


Figure 93. Relative Incapacitation Index Computer Predictions For a .357 Caliber Bullets With  $C_D = .45$  and Mass = 158 grains. (Data are .357, 148 grain WC bullets.)

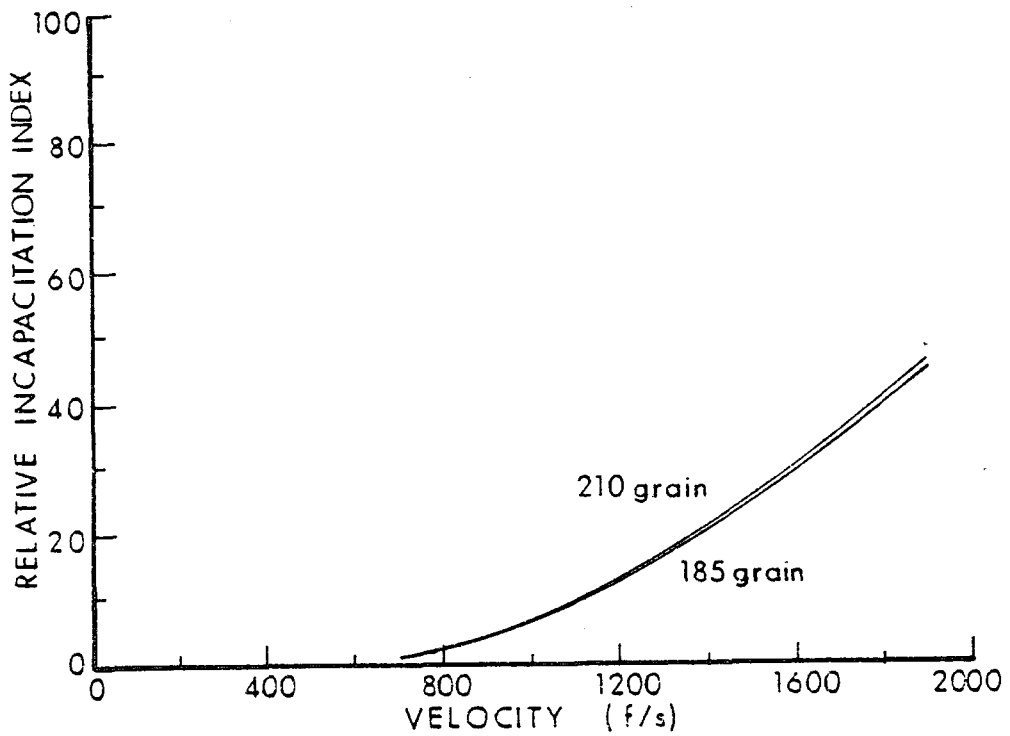


Figure 94. Relative Incapacitation Index Computer Predictions For a .45 Caliber Bullets With  $C_D = .30$ .

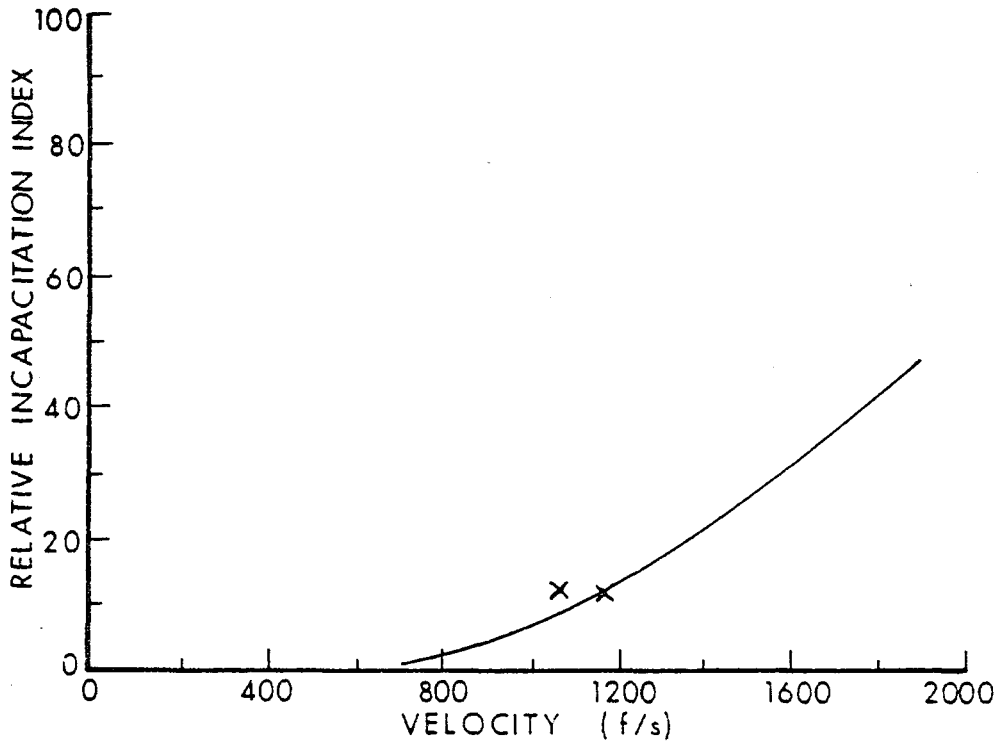


Figure 95. Relative Incapacitation Index Computer Predictions For a .45 Caliber Bullet With  $C_D = .45$  and Mass = 230 Grains. (Data are .45, 230 grain bullets.)

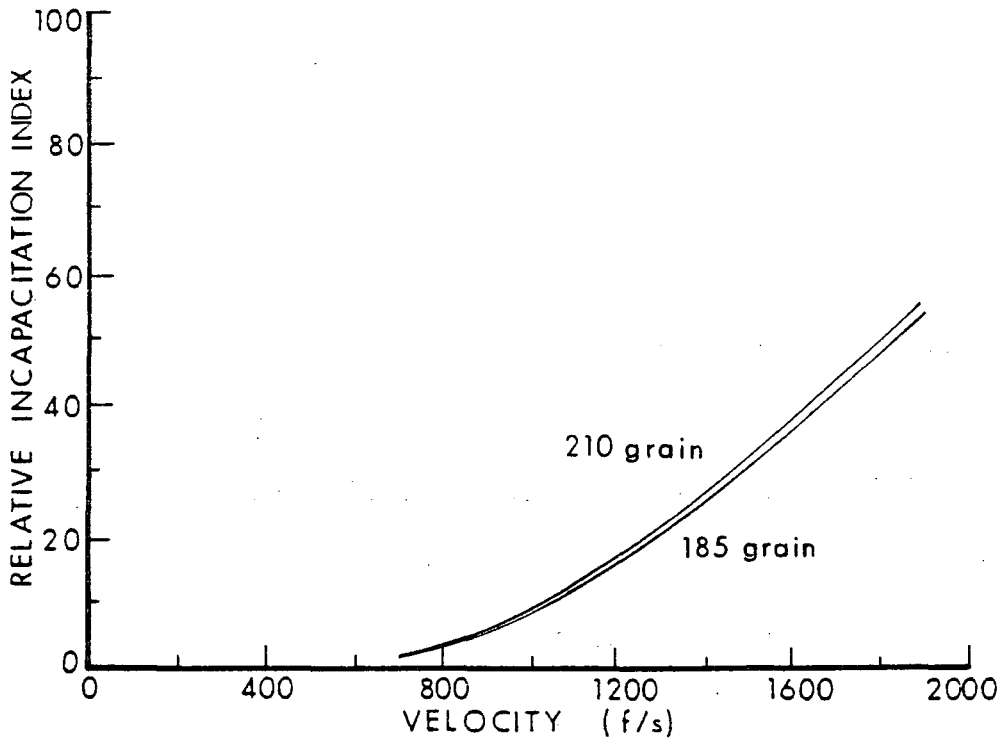


Figure 96. Relative Incapacitation Index Computer Predictions For a .45 Caliber Bullet With  $C_D = .37$ .

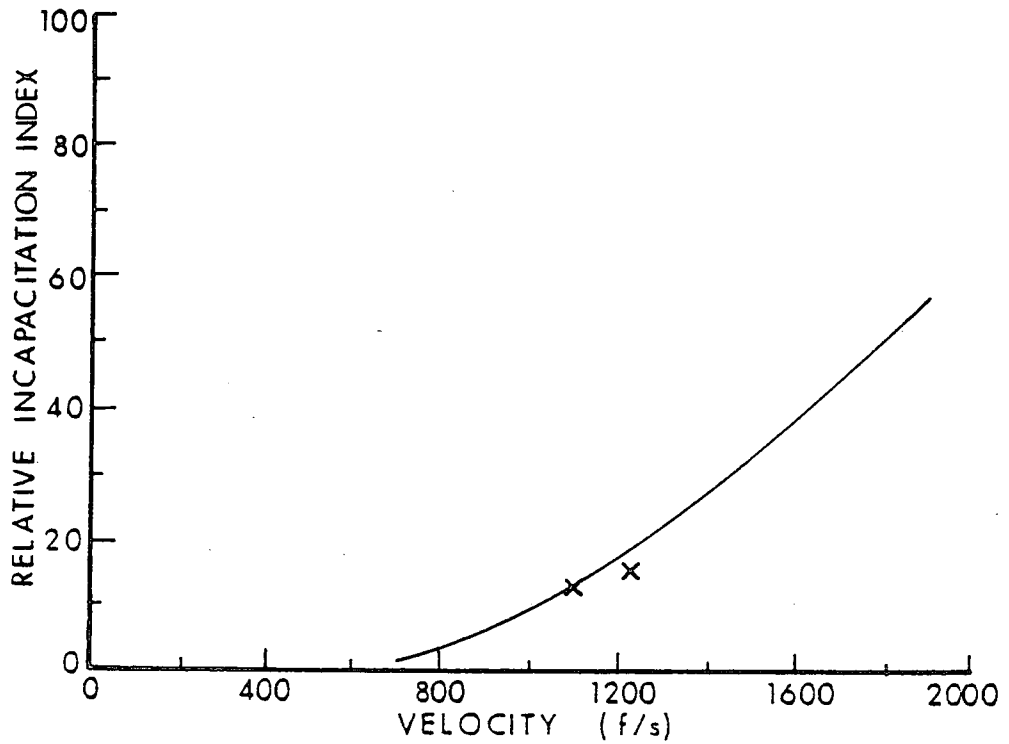


Figure 97. Relative Incapacitation Index Computer Predictions For a .45 Caliber Bullet With  $C_D = .37$  and Mass = 250 Grains. (Data are .45, 255 grain LRN bullets.)

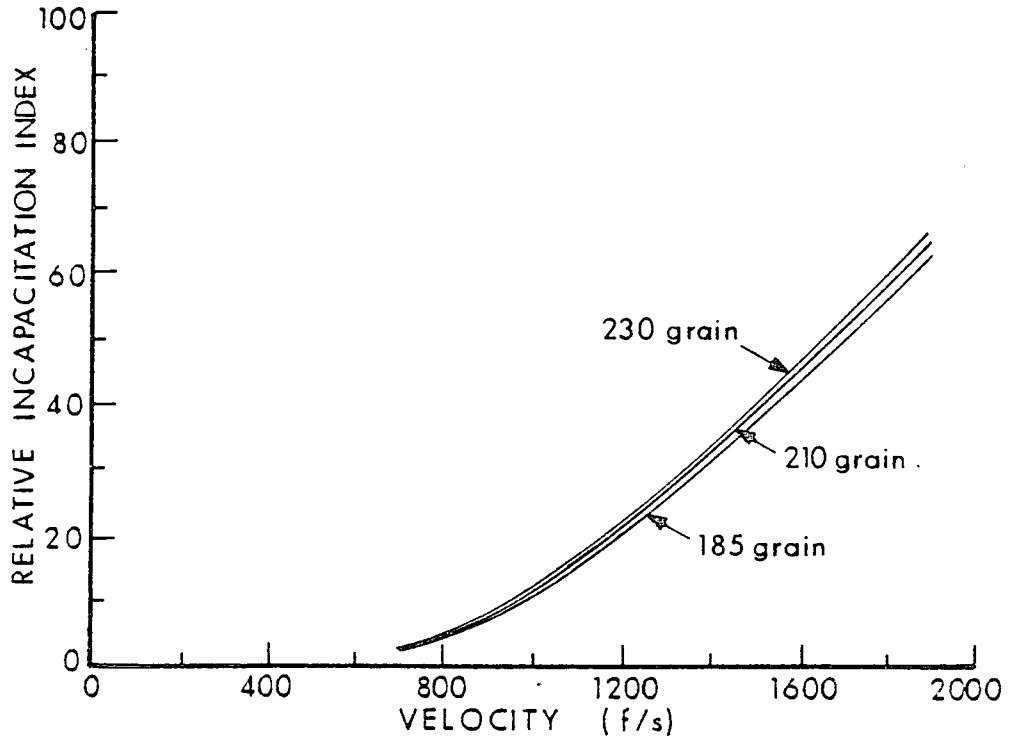


Figure 98. Relative Incapacitation Index Computer Predictions For a .45 Caliber Bullet With  $C_D = .45$ .

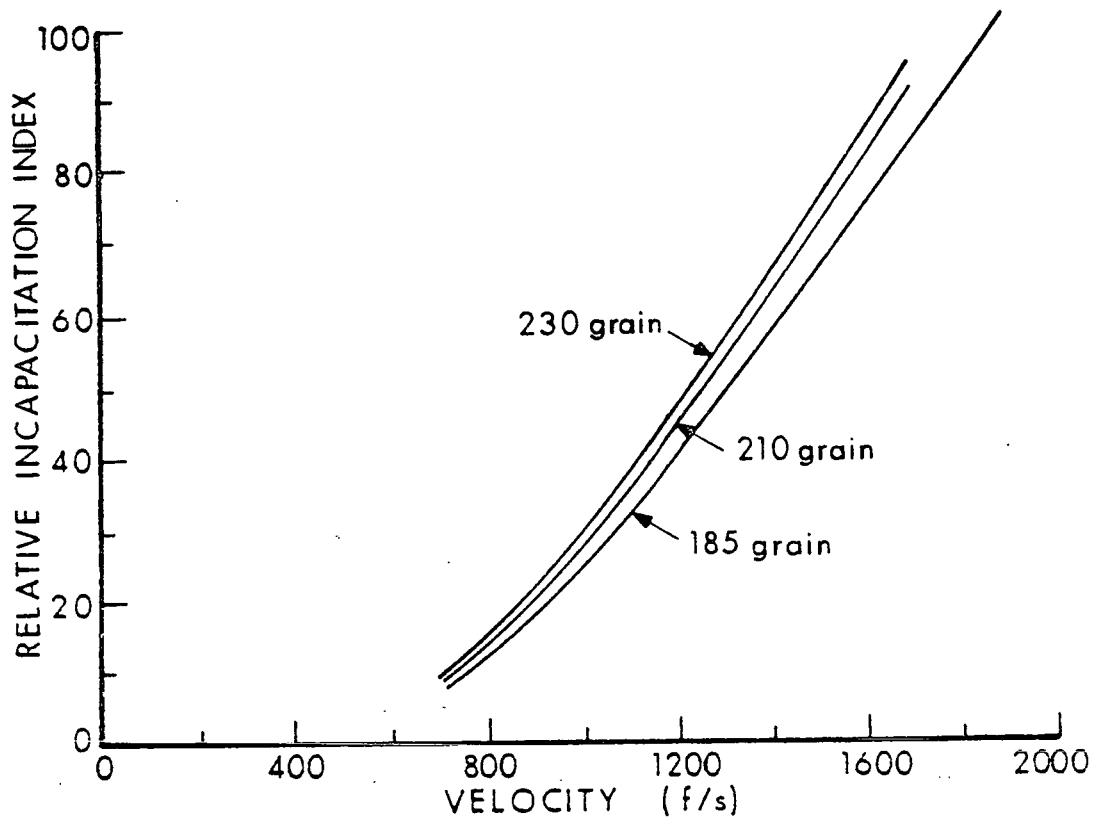


Figure 99. Relative Incapacitation Index Computer Predictions For a .45 Caliber Bullet With  $C_D = 1.20$ .

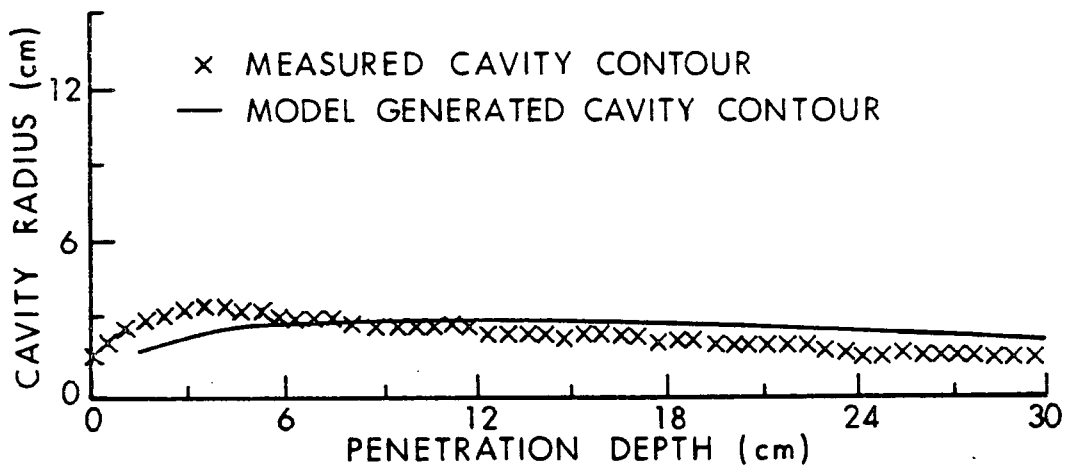


Figure 100. Comparison of a Measured Cavity Contour For a .357, 158 Grain JSP Bullet at 372 m/s Velocity and Model Generated Cavity Contour for a Similar Non-Deforming Bullet.

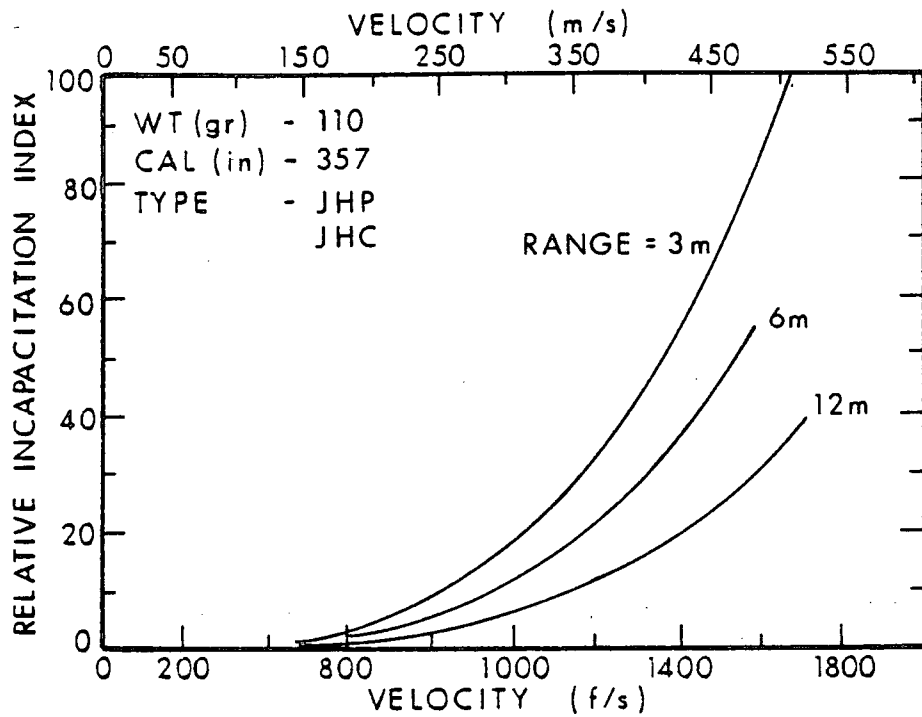


Figure 101. Effect of Engagement Range on the Relative Incapacitation Index.

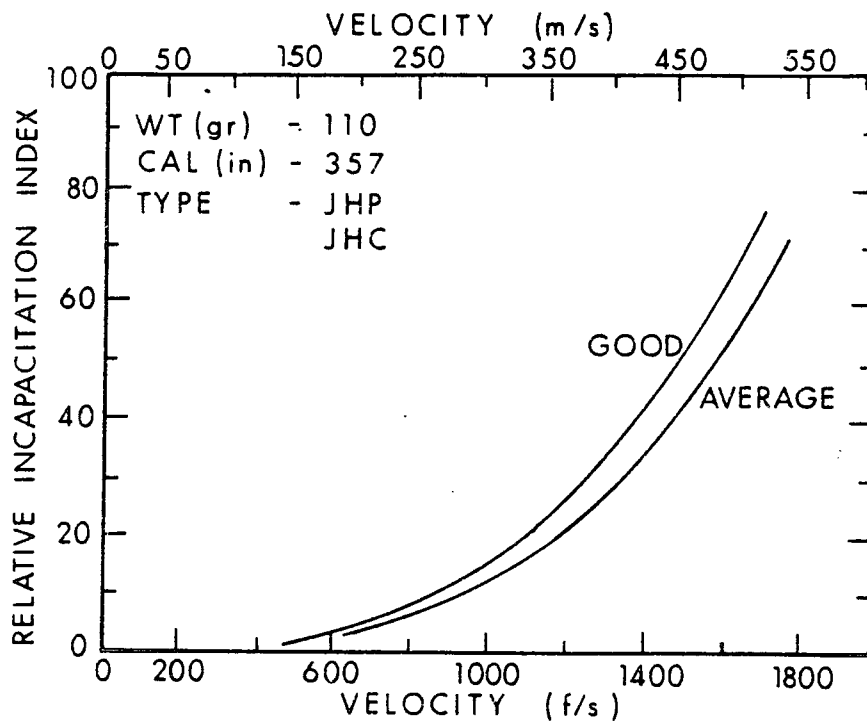


Figure 102. Effect of Shooter Accuracy on Relative Incapacitation Index. (Good = Group B shooters; Average = Group A shooters.)

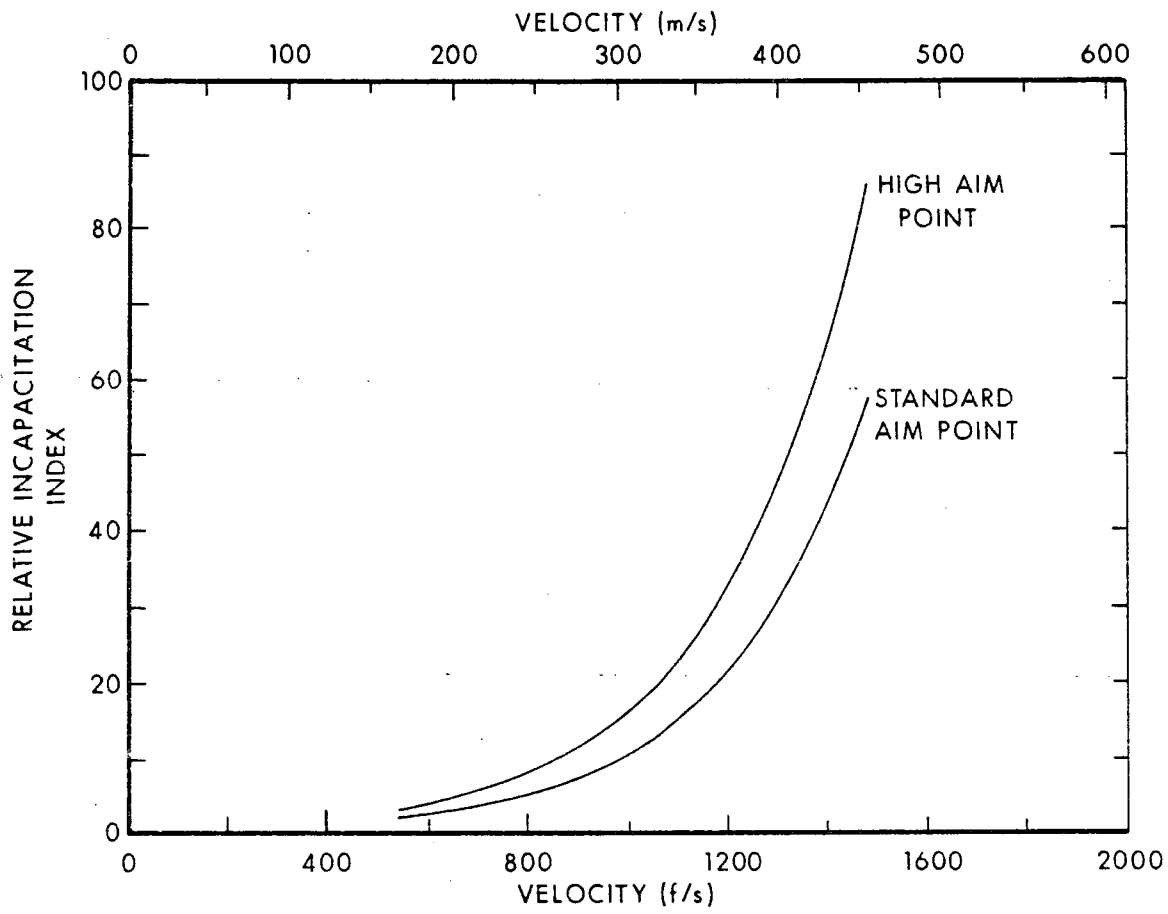


Figure .103. Effect of Aim Point on Relative Incapacitation Index. (Group a Shooters.)

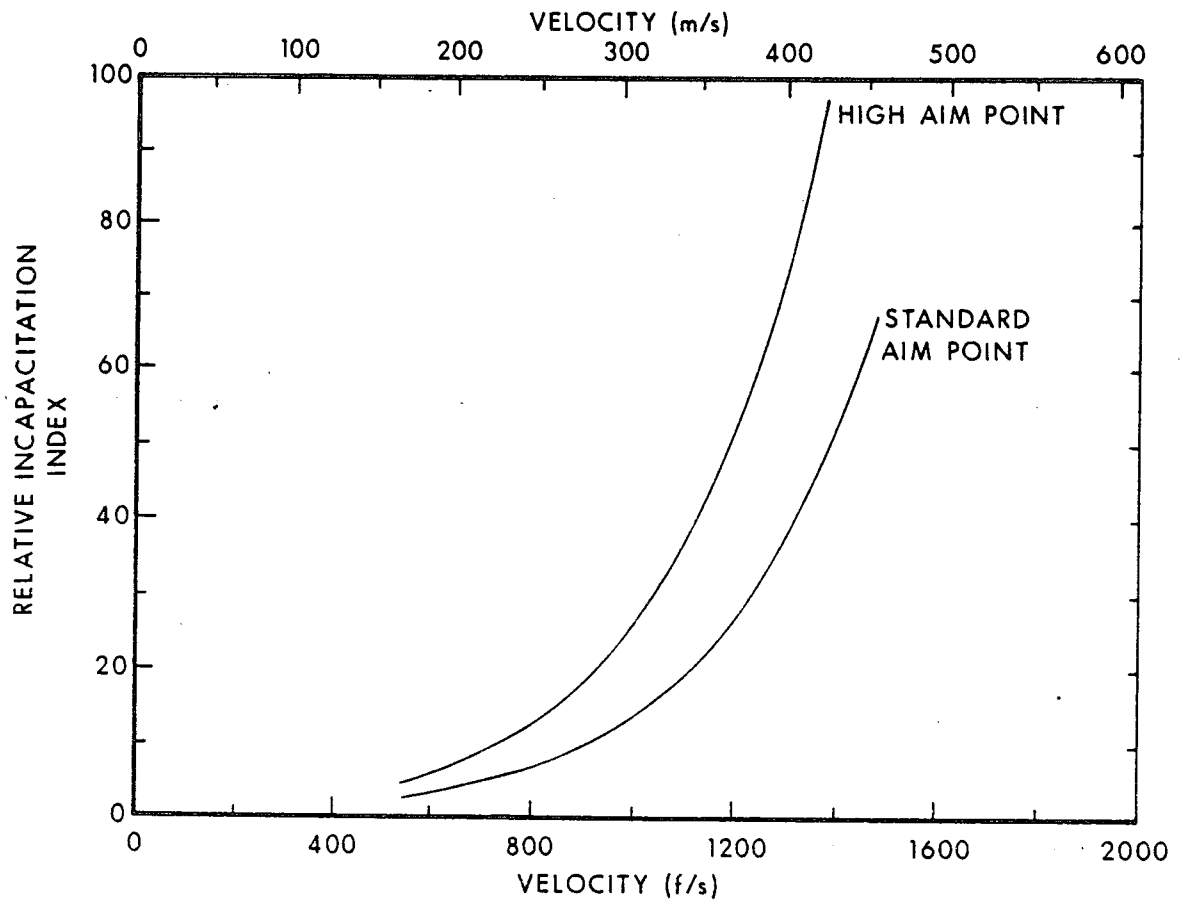


Figure 104. Effect of Aim Point on Relative Incapacitation Index. (Group B Shooters.)

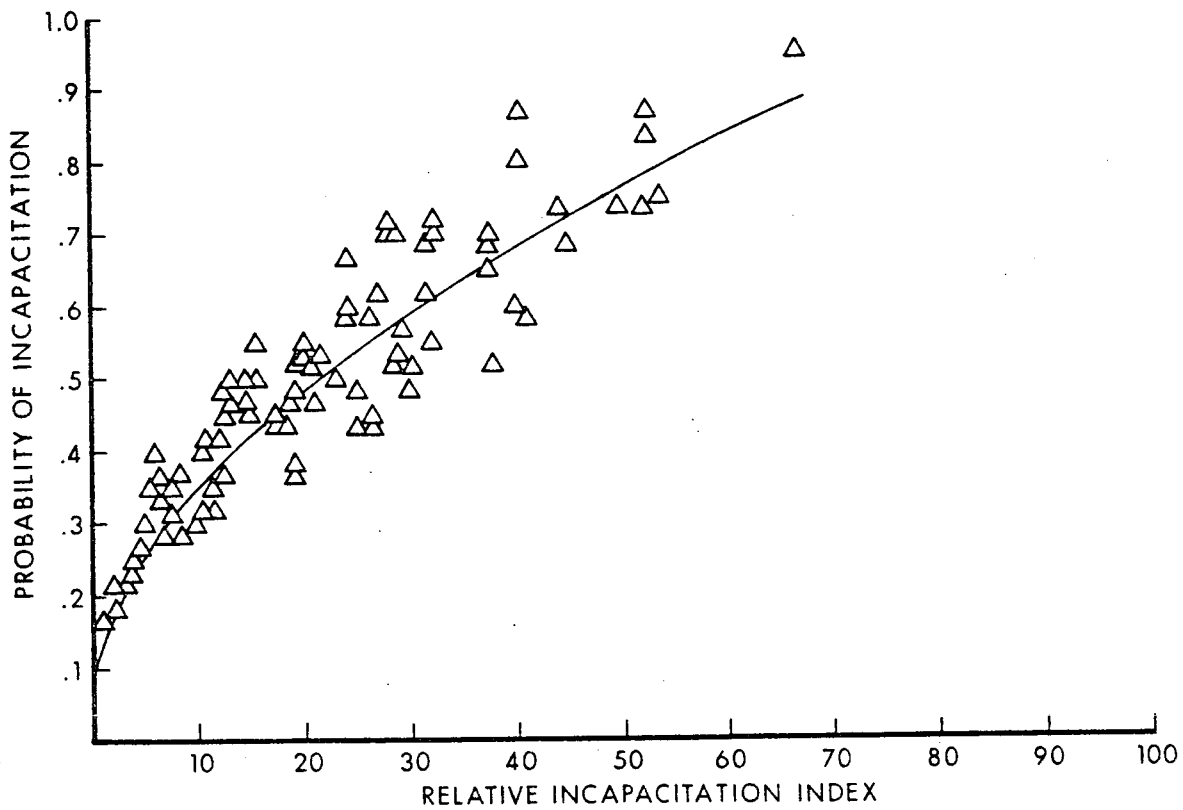


Figure 105. Relationship Between Probability of Instant Incapacitation and Relative Incapacitation Index.

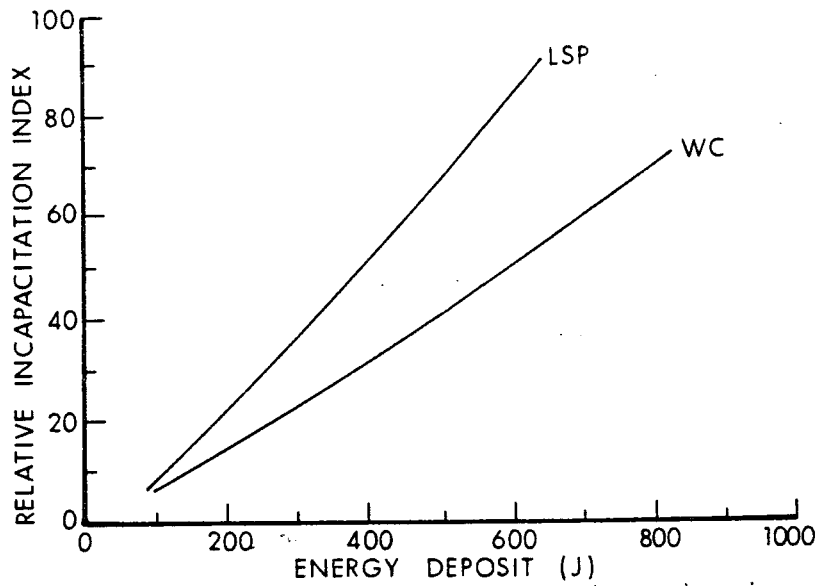


Figure 106. Relationship Between Energy Deposit and Relative Incapacitation Index.

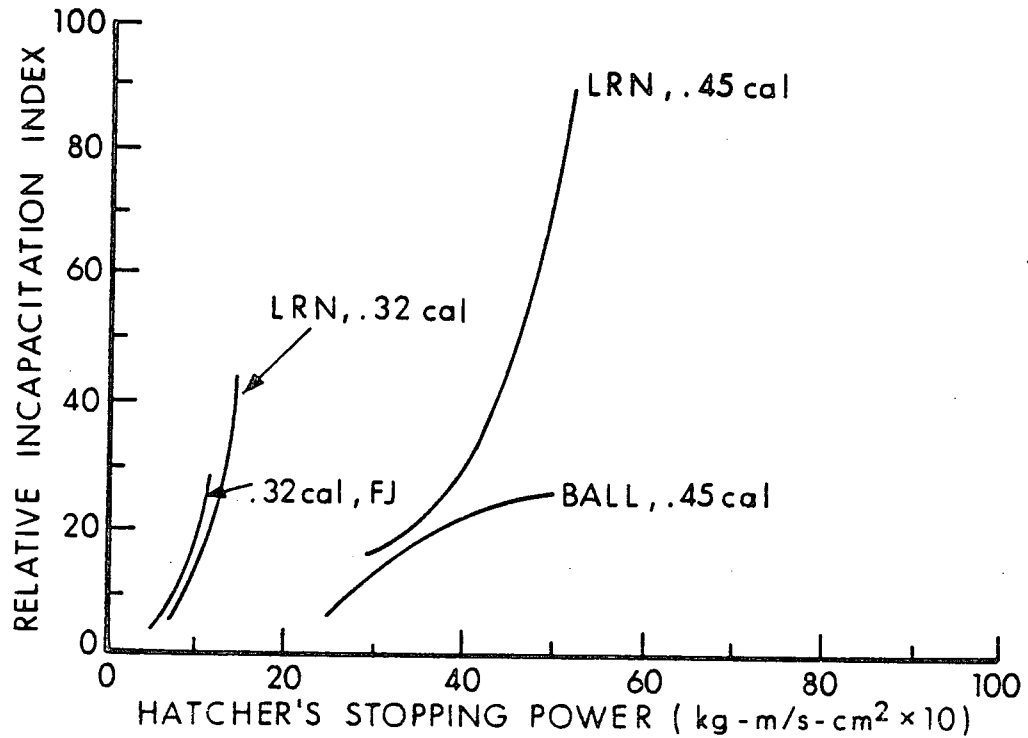


Figure 107. Relationship Between Hatcher's Formula and Relative Incapacitation Index.

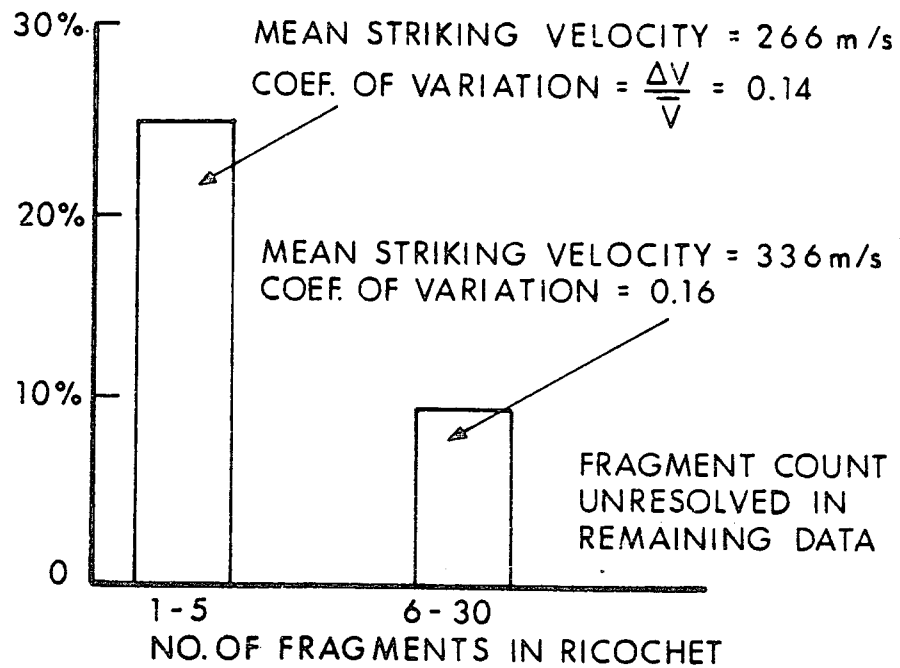


Figure 108. Histogram of Bullet Fragmentation on Ricochet.

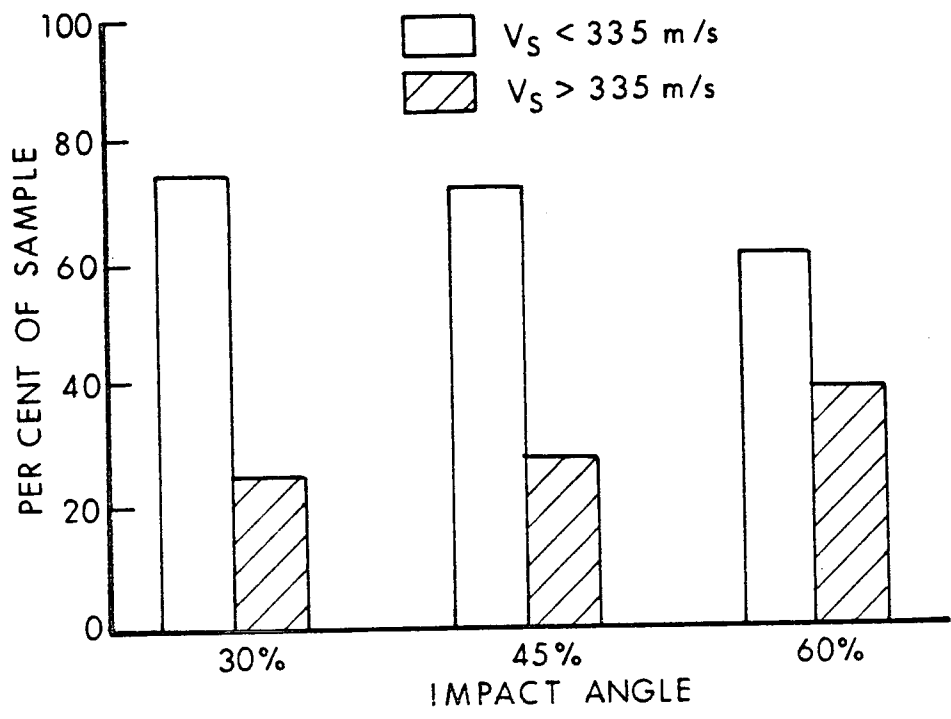


Figure 109. Effect of Impact Angle and Velocity on Bullet Breakup.

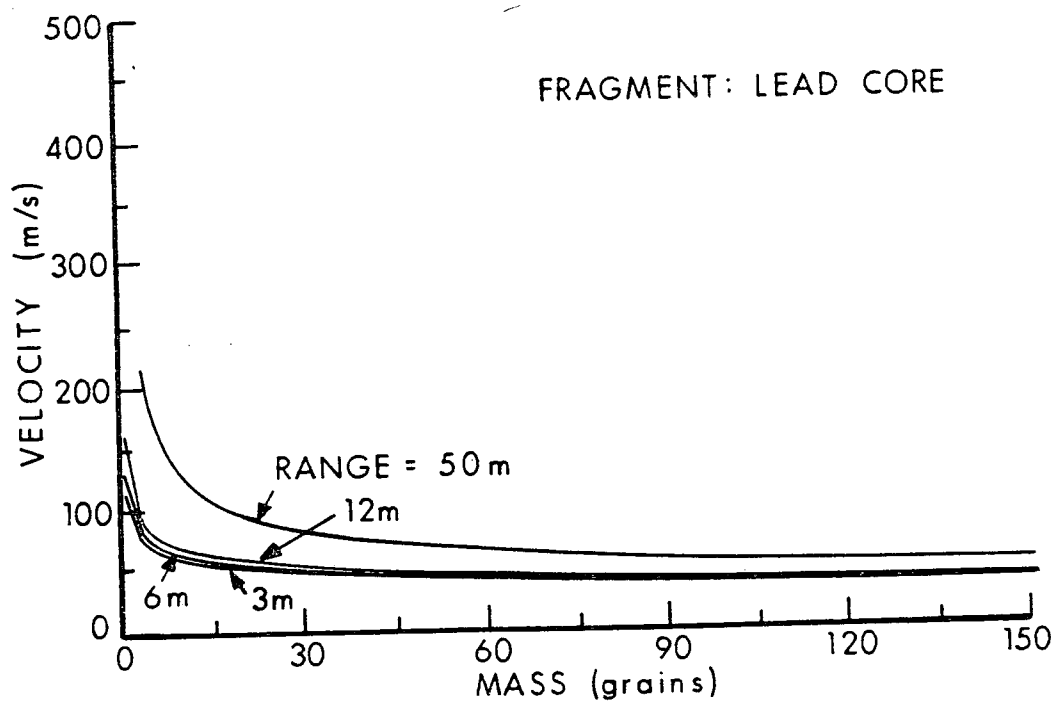


Figure 110. Safety Range For Lead Fragments.

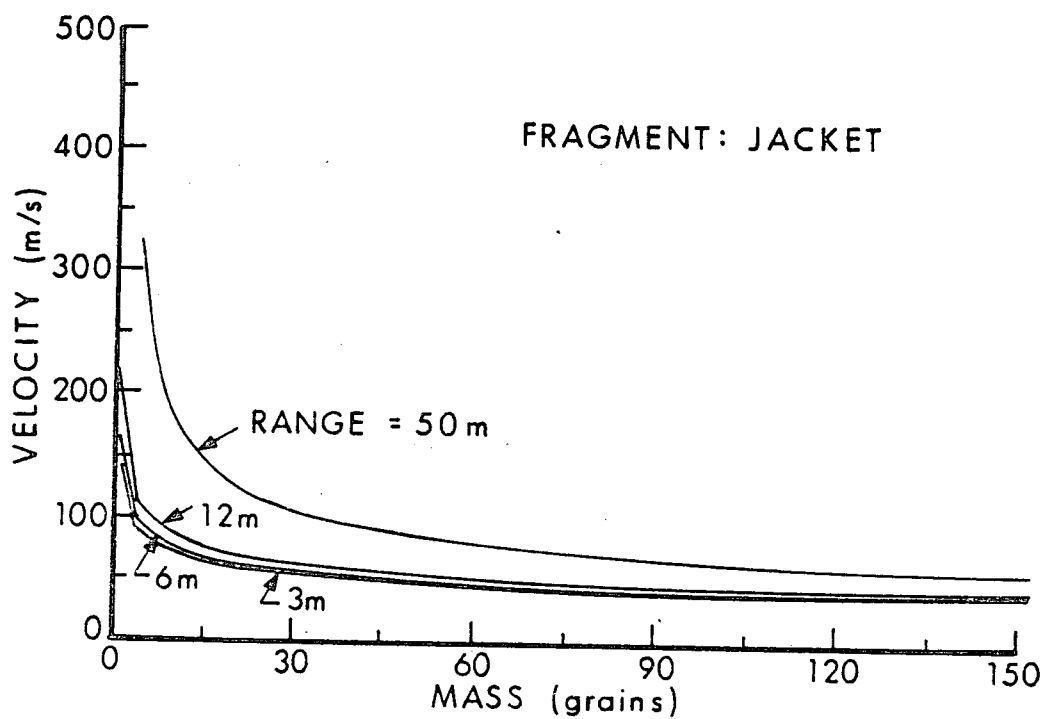


Figure 111. Safety Range For Bullet Jacket Fragments.

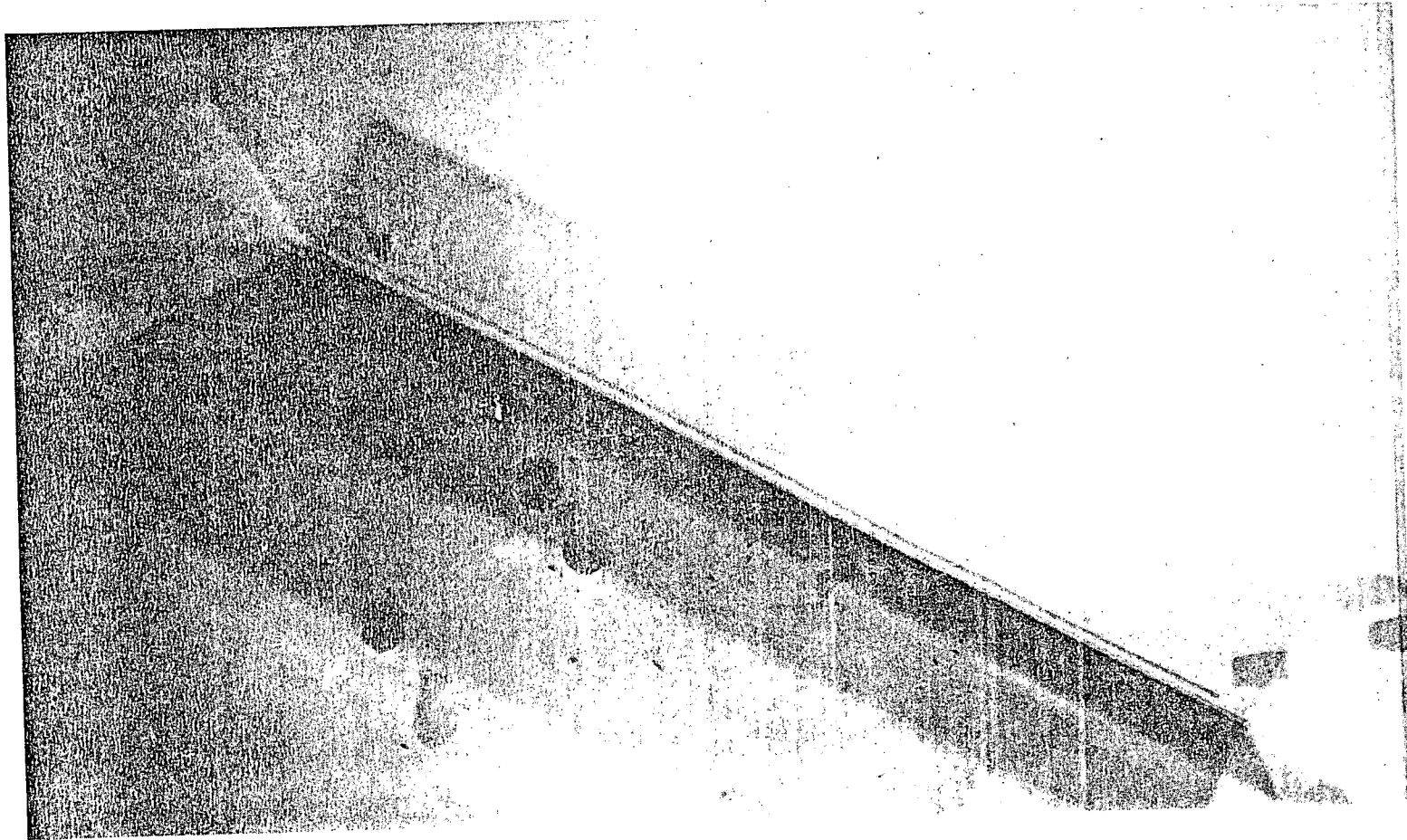


Figure 112. Impact of a .357 Magnum, 125 grain, JHP Bullet Against 1/8 inch Plate Glass. Velocity - 284 mps (933 fps)

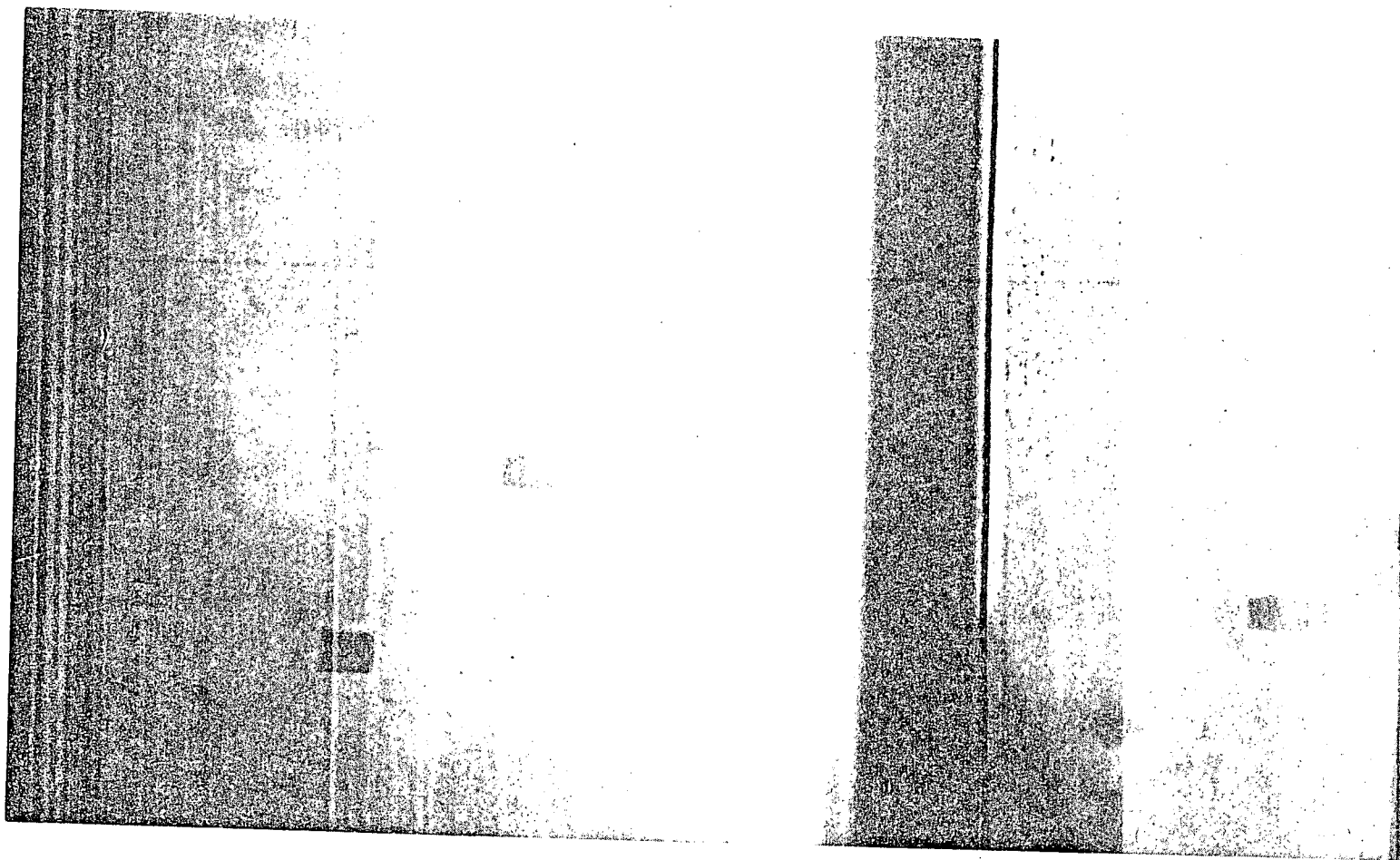


Figure 113. Impact of a .357 Magnum, 125 grain, JHP Bullet Against  
1/8 inch Plate Glass. Velocity - 194 mps (637 fps)

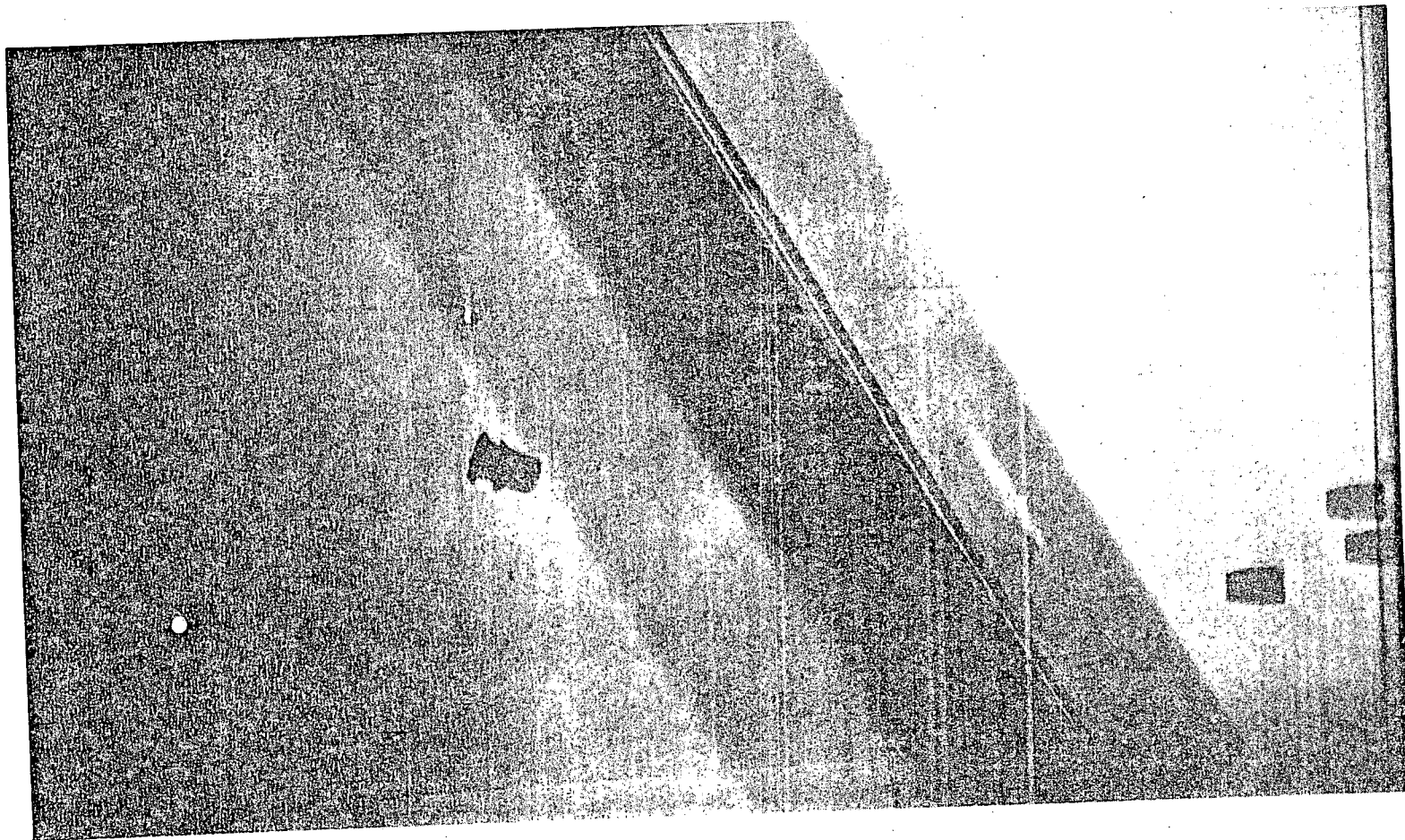


Figure 114. Impact of a .357 Magnum, 125 grain, JHP Bullet Against 1/8 inch Plate Glass. Velocity - 270 mps (887 fps)

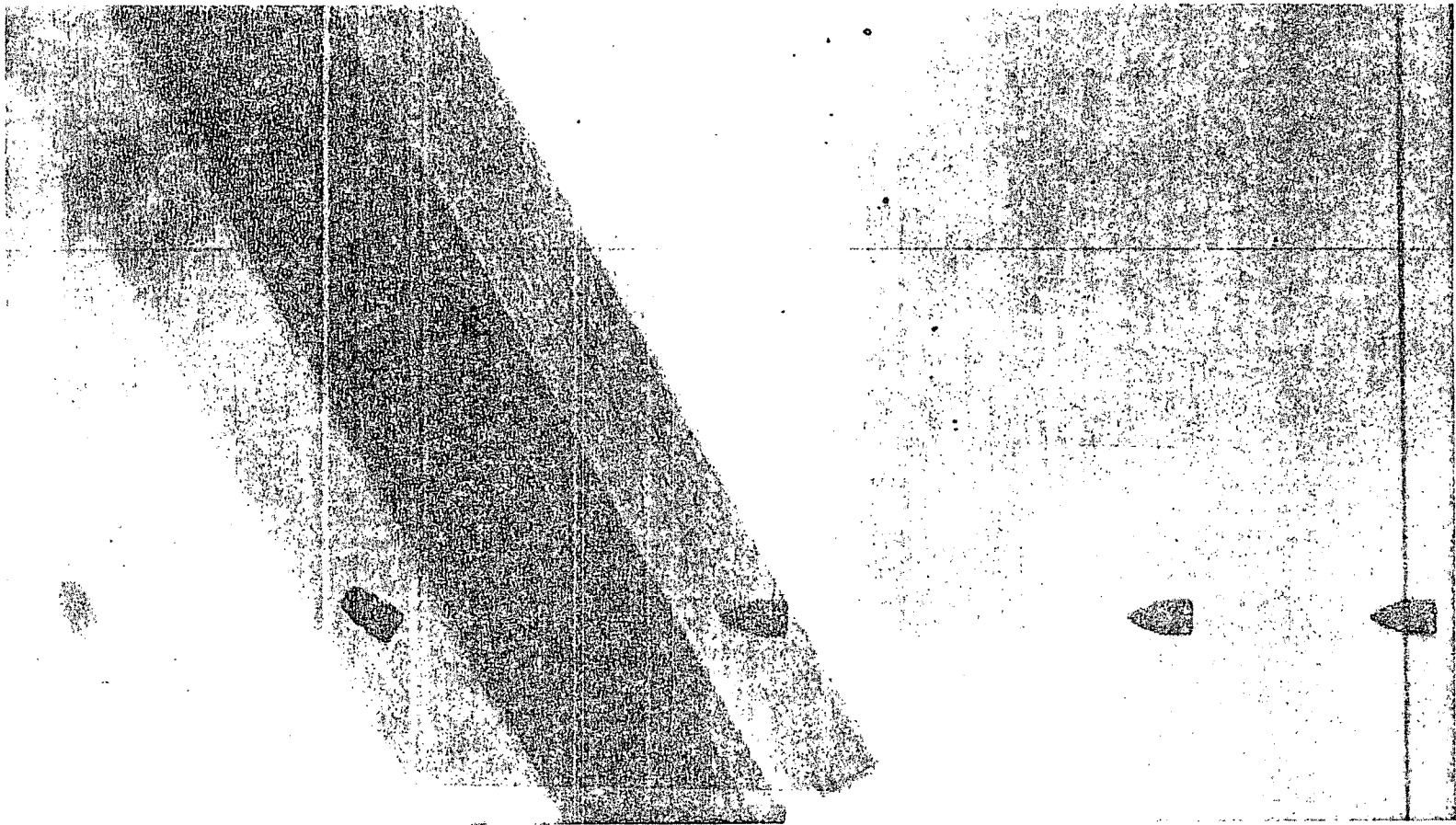


Figure 115. Impact of a .357 Magnum KTW Metal Piercing Bullet Against 1/8 inch Laminated Glass. Velocity - 644 mps (2114 fps)

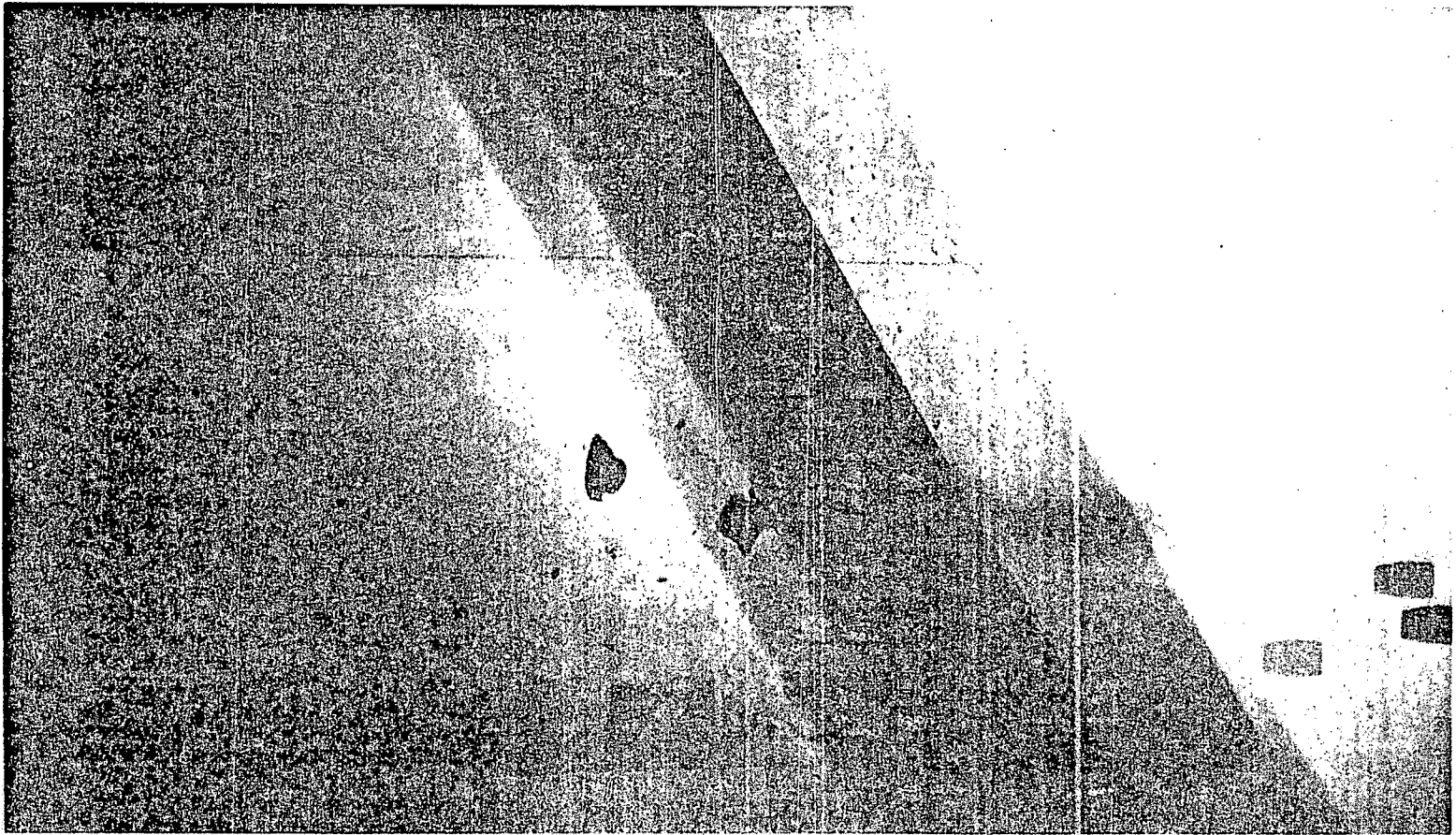


Figure 116. Impact of a .357 Magnum, 125 grain, JHP Bullet Against  
1/4 inch Laminated Glass. Velocity - 205 mps (674 fps)

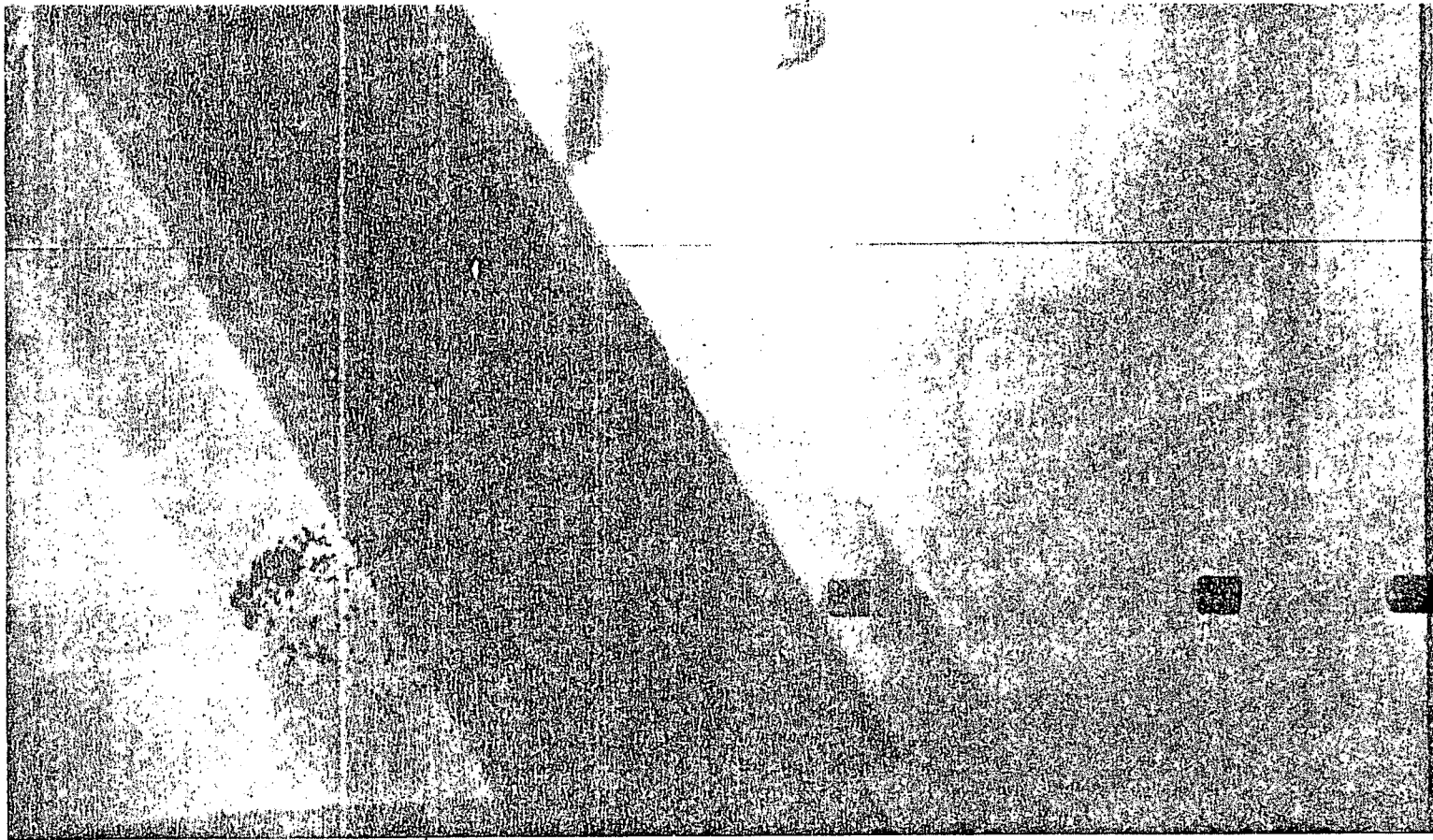


Figure 117. Impact of a .357 Magnum Safety Slug Against 1/4 inch Laminated Glass. Velocity - 601 mps (1972 fps)

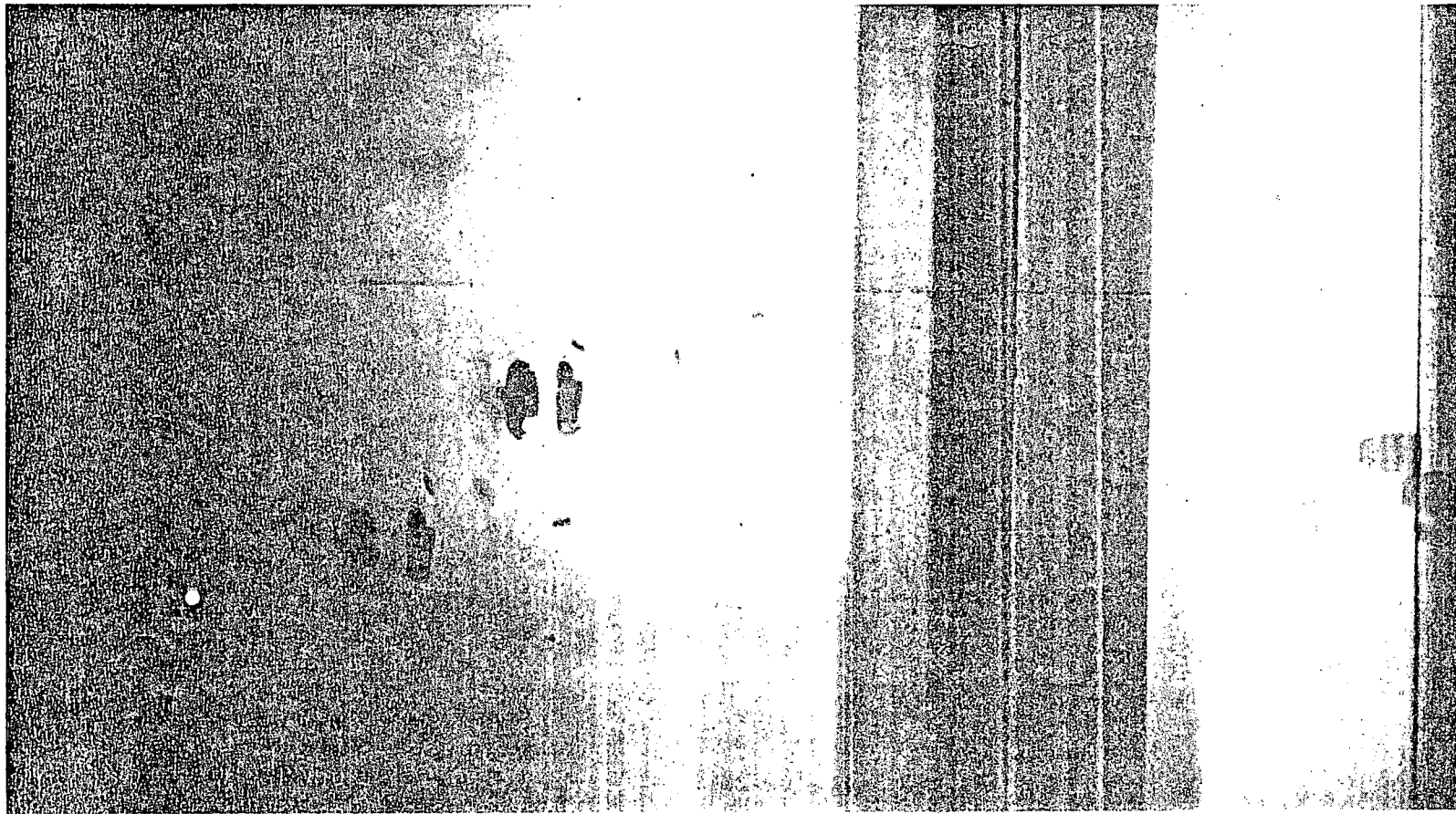


Figure 118. Impact of a .41 Magnum, 170 grain, JHP Bullet Against  
1/4 inch Laminated Glass. Velocity - 350 mps (1151 fps)

TABLE I

## Sedov's Ricochet Parameters

PARAMETER	DESCRIPTION
$\frac{tV\cos\theta}{c}$	non-dimensional time
$\cot\theta$	ratio of normal to tangential velocity components
$\theta$	angle of incidence at impact
$\frac{c\omega}{V\cos\theta}$	non-dimensional angular velocity at impact
$\frac{X_{cg}}{c}, \frac{Y_{cg}}{c}$	location of projectile center of gravity
$\frac{J}{\rho c^5}$	non-dimensional pitch plane moment of inertia
$\frac{m}{\rho c^3}$	non-dimensional projectile mass
$\frac{2F}{\rho c^2 V^2 \cos^2\theta}$	external force coefficient
$\frac{V\cos\theta}{\sqrt{cg}}$	the hydrodynamic Froude number
$\frac{\rho V\cos\theta c}{\mu}$	Reynolds number

- $c$  = projectile diameter  
 $t$  = time after impact  
 $V$  = impact speed  
 $\theta$  = impact angle  
 $\omega$  = angular velocity  
 $Y_{cg}, Y_{cg}$  = coordinates of center of gravity  
 $J$  = polar mass moment of inertia  
 $\rho$  = mass density of water  
 $F$  = external force  
 $g$  = gravitational constant  
 $\mu$  = viscosity coefficient for water

TABLE II. Sample Scan Output

SCAN 0 ( KO = 95155 ) covering round numbers 6 to 335 with:

ALL MANUFACTURERS  
 CONSTRUCTION CODES RN WC JSP LRN  
 MASSES (grains) - 148 to 158  
 CALIBERS - .357  
 STRIKING VELOCITIES (f/s) - 800 to 1400

RND. No.	ID	MASS(grains)	CALIBER	VS(f/s)
78	S+W,WC,.38SPEC	147.9	.357	820
80	S+W,LRN,.38SPEC	157.9	.357	869
81	S+W,JSP,.38SPEC	157.9	.357	1040
105	S+W,JSP,.357MAG	157.9	.357	1220
110	S+W,JSP,.357MAG	157.9	.357	1076
111	S+W,JSP,.357MAG	157.9	.357	1043
112	S+W,JSP,.357MAG	157.9	.357	954
188	SIERRA,JSP	157.9	.357	1128
189	SIERRA,JSP	157.9	.357	1263
190	SIERRA,JSP	157.9	.357	967
191	SIERRA,JSP	157.9	.357	853
200	SIERRA,JSP	157.9	.357	1154
201	SIERRA,JSP	157.9	.357	1299
262	HI-PRECISION,JSP	157.9	.357	1269
263	HI-PRECISION,JSP	157.9	.357	1125
267	HI-PRECISION,JSP	157.9	.357	1243
268	HI-PRECISION,JSP	157.9	.357	1092
289	W-W,JSP,.357MAG	150	.357	1289
301	W-W,LRN,.38SPEC	150	.357	928
302	W-W,LRN,.38SPEC	150	.357	1138
303	W-W,LRN,.38SPEC	150	.357	1259
304	W-W,LRN,.38SPEC	157.9	.357	944
305	W-W,LRN,.38SPEC	157.9	.357	1089
306	W-W,LRN,.38SPEC	157.9	.357	1250
311	W-W,RN,.38SPEC	157.9	.357	997
312	W-W,RN,.38SPEC	157.9	.357	1099
313	W-W,RN,.38SPEC	157.9	.357	1236
314	W-W,WC,.38SPEC	147.9	.357	869
315	W-W,WC,.38SPEC	147.9	.357	1046
317	W-W,JSP,.38SPEC	157.9	.357	1282
318	W-W,JSP,.38SPEC	157.9	.357	1141
319	W-W,JSP,.38SPEC	157.9	.357	987

32 rounds satisfy SCAN CODE 0

TABLE III. Vulnerability Index Parameters

<u>Range (meters)</u>	<u>Hit Distribution</u>
3	Group A (standard aim point)
6	Group A ( " " " )
12	Group A ( " " " )
6	Group B ( " " " )
6	Group A (high aim point)
6	Group B ( " " " )

TABLE IV

SCAN 82 ( K0= 71948 ) covering round numbers 6 to 917 with:

ALL MANUFACTURERS  
 CONSTRUCTION CODES JSP JFP  
 MASSES (grains) - 90  
 CALIBERS - .353 to .355  
 STRIKING VELOCITIES (f/s) - All

4 rounds satisfy SCAN CODE 82

RND. NO.	ID	MASS(GR)	DIAM.(IN)	VS(F/S)	RII
135	S+W,J SP,9M M	90.0	0.353	1558	31.50
136	S+W,J SP,9M M	90.0	0.353	1371	19.29
137	S+W,J SP,9M M	90.0	0.353	1076	6.67
139	S+W,J SP,9M M	90.0	0.353	843	3.91

A=-3.20687575804  
 B= 3.84511448E-03  
 C= 1105.837898399

MANUFACTURER	AVG DEV	NO. PTS.	% PTS.POS.
S+	-0.04	4	50.00

(See also Figure 24)

TABLE V

SCAN 86 ( K0= 71251 ) covering round numbers 6 to 917 with:

ALL MANUFACTURERS  
 CONSTRUCTION CODES FJ  
 MASSES (grains) - 100  
 CALIBERS - .353 to .355  
 STRIKING VELOCITIES (f/s) - All

RND. NO.	ID	MASS(GR)	DIAM.(IN)	VS(F/S)	RII
73	S+W,F J,9MM	100.0	0.353	1646	29.99

A=-9.14450233E-03  
 B= 2.37736550E-03  
 C=-670.723217681

MANUFACTURER	AVG DEV	NO. PTS.	% PTS.POS.
S+	-3.09	1	0.00

(See also Figure 25)

TABLE VI

SCAN 63 ( K0= 71273 ) covering round numbers 6 to 917 with:

ALL MANUFACTURERS  
 CONSTRUCTION CODES PP  
 MASSES (grains) - 100  
 CALIBERS - .353 to .355  
 STRIKING VELOCITIES (f/s) - All

5 rounds satisfy SCAN CODE 63

RND. NO.	ID	MASS(GR)	DIAM.(IN)	VS(F/S)	RII
60	W-W,P P,9MM	100.0	0.353	1568	48.78
61	W-W,P P,9MM	100.0	0.353	708	3.50
62	W-W,P P,9MM	100.0	0.353	977	7.12
63	W-W,P P,9MM	100.0	0.353	1154	10.43
64	W-W,P P,9MM	100.0	0.353	1348	31.40

A=-3.084359160868  
 B= 4.10145406E-03  
 C= 1005.06277529

MANUFACTURER	AVG DEV	NO. PTS.	% PTS.POS.
W-	-0.00	5	60.00

(See also Figure 26)

TABLE VII

SCAN 85 ( K0= 71968 ) covering round numbers 6 to 917 with:

ALL MANUFACTURERS  
 CONSTRUCTION CODES  
 MASSES (grains) - 100  
 CALIBERS - .353 to .355  
 STRIKING VELOCITIES (f/s) - All

JSP

JFP

RND. NO.	ID	MASS(GR)	DIAM.(IN)	VS(F/S)	RII
72	S+W,J SP,9M M	100.0	0.353	1519	39.98

A=-3.52531725E-03

B= 2.74871135E-03

C=-684.0920454629

MANUFACTURER	AVG DEV	NO. PTS.	% PTS.POS.
S+	-1.33	1	0.00

S+

-1.33

1

0.00

(See also Figure 27)

TABLE VIII

SCAN 8 ( K0= 71911 ) covering round numbers 6 to 917 with:

All MANUFACTURERS  
 CONSTRUCTION CODES JHP JHC  
 MASSES (grains) - 100  
 CALIBERS - .353 to .355  
 STRIKING VELOCITIES (f/s) - All

11 rounds satisfy SCAN CODE 8

RND. NO.	ID	MASS(GR)	DIAM.(IN)	VS(F/S)	RII
75	S+W,J HP,9M M	100.0	0.353	1512	44.18
131	S+W,J HP,9M M	100.0	0.353	1377	27.17
132	S+W,J HP,9M M	100.0	0.353	1099	15.11
133	S+W,J HP,9M M	100.0	0.353	836	3.57
134	S+W,J HP,9M M	100.0	0.353	600	1.27
490	SPEER, JHP,9M M	100.0	0.353	1440	44.82
491	SPEER, JHP,9M M	100.0	0.353	1486	36.43
492	SPEER, JHP,9M M	100.0	0.353	1246	32.06
493	SPEER, JHP,9M M	100.0	0.353	1210	29.19
494	SPEER, JHP,9M M	100.0	0.353	974	15.86
495	SPEER, JHP,9M M	100.0	0.353	875	7.27

A= 5.638407692003  
 B= 2.76390508E-04  
 C=-3411.507895403

MANUFACTURER	AVG DEV	NO.	PTS.	% PTS.POS.
S+	-2.44	5	20.00	
SP	+2.71	6	66.66	

(See also Figure 28)

TABLE IX

SCAN 87 ( K0= 71081 ) covering round numbers 6 to 917 with:

A11 MANUFACTURERS  
 CONSTRUCTION CODES FJ  
 MASSES (grains) - 115  
 CALIBERS - .353  
 STRIKING VELOCITIES (f/s) - A11

RND. NO.	ID	MASS(GR)	DIAM.(IN)	VS(F/S)	RII
74	S+W,F J,9MM	115.0	0.353	1325	18.75

A=-2.44586917E-03  
 B= 2.72627309E-03  
 C=-831.5696403531

MANUFACTURER	AVG DEV	NO. PTS.	% PTS.POS.
S+	-1.00	1	0.00

(See also Figure 29)

TABLE X

SCAN 64 ( K0= 71303 ) covering round numbers 6 to 917 with:

ALL MANUFACTURERS  
 CONSTRUCTION CODES PP  
 MASSES (grains) - 115  
 CALIBERS - .353 to .355  
 STRIKING VELOCITIES (f/s) - All

RND. NO.	ID	MASS(GR)	DIAM.(IN)	VS(F/S)	RII
65	W-W,P P,9MM	115.0	0.353	1371	12.56

A=-1.16236775E-02  
 B= 2.17941033E-03  
 C=-359.9430776983

MANUFACTURER	AVG DEV	NO. PTS.	% PTS.POS.
W-	-2.53	1	0.00

(See also Figure 30)

TABLE XI

SCAN 83 ( K0= 71941 ) covering round numbers 6 to 917 with:

ALL MANUFACTURERS  
 CONSTRUCTION CODES JHP JHC  
 MASSES (grains) - 115  
 CALIBERS - .353 to .355  
 STRIKING VELOCITIES (f/s) - A11

11 rounds satisfy SCAN CODE 83

RND. NO.	ID	MASS(GR)	DIAM.(IN)	VS(F/S)	RII
76	S+W,J HP,9M M	115.0	0.353	1400	41.36
127	S+W,J HP,9M M	115.0	0.353	1253	22.33
128	S+W,J HP,9M M	115.0	0.353	1069	13.63
129	S+W,J HP,9M M	115.0	0.353	862	4.42
130	S+W,J HP,9M M	115.0	0.353	511	1.49
874	REM,JH P,9MM	115.0	0.353	1417	45.25
875	REM,JH P,9MM	115.0	0.353	1286	37.62
876	REM,JH P,9MM	115.0	0.353	1263	37.83
877	REM,JH P,9MM	115.0	0.353	1181	37.83
878	REM,JH P,9MM	115.0	0.353	1010	15.41
879	REM,JH P,9MM	115.0	0.353	856	3.33

NO X

A= .441116438577  
 B= 2.86405759E-03  
 C=-797.6466613514

MANUFACTURER	AVG DEV	NO. PTS.	% PTS.POS.
S+	-3.92	5	20.00
RE	+3.98	6	83.33

(See also Figure 31)

TABLE XII

SCAN 107 ( K0= 71299 ) covering round numbers 857 to 917 with:

All MANUFACTURERS  
 CONSTRUCTION CODES FJ  
 MASSES (grains) - 124  
 CALIBERS - .353 to .355  
 STRIKING VELOCITIES (f/s) - All

RND. NO.	ID	MASS(GR)	DIAM.(IN)	VS(F/S)	RII
880	REM,FJ ,9MM	123.9	0.353	1394	31.42
881	REM,FJ ,9MM	123.9	0.353	1335	31.42
882	REM,FJ ,9MM	123.9	0.353	1217	18.61
883	REM,FJ ,9MM	123.9	0.353	1161	14.82

A= 1.36366961E-03  
 B= 3.03046062E-03  
 C=-964.1634308413

MANUFACTURER	AVG DEV	NO. PTS.	% PTS.POS.
RE	+0.32	4	75.00

(See also Figure 32)

TABLE XIII

SCAN 103 ( K0= 71321 ) covering round numbers 490 to 917 with:

ALL MANUFACTURERS  
 CONSTRUCTION CODES RN  
 MASSES (grains) - 125  
 CALIBERS - .353 to .355  
 STRIKING VELOCITIES (f/s) - ALL

RND. NO.	ID	MASS(GR)	DIAM.(IN)	VS(F/S)	RII
497	SPEER, RN,9MM	125.0	0.353	1371	24.33

A=-5.36144609E-03  
 B= 2.71962101E-03  
 C=-616.291409314

MANUFACTURER	AVG DEV	NO. PTS.	% PTS.POS.
SP	-2.10	1	0.00

(See also Figure 33)

TABLE XIV

SCAN 102 ( K0= 71563 ) covering round numbers 480 to 917 with:

All MANUFACTURERS  
 CONSTRUCTION CODES JSP  
 MASSES (grains) - 125  
 CALIBERS - .353 to .355  
 STRIKING VELOCITIES (f/s) - All

6 rounds satisfy SCAN CODE 102

RND. NO.	ID	MASS(GR)	DIAM.(IN)	VS(F/S)	RII
485	SPEER, JSP,9M M	125.0	0.353	1351	59.44
486	SPEER, JSP,9M M	125.0	0.353	1269	27.39
487	SPEER, JSP,9M M	125.0	0.353	1263	27.81
488	SPEER, JSP,9M M	125.0	0.353	1128	14.91
489	SPEER, JSP,9M M	125.0	0.353	1069	10.06
496	SPEER, JSP,9M M	125.0	0.353	875	7.17

A=-22.16397211567  
 B= 1.34179180E-02  
 C= 10851.68361002

MANUFACTURER	AVG DEV	NO. PTS.	% PTS.POS.
SP	+0.23	6	33.33

(See also Figure 34)

TABLE XV

SCAN 26 ( K0= 72548 ) covering round numbers 6 to 917 with:

ALL MANUFACTURERS  
 CONSTRUCTION CODES JSP JFP  
 MASSES (grains) - 90  
 CALIBERS - .357  
 STRIKING VELOCITIES (f/s) - A11

RND. NO.	ID	MASS(GR)	DIAM.(IN)	VS(F/S)	RII
77	S+W,J SP,.3 8SPEC	90.0	0.357	1348	22.74
138	S+W,J SP,9M M	90.0	0.357	436	0.46

A=-1.51730603E-02  
 B= 2.87124095E-03  
 C=-836.1191135533

MANUFACTURER	AVG DEV	NO. PTS.	% PTS.POS.
S+	-1.36	2	0.00

(See also Figure 35)

TABLE XVI

SCAN 60 ( K9= 73774 ) covering round numbers 6 to 917 with:

A11 MANUFACTURERS  
 CONSTRUCTION CODES HEMIJSP  
 MASSES (grains) - 90  
 CALIBERS - .357  
 STRIKING VELOCITIES (f/s) - A11

3 rounds satisfy SCAN CODE 60

RND. NO.	ID	MASS(GR)	DIAM.(IN)	VS(F/S)	RII
117	S+W,HE MIJSP	90.0	0.357	1250	16.24
118	S+W,HE MIJSP	90.0	0.357	1030	7.13
119	S+W,HE MIJSP	90.0	0.357	777	4.29

A=-8.408132122255  
 B= 6.60067664E-03  
 C= 3681.056570682

MANUFACTURER	AVG DEV	NO. PTS.	% PTS.POS.
S+	-0.00	3	33.33

(See also Figure 36)

TABLE XVII

SCAN 91 ( K0= 71850 ) covering round numbers 6 to 917 with:

ALL MANUFACTURERS  
 CONSTRUCTION CODES MP  
 MASSES (grains) - 90  
 CALIBERS - .357  
 STRIKING VELOCITIES (f/s) - ALL

RND. NO.	ID	MASS(GR)	DIAM.(IN)	VS(F/S)	RII
283	KTW,M P,.35 7MAG	89.9	0.357	2033 NO X	42.44
284	KTW,M P,.38 SPEC	89.9	0.357	1479 NO X	32.69

A=-4.68891083E-02  
 B= 2.15139262E-03  
 C=-369.9821627931

MANUFACTURER	AVG DEV	NO. PTS.	% PTS.POS.
KT	-6.71	2	50.00

(See also Figure 37)

TABLE XVIII

SCAN 106 ( K0= 72081 ) covering round numbers 857 to 917 with:

All MANUFACTURERS  
 CONSTRUCTION CODES JHP  
 MASSES (grains) - 95  
 CALIBERS - .357  
 STRIKING VELOCITIES (f/s) - All

4 rounds satisfy SCAN CODE 106

RND. NO.	ID	MASS(GR)	DIAM.(IN)	VS(F/S)	RII
861	REM,JH P,38SP	95.0	0.357	800	3.31
862	REM,JH P,38SP	95.0	0.357	853	5.28
863	REM,JH P,38SP	95.0	0.357	977	13.41
864	REM,JH P,38SP	95.0	0.357	1397	36.63

A= 17.66599655536  
 B=-4.92163066E-03  
 C=-10042.07959894

MANUFACTURER	AVG DEV	NO. PTS.	% PTS.POS.
RE	+0.00	4	50.00

(See also Figure 38)

TABLE XVIX

SCAN 2 ( .K0= 72511 ) covering round numbers 74 to 917 with:

A11 MANUFACTURERS  
 CONSTRUCTION CODES JHP JHC  
 MASSES (grains) - 100  
 CALIBERS - .357  
 STRIKING VELOCITIES (f/s) - A11

5 rounds satisfy SCAN CODE 2

RND. NO.	ID	MASS(GR)	DIAM.(IN)	VS(F/S)	RII
167	ZERO, JHP	100.0	0.357	1292	22.64
168	ZERO, JHP	100.0	0.357	761	5.00
169	ZERO, JHP	100.0	0.357	1085	17.68
170	ZERO, JHP	100.0	0.357	938	14.00
171	ZERO, JHP	100.0	0.357	508	0.96

A= 6.060524075061  
 B=-4.13052697E-04  
 C=-3010.963354593

MANUFACTURER	AVG DEV	NO. PTS.	% PTS.POS.
ZE	+0.07	5	60.00

(See also Figure 39)

TABLE XX

SCAN 114 ( K0= 72133 ) covering round numbers 372 to 917 with:

A11 MANUFACTURERS  
 CONSTRUCTION CODES JSP  
 MASSES (grains) - 110  
 CALIBERS - .357  
 STRIKING VELOCITIES (f/s) - A11

6 rounds satisfy SCAN CODE 114

RND. NO.	ID	MASS(GR)	DIAM.(IN)	VS(F/S)	RII
471	SUPERV EL,JSP ,38SP	110.0	0.357	1135	15.12
474	SUPERV EL,JSP ,38SP	110.0	0.357	1230	20.81
475	SUPERV EL,JSP ,38SP	110.0	0.357	1138	16.19
476	SUPERV EL,JSP ,38SP	110.0	0.357	980	10.55
477	SUPERV EL,JSP ,38SP	110.0	0.357	898	6.39
478	SUPERV EL,JSP ,38SP	110.0	0.357	803	4.90

A= 2.760793982647  
 B= 1.49707574E-03  
 C=-1931.716267668

MANUFACTURER	AVG DEV	NO. PTS.	% PTS.POS.
SU	+0.01	6	66.66

(See also Figure 40)

TABLE XXI

SCAN 3 ( K0= 72531 ) covering round numbers 30 to 917 with:

A11 MANUFACTURERS  
 CONSTRUCTION CODES  
 MASSES (grains) - 110  
 CALIBERS - .357  
 STRIKING VELOCITIES (f/s) - A11

JHP

JHC

78 rounds satisfy SCAN CODE 3

RND. NO.	ID	MASS(GR)	DIAM.(IN)	VS(F/S)		RII
31	W-W,JH P,.357 MAG	110.0	0.357	1637	NO X	38.97
33	W-W,JH P,.357 MAG	110.0	0.357	1325	NO X	21.12
34	W-W,JH P,.357 MAG	110.0	0.357	1197	NO X	19.27
35	W-W,JH P,.357 MAG	110.0	0.357	1085		19.01
36	W-W,JH P,.357 MAG	110.0	0.357	1049		16.82
37	W-W,JH P,.357 MAG	110.0	0.357	912		12.67
38	W-W,JH P,.357 MAG	110.0	0.357	711		4.95
84	S+W,J HP,.3 8SPEC	110.0	0.357	1292		29.45
85	S+W,J HP,.3 57MAG	110.0	0.357	1725		60.31
102	S+W,J HP,.3 57MAG	110.0	0.357	774		4.76
106	S+W,J HP,.3 57MAG	110.0	0.357	1118		16.74
113	S+W,J HP,.3 57MAG	110.0	0.357	1122		18.42
114	S+W,J HP,.3 57MAG	110.0	0.357	1020		12.55
115	S+W,J HP,.3 57MAG	110.0	0.357	856		5.66
116	S+W,J HP,.3 57MAG	110.0	0.357	623		2.23
124	S+W,J HP,.3 8SPEC	110.0	0.357	971		3.02
125	S+W,J HP,.3 8SPEC	110.0	0.357	721		6.80
126	S+W,J HP,.3 8SPEC	110.0	0.357	869		6.05
140	W-W,J HP,.3 8SPEC	110.0	0.357	1335		26.35
141	W-W,J HP,.3 8SPEC	110.0	0.357	1184		22.70
142	W-W,J HP,.3 8SPEC	110.0	0.357	1013		15.64
143	W-W,J HP,.3 8SPEC	110.0	0.357	784		5.09
144	W-W,J HP,.3 8SPEC	110.0	0.357	656		2.24
158	HORNAD Y,JHP	110.0	0.357	1328		27.17
159	HORNAD Y,JHP	110.0	0.357	472		1.11
160	HORNAD Y,JHP	110.0	0.357	734		4.17
161	HORNAD Y,JHP	110.0	0.357	961		9.79
162	HORNAD Y,JHP	110.0	0.357	1102		16.45
172	SIERRA ,JHP	110.0	0.357	1286		31.12
173	SIERRA ,JHP	110.0	0.357	1079		13.09
174	SIERRA ,JHP	110.0	0.357	938		11.93
175	SIERRA ,JHP	110.0	0.357	787		5.81
193	SIERRA ,JHP	110.0	0.357	1443		33.91
194	SIERRA ,JHP	110.0	0.357	1122		11.39
195	SIERRA ,JHC	110.0	0.357	1289		27.66
208	ZERO, JHP	110.0	0.357	1489		44.14
209	ZERO, JHP	110.0	0.357	1351		36.57

210	ZERO, JHP	110.0	0.357	1194	24.10
211	HORNAD Y,JHP	110.0	0.357	1532	48.60
212	HORNAD Y,JHP	110.0	0.357	1364	33.56
213	HORNAD Y,JHP	110.0	0.357	1193	22.13
220	ZERO, JHP	110.0	0.357	1023	13.78
221	ZERO, JHP	110.0	0.357	958	10.67
222	ZERO, JHP	110.0	0.357	872	6.30
223	HORNAD Y,JHP	110.0	0.357	1079	14.94
224	HORNAD Y,JHP	110.0	0.357	980	9.80
225	HORNAD Y,JHP	110.0	0.357	905	7.31
259	HI-PRE CISION ,JHP	110.0	0.357	1279	21.80
260	HI-PRE CISION ,JHP	110.0	0.357	1128	13.31
261	HI-PRE CISION ,JHP	110.0	0.357	866	5.56
264	HI-PRE CISION ,JHP	110.0	0.357	1341	27.76
265	HI-PRE CISION ,JHP	110.0	0.357	1167	16.86
266	HI-PRE CISION ,JHP	110.0	0.357	1023	9.15
286	W-W,J HP,.3 57MAG	110.0	0.357	1279	34.74
287	W-W,J HP,.3 57MAG	110.0	0.357	1020	20.24
288	W-W,J HP,.3 57MAG	110.0	0.357	803	9.98
294	W-W,J HP,.3 8SPEC	110.0	0.357	1246	37.01
295	W-W,J HP,.3 8SPEC	110.0	0.357	1072	21.43
296	W-W,J HP,.3 8SPEC	110.0	0.357	889	13.17
297	W-W,J HP,.3 8SPEC	110.0	0.357	685	4.52
390	SPEER, JHP,38 CAL	110.0	0.357	1410	45.36
391	SPEER, JHP,38 CAL	110.0	0.357	1167	29.32
392	SPEER, JHP,38 CAL	110.0	0.357	849	9.58
424	SPEER, JHP,38 CAL	110.0	0.357	1469	51.25
425	SPEER, JHP,38 CAL	110.0	0.357	1443	46.84
426	SPEER, JHP,38 CAL	110.0	0.357	1299	36.20
479	SUPERV EL,JHP ,38SP	110.0	0.357	1371	49.30
480	SUPERV EL,JHP ,38SP	110.0	0.357	1243	38.62
481	SUPERV EL,JHP ,38SP	110.0	0.357	1151	25.04
482	SUPERV EL,JHP ,38SP	110.0	0.357	987	11.72
483	SUPERV EL,JHP ,38SP	110.0	0.357	915	8.27
484	SUPERV EL,JHP ,38SP	110.0	0.357	790	5.53
501	SPEER, JHP,35 7	110.0	0.357	1633	69.92
502	SPEER, JHP,35 7	110.0	0.357	1699	64.68
503	SPEER, JHP,35 7MAG	110.0	0.357	1397	31.90
504	SPEER, JHP,35 7MAG	110.0	0.357	1266	27.82
505	SPEER, JHP,35 7	110.0	0.357	971	12.80
506	SPEER, JHP,35 7	110.0	0.357	780	4.61

A= 2.685827088166

B= 1.48286991E-03

C=-1639.961723535

MANUFACTURER	AVG DEV	NO. PTS.	% PTS.POS.
HI	-4.06	6	0.00
S+	-1.84	11	27.27
SI	-1.50	7	28.57
HO	-0.91	11	27.27
ZE	+0.72	6	50.00
W-	+0.72	19	68.42
SP	+3.71	12	75.00
SU	+5.47	6	50.00

(See also Figure 41)

TABLE XXII

SCAN 73 ( K0= 72618 ) covering round numbers 6 to 917 with:

ALL MANUFACTURERS  
 CONSTRUCTION CODES                      JSP                      JFP  
 MASSES (grains) - 125  
 CALIBERS - .357  
 STRIKING VELOCITIES (f/s) - All

13 rounds satisfy SCAN CODE 73

RND. NO.	ID	MASS(GR)	DIAM.(IN)	VS(F/S)	RII
180	SIERRA ,JSP	125.0	0.357	1276	18.60
181	SIERRA ,JSP	125.0	0.357	1108	13.60
182	SIERRA ,JSP	125.0	0.357	925	7.89
183	SIERRA ,JSP	125.0	0.357	626	1.78
205	SIERRA ,JSP	125.0	0.357	1374	38.95
206	SIERRA ,JSP	125.0	0.357	1227	19.40
207	SIERRA ,JSP	125.0	0.357	1167	16.03
393	SPEER, JSP, 38 CAL	125.0	0.357	1407	45.50
394	SPEER, JSP, 38 CAL	125.0	0.357	1066	27.13
395	SPEER, JSP, 38 CAL	125.0	0.357	734	6.19
427	SPEER, JSP, 38 CAL	125.0	0.357	780	5.04
428	SPEER, JSP, 38 CAL	125.0	0.357	1309	34.90
429	SPEER, JSP, 38 CAL	125.0	0.357	1013	14.44

A= 3.833194355271

B= 9.99823834E-04

C=-2303.088990996

MANUFACTURER	AVG DEV.	NO.	PTS.	% PTS.POS.
SI	-2.76	7		14.28
SP	+4.82	6		33.33

(See also Figure 42)

TABLE XXIII

SCAN 10 ( K0= 72561 ) covering round numbers 6 to 917 with:

ALL MANUFACTURERS  
CONSTRUCTION CODES

JHP

JHC

MASSES (grains) - 125

CALIBERS - .357

STRIKING VELOCITIES (f/s) - All

62 rounds satisfy SCAN CODE 10

RND. NO.	ID	MASS(GR)	DIAM.(IN)	VS(F/S)	RII
7	REM,J HP,.3 8SPEC	125.0	0.357	1167 NO X	14.31
9	REM,J HP,.3 8SPEC	125.0	0.357	1003 NO X	15.10
10	REM,J HP,.3 8SPEC	125.0	0.357	987 NO X	14.99
11	REM,J HP,.3 8SPEC	125.0	0.357	866 NO X	7.15
12	REM,J HP,.3 8SPEC	125.0	0.357	790 NO X	4.99
13	REM,J HP,.3 8SPEC	125.0	0.357	675 NO X	2.72
83	S+W,J HP,.3 8SPEC	125.0	0.357	1079	19.07
88	S+W,J HP,.3 57MAG	125.0	0.357	1784	71.75
89	S+W,J HP,.3 8SPEC	125.0	0.357	541	1.33
90	S+W,J HP,.3 8SPEC	125.0	0.357	994	13.99
91	S+W,J HP,.3 8SPEC	125.0	0.357	853	7.43
92	S+W,J HP,.3 8SPEC	125.0	0.357	626	2.24
93	S+W,J HP,.3 8SPEC	125.0	0.357	1837	69.59
94	S+W,J HP,.3 57MAG	125.0	0.357	685	2.81
95	S+W,J HP,.3 57MAG	125.0	0.357	1269	26.85
96	S+W,J HP,.3 57MAG	125.0	0.357	1164	15.05
97	S+W,J HP,.3 57MAG	125.0	0.357	1007	9.56
98	S+W,J HP,.3 57MAG	125.0	0.357	915	6.02
99	S+W,J HP,.3 57MAG	125.0	0.357	820	5.28
145	HORNAD Y,JHP	125.0	0.357	1259	25.15
146	HORNAD Y,JHP	125.0	0.357	764	6.70
147	HORNAD Y,JHP	125.0	0.357	948	8.51
148	HORNAD Y,JHP	125.0	0.357	1131	20.68
163	ZERO, JHP	125.0	0.357	1256	23.71
164	ZERO, JHP	125.0	0.357	1069	19.13
165	ZERO, JHP	125.0	0.357	938	12.18
166	ZERO, JHP	125.0	0.357	725	5.59
176	SIERRA ,JHP	125.0	0.357	1269	28.36
177	SIERRA ,JHP	125.0	0.357	1082	13.82
178	SIERRA ,JHP	125.0	0.357	398	10.00
179	SIERRA ,JHP	125.0	0.357	754	4.93
196	SIERRA ,JHP	125.0	0.357	1122	12.92
197	SIERRA ,JHP	125.0	0.357	1358	33.89
202	ZERO, JHP	125.0	0.357	1404	34.20
203	ZERO, JHP	125.0	0.357	1243	25.80
204	ZERO, JHP	125.0	0.357	1181	27.05

214	HORNAD Y,JHP	125.0	0.357	1397	38.15
215	HORNAD Y,JHP	125.0	0.357	1233	31.51
216	HORNAD Y,JHP	125.0	0.357	1174	22.49
217	ZERO, JHP	125.0	0.357	977	15.77
218	ZERO, JHP	125.0	0.357	931	10.69
219	ZERO, JHP	125.0	0.357	836	5.05
226	HORNAD Y,JHP	125.0	0.357	1046	12.04
228	HORNAD Y,JHP	125.0	0.357	810	7.40
396	SPEER, JHP,38 CAL	125.0	0.357	1430	51.13
397	SPEER, JHP,38 CAL	125.0	0.357	1112	25.77
398	SPEER, JHP,38 CAL	125.0	0.357	754	6.98
430	SPEER, JHP,38 CAL	125.0	0.357	1335	48.46
431	SPEER, JHP,38 CAL	125.0	0.357	1256	39.97
432	SPEER, JHP,38 CAL	125.0	0.357	1036	20.48
857	REM,JH P,38CA L	125.0	0.357	1305	40.60
858	REM,JH P,38CA L	125.0	0.357	1095	23.01
859	REM,JH P,38CA L	125.0	0.357	1020	18.39
860	REM,JH P,38CA L	125.0	0.357	698	2.36
865	REM,JH P,38SP	125.0	0.357	823	36.63
866	REM,JH P,38SP	125.0	0.357	846	4.69
867	REM,JH P,38SP	125.0	0.357	882	6.07
891	REM,JH P,357M AG	125.0	0.357	1410	51.78
892	REM,JH P,357M AG	125.0	0.357	1256	51.78
893	REM,JH P,357M AG	125.0	0.357	1135	30.50
894	REM,JH P,357	125.0	0.357	951	8.21
895	REM,JH P,357M AG	125.0	0.357	754	3.73

A= 4.268997195447

B= 8.61674999E-04

C=-2512.299363429

MANUFACTURER AVG DEV NO. PTS. % PTS.POS.

S+	-3.65	13	30.76
SI	-2.33	6	33.33
HO	-0.59	9	44.44
ZE	-0.36	10	50.00
RE	+3.96	18	50.00
SP	+7.94	6	100.00

(See also Figure 43)

TABLE XXIV

SCAN 98 ( K0= 72171 ) covering round numbers 370 to 917 with:

A11 MANUFACTURERS  
 CONSTRUCTION CODES JHP  
 MASSES (grains) - 140  
 CALIBERS - .357  
 STRIKING VELOCITIES (f/s) - A11

6 rounds satisfy SCAN CODE 98

RND. NO.	ID	MASS(GR)	DIAM.(IN)	VS(F/S)	RII
399	SPEER, JHP,38 CAL	140.0	0.357	1512	60.94
400	SPEER, JHP,38 CAL	140.0	0.357	1033	24.78
401	SPEER, JHP,38 CAL	140.0	0.357	761	8.46
402	SPEER, JHP,38 CAL	140.0	0.357	1417	51.68
433	SPEER, JHP,38 CAL	140.0	0.357	1240	46.42
434	SPEER, JHP,38 CAL	140.0	0.357	1003	26.30

A= 8.473826178012  
 B=-1.05642851E-03  
 C=-4214.57575316

MANUFACTURER	AVG DEV	NO. PTS.	% PTS.POS.
SP	+0.06	6	66.66

(See also Figure 44)

TABLE XXV

SCAN 99 ( K0= 72183 ) covering round numbers 270 to 917 with:

ALL MANUFACTURERS  
 CONSTRUCTION CODES JHP  
 MASSES (grains) - 146  
 CALIBERS - .357  
 STRIKING VELOCITIES (f/s) - ALL

6 rounds satisfy SCAN CODE 99

RND: NO.	ID	MASS(GR)	DIAM.(IN)	VS(F/S)	RII
403	SPEER, JHP, 38 CAL	146.0	0.357	1295	36.12
404	SPEER, JHP, 38 CAL	146.0	0.357	731	6.21
408	SPEER, JHP, 38 CAL	146.0	0.357	1076	28.48
435	SPEER, JHP, 38 CAL	146.0	0.357	1318	33.54
436	SPEER, JHP, 38 CAL	146.0	0.357	1194	30.42
437	SPEER, JHP, 38 CAL	146.0	0.357	1148	38.73

A=-1.27993606E-02  
 B= 3.01676941E-03  
 C=-242.5007425015

MANUFACTURER	AVG DEV	NO. PTS.	2 PTS. POS.
SP	+1.16	6	50.00

(See also Figure 45)

TABLE XXVI

SCAN 42 ( K0= 71950 ) covering round numbers 6 to 917 with:

A11 MANUFACTURERS  
 CONSTRUCTION CODES WC  
 MASSES (grains) - 148  
 CALIBERS - .357  
 STRIKING VELOCITIES (f/s) - A11

21 rounds satisfy SCAN CODE 42

RND. NO.	ID	MASS(GR)	DIAM.(IN)	VS(F/S)	RII
57	W-W,W C,.	38SPEC 147.9	0.357	390	11.16
78	S+W,W C,.38	SPEC 147.9	0.357	820	10.66
314	W-W,W C,.38	SPEC 147.9	0.357	869	17.42
315	W-W,W C,.38	SPEC 147.9	0.357	1046	26.58
316	W-W,W C,.38	SPEC 147.9	0.357	1624	40.33
366	W-W,W C,38SP	EC 147.9	0.357	1013	23.38
367	W-W,W C,38SP	EC 147.9	0.357	780	12.38
405	SPEER, WC,38C	AL 147.9	0.357	1794	56.20
406	SPEER, WC,38C	AL 147.9	0.357	1338	33.65
407	SPEER, WC,38C	AL 147.9	0.357	902	14.61
409	SPEER, WC,38C	AL 147.9	0.357	941	15.15
410	SPEER, WC,38C	AL 147.9	0.357	1161	27.16
438	SPEER, WC,38C	AL 147.9	0.357	1709	50.64
439	SPEER, WC,38C	AL 147.9	0.357	1689	50.63
440	SPEER, WC,38C	AL 147.9	0.357	1624	46.88
441	SPEER, WC,38C	AL 147.9	0.357	1387	43.99
442	SPEER, WC,38C	AL 147.9	0.357	1092	22.77
443	SPEER, WC,38C	AL 147.9	0.357	984	16.61
903	REM,WC ,38SP	147.9	0.357	869	17.42
909	REM,WC ,38SP	147.9	0.357	961	24.49
910	REM,WC ,38SP	147.9	0.357	1433	34.52

A= 1.260402154507  
 B= 1.52503957E-03  
 C= 186.5770153893

MANUFACTURER	AVG DEV	NO. PTS.	% PTS.POS.
S+	-4.79	1	0.00
SP	+0.01	11	36.36
W-	+0.33	6	66.66
RE	+1.89	3	66.66

(See also Figure 46)

TABLE XXVII

SCAN 38 ( K0= 72523 ) covering round numbers 6 to 917 with:

ALL MANUFACTURERS  
 CONSTRUCTION CODES L LRN RN  
 MASSES (grains) - 150  
 CALIBERS - .357  
 STRIKING VELOCITIES (f/s) - All

5 rounds satisfy SCAN CODE 38

RND. NO.	ID	MASS(GR)	DIAM.(IN)	VS(F/S)	RII
66	W-W,L ,.38 LC	150.0	0.357	813	5.63
68	W-W,L ,.38 SPEC	150.0	0.357	1135	10.85
301	W-W,L RN,.3 8SPEC	150.0	0.357	928	7.76
302	W-W,L RN,.3 8SPEC	150.0	0.357	1138	12.61
303	W-W,L RN,.3 8SPEC	150.0	0.357	1259	25.13

A=-13.17843674403

B= 9.04175349E-03

C= 6197.297802882

MANUFACTURER	AVG DEV	NO. PTS.	% PTS.POS.
W-	+0.15	5	40.00

(See also Figure 47)

TABLE XXVIII

SCAN 37 ( K0= 72668 ) covering round numbers 6 to 917 with:

ALL MANUFACTURERS  
 CONSTRUCTION CODES JSP JFP  
 MASSES (grains) - 150  
 CALIBERS - .357  
 STRIKING VELOCITIES (f/s) - All

RND. NO.	ID	MASS(GR)	DIAM.(IN)	VS(F/S)	RII
289	W-W,J SP,.3	57MAG 150.0	0.357	1289	29.07

A=-6.76358390E-04  
 B= 2.98354213E-03  
 C=-592.1552588635

MANUFACTURER	AVG DEV	NO. PTS.	% PTS.POS.
W-	-0.49	1	0.00

(See also Figure 48)

TABLE XXIX

SCAN 46 ( K0= 72611 ) covering round numbers 6 to 917 with:

A11 MANUFACTURERS  
 CONSTRUCTION CODES JHP JHC  
 MASSES (grains) - 150  
 CALIBERS - .357  
 STRIKING VELOCITIES (f/s) - A11

6 rounds satisfy SCAN CODE 46

RND. NO.	ID	MASS(GR)	DIAM.(IN)	VS(F/S)	RII
184	SIERRA ,JHP	150.0	0.357	1148	28.55
185	SIERRA ,JHP	150.0	0.357	958	12.47
186	SIERRA ,JHP	150.0	0.357	803	7.09
187	SIERRA ,JHP	150.0	0.357	498	0.79
198	SIERRA ,JHP	150.0	0.357	1118	13.92
199	SIERRA ,JHP	150.0	0.357	1335	42.05

A= 3.384355727232  
 B= 1.40351211E-03  
 C=-2137.976826352

MANUFACTURER	AVG DEV	NO. PTS.	% PTS.POS.
SI	+0.47	6	66.66

(See also Figure 49)

TABLE XXX

SCAN 39 ( K0= 72539 ) covering round numbers 6 to 917 with:

A11 MANUFACTURERS  
 CONSTRUCTION CODES L LRN RN  
 MASSES (grains) - 158  
 CALIBERS - .357  
 STRIKING VELOCITIES (f/s) - A11

18 rounds satisfy SCAN CODE 39

RND. NO.	ID	MASS(GR)	DIAM.(IN)	VS(F/S)	RII
49	W-W,L ,.357 MAG	157.9	0.357	1125	31.99
50	W-W,L ,.357 MAG	157.9	0.357	770	4.53
51	W-W,L ,.357 MAG	157.9	0.357	1085	13.54
52	W-W,L ,.357 MAG	157.9	0.357	377	7.78
53	W-W,L ,.357 MAG	157.9	0.357	997	8.98
67	W-W,L ,.38 SPEC	157.9	0.357	938	10.51
80	S+W,L RN,.3 8SPEC	157.9	0.357	869	3.20
304	W-W,L RN,.3 8SPEC	157.9	0.357	944	8.15
305	W-W,L RN,.3 8SPEC	157.9	0.357	1089	11.50
306	W-W,L RN,.3 8SPEC	157.9	0.357	1250	17.26
311	W-W,R N,.38 SPEC	157.9	0.357	997	8.52
312	W-W,R N,.38 SPEC	157.9	0.357	1099	9.55
313	W-W,R N,.38 SPEC	157.9	0.357	1236	13.02
868	REM,RN ,38SP	157.9	0.357	1266	29.39
869	REM,RN ,38SP	157.9	0.357	1233	13.62
870	REM,RN ,38SP	157.9	0.357	1079	9.65
899	REM,L, 357MAG	157.9	0.357	1250	36.47
900	REM,L, 357MAG	157.9	0.357	1181	13.38

A=-5.033894694484

B= 5.26967465E-03

C= 1916.501103882

MANUFACTURER AVG DEV NO. PTS. % PTS.POS.

S+	-2.55	1	0.00
W-	+0.84	12	50.00
RE	+1.74	5	40.00

(See also Figure 50)

TABLE XXXI

SCAN 41 ( K0= 72207 ) covering round numbers 6 to 917 with:

A11 MANUFACTURERS  
 CONSTRUCTION CODES SWC  
 MASSES (grains) - 158  
 CALIBERS - .357  
 STRIKING VELOCITIES (f/s) - A11

14 rounds satisfy SCAN CODE 41

RND. NO.	ID	MASS(GR)	DIAM.(IN)	VS(F/S)	RII
58	W-W,S WC,.3 8SPEC	157.9	0.357	1128	23.12
79	S+W,S WC,.3 8SPEC	157.9	0.357	875	3.93
307	W-W,S WC,.3 8SPEC	157.9	0.357	790	8.26
308	W-W,S WC,.3 8SPEC	157.9	0.357	859	11.47
309	W-W,S WC,.3 8SPEC	157.9	0.357	1125	30.35
413	SPEER, SWC,38 CAL	157.9	0.357	1719	57.84
414	SPEER, SWC,38 CAL	157.9	0.357	1223	32.58
444	SPEER, SWC,38 CAL	157.9	0.357	1463	63.72
445	SPEER, SWC,38 CAL	157.9	0.357	1381	58.00
446	SPEER, SWC,38 CAL	157.9	0.357	1131	40.11
447	SPEER, SWC,38 CAL	157.9	0.357	1177	19.94
901	REM,SW C,38SP	157.9	0.357	1364	42.78
902	REM,SW C,38SP	157.9	0.357	1145	24.53
903	REM,SW C,38SP	157.9	0.357	1082	10.11

NO X

A= 6.729291308774  
 B=-7.33217328E-05  
 C=-3918.064161714

MANUFACTURER	AVG DEV	NO. PTS.	% PTS.POS.
S+	-4.97	1	0.00
RE	-3.76	3	0.00
W-	+2.95	4	75.00
SP	+3.98	6	66.66

(See also Figure 51)

TABLE XXXII

SCAN 40 ( KO= 72209 ) covering round numbers 30 to 917 with:

A11 MANUFACTURERS  
 CONSTRUCTION CODES LHP  
 MASSES (grains) - 158  
 CALIBERS - .357  
 STRIKING VELOCITIES (f/s) - A11

13 rounds satisfy SCAN CODE 40

RND. NO.	ID		MASS(GR)	DIAM.(IN)	VS(F/S)	RII
39	W-W,LH P,.38	SPEC	157.9	0.357	1151	28.96
40	W-W,LH P,.38	SPEC	157.9	0.357	725	8.55
41	W-W,LH P,.38	SPEC	157.9	0.357	1181	32.63
42	W-W,LH P,.38	SPEC	157.9	0.357	1295	32.33
44	W-W,LH P,.38	SPEC	157.9	0.357	830	14.66
45	W-W,LH P,.38	SPEC	157.9	0.357	1046	21.64
292	W-W,L HP,.3	57MAG	157.9	0.357	1177	41.08
321	W-W,L HP,.3	8SPEC	157.9	0.357	1312	51.45
322	W-W,L HP,.3	8SPEC	157.9	0.357	1171	47.10
323	W-W,L HP,.3	8SPEC	157.9	0.357	951	20.57
324	W-W,L HP,.3	8SPEC	157.9	0.357	830	13.43
325	W-W,L HP,.3	8SPEC	157.9	0.357	774	5.95
326	W-W,L HP,.3	8SPEC	157.9	0.357	557	2.73

A= 4.858814531264  
 B= 5.7979219E-04  
 C=-2353.228014494

MANUFACTURER	AVG DEV	NO. PTS.	%PTS.POS.
W-	+0.50	13	61.53

(See also Figure 52)

TABLE XXXIII

SCAN 72 ( KO= 72634 ) covering round numbers 6 to 917 with:

ALL MANUFACTURERS  
 CONSTRUCTION CODES JSP JFP  
 MASSES (grains) - 158  
 CALIBERS - .357  
 STRIKING VELOCITIES (f/s) - All

41 rounds satisfy SCAN CODE 72

RND. NO.	ID	MASS(GR)	DIAM.(IN)	VS(F/S)	RII	
59	W-W,J SP,.3	57MAG	157.9	0.357	1601	79.36
81	S+W,J SP,.3	8SPEC	157.9	0.357	1040	17.15
86	S+W,J SP,.3	57MAG	157.9	0.357	1561	52.16
103	S+W,J SP,.3	57MAG	157.9	0.357	754	2.54
105	S+W,J SP,.3	57MAG	157.9	0.357	1220	17.32
110	S+W,J SP,.3	57MAG	157.9	0.357	1076	18.82
111	S+W,J SP,.3	57MAG	157.9	0.357	1043	16.87
112	S+W,J SP,.3	57MAG	157.9	0.357	954	7.12
149	HORNAD Y,JFP		157.9	0.357	1049	17.57
150	HORNAD Y,JFP		157.9	0.357	987	13.99
151	HORNAD Y,JFP		157.9	0.357	790	4.39
152	HORNAD Y,JFP		157.9	0.357	1236	32.05
188	SIERRA ,JSP		157.9	0.357	1128	13.96
189	SIERRA ,JSP		157.9	0.357	1263	21.39
190	SIERRA ,JSP		157.9	0.357	967	8.32
191	SIERRA ,JSP		157.9	0.357	853	9.19
192	SIERRA ,JSP		157.9	0.357	590	1.88
200	SIERRA ,JSP		157.9	0.357	1154	15.44
201	SIERRA ,JSP		157.9	0.357	1299	27.60
232	HORNAD Y,JSP		157.9	0.357	1578	75.83
234	HORNAD Y,JFP		157.9	0.357	1145	16.69
262	HI-PRE CISION ,JSP		157.9	0.357	1269	16.55
263	HI-PRE CISION ,JSP		157.9	0.357	1125	12.68
267	HI-PRE CISION ,JSP		157.9	0.357	1243	16.43
268	HI-PRE CISION ,JSP		157.9	0.357	1092	12.58
317	W-W,J SP,.3	8SPEC	157.9	0.357	1282	22.21
318	W-W,J SP,.3	8SPEC	157.9	0.357	1141	16.51
319	W-W,J SP,.3	8SPEC	157.9	0.357	987	17.47
320	W-W,J SP,.3	8SPEC	157.9	0.357	774	8.04
415	SPEER, JSP,38 CAL		157.9	0.357	1683	67.80
416	SPEER, JSP,38 CAL		157.9	0.357	1328	39.35
417	SPEER, JSP,38 CAL		157.9	0.357	1010	22.27
448	SPEER, JSP,38 CAL		157.9	0.357	1364	58.09
472	SPEER, JSP,38 CAL		157.9	0.357	1102	20.20
473	SPEER, JSP,38 CAL		157.9	0.357	1023	17.25

507	SPEER, JSP,35 7	157.9	0.357	1761	37.16
508	SPEER, JSP,35 7	157.9	0.357	951	8.14
509	SPEER, JSP,35 7	157.9	0.357	787	4.03
896	REM,JS P,357M AG	157.9	0.357	1292	27.56
897	REM,JS P,357M AG	157.9	0.357	1167	27.56
898	REM,JS P,357M AG	157.9	0.357	1053	8.56

A= 2.284496287811

B= 1.79523251E-03

C=-1626.224818408

MANUFACTURER	AVG DEV	NO. PTS.	% PTS.POS.
HI	-6.59	4	0.00
SI	-1.85	7	28.57
S+	-0.62	7	42.85
RE	+0.50	3	33.33
W-	+3.73	5	60.00
SP	+3.73	9	55.55
HO	+4.07	6	66.66

(See also Figure 53)

TABLE XXXIV

SCAN 7 ( K0= 72627 ) covering round numbers 6 to 917 with:

ALL MANUFACTURERS

CONSTRUCTION CODES

JHP

JHC

MASSES (grains) - 158

CALIBERS - .357

STRIKING VELOCITIES (f/s) - All

41 rounds satisfy SCAN CODE 7

RND. NO.	ID	MASS(GR)	DIAM.(IN)	VS(F/S)	RII
14	W-W,J HP,.3 57MAG	157.9	0.357	1748 NO X	81.84
17	W-W,J HP,.3 57MAG	157.9	0.357	1532 NO X	32.80
18	W-W,J HP,.3 57MAG	157.9	0.357	1509 NO X	32.55
20	W-W,J HP,.3 57MAG	157.9	0.357	1335 NO X	64.78
21	W-W,J HP,.3 57MAG	157.9	0.357	1204 NO X	21.34
22	W-W,J HP,.3 57MAG	157.9	0.357	1125 NO X	31.23
23	W-W,J HP,.3 57MAG	157.9	0.357	1131 NO X	24.16
24	W-W,JH P,.357 MAG	157.9	0.357	1069 NO X	17.52
25	W-W,JH P,.357 MAG	157.9	0.357	948 NO X	33.51
26	W-W,JH P,.357 MAG	157.9	0.357	912 NO X	20.42
27	W-W,JH P,.357 MAG	157.9	0.357	994 NO X	10.55
28	W-W,JH P,.357 MAG	157.9	0.357	1066 NO X	21.10
29	W-W,JH P,.357 MAG	157.9	0.357	715 NO X	3.79
30	W-W,JH P,.357 MAG	157.9	0.357	990 NO X	24.02
82	S+W,J HP,.3 8SPEC	157.9	0.357	1046	13.06
87	S+W,J HP,.3 57MAG	157.9	0.357	1469	57.33
100	S+W,J HP,.3 57MAG	157.9	0.357	505	0.99
101	S+W,J HP,.3 57MAG	157.9	0.357	787	7.26
104	S+W,J HP,.3 57MAG	157.9	0.357	1217	26.70
107	S+W,J HP,.3 57MAG	157.9	0.357	905	8.83
108	S+W,J HP,.3 57MAG	157.9	0.357	1135	14.73
109	S+W,J HP,.3 57MAG	157.9	0.357	1154	20.22
121	S+W,J HP,.3 8SPEC	157.9	0.357	1282	36.49
122	S+W,J HP,.3 8SPEC	157.9	0.357	1263	34.29
123	S+W,J HP,.3 8SPEC	157.9	0.357	757	7.35
154	HORNAD Y,JHP	157.9	0.357	1295	37.63
155	HORNAD Y,JHP	157.9	0.357	1145	23.90
156	HORNAD Y,JHP	157.9	0.357	994	12.13
157	HORNAD Y,JHP	157.9	0.357	849	7.25
229	HORNAD Y,JHP	157.9	0.357	1397	49.05
230	HORNAD Y,JHP	157.9	0.357	1286	41.88
231	HORNAD Y,JHP	157.9	0.357	1141	27.75
290	W-W,J HP,.3 57MAG	157.9	0.357	1276	44.88
298	W-W,J HP,.3 8SPEC	157.9	0.357	1250	53.51
299	W-W,J HP,.3 8SPEC	157.9	0.357	1099	37.88

300	W-W,J	HP,.3	8SPEC	157.9	0.357	954	21.04
327	W-W,J	HP,.3	8SPEC	157.9	0.357	875	19.64
328	W-W,J	HP,.3	8SPEC	157.9	0.357	688	6.55
904	REM,JH	P,357M	AG	157.9	0.357	1289	50.17
906	REM,JH	P,357M	AG	157.9	0.357	1053	19.86
907	REM,JH	P,357M	AG	157.9	0.357	882	7.17

A= 5.463773587451

B= 2.41878706E-04

C=-2826.097748446

MANUFACTURER    AVG DEV    NO. PTS.    % PTS.POS.

S+	-2.23	11	45.45
H0	+0.44	7	57.14
RE	+2.83	3	33.33
W-	+3.48	20	60.00

(See also Figure 54)

TABLE XXXV

SCAN 93 ( K0= 71986 ) covering round numbers 6 to 917 with:

ALL MANUFACTURERS  
 CONSTRUCTION CODES MP  
 MASSES (grains) - 158  
 CALIBERS - 357  
 STRIKING VELOCITIES (f/s) - ALL

5 rounds satisfy SCAN CODE 93

RND. NO.	ID	MASS(GR)	DIAM.(IN)	VS(F/S)	RII	
55	W-W, M P,. 35	7MAG	157.9	0.357	1578	15.96
291	W-W, M P,. 35	7MAG	157.9	0.357	1282	23.71
871	REM, MP, 385P		157.9	0.357	1345	14.76
872	REM, MP, 385P		157.9	0.357	1230	13.38
873	REM, MP, 385P		157.9	0.357	1099	7.47

A=-2.11528401E-03  
 B= 2.77168214E-03  
 C=-993.161798543

MANUFACTURER	AVG DEV	NO. PTS.	% PTS. POS.
W-	-9.31	2	50.00
RE	-2.06	3	0.00

(See also Figure 55)

TABLE XXXVI

SCAN 111 ( K0= 72261 ) covering round numbers 857 to 917 with:

A11 MANUFACTURERS  
 CONSTRUCTION CODES JHP  
 MASSES (grains) - 185  
 CALIBERS - .357  
 STRIKING VELOCITIES (f/s) - A11

RND. NO.	ID	MASS(GR)	DIAM.(IN)	VS(F/S)	RII
905	REM,JH P,357M AG	185.0	0.357	1161	36.21

A= 4.03287990E-04  
 B= 3.75260300E-03  
 C=-898.7414499336

MANUFACTURER	AVG DEV	NO. PTS.	% PTS.POS.
RE	+0.16	1	100.00

(See also Figure 56)

TABLE XXXVII

SCAN 112 ( K0= 71909 ) covering round numbers 857 to 917 with:

A11 MANUFACTURERS  
 CONSTRUCTION CODES L  
 MASSES (grains) - 200  
 CALIBERS - .357  
 STRIKING VELOCITIES (f/s) - A11

RND. NO.	ID	MASS(GR)	DIAM.(IN)	VS(F/S)	R11
911	REM,L, 33SP	200.0	0.357	1302	29.44
912	REM,L, 33SP	200.0	0.357	1207	18.52
913	REM,L, 33SP	200.0	0.357	1069	18.52

A=-4.06476920E-03  
 B= 2.92772630E-03  
 C=-517.4344932663

MANUFACTURER	AVG DEV	NO. PTS.	% PTS.POS.
RE	-0.04	3	33.33

(See also Figure 57)

TABLE XXXVIII

SCAN 43 ( K0= 71682 ) covering round numbers 271 to 917 with:

ALL MANUFACTURERS  
 CONSTRUCTION CODES SS  
 MASSES (grains) - All  
 CALIBERS - .357  
 STRIKING VELOCITIES (f/s) - All

3 rounds satisfy SCAN CODE 43

RND. NO.	ID	MASS(GR)	DIAM.(IN)	VS(F/S)	RII
272	MBA,S S,.38 SPEC	63.9	0.357	1007 NO X	9.37
273	MBA,S S,.38 SPEC	63.9	0.357	1053 NO X	18.21
274	MBA,S S,.38 SPEC	63.9	0.357	807 NO X	0.89

A=-30.82212493421  
 B= 2.34343443E-02  
 C= 9525.324936997

MANUFACTURER	AVG DEV	NO. PTS.	% PTS.POS.
MB	+0.00	3	66.66

(See also Figure 58)

TABLE XXXIX

SCAN 44 ( K0= 71895 ) covering round numbers 274 to 917 with:

All MANUFACTURERS  
 CONSTRUCTION CODES SSG  
 MASSES (grains) - All  
 CALIBERS - .357  
 STRIKING VELOCITIES (f/s) - All

6 rounds satisfy SCAN CODE 44

RND. NO.	ID	MASS(GR)	DIAM.(IN)	VS(F/S)	RII
275	GLASER ,SSG,, 357MAG	96.4	0.357	2181 NO X	66.88
276	GLASER ,SSG,, 38SPEC	96.4	0.357	1889 NO X	52.39
277	GLASER ,SSG,, 38SPEC	96.4	0.357	1860 NO X	62.14
278	GLASER ,SSG,, 357MAG	96.4	0.357	2158 NO X	77.17
281	GLASER ,SSG,, 357MAG	96.4	0.357	1328 NO X	29.39
282	GLASER ,SSG,, 357MAG	96.4	0.357	1443 NO X	33.20

A= 5.443886376076  
 B= 7.69727668E-05  
 C=-2914.878473997

MANUFACTURER	AVG DEV	NO. PTS.	% PTS.POS.
GL	+0.17	6	50.00

(See also Figure 59)

TABLE XL

SCAN 89 ( K0= 83251 ) covering round numbers 6 to 917 with:

ALL MANUFACTURERS  
 CONSTRUCTION CODES JHP JHC  
 MASSES (grains) - 170  
 CALIBERS - .41  
 STRIKING VELOCITIES (f/s) - A11

RND. NO.	ID	MASS(GR)	DIAM.(IN)	VS(F/S)	RII
258	SIERRA ,JHP	170.0	0.409	1164	16.78

A=-1.63011812E-03  
 B= 2.80051558E-03  
 C=-489.946793937

MANUFACTURER	AVG DEV	NO. PTS.	% PTS.POS.
SI	-0.31	1	0.00

(See also Figure 60)

TABLE XLI

SCAN 101 ( K0= 82891 ) covering round numbers 460 to 917 with:

ALL MANUFACTURERS  
 CONSTRUCTION CODES JHP  
 MASSES (grains) - 200  
 CALIBERS - .41  
 STRIKING VELOCITIES (f/s) - All

6 rounds satisfy SCAN CODE 101

RND. NO.	ID	MASS(GR)	DIAM.(IN)	VS(F/S)	RII
463	SPEER, JHP, 41 MAG	200.0	0.409	1305	49.52
464	SPEER, JHP, 41 MAG	200.0	0.409	1161	32.73
465	SPEER, JHP, 41 MAG	200.0	0.409	1036	32.16
466	SPEER, JHP, 41 MAG	200.0	0.409	1368	50.19
467	SPEER, JHP, 41 MAG	200.0	0.409	1174	38.79
468	SPEER, JHP, 41 MAG	200.0	0.409	1092	44.96

A=-2.629323033323  
 B= 3.22958938E-03  
 C= 2939.900797912

MANUFACTURER	AVG DEV	NO. PTS.	% PTS.POS.
SP	+0.27	6	33.33

(See also Figure 61)

TABLE XLII

SCAN 113 ( K0= 82729 ) covering round numbers 857 to 917 with:

A11 MANUFACTURERS  
 CONSTRUCTION CODES L  
 MASSES (grains) - 210  
 CALIBERS - .411  
 STRIKING VELOCITIES (f/s) - A11

4 rounds satisfy SCAN CODE 113

RND. NO.	ID	MASS(GR)	DIAM.(IN)	VS(F/S)	RII
914	REM,L, 41MAG	210.0	0.411	1430	76.04
915	REM,L, 41MAG	210.0	0.411	1263	38.81
916	REM,L, 41MAG	210.0	0.411	1158	21.96
917	REM,L, 41MAG	210.0	0.411	1089	15.84

A= 6.168620175805  
 B= 1.28604390E-03  
 C=-5252.00040152

MANUFACTURER	AVG DEV	NO.	PTS.	% PTS.POS.
RE	-0.00	4		50.00

(See also Figure 62)

TABLE XLIII

SCAN 110 ( K0= 82933 ) covering round numbers 857 to 917 with:

All MANUFACTURERS  
 CONSTRUCTION CODES JSP  
 MASSES (grains) - 210  
 CALIBERS - .41  
 STRIKING VELOCITIES (f/s) - All

5 rounds satisfy SCAN CODE 110

RND. NO.	ID	MASS(GR)	DIAM:(IN)	VS(F/S)	RII
886	REM,JS P,41MA G	210.0	0.409	1276	55.61
887	REM,JS P,41MA G	210.0	0.409	1210	40.37
888	REM,JS P,41MA G	210.0	0.409	1141	20.52
889	REM,JS P,41MA G	210.0	0.409	1145	27.51
890	REM,JS P,41MA G	210.0	0.409	974	12.27

A=-22.62956492331  
 B= 1.40939623E-02  
 C= -11104.99248334

MANUFACTURER	AVG DEV	NO.	PTS.	% PTS.POS.
RE	+0.08	5		60.00

(See also Figure 63)

TABLE XLIV

SCAN 32 ( K0= 83331 ) covering round numbers 6 to 917 with:

ALL MANUFACTURERS  
 CONSTRUCTION CODES JHP JHC  
 MASSES (grains) - 210  
 CALIBERS - .41  
 STRIKING VELOCITIES (f/s) - All

RND. NO.	ID	MASS(GR)	DIAM.(IN)	VS(F/S)	RII
252	HORNAD Y,JHP	210.0	0.409	1164	49.52
253	HORNAD Y,JHP	210.0	0.409	1030	29.44
254	HORNAD Y,JHP	210.0	0.409	915	20.07
255	HORNAD Y,JHP	210.0	0.409	856	14.51
256	HORNAD Y,JHP	210.0	0.409	725	5.58
257	SIERRA ,JHP	210.0	0.409	1158	17.84

A=-1.76702513E-02  
 B= 3.66871359E-03  
 C=-653.0391049244

MANUFACTURER	AVG DEV	NO. PTS.	% PTS.POS.
SI	-21.13	1	0.00
HO	+5.28	5	30.00

(See also Figure 64)

TABLE XLV

SCAN 100 ( K0= 82953 ) covering round numbers 459 to 917 with:

A11 MANUFACTURERS  
 CONSTRUCTION CODES JSP  
 MASSES (grains) - 220  
 CALIBERS - .41  
 STRIKING VELOCITIES (f/s) - A11

5 rounds satisfy SCAN CODE 100

RND. NO.	ID	MASS(GR)	DIAM.(IN)	VS(F/S)	R11
460	SPEER, JSP,41 MAG	220.0	0.409	1295	50.88
461	SPEER, JSP,41 MAG	220.0	0.409	1174	22.54
462	SPEER, JSP,41 MAG	220.0	0.409	951	11.55
469	SPEER, JSP,41 MAG	220.0	0.409	1253	43.01
470	SPEER, JSP,41 MAG	220.0	0.409	1102	21.32

A=-15.27478457398  
 B= 1.03597923E-02  
 C= 7497.572173207

MANUFACTURER	AVG DEV	NO.	PTS.	% PTS.POS.
SP	+0.14	5		40.00

(See also Figure 65)

TABLE XLVI

SCAN 115 ( K0= 86473 ) covering round numbers 372 to 917 with:

All MANUFACTURERS  
 CONSTRUCTION CODES JSP  
 MASSES (grains) - 180  
 CALIBERS - .427 to .429  
 STRIKING VELOCITIES (f/s) - All

RND. NO.	ID	MASS(GR)	DIAM.(IN)	VS(F/S)	RII
372	SUPERV EL,JSP	,44MAG 180.0	0.427	1601	44.53

A=-6.83223051E-03  
 B= 2.45934328E-03  
 C=-126.3702707803

MANUFACTURER	AVG DEV	NO. PTS.	% PTS.POS.
SU	-2.53	1	. 0.00

(See also Figure 66)

TABLE XLVII

SCAN 54 ( K0= 86651 ) covering round numbers 243 to 917 with:

All MANUFACTURERS  
 CONSTRUCTION CODES JHP  
 MASSES (grains) - 180  
 CALIBERS - .429  
 STRIKING VELOCITIES (f/s) - All

RND. NO.	ID	MASS(GR)	DIAM.(IN)	VS(F/S)	RII
243	SIERRA ,JHP	180.0	0.429	1217	16.23

A=-2.49956217E-03  
 B= 2.55065907E-03  
 C=-353.3126339531

MANUFACTURER	AVG DEV	NO. PTS.	% PTS.POS.
SI	-0.40	1	0.00

(See also Figure 67)

TABLE XLVIII

SCAN 55 ( K0= 86691 ) covering round numbers 235 to 917 with:

ALL MANUFACTURERS  
 CONSTRUCTION CODES JHP  
 MASSES (grains) - 200  
 CALIBERS - .429  
 STRIKING VELOCITIES (f/s) - All

11 rounds satisfy SCAN CODE 55

RND. NO.	ID	MASS(GR)	DIAM.(IN)	VS(F/S)	RII
235	HORNAD Y,JHP	200.0	0.429	1108	28.14
236	HORNAD Y,JHP	200.0	0.429	1043	24.20
237	HORNAD Y,JHP	200.0	0.429	971	19.81
238	HORNAD Y,JHP	200.0	0.429	872	13.29
244	HORNDA Y,JHP	200.0	0.429	757	7.20
245	HORNDA Y,JHP	200.0	0.429	1227	53.91
387	SPEER, JHP,44 MAG	200.0	0.429	1128	48.51
388	SPEER, JHP,44 MAG	200.0	0.429	935	27.11
389	SPEER, JHP,44 MAG	200.0	0.429	731	7.66
451	SPEER, JHP,44 MAG	200.0	0.429	1240	56.82
452	SPEER, JHP,44 MAG	200.0	0.429	1105	39.26

A= 3.666153538256  
 B= 1.69946042E-03  
 C=-2163.581009684

MANUFACTURER	AVG DEV	NO. PTS.	% PTS.POS.
HO	-2.90	6	0.00
SP	+4.37	5	100.00

(See also Figure 68)

TABLE XLIX

SCAN 97 ( K0= 86541 ) covering round numbers 370 to 917 with:

A11 MANUFACTURERS  
 CONSTRUCTION CODES JHP  
 MASSES (grains) - 225  
 CALIBERS - .427 to .429  
 STRIKING VELOCITIES (f/s) - A11

RND. NO.	ID	MASS(GR)	DIAM.(IN)	VS(F/S)	RII
334	SPEER, JHP,44	225.0	0.429	1181	46.90
335	SPEER, JHP,44	225.0	0.429	997	34.80
336	SPEER, JHP,44	225.0	0.429	826	11.17
457	SPEER, JHP,44 MAG	225.0	0.429	1167	43.12
458	SPEER, JHP,44 MAG	225.0	0.429	1158	38.86
459	SPEER, JHP,44 MAG	225.0	0.429	997	30.90

A=-1.31463143E-02  
 B= 3.94006022E-03  
 C=-771.1731238753

MANUFACTURER	AVG DEV	NO. PTS.	% PTS.POS.
SP	-0.67	6	50.00

(See also Figure 69)

TABLE L

SCAN 96 ( K0= 86571 ) covering round numbers 370 to 917 with:

All MANUFACTURERS  
 CONSTRUCTION CODES SWC  
 MASSES (grains) - 240  
 CALIBERS - .427 to .429  
 STRIKING VELOCITIES (f/s) - All

6 rounds satisfy SCAN CODE 96

RND. NO.	ID	MASS(GR)	DIAM.(IN)	VS(F/S)	RII
381	SPEER, SWC,4 4	240.0	0.429	1243	47.23
382	SPEER, SWC,4 4	240.0	0.429	1141	27.61
383	SPEER, SWC,4 4	240.0	0.429	872	7.50
454	SPEER, SWC,44 MAG	240.0	0.429	1348	25.92
455	SPEER, SWC,44 MAG	240.0	0.429	1007	13.84
456	SPEER, SWC,44 MAG	240.0	0.429	1056	14.48

A= 16.95871495063  
 B=-4.72439460E-03  
 C=-9532.682252896

MANUFACTURER	AVG DEV	NO. PTS.	% PTS.POS.
SP	+1.04	6	50.00

(See also Figure 70)

TABLE LI

SCAN 95 ( K0= 86593 ) covering round numbers 370 to 917 with:

ALL MANUFACTURERS  
 CONSTRUCTION CODES JSP  
 MASSES (grains) - 240  
 CALIBERS - .427 to .429  
 STRIKING VELOCITIES (f/s) - All

12 rounds satisfy SCAN CODE 95

RND. NO.	ID	MASS(GR)	DIAM.(IN)	VS(F/S)	RII
370	SPEER, JSP,44 MAG	240.0	0.427	1233	76.05
373	SPEER, JSP,44 MAG	240.0	0.429	1085	40.49
374	SPEER, JSP,44 MAG	240.0	0.429	935	28.31
375	SPEER, JSP,44 MAG	240.0	0.429	862	18.57
376	SPEER, JSP,44	240.0	0.429	1092	26.59
377	SPEER, JSP,44	240.0	0.429	1204	45.73
378	SPEER, JSP,44	240.0	0.429	1135	33.99
379	SPEER, JSP,44	240.0	0.429	839	13.25
380	SPEER, JSP,44	240.0	0.429	1302	67.65
449	SPEER, JSP,44 MAG	240.0	0.429	1213	46.90
450	SPEER, JSP,44 MAG	240.0	0.429	1279	59.77
453	SPEER, JSP,44 MAG	240.0	0.429	980	16.35

A=-3.986962375353

B= 5.12413614E-03

C= 2044.717604744

MANUFACTURER	AVG DEV	NO. PTS.	% PTS.POS.
SP	+0.72	12	33.33

(See also Figure 71)

TABLE LII

SCAN 56 ( K0= 86771 ) covering round numbers 239 to 917 with:

ALL MANUFACTURERS  
 CONSTRUCTION CODES JHP  
 MASSES (grains) - 240  
 CALIBERS - .429  
 STRIKING VELOCITIES (f/s) - ALL

10 rounds satisfy SCAN CODE 56

RND. NO.	ID	MASS(GR)	DIAM.(IN)	VS(F/S)	RII
239	HORNAD Y, JHP	240.0	0.429	1118	38.28
240	HORNAD Y, JHP	240.0	0.429	1036	28.83
241	HORNAD Y, JHP	240.0	0.429	994	26.49
242	HORNAD Y, JHP	240.0	0.429	859	14.68
246	HORNAD Y, JHP	240.0	0.429	774	11.19
247	HI-PRECISION, JHP	240.0	0.429	1141	40.86
248	HI-PRECISION, JHP	240.0	0.429	1164	38.09
249	HI-PRECISION, JHP	240.0	0.429	994	27.77
250	HI-PRECISION, JHP	240.0	0.429	889	17.92
251	SIERRA, JHP	240.0	0.429	1210	15.90

A= 6.420674639184  
 B=-1.93650849E-05  
 C=-3121.181150618

MANUFACTURER	AVG DEV	NO. PTS.	% PTS. POS.
SI	-29.65	1	0.00
HO	+0.00	5	60.00
HI	+0.06	4	50.00

(See also Figure 72)

TABLE LIII

SCAN 90 ( K0= 92468 ) covering round numbers 6 to 917 with:

ALL MANUFACTURERS  
 CONSTRUCTION CODES HEMIJHP  
 MASSES (grains) - 170  
 CALIBERS - .45  
 STRIKING VELOCITIES (f/s) - All

RND. NO.	ID	MASS(GR)	DIAM.(IN)	VS(F/S)	RII
269	HI-PRE C,HEMI JHP	170.0	0.450	1279	41.04
270	HI-PRE C,HEMI JHP	170.0	0.450	1122	32.94
271	HI-PRE C,HEMI JHP	170.0	0.450	951	13.47

A=-4.75961025E-03  
 B= 3.52057612E-03  
 C=-753.9400377023

MANUFACTURER	AVG DEV	NO. PTS.	% PTS.POS.
HI	-0.57	3	66.66

(See also Figure 73)

TABLE LIV

SCAN 123 ( K0= 90861 ) covering round numbers 917 to 924 with:

ALL MANUFACTURERS  
 CONSTRUCTION CODES JHP  
 MASSES (grains) - 185  
 CALIBERS - 45  
 STRIKING VELOCITIES (f/s) - ALL

7 rounds satisfy SCAN CODE 123

RND. NO.	ID	MASS(GR)	DIAM.(IN)	VS(F/S)	RII
918	REM, JHP, 45AC P	185.0	0.450	1109	40.41
919	REM, JHP, 45AC P	185.0	0.450	1155	46.35
920	REM, JHP, 45AC P	185.0	0.450	1180	54.65
921	REM, JHP, 45AC P	185.0	0.450	1088	38.30
922	REM, JHP, 45AC P	185.0	0.450	1009	36.04
923	REM, JHP, 45AC P	185.0	0.450	933	22.00
924	REM, JHP, 45AC P	185.0	0.450	805	8.88

A= 17.87498265475  
 B=-5.17721571E-03  
 C=-9269.667489503

MANUFACTURER	AVG DEV	NO. PTS.	% PTS.	POS.
RE	+0.08	7	28.57	

(See also Figure 74)

TABLE LV

SCAN 108 ( K0= 91024 ) covering round numbers 857 to 917 with:

All MANUFACTURERS  
 CONSTRUCTION CODES WC  
 MASSES (grains) - 185  
 CALIBERS - .45 to .454  
 STRIKING VELOCITIES (f/s) - All

RND. NO.	ID	MASS(GR)	DIAM.(IN)	VS(F/S)	RII
884	REM,WC ,45ACP	185.0	0.451	1230	22.06

A=-2.64193664E-02  
 B= 2.79817047E-03  
 C=-175.5762192963

MANUFACTURER	AVG DEV	NO. PTS.	% PTS.POS.
RE	-4.34	1	0.00

(See also Figure 75)

TABLE LVI

SCAN 30 ( K0= 91291 ) covering round numbers 335 to 917 with:

ALL MANUFACTURERS  
 CONSTRUCTION CODES SWC  
 MASSES (grains) - 200  
 CALIBERS - .45 to .454  
 STRIKING VELOCITIES (f/s) - All

RND. NO.	ID	MASS(GR)	DIAM.(IN)	VS(F/S)	RII
515	SPEER, SWC,4 5CAL	200.0	0.453	1489	39.32
516	SPEER, SWC,4 5CAL	200.0	0.453	1210	15.33
517	SPEER, SWC,4 5CAL	200.0	0.453	1026	15.58

A=-4.37363520E-03  
 B= 2.41496355E-03  
 C= 37.48117692936

MANUFACTURER	AVG DEV	NO. PTS.	% PTS.POS.
SP	-0.33	3	66.66

(See also Figure 76)

TABLE LVII

SCAN 104 ( K0= 121291 ) covering round numbers 515 to 917 with:

All MANUFACTURERS  
 CONSTRUCTION CODES JHP  
 MASSES (grains) - 200  
 CALIBERS - .45 to .454  
 STRIKING VELOCITIES (f/s) - 0 to 3000

5 rounds satisfy SCAN CODE 104

RND. NO.	ID	MASS(GR)	DIAM.(IN)	VS(F/S)	RII
518	SPEER, JHP,4 5CAL	200.0	0.453	1509	94.37
519	SPEER, JHP,4 5CAL	200.0	0.453	1227	53.12
520	SPEER, JHP,4 5CAL	200.0	0.453	1046	39.71
521	SPEER, JHP,4 5CAL	200.0	0.453	928	24.78
522	SPEER, JHP,4 5CAL	200.0	0.453	620	5.48

A= 5.877362611534  
 B= 2.93918304E-04  
 C=-2701.609584763

MANUFACTURER	AVG DEV	NO.	PTS.	% PTS.POS.
SP	+0.05	5		40.00

(See also Figure 77)

TABLE LVIII

SCAN 81 ( K0= 91341 ) covering round numbers 335 to 917 with:

All MANUFACTURERS  
 CONSTRUCTION CODES JHP  
 MASSES (grains) - 225  
 CALIBERS - .45 to .454  
 STRIKING VELOCITIES (f/s) - All

4 rounds satisfy SCAN CODE 81

RND. NO.	ID	MASS(GR)	DIAM.(IN)	VS(F/S)	RII
510	SPEER, JHP,45 CAL	225.0	0.453	1387	73.97
512	SPEER, JHP,45 CAL	225.0	0.453	1217	36.15
513	SPEER, JHP,45 CAL	225.0	0.453	1108	50.08
514	SPEER, JHP,45 CAL	225.0	0.453	954	22.72

A= 5.374178693116  
 B= 4.83344163E-04  
 C=-2527.46017364

MANUFACTURER	AVG DEV	NO. PTS.	% PTS.POS.
SP	+0.98	4	50.00

(See also Figure 78)

TABLE LIX

SCAN 57 ( K0= 91558 ) covering round numbers 69 to 917 with:

ALL MANUFACTURERS  
 CONSTRUCTION CODES FJ FMJ  
 MASSES (grains) - 230  
 CALIBERS - .45 to .454  
 STRIKING VELOCITIES (f/s) - All

RND. NO.	ID	MASS(GR)	DIAM.(IN)	VS(F/S)	RII
69	W-W,F J,.45 AUTO	230.0	0.453	1059	12.51
334	W-W,F MJ,.4 SACP	230.0	0.451	1164	12.42

A=-4.44360010E-03  
 B= 2.77197163E-03  
 C=-536.5915478282

MANUFACTURER	AVG DEV	NO. PTS.	% PTS.POS.
W-	-1.12	2	50.00

(See also Figure 79)

TABLE LX

SCAN 109 ( K0= 91104 ) covering round numbers 857 to 917 with:

ALL MANUFACTURERS  
 CONSTRUCTION CODES MC  
 MASSES (grains) - 230  
 CALIBERS - .45 to .454  
 STRIKING VELOCITIES (f/s) - All

RND. NO.	ID	MASS(GR)	DIAM.(IN)	VS(F/S)	RII
885	REM,MC ,45ACP	230.0	0.450	1243	21.30

A=-2.79182674E-03  
 B= 2.92603370E-03  
 C=-615.0977736153

MANUFACTURER	AVG DEV	NO. PTS.	% PTS.POS.
RE	-1.81	1	0.00

(See also Figure 80)

TABLE LXI

SCAN 105 ( K0= 91391 ) covering round numbers 520 to 917 with:

ALL MANUFACTURERS  
 CONSTRUCTION CODES SWC  
 MASSES (grains) - 250  
 CALIBERS - .45 to .454  
 STRIKING VELOCITIES (f/s) - All

RND. NO.	ID	MASS(GR)	DIAM.(IN)	VS(F/S)	RII
523	SPEER, SWC,4	5CAL 250.0	0.453	1384	78.37
524	SPEER, SWC,4	5CAL 250.0	0.453	1305	44.08
525	SPEER, SWC,4	5CAL 250.0	0.453	1223	34.17

A=-2.14004939E-03  
 B= 3.26195589E-03  
 C=-421.5422303956

MANUFACTURER	AVG DEV	NO. PTS.	% PTS.POS.
SP	-0.03	3	33.33

(See also Figure 81)

TABLE LXII

SCAN 92 ( K0= 91733 ) covering round numbers 6 to 917 with:

ALL MANUFACTURERS  
 CONSTRUCTION CODES L LRN RN  
 MASSES (grains) - 255  
 CALIBERS - .45 to .454  
 STRIKING VELOCITIES (f/s) - A11

RND. NO.	ID	MASS(GR)	DIAM.(IN)	VS(F/S)	RII
329	W-W,L RN,.4 5ACP	255.0	0.451	1099	13.26
330	W-W,L RN,.4 5ACP	255.0	0.451	1230	15.57

A=-8.73011535E-03  
 B= 2.60455964E-03  
 C=-237.2371301171

MANUFACTURER	AVG DEV	NO. PTS.	% PTS.POS.
W-	-2.63	2	0.00

(See also Figure 82)

TABLE LXIII

## Performance of Commercially Available Handgun Ammunition

CALIBER	WEIGHT (grains)	BULLET TYPE	MANUFACTURER	BARREL LENGTH (in)	VELOCITY			RI INDEX
					NOMINAL* (fps)	MEASURED (fps)	(mps)	
122 CAL	37	LHP	WINCH-WESTERN	2.00	1365	872	265	2.3
9MM	96	SAFETY SLUG	DEADEYE ASSOC	4.00	1365	1839	560	54.5
9MM	100	FJ(FMC)	SMITH+WESSON	4.00	1250	1341	408	15.2
9MM	100	JHP	SPEER	4.00	1315	1188	363	24.8
9MM	115	FJ(FMC)	BROWNING	4.00	1140	1067	325	9.2
9MM	115	FJ(FMC)	SMITH+WESSON	4.00	1145	1192	363	10.3
9MM	115	FJ(FMC)	WINCHESTER	4.00	1140	1126	343	9.7
9MM	115	JHP	REMINGTON	4.00	1160	1192	363	28.2
9MM	115	JHP	SMITH+WESSON	4.00	1145	1193	363	20.4
9MM	115	JSP(POWER POINT)	WESTERN SUP-X	4.00	1160	1272	387	12.0
9MM	124	FJ(FMC)	REMINGTON	4.00	1120	1084	330	8.0
9MM	125	JSP	SPEER	4.00	1120	1058	322	10.1
.357 MAG	96	SAFETY SLUG	DEADEYE ASSOC	2.00	1120	1615	492	43.3
.357 MAG	96	SAFETY SLUG	DEADEYE ASSOC	4.00	1120	1725	525	49.0
.357 MAG	110	JHP	SMITH+WESSON	4.00	1800	1226	373	21.9
.357 MAG	110	JHP	SMITH+WESSON	2.00	1800	1044	318	12.5
.357 MAG	110	JHP	SPEER	4.00	1700	1246	379	28.7
.357 MAG	110	JHP	SPEER	2.00	1700	1178	359	24.6
.357 MAG	110	JHP	WESTERN SUP-X	4.00	1500	1309	398	29.9
.357 MAG	110	JHP	WESTERN SUP-X	2.75	1500	1258	383	26.4
.357 MAG	125	JHP	SMITH+WESSON	4.00	1775	1227	373	22.9
.357 MAG	125	JHP	SMITH+WESSON	2.00	1775	1188	362	20.3
.357 MAG	125	JHP	SPEER	4.00	1900	1301	396	39.7
.357 MAG	125	JHP	SPEER	2.00	1900	1161	353	30.3
.357 MAG	125	JHP	REMINGTON	4.00	1675	1366	416	40.8
.357 MAG	125	JHP	REMINGTON	2.00	1675	1173	357	27.0
.357 MAG	140	JHP	SPEER	4.00	1780	1221	372	41.8
.357 MAG	140	JHP	SPEER	2.00	1780	1125	342	34.5

TABLE LXII (CONTINUED)

## Performance of Commercially Available Handgun Ammunition

CALIBER	WEIGHT (grains)	BULLET TYPE	MANUFACTURER	BARREL LENGTH (in)	VELOCITY			RI INDEX
					NOMINAL* (fps)	MEASURED (fps)	(mps)	
.357 MAG	158	JHP	SMITH+WESSON	4.00	1050	1116	340	22.3
.357 MAG	158	JHP	SMITH+WESSON	2.00	1050	982	299	14.6
.357 MAG	158	JSP(III-VEL)	FEDERAL	4.00	1550	1255	382	29.3
.357 MAG	158	JSP(III-VEL)	FEDERAL	2.00	1550	1195	364	25.2
.357 MAG	158	JSP	SMITH+WESSON	4.00	1500	1168	356	19.2
.357 MAG	158	JSP	SMITH+WESSON	2.00	1500	1091	332	15.1
.357 MAG	158	JSP	SPEER	4.00	1625	1156	352	22.9
.357 MAG	158	JSP	SPEER	2.00	1625	1030	313	16.6
.357 MAG	158	LRN(LUBALOY)	WESTERN SUP-X	4.00	1410	1230	374	21.0
.357 MAG	158	LRN(LUBALOY)	WESTERN SUP-X	2.00	1410	1169	356	16.7
.357 MAG	158	SWC	REMINGTON	4.00	1410	1088	331	17.3
.357 MAG	158	SWC	REMINGTON	2.00	1410	958	291	9.3
.38 SPEC	90	JSP(HEMI)	SMITH+WESSON	4.00	1350	1158	352	11.2
.38 SPEC	90	JSP(HEMI)	SMITH+WESSON	2.00	1350	1053	320	7.7
.38 SPEC	90	JSP	SMITH+WESSON	4.00	1350	1118	340	9.6
.38 SPEC	90	JSP	SMITH+WESSON	2.00	1350	975	297	6.1
.38 SPEC	90	MP	KTW	4.00	1030	922	281	4.6
.38 SPEC	90	MP	KTW	2.00	1030	734	223	2.8
.38 SPEC	95	JHP(+P)	REMINGTON	4.00	985	1187	361	28.9
.38 SPEC	95	JHP(+P)	REMINGTON	2.00	985	1019	310	16.4
.38 SPEC	96	SAFETY SLUG	DEADEYE ASSOC	4.00	1800	1585	483	41.8
.38 SPEC	96	SAFETY SLUG	DEADEYE ASSOC	2.00	1800	1496	455	37.2
.38 SPEC	110	JHP	SMITH+WESSON	4.00	1380	1014	309	11.3
.38 SPEC	110	JHP	SMITH+WESSON	2.00	1380	888	270	6.8
.38 SPEC	110	JHP	SPEER	4.00	1245	857	261	11.4
.38 SPEC	110	JHP	SPEER	2.00	1245	789	240	8.6
.38 SPEC	110	JHP	SUPER VEL	4.00	1370	1159	353	25.3

TABLE LXII (CONTINUED)

## Performance of Commercially Available Handgun Ammunition

CALIBER	WEIGHT (grains)	BULLET TYPE	MANUFACTURER	BARREL LENGTH (in)	VELOCITY			RI INDEX
					NOMINAL*	MEASURED		
					(fps)	(fps)	(mps)	
.38 SPEC	110	JHP	SUPER VEL	2.00	1370	1148	349	24.8
.38 SPEC	110	JHP(LOT-Q4070)	WINCH-WESTERN	4.00	####	1106	337	17.9
.38 SPEC	110	JHP(LOT-Q4070)	WINCH-WESTERN	2.00	####	956	291	11.6
.38 SPEC	110	JSP	SUPER VEL	4.00	1370	1202	366	19.2
.38 SPEC	110	JSP	SUPER VEL	2.00	1370	1076	327	13.1
.38 SPEC	125	JHP	SMITH+WESSON	4.00	1350	900	274	5.9
.38 SPEC	125	JHP	SMITH+WESSON	2.00	1350	716	218	3.0
.38 SPEC	125	JHP	SMITH+WESSON	4.00	1350	1002	305	10.2
.38 SPEC	125	JHP	SMITH+WESSON	2.00	1350	899	274	5.8
.38 SPEC	125	JHP(+P)	SPEER	4.00	1425	1006	306	21.9
.38 SPEC	125	JHP(+P)	SPEER	2.00	1425	931	283	18.7
.38 SPEC	125	JSP(+P)	SPEER	4.00	1425	1047	319	19.4
.38 SPEC	125	JSP(+P)	SPEER	2.00	1425	983	299	16.7
.38 SPEC	125	JSP	SMITH+WESSON	4.00	1350	1064	324	15.4
.38 SPEC	125	JSP	SMITH+WESSON	2.00	1350	896	273	8.6
.38 SPEC	125	JSP	3-D	4.00	1085	1091	332	16.6
.38 SPEC	125	JSP	3-D	2.00	1085	957	291	10.8
.38 SPEC	125	JHP	REMINGTON	4.00	1160	1108	337	23.2
.38 SPEC	125	JHP	REMINGTON	2.00	1160	911	277	13.9
.38 SPEC	140	JHP(+P)	SPEER	4.00	1200	978	298	23.0
.38 SPEC	140	JHP(+P)	SPEER	2.00	1200	897	273	17.0
.38 SPEC	148	WC	BROWNING	4.00	770	731	222	13.9
.38 SPEC	148	WC	BROWNING	2.00	770	618	188	12.2
.38 SPEC	148	WC	REMINGTON	4.00	770	741	225	15.9
.38 SPEC	148	WC	REMINGTON	2.00	770	700	213	15.3
.38 SPEC	148	WC	FEDERAL	4.00	770	737	224	14.3
.38 SPEC	148	WC	FEDERAL	2.00	770	674	205	13.3
.38 SPEC	148	WC	SMITH+WESSON	4.00	800	726	221	9.0
.38 SPEC	148	WC	SMITH+WESSON	2.00	800	662	201	8.0
.38 SPEC	148	WC	SPEER	4.00	825	679	206	13.1

TABLE LXII (CONTINUED)

## Performance of Commercially Available Handgun Ammunition

CALIBER	WEIGHT (grains)	BULLET TYPE	MANUFACTURER	BARREL LENGTH (in)	VELOCITY			RI INDEX
					NOMINAL*	MEASURED (fps)	(mps)	
.38 SPEC	148	WC	SPEER	2.00	825	652	198	12.7
.38 SPEC	148	WC(CLEAN CUTTING)	WESTERN	4.00	770	696	212	13.6
.38 SPEC	148	WC(CLEAN CUTTING)	WESTERN	2.00	770	618	188	12.6
.38 SPEC	158	JHP	SMITH+WESSON	4.00	1050	1047	319	18.2
.38 SPEC	158	JHP	SMITH+WESSON	2.00	1050	950	289	12.9
.38 SPEC	158	JSP	SMITH+WESSON	4.00	1050	828	252	5.5
.38 SPEC	158	JSP	SMITH+WESSON	2.00	1050	730	222	3.3
.38 SPEC	158	LRN	WINCHESTER	4.00	855	919	280	7.5
.38 SPEC	158	LRN	WINCHESTER	2.00	855	780	237	5.5
.38 SPEC	158	LRN(+P)	FEDERAL	4.00	1090	999	304	9.4
.38 SPEC	158	LRN(+P)	FEDERAL	2.00	1090	947	288	8.1
.38 SPEC	158	LRN	FEDERAL	4.00	855	795	242	5.6
.38 SPEC	158	LRN	FEDERAL	2.00	855	632	192	4.6
.38 SPEC	158	LRN	REMINGTON	4.00	855	749	228	6.1
.38 SPEC	158	LRN	REMINGTON	2.00	855	694	211	5.7
.38 SPEC	158	LRN	SPEER	4.00	975	749	228	4.4
.38 SPEC	158	LRN	SPEER	2.00	975	635	193	3.8
.38 SPEC	158	LRN	SMITH+WESSON	4.00	910	708	215	1.5
.38 SPEC	158	LRN	SMITH+WESSON	2.00	910	626	190	1.2
.38 SPEC	158	LHP	WINCH-WESTERN	4.00	855	915	278	17.2
.38 SPEC	158	LHP	WINCH-WESTERN	2.00	855	805	245	11.5
.38 SPEC	158	SWC	FEDERAL	4.00	855	823	250	9.7
.38 SPEC	158	SWC	FEDERAL	2.00	855	796	242	8.7
.38 SPEC	158	SWC	SMITH+WESSON	4.00	1060	875	266	3.9
.38 SPEC	158	SWC	SMITH+WESSON	2.00	1060	678	206	7.4
.38 SPEC	158	SWC	SMITH+WESSON	4.00	850	1006	306	10.8
.38 SPEC	158	SWC	SMITH+WESSON	2.00	850	870	265	3.7
.38 SPEC	158	SWC	SPEER	4.00	975	803	244	10.0
.38 SPEC	158	SWC	SPEER	2.00	975	640	195	5.7
.38 SPEC	158	SWC	WINCHESTER	4.00	855	924	281	14.2

TABLE LXII (CONTINUED)

## Performance of Commercially Available Handgun Ammunition

CALIBER	WEIGHT (grains)	BULLET TYPE	MANUFACTURER	BARREL LENGTH (in)	VELOCITY			RI INDEX
					NOMINAL* (fps)	MEASURED (fps)	(mps)	
.38 SPEC	158	SWC	WINCHESTER	2.00	855	799	237	8.8
.38 SPEC	200	LRN	REMINGTON	4.00	730	647	197	2.9
.38 SPEC	200	LRN	REMINGTON	2.00	730	593	180	2.3
.38 SPEC	200	LRN	SPEER	4.00	850	710	216	3.8
.38 SPEC	200	LRN	SPEER	2.00	850	598	182	2.4
.38 SPEC	200	LRN(LUBALOY)	WESTERN SUP-X	4.00	730	626	190	2.7
.38 SPEC	200	LRN(LUBALOY)	WESTERN SUP-X	2.00	730	592	180	2.4
.41 MAG	210	JSP	REMINGTON	4.00	1500	1260	384	51.6
.41 MAG	210	SWC	REMINGTON	4.00	1050	944	287	6.2
.44 MAG	180	JSP	SUPER VEL	4.00	1995	1495	455	33.5
.44 MAG	200	JHP	SPEER	4.00	1675	1277	389	67.3
.44 MAG	240	JHP	BROWNING	4.00	1330	1257	383	50.1
.44 MAG	240	JHP	REMINGTON	4.00	1470	1229	374	47.3
.44 MAG	240	JSP	SPEER	4.00	1650	1203	366	49.0
.44 MAG	240	SWC	BROWNING	4.00	1470	1311	399	32.9
.44 MAG	240	SWC	REMINGTON	4.00	1470	1286	391	32.2
.44 MAG	240	SWC	WINCH-WESTERN	4.00	1470	1330	405	33.4
.45 AUTO	185	JHP	REMINGTON	5.00	950	895	272	18.0
.45 AUTO	185	WC(TARGETMASTER)	REMINGTON	5.00	775	821	250	3.5
.45 AUTO	185	WC	FEDERAL	5.00	775	751	228	6.3
.45 AUTO	230	FJ	REMINGTON	5.00	855	839	255	5.4
.45 AUTO	230	FJ	WINCH-WESTERN	5.00	850	740	225	2.6
.45 LC	255	LRN	WINCH-WESTERN	7.50	860	821	250	3.7

\* - Advertised Velocity

#### - Velocity not available

TABLE LXIV. Effective Coefficients for Typical Bullet Shapes Assuming No Deformation

<u>C<sub>D</sub></u>	<u>Typical Bullets</u>
.3	Ball (full jacket) parabolic nose, power point
.37	Round nose, sphere, or hemi
.45	Semi-wadcutter, jacketed soft point
1.2	Wadcutter

TABLE LXV. Matrix of Nondeforming Projectiles Examined with the Cavity Model

<u>Caliber</u>	<u>Drag Coefficients</u>	<u>Mass (grains)</u>
.357		110
	.30, .37, .45, 1.2	125
		158
	.37	166 (Lead sphere)
.45		185
	.30, .37, .45, 1.2	210
		230
	.37	.30 (Lead sphere)

TABLE LXVI

Caliber Class	Common Brick	Concrete Block 6" thick	Urban Dwell walls other than brick	1/8" window glass	1/4" laminated window glass	Common Auto-mobile Body	Lightly Armored Automobile Body	Office Building (Exterior)	Office Building Interior Walls
22 LR to 32 ACP	R	R	P R	P	P	P	R	R	P R
38 SP to 357 MAG	R	R	P R	P	P	P	R	R	P R
41 MAG through 45 CAL	R	R	P R	P	P	P	R	P R	P R

P = penetration possible  
R = lethal ricochet possible

•

•

•

•



2

2

2

